DOCTOR OF PHILOSOPHY

Investigation of Alternative Water Heating Methods

Fadl, Mohamed Sakr

Award date:
2014

Awarding institution:
Coventry University

Investigation of Alternative Water Heating Methods

By

Mohamed Sakr Fadl

For the degree of Doctor of Philosophy

December, 2014

Coventry University

Abstract

Water heating contributes an important proportion of residential energy consumption all around the world. Internationally, domestic potable water heating contributes between 15% and 40% of energy consumption within residential dwelling, electricity and natural gas are the major fuels reported in use for domestic water heating.

Different kinds of domestic hot-water production systems exist. The operational cost, environmental effect and performance of these systems differ according to various energy sources, climates, system types and system designs. Therefore design of water heating systems for household and industry are more subject to optimization, in order to improve thermal performance and minimize losses.

One of the most common types of water heating technologies is TEWHs (Tankless electric water heater). These high-power water heaters heat water instantly as it flows through the heater. (TEWHs) are compact, will not run out of hot water and have no standby energy losses but have to be wired to the electric consumer unit.

The research work carried out and reported in this thesis is divided into three main parts. Firstly, influences by employing different inlet–outlet port arrangements, heating tank shapes and electric coil configurations on the thermal performance of the tankless electric water heater were investigated experimentally and numerically. Results were obtained for four operation water rates of 0.06, 0.08, 0.10 and 0.12 L/s. The analysis and design optimization are based on the transient temperature profile of the outlet water, the transient temperature distribution of the water inside the heating tank, flow profile of fluid flowing inside the heating tank and heat transfer between the heating elements and fluid, and also the temperature distribution on the surface of the heating elements. The characteristic performance of the heater with different configurations is analyzed and the best one is identified and proposed to use in practice especially the heater with horizontally inclined inlet ports.

It is found that, the heaters with horizontal inclined inlet angle ports are successful in promoting good thermal distribution inside the heating tank, however, the degree of flow mixing produced by each design is found to have a significant impact on the heater thermal performance.

Meanwhile the new heater fixture provides more hot water at almost constant temperature in the first mean residence time, which is of prime concern for the user.

In the second part of the simulation, eleven different heating tank shapes were simulated, included two different structures of heating elements coils (external and internal legs) both have the same heating power rating and length. The heating tank diameter varied from (58, 66 to 73.2 mm) and with different inlet port positions.

The numerical results demonstrated that the shape of the heating tank has significant influence on the water mixing and circulation inside the heating tank heating tank, Furthermore, modification of the heating elements coils structure and geometry of the heating tank could be significant benefit to assist in smoothing the flow of fluid from inlet to outlet through the heating tank so that the heating elements do not interfere with the flow of fluid through the heating tank. In addition, improve both heating efficiency, reduce occurrence of heater failure and more likely to improve durability.

Secondly, experimental investigations were carried out to observe the advantage of using PCM in thermal energy storage system. The experimental findings indicate that the use of PCM helps to stabilize the system temperature to an allowable working temperature of 40 ^{o}C and extends the usage time. The results show that inclusion of a PCM in water tanks for domestic hot-water supply is a very promising technology. It would allow the user to have hot-water for longer period of time even without exterior energy supply. Additionally, further studies should focus on optimizing latent heat thermal energy storage with heat transfer enhancement methods.

Finally, an attempt of utilizing Ohmic heating method to generate heat in water as an alternative heating method rather than using electric heating coils has been studied experimentally. The effects of applied voltage, electrode gaps, electrode types and electrical conductivity of water during Ohmic heating were investigated. Heat was generated within the water using alternating electric current at frequency of 60 Hz, the range of voltage gradients were 26.31–87.0 V/cm.

One major output of this research is the assessment operating parameters during Ohmic heating which adds a new perspective to system analysis and design Ohmic heating system for water heating process.

The results indicate that Ohmic heating provides rapid and uniform heating method within less heating time. However, more studies are needed for continuous Ohmic heating system, modeling for commercial production as well as economical evaluation of the system.

Industrial relevance

In the present study, innovative methods to improve the thermal performance of tankless electric water heaters were applied. Some experimental and numerical models were developed and validated in this work for the industry to apply them for producing more robust and efficient heating systems, also, this work also show that the quality attributes of Ohmic heating is better than those of conventional water heating in many aspects.

Acknowledgements

Thanks to God the merciful, who guided me along the years until this work was accomplished. Thanks go to the many people who have supported me throughout my PhD journey.

The author wishes to express his sincere gratitude for Dr Shuli Liu and Prof Peter Claisse for their supervision and valuable advice during the work.

I gratefully acknowledge the funding received towards my PhD from the Coventry University PhD studentship. I am also grateful the financial support from Triton Showers is gratefully acknowledged. I also thank Mr. Hezar Qasim and Mr. Robin Brash (Triton Showers) for their excellent technical assistance.

My special thanks to all the technicians of the John Lang Building at Coventry University, Ian Breakwell, Terry Teeling, Kieran Teeling, and Steve Hutton.

These acknowledgments would not be complete without thanking my family for their constant support and care. Finally, I would like to mention two other people who are very important in my life: My wife, Roqaya Sadek and my little son, Kareem. I thank Roqaya for everything. I could not have accomplished my goal without her unfaltering support, encouragement, and inspiration. During the past four years, she stubbornly refused to allow my mind's stressed and exhausted state to distort reality. She also selflessly accepted my lack of attention and time. I thank my little son for making me so happy with his cute smile and engaging me lot at home

May all who helped me in preparing the manuscript also receive my deep gratitude.

Contents

List of Figures

Chapter (1)

Chapter (2)

Chapter (3)

Chapter (4)

Chapter (5)

Chapter (6)

Chapter (7)

List of Tables

Chapter (2)

Chapter (3)

Chapter (5)

Chapter (6)

Chapter (7)

Appendices

List of Variables

C_p	Specific heat capacity (J/kg ^oC)
C_1, C_2, C_μ	constant of the *k*–*ε* model
D	Tank inner diameter(m)
d	Pipe inner diameter (m)
f	friction factor (-)
H	Twist pitch length (m)
I	Current (A)
k	Turbulence kinetic energy (m^2/s^2)
L	Length of computational domain (m)
m	Mass of the sample (kg)
m^o	Water mass flow rate (kg/s)
n	Temperature factors (S/m ^oC)
Nu	Nusselt number
P	Electrical power given to the system (J)
p	Pressure (Pa)
Pr	Prandtl number
Q	Energy required to heat the sample (J)
Q_{ele}	Electrical power given to the system (W)
Q_f	Energy transferred to the water (W)
R^2	Determination of coefficient (–)
Re	Reynolds number
SPC	System performance coefficient (–)

T	Temperature (^oC)
t	Time (second)
T_f	Final temperature of sample (^oC)
T^i	Initial temperature of sample (^oC)
T_{in}	Water inlet temperature (^oC)
T_{out}	Water outlet temperature (^oC)
$\vec{u}$	Velocity vector (m/s)
V	Voltage applied (V)
V	Computational domain volume (m^3)
w	wall
X	Gap between the electrodes (mm)
y	Twist ratio (-)

Greek Symbols

ε	Turbulence energy dissipation rate (m^2/s^3)
$\bar{\varepsilon}$	Global power dissipation rate per fluid mass unit (W/kg)
η	Heat transfer enhancement efficiency
k	Thermal conductivity (W/m K)
k_{eff}	Effective thermal conductivity (W/m K)
μ, μ_T μ_{eff}	Laminar, turbulent and effective viscosity (Pa s)
υ	Fluid kinematic viscosity (m^2/s)
ρ	Mass density (kg/m^3)
σ	Temperature standard deviation (K)
σ_k, σ_ε	Turbulent Prandtl numbers for k–ε
σ	Electrical conductivity (S/m)

τ	Time(second)
$\bar{\bar{\tau}}$	Stress tensor (Pa)

Subscripts

i	inner diameter

Abbreviations

CFD	Computational fluid dynamics
DDIR	Discrete double-inclined ribs
DWs	Delta-winglet type vortex generators
ETWHs	Electric tankless water heaters
HWTs	Hot water tanks
MT-VG	Multiple twisted tape vortex generators
O-DWT	Oblique delta-winglet twisted tape
OH	Ohmic heating
PCM	Phase change materials
POU	Point-of-use
PT-A	Peripherally-cut twisted tape with alternate axis
P-TT	Plain twisted tapes
S-DWT	Straight delta-winglet twisted tape
SEWHs	Storage-type electrical water-heaters
STT	Serrated twisted tape
TCEs	Thermal conductivity enhancers
TES	Thermal energy storage
TT	Typical twisted tape
TWHs	Tankless Water Heaters

WN-TT	Twisted tape consisting wire nails
WT	Twisted tape with wings
WVG	Winglet vortex generator
WVGs	Winglet type vortex generators

Chapter (1)

1. Introduction

1.1. Background

Water heating is one of the most energy-consumptive activities in a household. Internationally, domestic potable water heating contributes between 15% and 40% of energy consumed within residential dwellings (Bourke et al., 2014). Different kinds of domestic hot-water production systems are available. These include tankless water heaters, condensing water heaters, heat pump water heaters, and solar water heaters, etc. All of these different water heating technologies could provide energy savings to homeowners. The operating cost, environmental effect and performance of these systems differ according to energy source, climate, system type, and system design (Ibrahim et al., 2014). Hence, the proper choice of a domestic hot-water system could significantly save energy, protect the environment and reduce operating costs.

In recent years Electric Tankless Water Heaters has been strongly promoted as a clean, quiet, efficient and convenient way of heating water. Whether it is for small quantities of water from a sink heater or an instantaneous shower or whether it is for larger quantities for general household use, there is a wide variety of products and methods of heating the water economically. Where smaller, and infrequent quantities of water are required, convenience and space are generally the overriding factors to be considered.

Electric Tankless Water Heaters (ETWHs) are sold in large numbers in many countries and are seen as an efficient means of producing domestic hot water with a far smaller carbon footprint than either gas storage water heaters with insulated central flues, or electric storage water heaters powered by thermally generated electricity and count as one of green building solution.

In general, Tankless Water Heaters (TWHs), also called instantaneous or demand water heaters, have both advantages and disadvantages when compared to storage water heaters.

Some of the advantages are that they are smaller, have a longer life, can provide a continuous stream of heated water and typically use less energy than their storage counterparts. Two main disadvantages are that they require a large power input and that the outlet temperature is difficult to control (Henze et al., 2009). Tankless water heaters are often installed throughout a household at more than one point-of-use (POU), far from the central water heater or larger models may still be used to provide all the hot water requirements for an entire house (Green Energy Efficient Homes, 2014). Point-of-use water heaters are usually fitted into existing dwellings. They are particularly useful where extensions and alterations are being undertaken, as they need only a cold water supply, usually mains cold water. Probably the most common point-of-use water heater is the instantaneous shower, which is often used on the first floor of two storey dwellings as the head pressure from the cold water cistern is sometimes insufficient to provide a high enough water flow and can be a more economic solution than the power shower. Point-of use water heaters can also be appropriate for the growing markets of holiday lets and second homes, where usage can be very varied and irregular.

1.2. Description of Electric Tankless Water Heating Technology

The Electric Tankless Water Heater works by using electric heating elements that are activated by the flow of water when there is demand for hot water (e.g. some are take a hot shower, a hot water tap is opened for a sink, washing machine, etc.). The tankless water heater's water flow turbine senses the flow and starts the heating process; the pressure inflates a diaphragm which closes the electrical contacts of the heater coil with the live contacts, turning on the device. Once the water is stopped, the device turns off automatically. Since it does not store hot water in anticipation of demand, there is no storage tank. Tankless water heaters are available in either electric or natural gas models (Milward, 2005).

In electric tankless water heaters, the heating elements convert electric energy into heat, and the elements are usually placed in direct contact with the water so that the heat is directly transferred into the flow. The electric elements heat up when the flow of water begins and will be turn off when the water flow stops. Figure 1.1 shows the internal components of typical electric tankless water heaters.

The heating element of an electric shower is made from a coil made of nickel or an alloy of nickel and chromium or can even be made of sheathed heater element, like the ones used in oil heaters, radiators or irons, they provide more safety as there is insulation between the electric parts and the water. Due to electrical safety standards, modern electric showers are made of plastic instead of the metallic casings like in the past. As an electrical appliance which works with higher electrical currents than a washer or a dryer machine (Amatore et al., 1998).

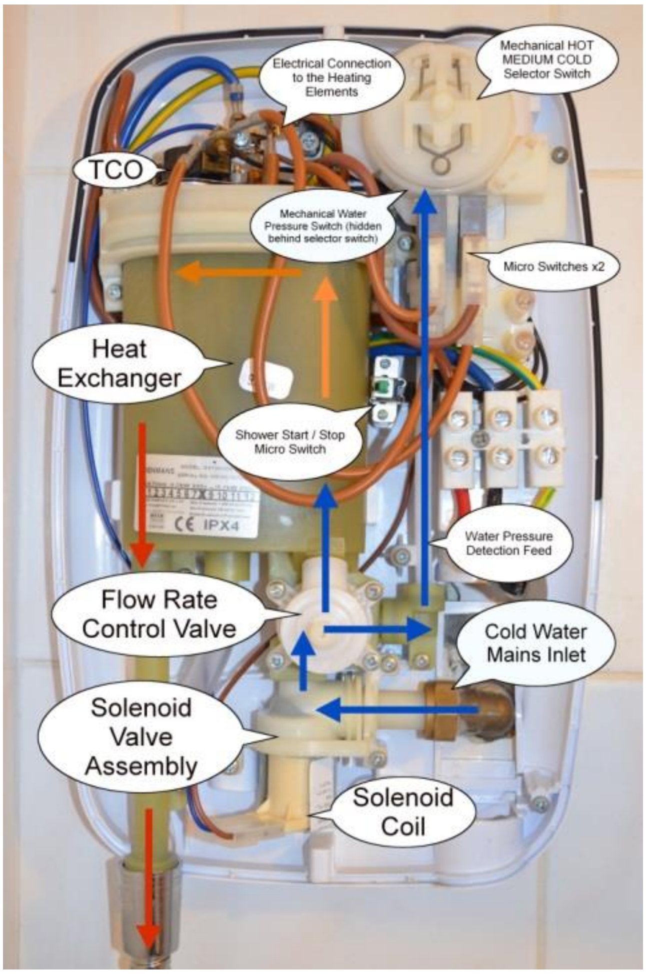

Figure 1-1 The components of electric tankless water heater

The advantages and disadvantage of the instantaneous water heater have been summarized by Milward and Prijyanonda (Milward and Prijyanonda, 2005) and Ibrahim et al (Ibrahim et al., 2014)

Advantages

- No hot-water storage, and thus standby heat loss is eliminated.
- Higher energy factor than conventional storage units, noting that the energy factor is defined as a measure of the portion of input energy that is transferred to the hot water.
- Lower operating cost compared to conventional storage units.
- Unlimited hot-water supply as water is heated while passing through the system.
- The temperature of a certain hot-water flow is constant.
- Their compact size use less physical space.
- Longer life expectancy than conventional storage units.

Disadvantages

- Start-up delay as water is heated upon demand.
- Minimum flow rate threshold, below which the unit will not activate, is required.
- May not be able to serve simultaneous multiple draws of hot water.
- For electrical type, high instantaneous power is needed.
- Yearly maintenance is needed to prevent water-flow restriction due to calcium build up.

1.3. Statement of the Problem

In light of the above background, it is clear that there is rapid growth of electric energy consumption for residential purposes and has become phenomenal in all over the world. One of the major application usages of electrical energy is domestic water heating especially. Because of such large amount of energy demand, there is increasing interest in more efficient units. One key aspect for the design of an efficient and reliable instantaneous electric water heater is thermal stresses arising during transient operation. If the stresses exceed the fatigue limits of the material, the lifetime of the heating element coils is shortened.

The presented work aims to develop a novel electric tankless water heater in order to minimize any area of flow rate to avoid such issues as hot spot being formed on the heating elements, promote uniform heating of the fluid in the heating tank, evaluating of using PCM to protecting subsequent shower users from scalding and potential application of using Ohmic heating principles as an alternative water heating methods in future.

1.3.1.Objectives

1. To investigate various parameters that affect tankless electric water heater thermal performance such as water mixing characteristics inside the heating tank with different cold water inlet velocities and configurations.
2. To compare the effect of different heating tank shapes and electrical heating coil structures.
3. To assess the effect of using PCM as thermal energy storage to remove and storage the heat from the heating tank after turn-off the heater experimentally under various operation conditions.
4. To evaluate the potential application of using Ohmic heating principles as an alternative water heating methods in future; research is needed on methods for measurements and testing equipment design. The Ohmic heating method seems to be ambiguous and needs more investigations.

1.4. Research Methodology

In order to achieve the above objectives, the proposed research methodologies are listed below:

1. Design and construct experimental facility to investigate the effect of inlet angles on the thermal performance of tankless electric water heating system. The experimental program has been performed for twelve different inlet angles. For

each inlet–outlet configuration, experiments have been carried out with draw-off flow rates of (0.06, 0.08, 0.10 and 0.12 kg/s).

2. 3D numerical simulation models for an instantaneous electric water, to predict flow mixing in the heating tank, for various modifications such as different inlet angles, different tank shapes and heater coil structures.
3. Experimentally evaluate the effect of using PCM for thermal management of tankless water heater. Experiments will be perform on prototype water tank that are designed and constructed to study the effect of the presence of PCM on transient performance of the heating system.
4. Design, build and assessment the thermal performance of an Ohmic heating apparatus in bench scale for water heating based on different parameters such as, voltage gradient, electrical conductivity, heating rate and electrode materials.

It is anticipated that the results put forward in this thesis will encourage designers and researchers in the field of water heating systems to dwell more on the flow characteristics, heat transfer aspects in the water heating system to provide better performance and efficiency of the system as a whole.

1.5. Structure of the Thesis

This thesis is organized in 8 chapters; the individual content of each chapter is given in the following paragraphs as described below:

Chapter 1 provides an introduction and a general description of the work carried out in the project, including the main aims, objectives and methodologies of the study.

Chapter 2 reviews of existing research work on heat transfer enhancement, thermal energy storage and the Ohmic heating concept.

Chapter 3 explains the experimental set-up of heating system include the test rig, the water supply units, the test section, the inlet configuration angles and the experimental procedure.

Chapter 4 includes the experimental results and discussions of the experimental work, the analysis based on the selection of the best inlet angle configuration to promote thermal performance of the heating system and maximize mixing during water heating inside the heating tank of instantaneous electric water heaters under different discharge rates. Such ability has the most significant impact on the heater capability of supplying its water capacity at the temperature and rate, which satisfy the needs of the user.

Chapter 5 explains the simulation framework and methodology, gives background information on CFD solution procedure, geometry generation, mesh generation, specification of boundary conditions, mathematical model and numerical methods, boundary conditions, solution procedure and solver setting monitoring solutions convergence, verification of the numerical simulation with experimental results and evaluation the effect of heating element and tank geometrical structures on the heating system thermal performance.

Chapter 6 includes the experimental setup and investigation of the advantage by using PCM in thermal energy storage system. The affecting factors were investigated such as stored water and PCM initial temperatures and storage time.

Chapter 7 concerns the Ohmic heating experimental apparatus includes Ohmic heating unit design, power supply system, dimensions of Ohmic heating unit includes electrodes sections and specifications, test procedure, and measured and calculated parameters such as the passing current, voltage, temperature, electric conductivity, heating rate. Experimental results and comparisons for different electrode materials were performed.

Chapter 8 finally concludes the research work by describing the outcomes of the study and provides recommendations for further work in this field.

In addition, five appendices are attached at the end of the thesis to provide more details and explanations for different parts.

Chapter (2)

2. Literature Review

Topic on the research of electric water heating has become a matter of great concern due to energy crisis all over the world; in the UK for example, the domestic sector currently accounts for one third of national energy consumption and one quarter of the UK greenhouse gas emissions. This is due to the heavy reliance on fossil fuels of domestic activities such as space and water heating. The majority (84%) of water heating in the UK is provided by natural gas with the rest supplied by electricity (Benjamin and Adisa, 2014).

Energy performance and environmental impact comparison of heating systems is a major topic that has already led to numerous publications (Pineau et al., 2013). This chapter summarizes the previous works on water heating systems with various heat transfer enhancement techniques include tank design, water inlet-outlet port configurations, fluid flow rate, thermal energy storage use of phase change materials, passive techniques to improve the convective heat transfer like insertion of twisted tapes and its geometry to improve the thermal performance of water heating systems. This chapter also discusses the methods to optimize and simulate the water heating systems and new methods that could be used in water heating such as Ohmic heating.

2.1 Design and Performance of Electric Water Heating Systems

Storage-type electrical water-heaters (SEWHs) are widely used in many countries all over the world for generating hot water in numerous domestic, commercial and industrial applications. In particular, they are very popular in the urban and suburban areas of developing countries, where the majority is the residential building stock consists of multi-family (multi-storey) buildings with individual domestic water heater for each apartment/unit. The disadvantage of storage-type domestic SEWHs is their excessive consumption of electrical energy (Hegazy and Diab, 2002).

There are numerous studies in the literature on the performance and design optimization of residential water heaters incorporating thermal storage vessels.

Sezai et al (Sezai et al., 2005) have studied experimentally the effect of using secondary heating element in storage type-domestic electric water heater to improve the energy utilization efficiencies, the results have illustrated that it is possible to design tank with dual heater giving the user the chance of switching between the elements depending on the amount of hot-water required.

Hegazy and Diab (Hegazy and Diab, 2001) experimentally investigated the effect of heating tank aspect ratio to improve the design for storage electric water heater. The results showed that the design improvements are very effective in enhancing the performances of such small capacity heaters as they could provide more hot water at almost constant temperature compared to conventional design EWHs, which is of prime concern for the user.

Also, Hegazy (Hegazy, 2007) experimentally investigated the effect of inlet design on the performance of storage-type domestic electrical water heaters for energy conservation using three different side-inlet geometries namely wedged, perforated, and slotted pipe-inlets, the results show an excellent performance for the slotted inlet.

The effect domestic electric hot water storage tank inlet and outlet arrangements have been studied by Fernández-Seara et al (Fernández-Seara et al., 2007). The experimental results have indicated that during dynamics operation the tank thermal performance strongly depends on the water inlet and outlet arrangement.

García-Marí et al (García-Marí et al., 2013) have studied the effect of two water inlet devices in a hot water storage tank during a thermal charge process: a sintered bronze conical diffuser (SBCD) and a conventional inlet elbow. The results obtained have shown that the SBCD favours water stratification during thermal charging with both low and high flow.

The effects of hot water withdrawal from the storage tank of a water heating system on the utilization percentage of solar heat gain, the mixing characteristics of hot water inside the storage tank with different inlet velocities of the supply cold water are studied by numerical simulations by (Gao et al., 2011), the numerical simulation results have shown that an increase in the inlet velocity of the supply cold water will result in a larger entrainment factor and stronger water mixing in the tank.

Ievers and Lin (Ievers and Lin, 2009) have studied numerically the hot water storage device using CFD, considering different operating conditions and tank geometries. The results show that increasing the tanks height/diameter aspect ratio, decreasing inlet/outlet flow rates and moving the inlet/outlet to the outer extremities of the tank all result in increasing levels of thermal stratification.

The effect of using different obstacles on thermal stratification in a cylindrical hot water tank have been analyzed numerically by Altuntop et al (Altuntop et al., 2005). The results indicated that placing obstacle in the tank provides better thermal stratification compared to the no obstacle case.

Shah and Furbo (Shah and Furbo, 2003) have studied theoretically and experimentally the effect of water inlet designs with different inlet flow rates on the thermal performance of solar storage tank. The results showed that the impact of the inlet design on the flow patterns in the tank and thus how the energy quality in a hot water tank is reduced with a poor inlet design.

Moeini and Khodadadi (Moeini and Khodadadi, 2013) have studied numerically and experimentally the thermal efficiency improvement of a residential natural gas-fired water heater in response to presence of a baffle, particularly designed for modifying the flow field within the water reservoir and enhancing heat transfer extracted into the water tank, the results have shown that baffle’s design is capable of lowering the natural gas consumption of the water heater by 4.95% under steady-state thermal efficiency test condition which meets the target of this research.

Many studies were performed on water heaters in order to analyze their performances under different conditions. One of these conditions is to minimize any areas of low water rate to avoid hot spots being formed on the heating element. In another study, it is desirable for the water flowing in the heating tank to be uniformly heated as much as is possible by the heating elements, also it is concluded in this study that it is undesirable for the outlet temperature to change during the shower time.

2.2 Heat Transfer Enhancements

Enhancing heat transfer surface is one of the most important processes in fluid engineering and is applied in numerous industrial applications to improve the thermal performance of hot water systems such as electric and gas water heaters. The design procedure of hot water systems is quite complicated, as it needs exact analysis of heat transfer rate, efficiency and pressure drop apart from issues such as long-term performance and the economic aspect of the equipment, so there is an increase in the demand for developing a new heat transfer enhancement techniques to decrease the size and the cost of the involving equipment.

One of the most important techniques used is passive heat transfer technique. These techniques if it is adapt in hot water systems will lead to improve the overall thermal performance significantly.

Whenever inserts technologies are used for the heat transfer enhancement, along with the improvement in the heat transfer rate, the pressure drop also increases, which induces the higher pumping cost. Therefore any augmentation device or methods utilized into the heating systems especially which uses heat exchangers should be optimized between the benefits of heat transfer coefficient and the higher pumping cost owing to the increased frictional losses. In general, heat transfer augmentation methods are classified into three broad categories:

- **Active method:** This method involves some external power input for the enhancement of heat transfer. Some examples of active methods include induced pulsation by cams and reciprocating plungers, the use of a magnetic field to disturb the seeded light particles in a flowing stream, mechanicals aids, surface vibration, fluid vibration, electrostatic fields, suction or injection and jet impingement requires an external activator/power supply to bring about the enhancement (Elshafei et al., 2008).
- **Passive method:** This method generally uses surface or geometrical modifications to the flow channel by incorporating inserts or additional devices. For example, inserts extra component, swirl flow devices, treated surface, rough surfaces,

extended surfaces, displaced enhancement devices, coiled tubes, surface tension devices and additives for fluids (Liebenberg et al., 2007).

- **Compound method:** Combination of the above two methods, such as rough surface with a twisted tape swirl flow device, or rough surface with fluid vibration, rough surface with twisted tapes (Alamgholilou and Esmaeilzadeh, 2012).

This section focuses on reviewing the passive methods to improve heat transfer in heating system which are using heat exchanger. The passive heat transfer augmentation methods as stated earlier do not need any external power input. For the convective heat transfer, one of the ways to enhance heat transfer rate is to increase the effective surface area and residence time of the heat transfer fluids. The passive methods are based on this principle, by employing several techniques to generate the swirl in the bulk of the fluids and disturb the actual boundary layer so as to increase effective surface area, residence time and consequently heat transfer coefficient in existing system. Although there are hundreds of passive methods to enhance the heat transfer performance, the following nine are most popular used in different aspects:

- **Treated surfaces:** They are heat transfer surfaces that have a fine-scale alteration to their finish or coating. The alteration could be continuous or discontinuous, where the roughness is much smaller than what affects single-phase heat transfer, and they are used primarily for boiling and condensing duties.
- **Rough surfaces:** They are generally surface modifications that promote turbulence in the flow field, primarily in single-phase flows, and do not increase the heat transfer surface area. Their geometric features range from random sand-grain roughness to discrete three-dimensional surface protuberances.
- **Extended surfaces:** They provide effective heat transfer enlargement. The newer developments have led to modified fin surfaces that also tend to improve the heat transfer coefficients by disturbing the flow field in addition to increasing the surface area.
- **Displaced enhancement devices:** These are the insert techniques that are used primarily in confined force convection. These devices improve the energy transfer

indirectly at the heat exchange surface by displacing the fluid from the heated or cooled surface of the duct/pipe with bulk fluid to the core flow.

- **Swirl flow devices:** They produce and superimpose swirl flow or secondary recirculation on the axial flow in a channel. These devices include helical strip or cored screw type tube inserts, twisted tapes. They can be used for single phase or two-phase flows heat exchanger.
- **Coiled tubes:** These techniques are suitable for relatively more compact heat exchangers. Coiled tubes produce secondary flows and vortices which promote higher heat transfer coefficient in single phase flow as well as in most boiling regions.
- **Surface tension devices:** These consist of wicking or grooved surfaces, which directly improve the boiling and condensing surface. These devices are most used for heat exchanger occurring phase transformation.

2.2.1 Important definitions terms commonly used in heat transfer augmentation

2.2.1.1 Thermal performance factor

Thermal performance factor is generally used to evaluate the performance of different inserts such as twisted tape, wire coil, etc., under a particular fluid flow condition. It is a function of the heat transfer coefficient, the friction factor and Reynolds number. For a particular Reynolds number, if an insert device can achieve significant increase of heat transfer coefficient with minimum raise of friction factor, the thermal performance factor of this device is good.

2.2.1.2 Overall enhancement ratio

The overall enhancement ratio is defined as the ratio of the heat transfer enhancement ratio to the friction factor ratio. This parameter is also used to compare different passive techniques for the same pressure drop. The overall enhancement ratio is expressed as:

$$\mathbf{Overall\ Enhancement\ Ratio} = \frac{\left(\frac{\mathbf{Nu}}{\mathbf{Nu_0}}\right)}{\left(\frac{\mathbf{f}}{\mathbf{f_0}}\right)^{\frac{1}{3}}} \qquad (2.1)$$

Where Nu, f, Nu_o and f_o are the Nusselt numbers and friction factors for a duct configuration with and without inserts respectively. The friction factor is a measurement of head loss or pumping power.

2.2.2 Twisted tape insert devices

Twisted tapes are the metallic strips twisted with some suitable techniques at desired shape and dimension, inserted in the flow. The twisted tape inserts are popular and widely used in heat exchangers for heat transfer augmentation besides twisted tape inserts promote heat transfer rates with less friction factor penalty on pumping power(Suresh, et al., 2005) and (Kumar and Prasad, 2000).

Insertion of twisted tapes in a tube provides a simple passive technique for enhancing the convective heat transfer by introducing swirl into the bulk flow and disrupting the boundary layer at the tube surface due to repeated changes in the surface geometry. That is to say such tapes induce turbulence and superimposed vortex motion (swirl flow) which induces a thinner boundary layer and consequently results in a better heat transfer coefficient and higher Nusselt number due to the changes in the twisted tape geometry. However, the pressure drop inside the tube will be increased by introducing the twisted-tape to insert. Hence a lot of researches have been carried out experimentally and numerically to investigate the optimal design and achieve the best thermal performance with less frication loss. The enhancement of heat transfer using twisted tapes depends on the Pitch and Twist ratio.

The twist ratio is defined as the ratio of pitch to inside diameter of the tube y=H/d, where H is the twist pitch length and d is the inside diameter of the tube.

Pitch is defined as the distance between two points that are on the same plane, measured parallel to the axis of a twisted tape.

2.2.2.1 Main categories of twisted tape

The most common used twisted tape can be classified into the following seven categories and some of the configuration sketches are displayed in Table 2-1.

- **Typical twisted tape:** These tapes have length equal to the length of exchanger tube (Kumar and Prasad, 2000), (Naga et al., 2010), (Jaisankar et al, 2009.a), (Wongcharee and Eiamsa-ard, 2011.a) and (Krishna et al., 2009).
- **Varying length, alternate-axes and pitches twisted tape:** These are distinguished from first category with regards that they are not having the length equal to length of the tube, but half length, ¾th length and ¼th length of section etc. (Eiamsa-ard et al, 2009.a), (Jaisankar et al., 2009.b) and (Jaisankar et al. 2009.c); or these are short length tapes with different pitches spaced or twist types connecting to each other with alternate axes (Wongcharee and Eiamsa-ard, 2011.b),(Seemawute and Eiamsa-ard, 2010) and (Eiamsa-ard et al., 2010.b).
- **Multiple twisted tapes:** More than one twist tapes are coupled used in one heat exchanger tube (Jaisankar et al., 2009.a) and (Eiamsa-ard et al., 2010.c).
- **Twisted tape with rod and varying spacer:** Twisted tape with rod and spacer to enhance the heat transfer rate (Jaisankar et al., 2009.b) and (Krishna et al., 2008).
- **Twisted Tape with attached fins and baffles:** Baffles are attached to the twisted tape at some intervals so as to achieve more augmentation (Jaisankar et al., 2009.c), (Eiamsa-ard et al., 2010.d) and (Wongcharee and Eiamsa-ard, 2011.a).
- **Twisted Tapes with slots, holes, cuts:** Slots and holes of suitable dimensions made in the twisted tape in order to create more turbulence (Murugesan et al., 2011), (Seemawute and Eiamsa-ard 2010.a), (Eiamsa-ard et al., 2010.e) and (Shababian et al., 2011).
- **Helical left-right twisted tape with screw:** The twisted tapes are shaped left-right helical and sometimes with screw element (Jaisankar et al, 2009.b, c), (Ibrahim et al., 2011) and (Moawed, 2011).
- **Tapes with different surface modifications:** Some insulating material is provided to tapes so that fin effect can be avoided. In some cases surface dimpled material used for tape fabrication (Eiamsa-ard, 2010.b), (Eiamsa-ard and Promvonge, 2010.c), (Murugesan et al., 2010) and (Thianpong et al., 2009).

These literatures presented in Tables 2-2, 2-3 and 2-4 investigated the effect of typical and developed twisted tapes on the heat transfer performance with different shape, angle and inserting locations at full-length dual and regularly-spaced dual twisted tapes, peripherally-cut twisted tape with serrated-edge insert and delta- winglet twisted tape. The thermal impacts of the oblique delta-winglet twisted tape (O-DWT), straight delta-winglet twisted tape (S-DWT) arrangements , serrated twisted tape (STT) peripherally-cut twisted tape with alternate axis (PT-A) and multiple twisted tape vortex generators (MT-VG) as swirl generators, for different heating fluid and wall conditions are investigated. All these investigations indicate the relationships between the enhancement of the heat transfer and the increase of the pressure drop inside the heat exchanger channels.

2.2.2.2 Impact of typical twist tapes on the enhancement efficiency

Large number of experimental work are carried out by researchers to investigate the thermohydraulic performance of various twisted tapes including the traditional simple twisted tapes, regularly spaced twisted tapes, varying length twisted tapes, tapes with different cut shapes, tapes with baffles and tapes with different surface modifications. The followings content will detail these reaches and display the finds from different researchers.

Kumar and Prasad (Kumar and Prasad, 2000) started to investigate the impact of the twist ratio on the enhancement efficiency for a solar water heater. When changed the twist ratios from 3.0 to 12.0 the heat transfer rate inside the solar collectors have been found increased by 18~70%, whereas the pressure drop increased by 87~132%. Synthetically consider the increase of heat transfer and pressure drop it is concluded that the twisted tape enhanced collectors would be preferable for higher grade energy collection to balance the pressure drop rather than for the solar collectors.

Continue research was carried out by Noothong et al (Noothong et al., 2006) regarding the influences of the twisted tape insertion with a twist ratio of 5.0 and 7.0 in a concentric double pipe heat exchanger. The results revealed that the twisted tape inserts induced the swirl or vortex motions which decrease the boundary layer thickness and enhance the heat transfer rate. The enhancement efficiency, Nusselt number (Nu) and friction factor all are reduced with the decreasing of the twist ratio. Furthermore, Naga et al (Naga et al., 2010), investigated the augmentations of turbulent flow heat transfer in a horizontal tube by varying the width of the twisted tape inserts with air as the working fluid. When the widths changed from 10 mm to 22 mm, the heat transfer rate are improved by 36% to 48% for the full width =26mm. This is because of that the centrifugal forces generate the spiral motion of the fluid.

Table 2-1 Configuration sketches of various twisted tapes

Table 2-2 Experimental works on the thermohydraulic performance of twisted tape

Table 2-3 Experimental works on the thermohydraulic performance of wire coils

Table 2-4 Configuration sketches of various wire coils various

2.2.2.3 Impact of twisted tape with alternate-axes, varying length and pitches on the enhancement efficiency

The alternate-axes, length and insert position of the twisted tape have differences enhancement effect on the heat transfer, hence researchers have carried out a lot researches (Eiamsa-ard et al., 2009), (Jaisankar et al., 2009 b) and (Eiamsa-ard et al., 2010 c). S. Eoamsa-ard et al, (Eiamsa-ard et al., 2009), studied the impact of the length of twist tape (LR) on the thermal performance, they found that: 1) the presence of the tube with short-length twisted tape insert yields higher heat transfer rate (Nu) up to 1.16, 1.22 and 1.27 times of the plain tube, while the friction factor up to 1.76, 1.88 and 1.99 times by applying LR = 0.29, 0.43 and 0.57, respectively; 2) the maximum heat transfer (Nu) and friction factor (f) is obtained for using the full-length tape; 2) the Nu and f values of the short-length twisted tape insert with LR = 0.29, 0.43 and 0.57, respectively, are about 14%, 9.5%, and 6.7%, and 21%, 15.3%, and 10.5% lower than these of the full-length twist tape .

S. Jaisankar et al, (Jaisankar et al., 2009 b) compared the heat transfer enhancement of full length and twisted twist fitted with rod and spacer. It is determined that the first has better effect than second. Some researchers such like Eiamsa-ard et al, (Eiamsa-ard et al., 2010 b). combined the alternate-axes and wings techniques together. They found that the twisted tape with alternate axes at the largest angle of attack will provide the highest Nusselt number, friction factors and thermal performance.

Meanwhile, Wongcharee et al (Wongcharee et al., (2011), further investigated the heat enhancement performance of clockwise and counter-clockwise alternate–axes twisted tape (T-A). The results indicate these: 1) the friction factor associated by T-A is higher than that induced by typical twisted tape (TT), and friction factor increases with the decrease of the twist ratio; 2) the friction factors of the tube with the T-A at y =3.0, 4.0 and 5.0 are respectively around 50%, 49% and 33% higher than those of the tube with the TT at the same twist ratio; 3) under the similar condition, the Nu associated by T-A is significantly higher than that associated by TT; 4) in the examined range, T-A yield higher Nu than TT by around 70.9% to 104.0%, in addition, Nu increases with the decreasing of twist ratio such like the T-A with twist ratio of 3.0 provides higher transfer rate than the T-A with twist ratio of 4.0 and 5.0 by 15.6% and 30.7%, respectively .

2.2.2.4 Impact of multi twisted tapes on the enhancement efficiency

From the previous research it is obvious that the twisted tape can improve the heat transfer efficiency, following this finds, Eiamsa-ard et al, (Eiamsa-ard et al., 2010 c) investigated the effect of dual and multiple twisted tape impacts on the heat transfer enhancement. The heat transfer rate for the dual twisted tapes is increased by 12% to 29% in comparison with the single tape at the twist ratios from 3.0 to 5.0 by generating strongly dual swirling flows inside the test tube. Depending on the flow conditions and twist ratio y, the increases in heat transfer rate over the plain tube are about 146%, 135% and 128% for y =3.0, 4.0 and 5.0, respectively. The smaller space ratio of the dual twisted tapes in tandem is more attractive in heat transfer application due to the higher enhancement efficiency than the single one. The multiple twisted tape vortex generators (MT-VG) were researched by S. Eiamsa-ard et al (Eiamsa-ard et al., 2010 d). The Nusselt numbers increase by 10% to 170% comparing with the values for the smooth channel, while the friction factors are 1.45 to 5.7 times of those of the smooth channel.

2.2.2.5 Impact of twisted tape with rod and varying spacers on the enhancement efficiency

The spacer distance will be another factor influencing the enhancement performance. Jaisankar et al, (Jaisankar et al., 2009 b) and Krishna et al,(Krishna et al., 2008) discovered that the heat enhancement in full length twisted tape is better than the twist fitted with rod and spacer; the decrease in heat transfer augmentation in twist with rod is minimum compared to twist with spacer; the decrease in friction factor is maximum for twist with spacer compared to twist with rod; and there is no appreciable increase in heat transfer enhancement in straight full twist insert with 2 in. spacer distance; meanwhile, Jaisankar also proved that there was 17% and 29% decrease of heat transfer with rod and spacer comparing to full length twist (Jaisankar et al. 2009 a,b,c).

2.2.2.6 Impact of twisted tape with attached fins and baffles on the enhancement efficiency

Usually, the wings, fins and baffles are attached alone the center line like shown in Table 2-1, or twisted tapes with wing shaped into triangle, rectangle and trapezoid (Eiamsa-ard et al., 2010 c) and (Eiamsa-ard et al., 2010 b). Researchers such like Eiamsa-srd et al, (Eiamsa-ard et al., 2010 c) studied the twisted tapes consisting of center wings and alternate-axes (WT-A). The effect of attack along the center line of the tape was studied. The results show that the heat transfer rate increases with the increasing of attack angle. Because the superior performance of the WT-A over those of the other tapes could be attributed to the combined effects of the following actions: a common swirling flow induced by the twisted tape; a vortex generated by the wing and a strong collision of the recombined streams behind each alternate point. This research group also investigated the thermal impact of oblique delta-winglet twisted tape (O-DWT) and straight delta-winglet twisted tape (S-DWT). The values of Nusselt number and friction factor in the test tube equipped with delta-winglet twisted tape are noticeably higher than those in the plain tube and also tube equipped with typical twisted tape.

The Nusselt number and friction factor increase with the decreasing of twist ratio and the increasing of the depth of wing cut ratio (DR); O-DWT gives higher Nusselt number and friction factor than that of the S-DWT; the thermal performance factor in the tube with O-DWT is greater than that with S-DWT and the factor increases with the decreasing of Reynolds number and the increasing of twist ratio; DWT performs better heat transfer enhancement than the typical twisted tape, and it indicates that the heat exchanger fitted with DWT is more compacted than the one with the typical twisted tape; therefore DWT can efficiently replace any of the TT with reduced heat exchanger size .

Wongcharee and Eiamsa-ard (Wongcharee and Eiamsa-ard, 2011) studied several of wing shape with alternate-axes instead of the depth of the wing, including triangle, rectangle and trapezoid. This group found these: 1) flow visualization by dye technique shows that apart from a common swirl flow, the twisted tapes with alternate axes and wings induce an additional fluid disturbance, signifying the excellent fluid mixing; 2) the twisted tapes consisted of both alternate-axes and wings offer superior heat transfer enhancement compared to the one with only alternate-axes and also the typical one, which thanks to the combined effects of the strong collision of fluid behind the alternate point, caused by alternate axis and the extra fluid disturbance near tube wall induced by wings; 3) for the twisted tapes with combined alternate axes and wings, the tape with trapezoidal wings provides the highest Nusselt number, friction factor as well as thermal performance factor, followed by the one with rectangular.

2.2.2.7 Impact of twisted tape with slots, holes, cuts on the enhancement efficiency

Slots, holes and cuts in the twisted tape can induce disturbance and swirling into the bulk flow, disrupt the laminar low, and increase the Nu number and the heat transfer rate. It has been proved by several researchers that this enchantment technology will result in better heat transfer and fluid flow characteristics Murugesan et al (Murugesan et al., 2011) and Seemawute and Eiamsa-ard (Seemawute and Eiamsa-ard , 2010). Eiamsa-ard et al (Eiamsa-ard et al., 2010b) investigated the influences of peripherally-cut twisted tape insert on heart transfer and thermal performance characteristics in laminar and turbulent tube flows. They discovered these: 1) the peripherally-cut twisted tape offered higher heat transfer rate, friction factor and also thermal performance factor compared to the typical twisted tape; 2) an additional turbulence of fluid in the vicinity of the tube wall and vorticity behind the cuts generated by the modified twisted tape contribute to the better heat transfer enhancement; 3) Nusselt number, friction factor as well as thermal performance factor associated by the peripherally-cut twisted tape were found to be increased with the increase of the tape depth ratio (DR) or the decrease of the tape width ratio (WR).

Murugesan et al (Murugesan et al., 2011) carried out a study of the heat transfer and pressure drop characteristics of turbulent flow in a tube fitted with a full length twisted tape coupled with trapezoidal-cut. The results show that for the twist ratio of 6.0, the mean Nusselt number and fanning friction factor for the trapezoidal-cut twisted tape are 1.37 and 1.97 times over the plain tube, respectively. When the twist ratio reduces to 4.4, the corresponding Nusselt number and fanning friction factor will increased to 1.72 and 2.85

times. These indicate that trapezoidal-cut induces significant enhancement of heat transfer coefficient and friction factor, in addition the impact will be heavier for a lower twist ratio.

Meanwhile, Seemawute and Eiamsa-ard (Seemawute and Eiamsa-ard, 2010) studied the combined impact of peripherally-cut twisted tape with alternate axis (PT-A) on the thermohydraulics of turbulent flow through a round tube. Thermal performance in a tube fitted with PT-A are consistently higher than those in the tube equipped with PT, TT and also in the plain tube. The combined actions induced by the PT-A are responsible for the improvement of heat transfer rate and friction factor by around 50% to 184% and 6 to 11 times, respectively compared to those in the plain tube. Following the trapezoidal-cut and peripherally-cut, Murugesan et al (Murugesan et al., 2011) investigated the effect of V-cut twisted tape insert on heat transfer, friction factor and thermal performance factor characteristics in a circular tube were investigated. The V-cut twisted tape offered a higher heat transfer rate, friction factor and also thermal performance factor rather than the plain twisted tape; in addition, the impact of the depth ratio was more dominant than that of the width ratio for all the Reynolds number; the thermal performance factors for all the cases are more than one indicating that the effect of heat transfer enhancement due to the enhancing tool is more dominant than the effect of the rising friction factor and vice versa.

2.2.2.8 Impact of helical twisted tape on the enhancement efficiency

Helical twisted tape is another kind of developed twisted tape to enhance the heat transfer rate inside the tube or pipe heat exchangers. Ibrahim (Ibrahim, 2011) studied the heat transfer and friction factor characteristics in the horizontal double pipes flat tubes. With full length of helical screw element, different twist ratio and spacer length were researched. The study shows that, the Nusslet number (Nu) and friction factor (f) decrease with the increase of twist ratio(y) value of the flat tube. Furthermore, Moawed (Moawed, 2011) investigated thermal influence of helical twisted tape on the elliptic tubes at different twist ratios y and pitch ratios under laminar flow condition. The results indicate that the average Nusslet number increases with the increase of the Reynolds number and the decrease of twist ratio; the Nusslet number of the plain elliptic tube is greater than that of the plain circular tube and the Nu of elliptic tubes containing a helical screw tapes is better than that of the plain elliptic tubes for all Re, twist ratio.

Sivashanmugam et al (Sivashanmugam et al., 2007) studied circular tube fitted with right-left helical screw inserts of equal length, unequal length of different twist ratio and full-length helical screw element at different twist ratio. The results show that the heat transfer coefficient enhancement for right-left helical screw inserts is higher than that for straight helical twist at a given twist ratio. For full-length helical screw element there is no much change of the heat transfer coefficient enhancement by increasing or decreasing the twist ratio, as the magnitude of swirl generated at the inlet or at the outlet is the same in the both of two cases. Thianpong et al (Thianpong et al., 2009) is another investigator group of these interesting enhancement technologies. They found these:

- The heat enhancement in helical and left–right twisted tape collectors is better than the plain tube collector.
- While comparing the left–right and helical twisted tape collector at the same twist ratio of 3.0, higher heat transfer and thermal performance are obtained from the left–right twisted tape collector.
- The increase of heat transfer and friction factor in left–right twisted tape collector is 3.75 and 1.42 times higher than plain tube collector respectively. The solar water heater with left–right twisted tape presents better heat transfer and overall thermal performance than that with the helical twisted tape.

2.2.2.9 Impact of twisted tapes with granulated surfaces on the enhancement efficiency

This section introduced another heat transfer enhancement technology called modified twist tape surface. Eiamsa-ard et al (Eiamsa-ard et al., 2010 a)presents a technology combined the cut and granulation, which is willing to induce more flow turbulent and break down the laminar flow layer with the willing to achieve higher heat transfer rate. With the surface granulation idea, Thianpong, et al (Thianpong et al., 2009), studied the friction and compound heat transfer behaviors in a dimpled tube fitted with a twisted tape swirl generator. They also studied the effects of the pitch and twist ratio on the average heat transfer coefficient and the pressure loss. The results reveal that both heat transfer coefficient and friction factor in the dimpled tube fitted with the twisted tape, are higher than those in the dimple tube acting alone and plain tube. It is also found that the heat transfer coefficient and friction factor in the combined devices increase as the pitch ratio and twist ratio decrease.

Murugesan et al (Murugesan et al., 2010), introduced the nails to the surface as shown in the Table 2-1. The tape's surface roughness was increased heavily, which lead additional turbulence offered by the wire nails besides the common swirling flow generated by the plain twisted tapes (P-TT). This spurs the Nusselt number, friction factor and thermal enhancement factor in the tube with twisted tape consisting wire nails (WN-TT) are respectively 1.08 to 1.31, 1.1 to 1.75 and 1.05 to 1.13 times of those in tube with plain twisted tapes (P-TT).

Saha (Saha, 2010) studied the twisted-tape inserts with and without oblique teeth. The axial corrugations in combination with twisted-tapes of all types with oblique teeth have been found performing better than those without oblique teeth in combination with axial corrugations.

Numerical simulation is another method to study the enhancement of heat transfer of various twist tapes in laminar and turbulent flow both for water and air. Eiamsa-ard, et al (Eiamsa-ard et al., 2010 d) developed a 3-D numerical model to study the swirling flow and convective heat transfer in a tube induced by loose-fit twisted tape insertion. The results show that the twisted tape inserts for y=2.5 with CR(clearance ratio)=0.0 (tight-fit), 0.1, 0.2 and 0.3 can enhance heat transfer rates up to 73.6%, 46.6%, 17.5% and 20%. The heat transfer augmentation is expected to involve the swirl flow formation between the tape and a tube wall. Chiu and Jang (Chiu and Jang, 2009) investigated the thermal–hydraulic characteristics of air flow inside a circular tube with different tube inserts by 3-D numerical model verified by experimental testing. Three kinds of tube inserts were studied including the longitudinal strip inserts with and without holes, and twisted-tape inserts with three different twisted angles. The heat transfer and fluid flow performance were analysed by a 3D turbulence model with the consideration of conjugate convective heat transfer in the flow field and heat conduction in the tube inserts.

Guo et al (Guo et al, 2011) studied the heat transfer and friction factor characteristics of laminar flow in a circular tube fitted with center-cleared twisted tape. The researchers demonstrated that the flow resistance can be reduced by narrow-width and center-cleared twisted tapes, however, the thermal behaviours are very different from each other. For tubes with narrow-width twisted tapes, the heat transfer and thermohydraulic performance are weakened by cutting off the tape edge. Contrarily, for tubes with center-cleared twisted tapes, the heat transfer can be even enhanced in the cases with a suitable central clearance ratio. All these indicated that the center-cleared twisted tape is a promising technique for laminar convective heat transfer enhancement. Furthermore, Shabanian et al (Shabanian et al., 2011) built up a CFD model to predict and explain the turbulence intensity and heat transfer enhancement in an air cooler equipped with different tubes inserts. The results illustrate that the predicted turbulence intensity of butterfly insert is higher than the jagged insert in the whole tube area. This can be the reason that more heat transfer rate is obtained by the butterfly insert compared to the jagged insert.

2.2.3 Coiled wire

The helical inserts are new addition to the family of inserts for enhancement of heat transfer. For the helical taps, the swirl moves in one direction along the helical and induce swirl in the flow, which increase the retention time of the flow and consequently provide better heat transfer performance over twisted tape insets. The high heat transfer with helical inserts is also accompanied by a higher pressure drop across the flow, but at low Reynolds number, helical tapes are used in solar water heating applications to drive heat transfer benefit. However inserts of different configuration are being used to meet the needs of higher heat dissipation rates. Wire coil inserts are currently used in the applications such as oil cooling devices, pre heaters or fire boilers. They show several advantages in relation to other enhancement techniques:

- Simple manufacturing process with low cost.
- Easy installation and removal.
- Preservation of original plain tube mechanical strength.
- Possibility of installation in an existing smooth tube heat exchanger.

- Fouling mitigation (in refineries, chemical industries and marine application).

The impacts of coiled wire on heat transfer enhancement inside tube and pipe heat exchanger are studied by (Gararcia et al, 2005) and (Yakut and Sahin, 2004). The vortex characteristics of tabulators, heat transfer rate and friction characteristics were considered as the criterions to evaluate the enhancement performance of coiled wire. Gararcia et al (Gararcia et al, 2005) experimentally studied the helical-wire-coils fitted inside a round tube in order to characterize their thermohydraulic behavior in laminar, transition and turbulent flows. Results have shown that, in laminar flow, wire coils behave as a smooth tube but accelerate transition to critical Reynolds numbers down to 700.

At the low Reynolds numbers about Re ≈700, transition from laminar to turbulent flow occurs in a gradual way. Within the transition region, heat transfer rate can be increased up to 200% when keep the pumping power constant. Wire coils have a predictable behavior within the transition region since they show continuous curves of friction factor and Nusselt number, which involves a considerable advantage over other enhancement techniques.

In turbulent flow, wire coils cause a high pressure drop which depends mainly on the pitch to wire-diameter ratio (p/e). In turbulent flow, the pressure drop and heat transfer are both increased by e up to nine times and four times respectively, compared to the empty smooth tube.

Therefore, it can be concluded that the wire coils do not cause obvious pressure drop and heat transfer rate increase, but induces the flow transition at a critical low Reynolds numbers at about 700. For pure turbulent flow, it can be stated that Prandtl number does not exert an influence on heat transfer augmentation. On the contrary, when working with high Prandtl number fluids within the transition region, wire coils produce the highest heat transfer increase. Meanwhile, the wired coils offer their best performance within the transition region where they present a considerable advantage over other enhancement techniques.

Following the pervious researches, Promvonge et al (Promvonge et al., 2008 a, b, c and d) experimentally studied the effects of wires coils with different square cross sections; coiled wires in conjunction with a snail-type swirl generator mounted at the tube entrance; wire coils in conjunction with twisted tapes used as a turbulator; and combined devices of the twisted tape (TT) and constant/periodically varying wire coil pitch ratio.

For the wires with square cross section, the Nusselt number augmentation tends to decrease rapidly with the rise of Reynolds number [40]. If wire coils are compared with a smooth tube at a constant pumping power, an increase in heat transfer is obtained, especially at low Reynolds number. Although fairly large differences have been observed among the analyzed coil wires, their evaluated performances are quite similar under the condition of Re = 5000, heat transfer enhancement efficiency (η) ≈ 1.2~1.3 and Re = 25,000, η≈1.1~1.15. Therefore, the coiled square wire should be applied to obtain a higher thermohydraulic performance, but it will lead more compact heat exchanger construction.

The use of the coiled wires in conjunction with a snail-type swirls generator results in a high increase of the pressure drop but provides considerable heat transfer augmentations. The heat transfer enhancement ratio is from 3.4 to 3.9, and the Nusselt number augmentation tends to decrease with the rise of Reynolds number (Promvonge et al., 2008 a).

The best operating regime for combined turbulators is at lower Reynolds number and the lowest values of the coil spring pitch and twist ratio. Similar with the coiled wires used in reference (Promvonge et al., 2008 b), the Nusselt number augmentation tends to decrease with the rise of Reynolds number. Comparing the combined turbulators consisted of wire coil and twisted tape with a smooth tube at a constant pumping power, a double increase in heat transfer performance is obtained especially at low Reynolds number.

Then Promvonge et al (Promvonge et al., 2008 c) investigated the combined devices consisted of the twisted tape (TT) and constant/periodically varying pitch ratio of the wire coil. They found that, at low Reynolds number, the device combined with TT at twist ratio of 3.0 and the DI-coil, provided the highest thermal performance which was around 6.3%, 13.7%, 2.4% and 3.7% higher than the wire coil alone, the TT alone, the TT with uniform wire coil, and the TT with D-coil, respectively.

Except the Promvonge's group, another two groups Gunes et al (Gunes et al., 2010) and Akhavan-Behabadi et al (Akhavan-Behabadi et al., 2010) also investigated the thermohydraulic behavior of coiled wires in tube and pipe heat exchangers in 2010. Gunes et al (Gunes et al., 2010) experimentally investigated the coiled wire inserted in a tube for a turbulent flow regime. The coiled wire has equilateral triangular cross section and was inserted separately from the tube wall. They discovered that the Nusselt number rises with the increase of Reynolds number and wire thickness, and the decrease of pitch ratio; the best operating regime of all coiled wire inserts is detected at low Reynolds number, which leads to more compact heat exchanger; the pitch increases, the vortex shedding frequencies decrease and the maximum amplitudes of pressure fluctuation of vortices produced by coiled wire turbulators occur with small pitches.

Meanwhile, Akhavan-Behabadi et al (Akhavan-Behabadi et al., 2010) investigated seven coiled wires with pitches from 12 mm to 69 mm, and wire diameters of 2.0 mm and 3.5 mm. These coiled wires are inserts inside a horizontal tube for heating the engine oil. The results show that the rise in fanning friction factor f due to the 2.0 mm thickness of the coiled wire insert for the Reynolds numbers less than 500. For Reynolds numbers higher than 500, the reduction in coil pitch causes an increase of the fanning friction factor.

Muñoz-Esparza and Sanmiguel-Rojas (Muñoz-Esparza and Sanmiguel-Rojas., 2011) employing the CFD simulation package investigated the heat transfer and fluid flow performance inside a round pipe with the helical wire coils inserts. They found that the friction factor becomes constant in the Re range of 600 ~ 850. The effect of the pitch on the friction factor has been addressed by performing a parametrical study with a pitch-periodic computational domain for wire coils within the dimensionless pitch range (p/d), $1.50 \leq p/d \leq 4.50$, and dimensionless wire diameter, $e/d = 0.074$, showing that the increase of p/d, decreases the friction factor.

Solanoa et al (Solanoa et al., 2012) used CFD to study the effect of helical wire on the enhancement of heat transfer in pipe subjected to uniform heat flux and laminar the flow. The results show that during the deceleration period of both oscillating semi-cycles, laminar eddies grow downstream of the wire and spread along the next helical pitch, promote radial mixing.

2.2.4 Swirl generators

Swirl flows have wide range of applications in various engineering areas such as chemical and mechanical mixing and separation devices, combustion chambers, turbo machinery, rocketry, fusion reactors, pollution control devices, etc. The utilization of swirl flows may lead to the heat and mass transfer enhancements. Problems of heat and mass transfer in swirl pipe flows are the practical importance in designing different heat exchangers, submerged burners, heat transfer promoters and chemical reactors.

Swirl flows result from an application of a spiral motion, a swirl velocity component (also called as ‘tangential’ or ‘azimuthal’ velocity component) being imparted to the flow by the use of various swirl-generating methods. Many researchers have studied the heat transfer characteristics of swirl flows by using various swirls. Generally, the swirling pipe flows are classified into two types: i) Continuous swirl flows, which maintain their characteristics over entire length of test section; and ii) decaying swirl flows. Additional difference in properties of swirl flows is related with the rate of swirl intensity.

This traditional classification of swirl flows is not sufficient for explanation of the heat and mass transfer in swirl flows. From the hydrodynamic point of view, the major problem is an incomplete understanding of the swirl flow parameters. Swirl flow is usually referred to a vortex structure with a central vortex core and an axial velocity component. Recent progress in study of these vortex structures reveals the direct relation between the type of vortex symmetry (left- or right-handed symmetry) and the appearance of swirl flows with jet-like or wake-like. In radial guide vane swirl generators, the flow direction changes from the radial direction to the axial direction

Yilmaz et al (Yilmaz et al., 2003) studied the effect of the geometry of the deflecting element in the radial guide vane swirl generator on the heat transfer and fluid friction characteristics in decaying swirl flow. The results show that an augmentation up to 150% in Nusselt number relative to that of the fully developed axial flow was obtained with a constant heat flux boundary condition. The exact segmentation depends upon the vane angles, Reynolds numbers and types of the swirl generators. They observed that the swirl generator with no deflecting element presented the highest Nusselt numbers and also the highest pressure drop in both the swirl generator and the tested pipe; the swirl generator with no deflecting element may be advantageous in terms of heat transfer enhancement and energy saving in comparison with swirl generators with a deflecting element; in swirling flow, increasing the Reynolds number and the vane angle increased the Nusselt number; to obtain lower pumping powers for the same heat transfer rate, higher vane angles and relatively lower Reynolds numbers must be employed.

A vortex generator with propeller-type geometry to produce swirl flow in a horizontal pipe was investigated by Sarac and Bali (Sarac and Bali, 2007). The heat transfer and pressure drop characteristics of decaying swirl flow through a circular pipe with a vortex generator were studied. They discovered that the Nusselt numbers increased from 18.1% to 163% which depends on the Reynolds number, the position of the vortex generator, the angle and the number of the vanes; with the decaying of the swirl flow, the heat transfer and pressure drop decreased gradually away from the axial; the inserts with six vanes resulted in more heat transfer values than those with four vanes.

Kurtbaş et al (Kurtbaş et al., 2009) devised a novel conical injector type swirl generator (CITSG) and experimentally examined the performances of heat transfer and pressure drop in a pipe with the CITSG. Moreover, circular holes with different numbers (N) of conical and cross-section areas (Ah) are drilled on the CITSG. They found that the Nu decreases with the increase of Reynolds number, the director angle (β), the director diameter (d), and with the decrease of the CITSG angle (α); the effect of the β on Nu_x is at negligible level for higher Re.

Eiamsa-ard et al (Eiamsa-ard et al, 2009) studied the heat transfer, friction loss and enhancement efficiency behaviors in a heat exchanger tube equipped with propeller type swirl generators at several pitch ratios (The swirl generator is used to create a decaying swirl in the tube flow). The results indicate that the use of the propeller leads to maximum enhancement efficiency up to 1.2. Thus, because of strong swirl or rotating flow, the propellers and their blade numbers become influential upon the heat transfer enhancement. The increase in friction factor from using the propeller is found to be 3~18 times over the plain tube. The heat transfer and the enhancement efficiency are found to increase with increasing the blade number (N) and the blade angle (θ) but to decrease with the rise of pitch ratio. Depending on Reynolds numbers, the increases in heat transfer rate are about 113%, 90%, and 73% above the plain tube, for PR=5.0, 7.0, and 10.0, respectively.

Yang et al (Yang et al., 2011) studied the heat transfer process of swirling flow issued into a heated convergent pipe with a convergent angle of 5° with respect to the pipe axis as shown in the Tables 2-5, 2-6, 2-7, 2-8, 2.9 and 2-10. A flat vane swirler situated at the entrance of the pipe is used to generate the swirling flow. The results show that the convergence of the pipe can accelerate the flow which has an effect to suppress the turbulence generated in the flow and reduce the heat transfer. However, in the region of weak swirl ($S = 0 \sim 0.65$), the Nusselt numbers increase with the increase of swirl numbers until $S = 0.65$, where the turbulence intensity is expected to be large enough and not suppressible. In the region of strong swirl ($S > 0.65$), where recirculation flow is expected to be generated in the core of the swirling flow, the heat transfer characteristic can be altered significantly. At very high swirl value ($S \geq 1.0$), the accelerated flow in the circumferential direction is expected to be dominant, which leads to suppress the turbulence and reduce the heat transfer.

Martemianov and Okulov (Martemianov and Okulov, 2004) developed a theoretical model of the heat transfer in the axisymmetric swirl pipe flows. The influences of vortex symmetry and vorticity distribution at the vortex core on the heat transfer enhancement were studied. The study shows that there are two types of vortex structures existing in the swirl flows with the same integral characteristics: vortices with left-handed helical symmetry and vortices with right-handed helical symmetry. The left-handed helical vortexes generate wake-like swirl flows and increase the heat transfer in comparison with the axial flow. Right-handed vortex structures generate jet-like swirl flows and can diminish heat transfer. The authors concluded that there are two major factors influencing the heat transfer enhancement: formation of the swirl flow with left hand helical vortex and modification of the near wall velocity profile of the inviscid flow due to the different vorticity distribution in the vortex core.

2.2.5 Conical ring

Promvonge (Promvonge, 2008d) studied different type of shapes and configuration of conical ring, conical ring integrated with twisted tape, conical-nozzles combined with swirl generator, free-spacing snail entry together with conical-nozzle turbulators, converging nozzle with different pitch ratios (PR), diverging nozzle arrangement, converging nozzle arrangement, V-nozzle turbulators, diamond-shaped turbulators in tandem arrangements. In 2006, Promvonge's research group found that the heat transfer in the circular tube is enhanced by the conical-nozzles combined with swirl generator, but induced higher energy loss of the fluid flow, which can be reduced at low Reynolds number. Therefore the applications of this kind of turbulators are more effectively at low Reynolds number rather than high Reynolds number. The same year, this group also investigated the impact of V-nozzle turbulators on heat transfer. The enhancement efficiency decreases by increasing the Reynolds number. The maximum enhancement efficiency obtained by using the V-nozzle with a PR value of 2.0, 4.0, and 7.0, are found to be 1.19, 1.14, and 1.09, respectively.

The enhancement efficiency increases as the pitch decreases and it generally will be lower at high Reynolds number for all pitches. Four more similar researches were carried out by Promvonge et al in 2007, they found these:

i) Inserts combined conical-ring and twisted-tape the enhancement efficiency tends to decrease with the rise of Reynolds number and to be nearly uniform for Reynolds number over 16,000. The larger the heat transfer and friction factor for all Reynolds numbers can be achieved at a smaller twist ratio; ii) C-nozzle turbulators and a snail with free-spacing entry can be employed effectively at low Reynolds number or in places where pumping power are not important but compact sizes and ease manufacture process are needed; iii) Despite very high friction, the conical-nozzle turbulators can be applied effectively in places where pumping power is not significantly taken into account but the compact size, ease of manufacture and installation are required; iv) V-nozzle alone provides the best thermal performance over other nozzle turbulator devices.

In 2008, Promvonge et al confirmed again the substantial increase in friction factor. Therefore, a diamond-shaped element is introduced into the turbulent tube flows by Promvonge et al (Promvonge et al., 2010). The heat transfer rate increase with the increasing of the cone angle and decreasing of the tail length ratio, which induces higher turbulence intensity imparted to the flow between the turbulators and the heating wall. Meanwhile, the turbulators are placed directly into the flow core causing high friction losses because of the high flow blockage.

Anvari et al (Anvari et al., 2011) studied the impact of conical ring inserts in transient regime. The insertion of turbulators has significant effect on the enhancement of heat transfer, especially the DR (Divergent rings) arrangement, and also increase the pressure drop. So tabulators can be used in places where the compact size is more significant than pumping power.

Kongkaitpaiboon et al (Kongkaitpaiboon et al., 2010) studied experimentally the influences of the PCR (perforated conical-rings) on the turbulent convective heat transfer, friction factor, and thermal performance factor. It is found that the PCR considerably diminishes the development of thermal boundary layer, leading to the heat transfer rate up to about 137% over that in the plain tube. Evidently, the PCRs can enhance heat transfer more efficient than the typical CR on the basis of thermal performance factor of around 0.92 at the same pumping power.

2.2.6 Ribs

Ribs are another technology enhancing the heat transfer rate. The heat transfer performances in discrete double-inclined ribs tube (DDIR-tube) were numerically and experimentally investigated by Meng et al (Meng et al., 2005) FLUENT 6.0 was used to solve the field synergy equation numerically. Numerical solution of the field synergy equation of laminar convection heat transfer in a straight circular tube together with other governing equations indicates that the multi-longitudinal vortex flow is the best way for heat transfer enhancement in laminar convection in tubes. The flow field of the DDIR-tube is similar to the optimal velocity field. The experimental results show that the DDIR-tube has better comprehensive heat transfer performance than the current heat transfer enhancement tubes. The present work indicates that new heat transfer enhancement techniques could be developed according to the optimum velocity field. Therefore the comprehensive performances of enhanced laminar heat transfer in DDIR-tube are better than that of the currently-known enhancement techniques.

Naphon et al (Naphon et al., 2006) experimentally studied the heat transfer and pressure drop characteristics in horizontal double pipes with helical ribs. Nine test sections with different characteristic parameters of: helical rib height to diameter, v/d = 0.12, 0.15, 0.19, and helical rib pitch to diameter, p/d = 1.05, 0.78, 0.63 are tested. The results show that the helical ribs have a significant effect on the heat transfer and pressure drop augmentations. The pressure drop across the tube with helical rib is produced by: i) drag forces exerted on the flow field by the helical rib, ii) flow blockage due to area reduction, iii) turbulence augmentation and4) rotational flow produced by the helical rib.

Li et al (Li et al., 2009) experimentally and numerically studied the turbulent heat transfer and flow resistance in an enhanced heat transfer in Discrete Double Incline Ribs (DDIR) tube. The results show that the heat transfer in the DDIR tube is enhanced from 100 to 120% contrasted with a plain tube and the pressure drop is increased from 170% to 250%. The heat transfer rate at the same pumping power is enhanced by 30 to 50%. The numerical simulations solved the three dimensional Reynolds-averaged Navier–Stokes equations with the standard k-e model in the commercial CFD code, Fluent. The numerical results agree well with the experimental data, with the largest discrepancy of 10% for the Nusselt numbers and 15% for the friction factors. Visualization of the flow field shows that in addition to the front and rear vortices around the ribs, main vortices and induced vortices are also generated by the ribs in the DDIR tube. The rear vortex and the main vortex contribute much to the heat transfer enhancement in the DDIR tubes.

Eiamsa et al (Eiamsa et al., 2008) investigated the louvered strips inserted in a concentric tube heat exchanger in 2008. The louvered strip was inserted into the tube to generate turbulent flow which helped to increase the heat transfer rate of the tube. Experimental results confirmed that the use of louvered strips leads to a higher heat transfer rate over the plain tube. The use of the louvered strip with backward arrangement leads to better overall enhancement ratio than that with forward arrangement around 9% to 24%.

Depaiwa et al (Depaiwa et al., 2010) experimentally studied the turbulent airflow through channel solar air heater with rectangular winglet vortex generator (WVG). The results present that the solar air heater channel with rectangular WVG provides significantly higher heat transfer rate and friction loss than the smooth wall channel. The use of larger attack angle value leads to higher heat transfer rate and friction loss than that of lower one. Chompookham et al (Chompookham et al., 2010) experimentally investigated the effect of combined wedge ribs and winglet type vortex generators (WVGs) in 2010. They used two types of wedge (right-triangle) ribs pointing downstream and upstream to create a reverse flow in the channel. The arrangements of both rib types placed inside the opposite channel walls are in-line and staggered arrays. The results show that the combined ribs and the WVGs show the significant increase in heat transfer rate and friction loss over the smooth channel.

Two more projects were published by Promvonge et al (Promvonge et al., 2010 and 2011). They experimentally studied the effects of combined ribs with delta-winglet type vortex generators (DWs) and integrated ribs with winglet type vortex generators (WVGs) on forced convection heat transfer and friction loss behaviours for turbulent airflow through a solar air heater channel. Results show that the Nusselt number and friction factor values for combined rib with DW are much higher than those for the rib/DW alone and have significant effect of the presence of the rib turbulator and the WVGs on the heat transfer rate and friction loss over the smooth wall channel. The values of Nusselt number and friction factor for utilizing both the rib and the WVGs are found to be considerably higher than those for using the rib or the WVGs alone.

Table 2-5 Configuration sketches of various swirl generators

Table 2-6 Experimental works on the thermohydraulic performance of swirl generators enhancement

Table 2-7 Experimental works on the thermohydraulic performance of conical rings enhancement

Table 2-8 Configuration sketches of various swirl conical ring

Table 2-9 Configuration sketches of insert ribs

Table 2-10 Experimental works on the thermohydraulic performance of insert ribs enhancement

2.3 Phase Change Materials (PCMs)

2.3.1 Thermal management using phase change materials

The operation of devices which generate heat requires a means by which the excess heat can be removed, as their reliability, durability, safety and performance depend significantly on temperature. This demand creates the need for efficient thermal management technologies. A number of factors influence the choice of cooling methodology used including: space, operating environment, heat dissipated, cost of materials and maintenance required (Mahmoud et al., 2013).

Of the several mesoscale technologies that have long been explored and practiced, the use of phase change materials (PCMs) is a passive cooling option (Fan et al., 2013), when PCMs is incorporated into traditional active cooling heat sinks to improve their performance by taking advantage of the thermal energy stored as latent heat (of fusion) upon melting.

The PCM for a particular application is selected such that the melting temperature of the PCM should be below than the maximum operating temperature of the device. The high latent heat of fusion of the PCMs is an important advantage that is helpful in achieving high storage density. Cycling stability makes the PCM suited for repeated use (Baby and Balaji., 2014).

The low thermal conductivity of most PCMs presents a significant challenge in the design of PCM-based electronic cooling systems. In order to overcome this drawback, researchers have proposed various heat transfer enhancement techniques, e.g., use of partitions/fins, graphite/metal matrices, dispersed high-conductivity particles in the PCM, multiple PCMs (Kandasamy et al., 2008)

Nayak et al (Nayak et al., 2006) carried out some basic studies to model the thermal performance of heat sinks with phase change materials and thermal conductivity enhancers. Three types of TCEs are studied, namely porous matrix, plate-type fins and rod-type fins. The results show that inserting aluminum matrix into Eicosane can offer an order-of-magnitude increase in thermal conductivity for the case of PCM with porous TCE matrix and the performance of the heat sink improves if the TCE material is distributed in the form of thinner fins.

Wang et al (Wang et al., 2008) have developed 2D conjugated computational model to study the hybrid PCM-based heat sinks. The results indicate that inclusion of PCM in the base heat sink will increase the thermal performance of the hybrid system under free convection conditions. Furthermore, constant and pulsed temperature difference between the input boundary temperature and melting point of the PCMs, aspect ratio, and various PCM properties are critical factors to affect the performance.

Dong-won and Yoo (Dong-won and Yoo, 2004) have simulated the transient loads of heat sink electronic components incorporating PCMs, the results of this study indicated that PCMs can potentially provide both energy savings for thermal management devices such as electric cooling fans, as well as size reduction of thermal management devices such as heat sinks.

2.3.2 Thermal energy storage

The use of a latent heat storage system using phase change materials (PCMs) is an effective way of storing thermal energy and has the advantages of high-energy storage density and the isothermal nature of the storage process (Sharma et al., 2009). For example, among the practical problems involved in solar energy systems is the need for an effective means by which the excess heat collected during periods of bright sunshine can be stored, preserved and later released for utilization during the night or other periods (Hasnain, 1998).

In the same time adding a PCM module at the top of the water tank in solar energy systems would give the system higher storage density, and compensate heat loss in the top layer, improve systems thermal stratification and reuse of waste heat (Mehling et al., 2003).

De Gracia et al (De Gracia et al., 2011) have used encapsulated phase change materials to improve thermal performance of domestic hot water cylinder. The increment in the thermal energy storage capacity of the system allows the use of low cost electricity during low peak periods.

Nabavitabatabayi et al (Nabavitabatabayi et al., 2014) have carried out numerical simulation to investigate the impact of operational and design parameters of using PCMs on the thermal performance of hot water tank. The simulation results demonstrate that the integration of enhanced PCMs to the hot water tank could shift the power demand to the off-peak for a longer period of time compared to pure PCMs due to the higher thermal conductivity and the enhanced heat transfer rate.

Nkwetta et al (Nkwetta et al., 2014) have concluded that the addition of PCM module into a hot water tank increases the amount of energy stored and this energy is directly proportional to the amount of PCM and using PCM in HWTs (Hot water tanks) increase energy savings and hot water discharging time. The combination of PCM in the HWT and the application of a control strategy can help to reduce the heating elements time thus reducing the energy consumption.

2.4 Fundamental Principles of Ohmic Heating

2.4.1 History

Ohmic heating concept is not new; it was used in the early 20th century where electric pasteurization of milk and other food materials was achieved by pumping the fluid between plates with a voltage difference between them (De Alwis et al., 1990) and (Palaniappan et al., 1991). Six states in the United States had commercial electrical pasteurizers in operation (Sastry and Palaniappan, 1992). In the design of Mc Connel and Olsson (Mcconnel et al., 1938) frankfurter sandwiches were cooked by passing through electric current for a predetermined time. Schade (Schade, 1951) described a blanching method of preventing the enzymatic discoloration of potato using Ohmic heating. It was thought at that time that lethal effects could be attributed to electricity. The technology virtually disappeared in succeeding years apparently due to the lack of suitable inert electrode materials and controls. Since that time, the technology has received limited interest, except for electro conductive thawing (De Alwis and Fryer, 1990). Within the past two decades, new and improved materials and designs for Ohmic heating have become available. The Electricity Council of Great Britain has patented a continuous-flow Ohmic heater and licensed the technology to APV Baker (Skudder, 1988).The particular interest in this technology stems from ongoing food industry interest in aseptic processing of liquid-particulate foods. Conventional aseptic processing systems for particulates rely on heating of the liquid phase which then transfers heat to the solid phase. Ohmic heating apparently offers an attractive alternative because it heats materials through internal heat generation.

2.4.2 Principles

An Ohmic heater also known as a joule heater is an electrical heating device that uses a liquid's own electrical resistance to generate the heat. Heat is produced directly within the fluid itself by Joule heating as alternating electric current (I) is passing through a conductive material of resistance (R), with the result energy generation causing temperature rise (Zell et al., 2009) Figure 2-1 illustrates the principles of Ohmic heating.

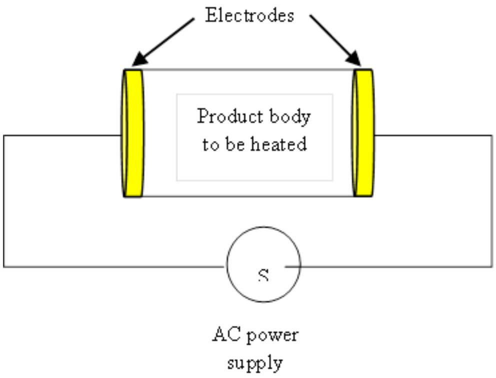

Figure 2-1 Schematic diagram illustrate the principle of Ohmic heating

The most commonly used heating techniques for liquids rely on heat transfer from a hot surface. This heat can be generated directly via an electrical heating element or indirectly from a hot medium (e.g. steam) via a heat exchanger (e.g. shell and tube, plate). These methods require a temperature gradient to transfer heat to the process liquid and as such the surfaces are at a higher temperature than the product. This can cause fouling of the surfaces for certain products which become burnt onto the hot surfaces reducing heat transfer rates and adversely affecting the product. A further issue with heat transfer is found when heating very viscous fluid and fluids with particulates where effective, even heat transfer is difficult to achieve. Ohmic heaters address the aforementioned problems by removing hot surfaces from the heating of the fluids.

2.4.3 Important definitions terms commonly used in Ohmic heating

2.4.3.1 Electrical conductivity

The electrical conductivity (σ) is a measure of how well a material accommodates the movement of an electric charge. It is the ratio of the current density to the electric field strength. Its SI derived unit is the Siemens per meter (s/m), for any material the electric conductivity can be calculate from the following equation (Zell et al., 2009), (Assiry et al., 2003) and (Salengke and Sastry, 2007).

$$\sigma = \frac{X}{A}\frac{I}{V} \tag{2.2}$$

Electrical conductivity of any sample is not constant and it is dependent on the material temperature (normally linearly) and it is increase with increased of the material temperature, the constant of the dependent electric conductivity relations for different electrical field strengths and concentrations are obtained using linear regression analysis using the following equation (Zell et al., 2009), (Tulsiyan et al., 2009) and (Castro et al., 2004):

$$\sigma_T = \sigma_i + n.T \tag{2.3}$$

Electric conductivity is a crucial factor in Ohmic heating, many different researchers reported the electric conductivity for different materials includes fresh fruits under Ohmic heating such as apple, pineapple, pear, strawberry and peach which their electric thermal conductivity in the range from (0.05 to 1.2) S/m (Assiry et al., 2010) and (Nguyen et al., 2013), pure water has poor electric conductivity and it is around 0.055μS/cm. The ions in solution control electric current transport, collection of electric conductivity for different material are listed below in Table. 2-11:

Table 2-11 Electric conductivity data for a range of different materials which have been heated successfully by the Ohmic heating

Material type	**Electric conductivity at 25 ^oC, S/m**
Beer	0.143
Black Coffee	0.182
Coffee with milk	0.357
Apple Juice	0.239
Chocolate 3% fat Milk	0.433
Tomato Juice	1.697
Sea water(TDS=44.00 mg/L)	5.8
Sea water(TDS=58.26 mg/L)	6.78
Sea water(TDS=57.78 mg/L)	6.75
Sea water(TDS=62.82 mg/L)	7.2
Meat(Pork)	0.64-0.86

2.4.3.2 Heating power

The energy (P) given to the Ohmic heating system to prescribed temperature are calculated by using the current (I) and voltage (ΔV) values during heating time (Δt) (Icier and Ilicali, 2005).

$$P=\sum VI\Delta t \tag{2.4}$$

2.4.3.3 Heating Rate

Due to the passing electrical current through the heating sample, a sensible heat is generated causing the temperature of the sample rise from T_i to T_f , the amount of heat give to the system can be calculate from the following equation

$$Q=m\ C_p\ (T_f-T_i) \tag{2.5}$$

2.4.3.4 Energy Efficiency

To evaluate performance of the heating process by using Ohmic heating method, the energy efficiency are calculated and evaluated. Energy efficiency is defined as (Nguyen et al., 2013).

$$\text{Energy Efficecny} = \frac{\text{Enery utilized to heat the sample}}{\text{Total input energy}} = \frac{\text{m cp } (T_f - T_i)}{\sum \text{VI } \Delta t} \tag{2.6}$$

2.4.4 Cons and pros of Ohmic heating

Comparative summary of the relative pros and cons identified for the Ohmic heating technologies as applied in different industry application are provided in Table 2-12. There are advantages and disadvantages should be considered depending on the purpose and objectives for considering heating application (Assiry et al., 2003 and 2010).

Table 2-12 Summarizing advantages and disadvantages of Ohmic heating

Advantages	Disadvantages	Suggestions for improvement
1. Temperature required achieved very quickly. 2. Rapid uniform heating of liquid with faster heating rates. 3. Reduced problems of surface fouling. 4. No residual heat transfer after shut off of the current. 5. Low maintenance costs and high energy conversion efficiencies. 6. Instant shutdown of the system. 7. Reduced maintenance costs because the lack of moving parts. 8. A quiet environmentally friendly system. 9. Reducing the risk of fouling on heat transfer surface.	1. Lack of generalized information. 2. Requested adjustment according to the conductivity of the dairy liquid. 3. Narrow frequency band. 4. Difficult to monitor and control. 5. Complex coupling between temperature and electrical field distribution.	1. Develop predictive, determinable and reliable models of Ohmic heating patterns. 2. Further research should be conducted to develop a reliable Feedback control to adjust the supply power according to the conductivity change of the dairy liquid. 3. Developing real-time temperature monitoring techniques for locating cold-spots and overheated regions during Ohmic heating. 4. Developing of adequate safety and quality-assurance protocols in order to commercialization Ohmic heating technology.

Since Ohmic heating use electrical energy, a comparison of Ohmic heating with other heating methods (such as heat pump heating, heat-resistance heating and microwave heating)was concluded in Table 2-13 .It is clear that Ohmic heating method is one of the efficient ways in heating applications.

Table 2-13 Comparison between Ohmic heating with other heating methods

	Principle	**Efficiency**	**Heating material**	**Operating parameters**
Ohmic heating	An electric current is passed through the heating sample, resulting in a temperature rise due to the conversion of the electric energy into heat	Provided 82–97% of energy saving while reducing the heating times by 90–95% compared to conventional heating (Castro et al., 2004). Energy efficiency close to 100% and uniform temperature distribution (Nguyen et al., 2013)	Liquid Solid Liquid Solid	Electrical conductivity pH of heating sample Voltage gradient
Heat resistance heating	An electric current flowing through a resistor converts electrical energy into heat energy	Converts nearly 100% of the energy in the electricity to heat	Liquid Solid Liquid Solid Gas	Depends on conductive, convective and radiative heat transfer coefficients

2.4.5 Ohmic heater design

Ohmic heating system contains at least two or more electrodes to impart current upon the fluid, electrode especially is a critical factor when designing Ohmic heating equipment, there are different designs depends on the electrodes locations and positions, the design can be set up either as static systems in container vessel or with continuous flow through them (Icier and Ilicali, 2005).

Basically, there are two widely design of Ohmic heating system, open geometry which makes clearing easier and reduce the effect of fouling and prevents damage to products (Simpson, 1994).

2.4.5.1 Electrode arrangement

Ohmic heater electrodes are typically arranged in one of four different configurations which optimize the operation.

2.4.5.1.1 Parallel plate configuration (transverse configuration)

Most suitable for low conductivity fluids (<5 S/m) and also offers a benefit where there are large solids particles with minimal shear force due to the completely unrestricted flow channel (Simpson, 1994). The electric field uniformity is optimized in this geometry improving even heating. The design can usually operate at standard voltages (e.g. 240V or 415V) as shown in Figure (2-2/a).

2.4.5.1.2 Parallel rod design

Typically used where considerations cost are paramount such as waste slurries. The design is much less expensive to construct than parallel plates or Collinear designs, but provides less even heating of the medium. As a result the fluid often must be mixed after heating to even out the temperature, reducing its suitability for heating solids without causing damage to them as shown in Figure (2-2/b).

2.4.5.1.3 Collinear design

Better option for high conductivity offering wider electrode spacing. The electrodes position can be in the fluid stream or as collars around a pipe which provides a fully unrestricted flow channel. For most applications this design requires a higher voltage than the parallel plate. Also the current distribution is less even and areas of high current density found at the leading edges of the electrodes can produce localized boiling and arcing as shown in Figure (2-2/c).

2.4.5.1.4 Staggered rod arrangement

A low cost option but can provide more even heating than the parallel rod design as shown in Figure (2-2/d).

Figure 2-2 Typical electrode arrangements in flow through Ohmic heating

2.4.5.2 Electrode design

Selection of suitable electrode to be used in an Ohmic heating is an important parameter that has to be considered (Assiry et al., 2010), (Samaranayake and Sastry, 2005), (Sarkis et al., 2013 a,b) and (Zell et al., 2011). Previous designs attempted to use different conductive electrode materials such as titanium, stainless steel, platinised-titanium, aluminum and graphite, electrodes are usually selected based on price and correction resistance which may affect the efficiency of the Ohmic heater, when the product quality is not essential such as waste treatment, low carbon electrodes are often employed, for high product quality applications metals such as stainless steel are preferred, in the same time the frequency of the power supply must be increased significant to prevent corrosion and apparent metal dissolution (Stancl and Zitny., 2010).

2.4.6 Important parameters of Ohmic heating

2.4.6.1 Electric conductivity

One of the most important parameter in Ohmic heating process is electric conductivity of the heating sample, because it depends on the temperature, frequency, concentration of electrolytes and applied voltage gradient (Assiry et al., 2006).The presence of ionic substances such as acids and salts increase conductivity, while the presence of no polar constituents like fata and lipids decreases it.

2.4.6.2 Current, voltage and applied Voltage

Icier (Icier , 2012), mentioned that current density which is the ratio between the current and electrode surface area is important to calculate the critical current density which are used in the design of the electrode dimension.

Voltage gradient used has effect on Ohmic heating times (Icier and Ilicali, 2002), the heat generation per unit time increase as the voltage gradient increases, that because the resistance of the heating sample to the current passing through it for any power applied is related to the heating sample composition and its electric conductivity (Zhu et al., 2010) and (Wang and Sastry, 1993.a, b).

2.4.6.3 Temperature

Electric conductivity of the heating sample is dependent on the temperature however in Ohmic heating; the work material temperature is changing very fast. Feedback control should be used to adjust the power applied during heating. Zell et al (Zell et al., 2009) has developed new thermocouple probes to monitor temperature changes during Ohmic heating; they found that, a triple-point probe is most satisfactory thermocouple for Ohmic heating applications. Marra et al (Marra et al., 2009) and Ye et al (Ye et al., 2004) have developed mathematical models to analyse and estimate heat transfer and temperature distributions during Ohmic heating. The designed models could be used to optimize the cell shape and electrode configurations.

2.4.6.4 Frequency

Waveform and frequency of applied voltage have effect on the electric conductivity values and the process of heating samples. In food industry, Lima et al (Lima and Sastry, 1999) reported that when the frequency of heating sample increased from 50.0 to 10000 Hz, the time required for the heating sample to reach 80 ^{o}C increased approximately sixfold. Amatore et al(Amatore et al., 1998), reported that conventional Ohmic heating under typical low frequency alternative current 50 to 60 Hz, could cause oxygen and hydrogen evolution due to the electrolysis of water. References (Zell et al., 2011), (Samaranayake and Sastry, 2005), (Castro et al., 2004), (Fryer et al., 1993), (Murphy et al., 1991), (Zhu et al., 2010), (Jakób et al., 2010) and (Tumpanuvatr and Jittanit, 2012) have used frequency varies from 50~60 Hz. Thus, attention needs to be paid to study the effect of frequency on Ohmic heating performance.

2.4.6.5 Flow properties

Total solid content (TDS), viscosity, acidity and alkalinity of the heating sample have effect on the Ohmic heating rate, Ghnimi et al (Ghnimi et al., 2008), have evaluated the Ohmic heating performance for highly viscous liquids, they reported that, higher viscous fluids tend to result in faster Ohmic heating than lower viscosity fluids. Others report vice versa .that conflict may due to different reactions occurring during Ohmic heating depending on their composition (Icier, 2012). Haldren et al (Haldren et al., 1990) have mentioned that pure water is not a good conductor of electricity and it has a conductivity of 0.055µS/cm. that because ions in solution is not helping electric current to transports.

2.4.7 Applications of Ohmic heating

2.4.7.1 Application of Ohmic heating in food industry

Applying Ohmic heating in food industry has developed significantly over the past two decades and the lack of that successes were related to solving electrode design problem such as electrode polarization and fouling (Singh and Heldman, 2014) in the same time Ohmic heating enables to heat the food at extremely rapid rate, in general from a few second to a few minutes (Sastry, 2008).

In the last decade researcher studied the effect of different parameters which effect on the performance of Ohmic heating efficiency such as pH of the heating fluid, electrode type …etc.

Samaranayake and Sastr (Samaranayake and Sastr, 2005) studied the effect of pH on electrochemical behavior of an electrode material is unique to the material itself using a 60 Hz sinusoidal alternating current, the experimental results show that, all the electrode materials exhibited intense electrode corrosion at pH 3.5 compared to that of the other pH values, although the titanium electrodes showed a relatively high corrosion resistance. Darvishi et al (Darvishi et al., 2013), investigated the behavior of pomegranate juice under Ohmic heating by applying voltage gradients in the range of 30–55 V/cm, the results showed that, as the voltage gradient increased, time and pH decreased.

Since the main critical parameter in Ohmic heating is the electric conductivity (σ), in a non-homogeneous material, such as soups containing slices of solid foods, the electric conductivity of the particle and its relation to fluid conductivity is pointed as a critical parameter to the understanding of particles heating rate under Ohmic heating (Darvishi et al., 2013).

Variation of electric conductivity with temperature of food products during Ohmic heating carried out by (Sarkis et al., 2013) and (Ye et al., 2003) they concluded that this increase mainly due to increase of ionic mobility and this phenomenon should be factored in to the design of continues Ohmic heaters.

2.4.7.2 Water distillation

Since seawater desalination need some form energy, Ohmic heating method can generate heat in seawater as an attempt to be utilized in destination process as an alternative heating methods rather than using steam boiler (Assiry et al., 2010), several studied carried out by (Assiry et al., 2003, 2010) they conclude that Ohmic heating can be applied for heating process of seawater with some limitations regarding to color change and more studied are need for pilot production system and modelling the potential use of Ohmic heading in desalination process.

Applying Ohmic heating methods in desalination process has an advantage especially at high heating rate due to the increasing the scaling outside the boiler tube in the traditional heating seawater in the MSF which lead to decrease the heat transfer coefficient and boiler tube also suffered from corrosion and erosion but in Ohmic heating there is no heat transfer limitations (Huang et al., 1997). In the same time applying Ohmic heating in desalination process have expected benefits such as reducing the need for maintenance and chemical activities and improve plant reliability and duration (Assiry, 2011).

2.4.7.3 Other industrial applications

One of the new important industrial application which Ohmic heating can be use is waste treatment such as sterilisation of animal wastes, heating of clay slip and other slurries, sewage sludge and compost leachate.

Previous studied by Murphy et al (Murphy et al., 1991) recommended that sewage sludge could be ohmically heated from room temperature to boiling point rapidly, uniformly and at energy efficiencies greater than 98%. Kanjanapongkul et al (Kanjanapongkul et al., 2010) developed a static Ohmic heating system to remove protein from fish mince (threadfin bream) wash water collected from a surimi production plant in order to improve water quality.

Ohmic heating has new approach to integrate with thermal energy storage such as electric thermal storage device (Marvin, 1986) salts are good at storing heat; they can be heated until they melt, and then stored in insulated containers. When the energy is needed, the molten salts can be pumped out to release their heat through a heat exchange system. Also Ohmic heating has significant effect of the fuel cell performance (Ho et al., 2010). Singdeo et al (Singdeo et al., 2011) have implemented Ohmic heating for generating heat in the start-up time for phosphoric acid doped PBI membrane based fuel cells, combining it with other heating techniques is found effective in reducing start-up times significantly.

2.4.7.4 Integration with thermal energy storage

Thermal energy storage (TES) systems based on latent heat is an emerging technology and currently is receiving great attention as a consequence of its advantages (Raluy et al., 2014)and (Gang, 2013) such as high heat of fusion (Gang et al., 2012). Especially TES systems in which molten salt is used as the storage medium are widely applied or under development worldwide (Gang et al., 2013, 2010 and 2012), as molten salt can offer the best balance of capacity, cost, efficiency and usability at high temperatures, as mentioned before, Ohmic heating performance increases with increasing ions on the heating solutions (Assiry et al., 2010), so there are potentials for using Ohmic heating to melt the salt and use this molten solution later for electricity generation in space heater (Marvin, 1986).

In the same time, there are significant advantages could be obtained using Ohmic heating for heat storage in salt hydrates phase change materials (PCMs) to reduce energy consumption or to transfer an energy load from one period to another (Gang et al., 2013, 2014). By heat and melt PCM during the night time and use this stored heat during the daytime, these positive impacts include peak load shifting, energy conservation and reduction in peak demand for network line companies and potential reduction in electricity consumption and savings for residential customers (Lin et al, 2007) and (Qureshi et al, 2011).

2.5 Conclusions

From literature review, it seems clear that water heating systems contribute an important proportion of residential energy consumption all around the world. Different kinds of domestic hot-water production systems exist, thus improve the thermal performance of water-heating systems is a prerequisite to recommend the proper choice among the existing systems or suggest new designs and approaches that would enhance reductions in energy consumption, environmental pollution and operating cost. Electric Heating Water Systems, Phase Change Materials (PCMs) and Ohmic Heating these subjects are related to the project researched in this thesis and the pre-reading and understanding of these technologies are necessary to progress the proposed research work.

In section 2.1, design and performance of electric heating water systems were reviewed, performance and design optimization of residential water heaters incorporating thermal storage vessels were discussed and it was pointed out that cold water inlet angle has important impact on the water heating system thermal performance.

In section 2.2, passive heat transfer technique to improve the overall thermal performance in hot water systems were summarized such as twisted tape, wire coil, swirl flow generator…..etc, it was found that:

- Variously developed twisted tape inserts are popular researched and used to strengthen the heat transfer efficiency for heat exchanger.
- Other several passive techniques such as ribs, conical nozzle, and conical ring, etc. are generally more efficient in the turbulent flow than in the laminar flow.
- In the selection of the tube inserts, the shape of the insert is important.
- Helical screw tape can help to promote higher heat transfer exchange rate than the use of twisted-tape because of that shorter pitch length leads to stronger swirling flow and longer residence time in the tube.
- Twisted tape in turbulent flow insert is not very effective.
- If the pressure drop is not concerned, twisted tape inserts are preferred in both laminar and turbulent regions.

In section 2.3, Phase change materials (PCMs) are regarded as a possible solution for thermal management and thermal energy storage in water heating system were reviewed. It was found that the combination of PCM in the HWT and the application of a control strategy can help to reduce the heating time thus reducing the energy consumption and it is possible to use PCMs as a traditional active cooling heat sinks to improve their heating systems performance by taking advantage of the thermal energy stored as latent heat.

In section 2.4, fundamental principles of Ohmic heating were reviewed, besides the common use of Ohmic heating in food industry. The intention of utilizing the Ohmic heating as an alternative new heating technology for water heating, water distillation, waste treatment and chemical processing has increased in the recent decades. Comprehensive review of Ohmic heating current applications, design configurations and operation parameters has been presented, from the literature review as discussed, it is concluded that:

- Ohmic heating has immense potential for achieving rapid and uniform heating.
- The success of Ohmic heating depends on the rate of heat generation in the system, electric conductivity of the heating substance, electric filed strength, residence time, applied electric frequency and the incident frequency.
- A vast amount of work is needed to complete understand all the effects produced by Ohmic heating.
- The economic studies will also play an important role in understand the overall cost and viability of commercial applications.
- There are still a lot of challenges and difficulties to control the rate of heat during Ohmic heating process due to change of electric conductivity of heating material.

Chapter (3)

3. Experimental Set-Up and Procedure (Effect on inlet angle)

3.1 Test Rig

The experimental facility shown in Figure 3-1 was designed and constructed to investigate the effect of inlet angles on the thermal performance of tankless electric water heaters. It is an open loop in which water as a working fluid is pumped and passed the test section to the atmosphere after being heated by two electric resistance coils. The test rig basically consists of two parts; the water supply unit with necessary adoptions and measuring devices and the test section.

3.2 Water Supply Unit

The water supply unit and its accessories consist of storage tanks, water pump, flow control valves and flow meter turbine as shown in Figure 3-2 The details of the flow meter turbine calibration is given in the appendix A.

Water is pumped by a pump (3) from storage tank (2), from which the water is discharged to the system. The flow rate of the incoming cold water was adjusted by using control valve (4) connected upstream of a calibrated flow meter turbine (5) which measured the flow rate of the water. Besides controlling the flow, the control valves also served as a major pressure drop in the system. Much care was taken in adjusting the opening of the inlet control valve so that the accuracy of the measured flow rate was always within ±0.2% or less. The cold water was supplied from a constant-head elevated tank to ensure steady-flow conditions. The water flow passes through the plastic test tube (10) and then discharged to the atmosphere.

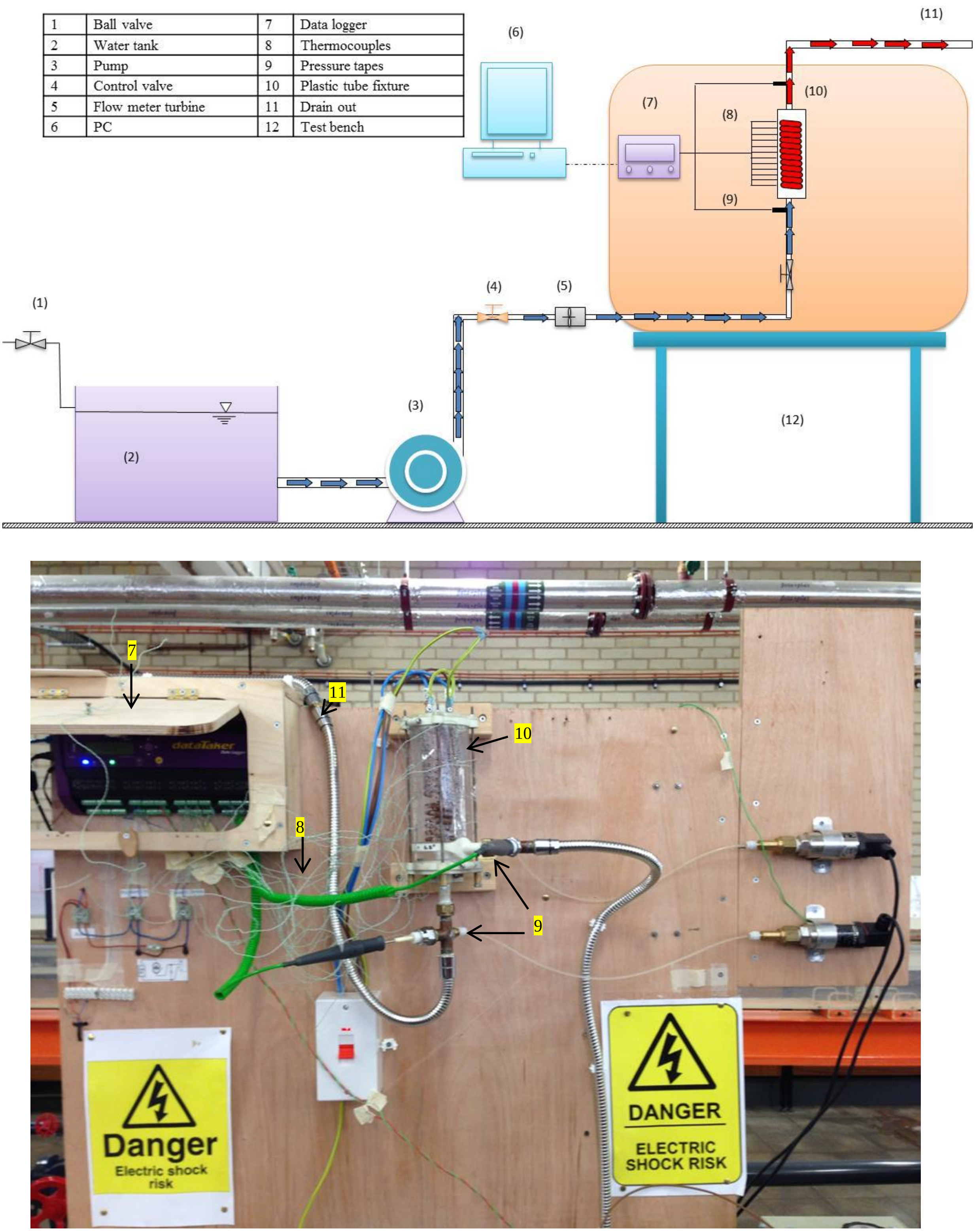

1	Ball valve	7	Data logger
2	Water tank	8	Thermocouples
3	Pump	9	Pressure tapes
4	Control valve	10	Plastic tube fixture
5	Flow meter turbine	11	Drain out
6	PC	12	Test bench

Figure 3-1 Schematic diagram for the experimental rig

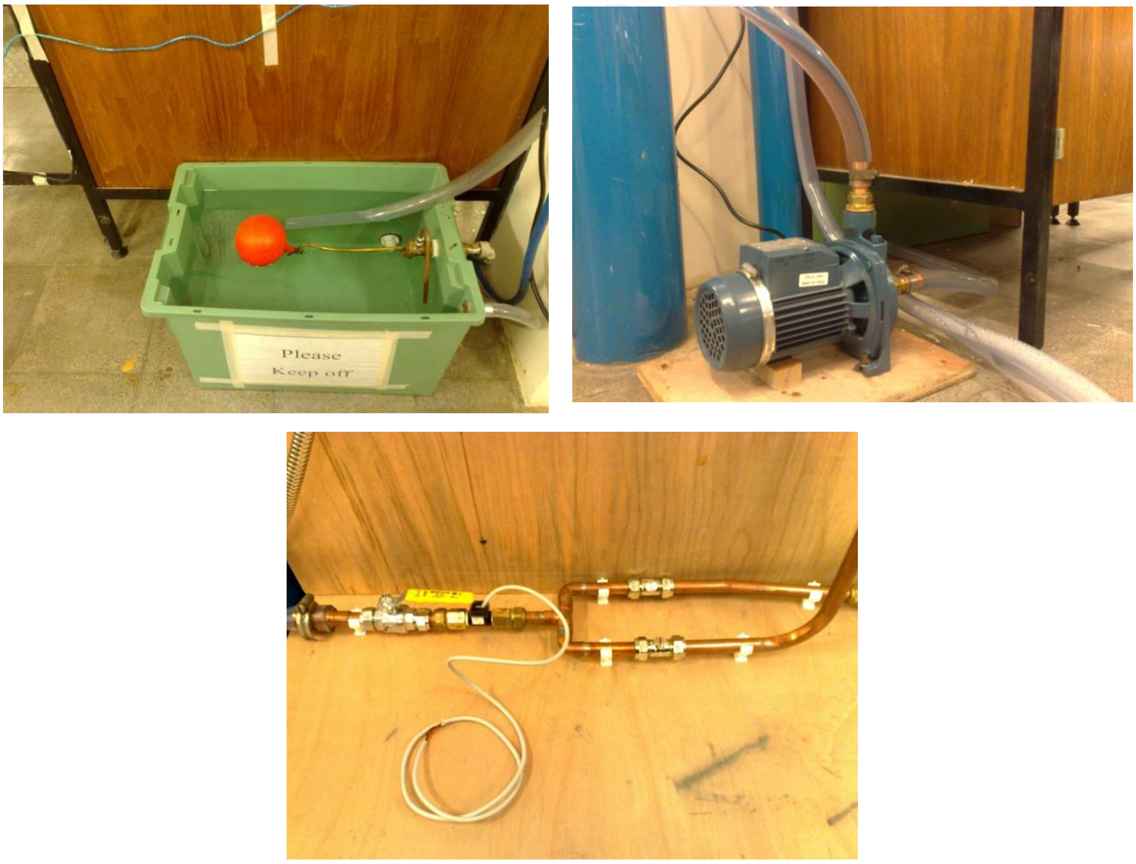

Figure 3-2 Water supply unit

3.2.1 Test Section

The test section (10) is shown schematically in Figure 3-3. It is a plastic tube of 73.2 mm inner diameter, 76 mm outer diameter and 200 mm in length (L/D_i = 2.73). The test section is clamped from both sides by flexile joints.

Transient temperature distributions of water body inside the tank were measured using 16 K-type (T_1, ……,T_{16}) thermocouples distributed along the tube surface at four levels (Y_1, Y_2, Y_3, Y_4), each level contains four thermocouples. Thermocouple junctions were fixed from a sealed opening in the tank side, each of 2 mm in diameter. The junctions of the thermocouples were located at 40, 80, 120 and 160 mm from the bottom of the tank as shown in Figure 3-4. Two more thermocouples were placed in the inlet and outlet ports for continuously monitoring the inflow and outflow water temperatures. Temperature signals were collected from the test heater by a data acquisition system based on a desktop computer. Data of water temperatures inside the tank were sampled at 1-s interval. Calibration of the thermocouples showed that the overall accuracy of the measurements was within ±0.2°C. The details of the thermocouples calibration is given in the Appendix B.

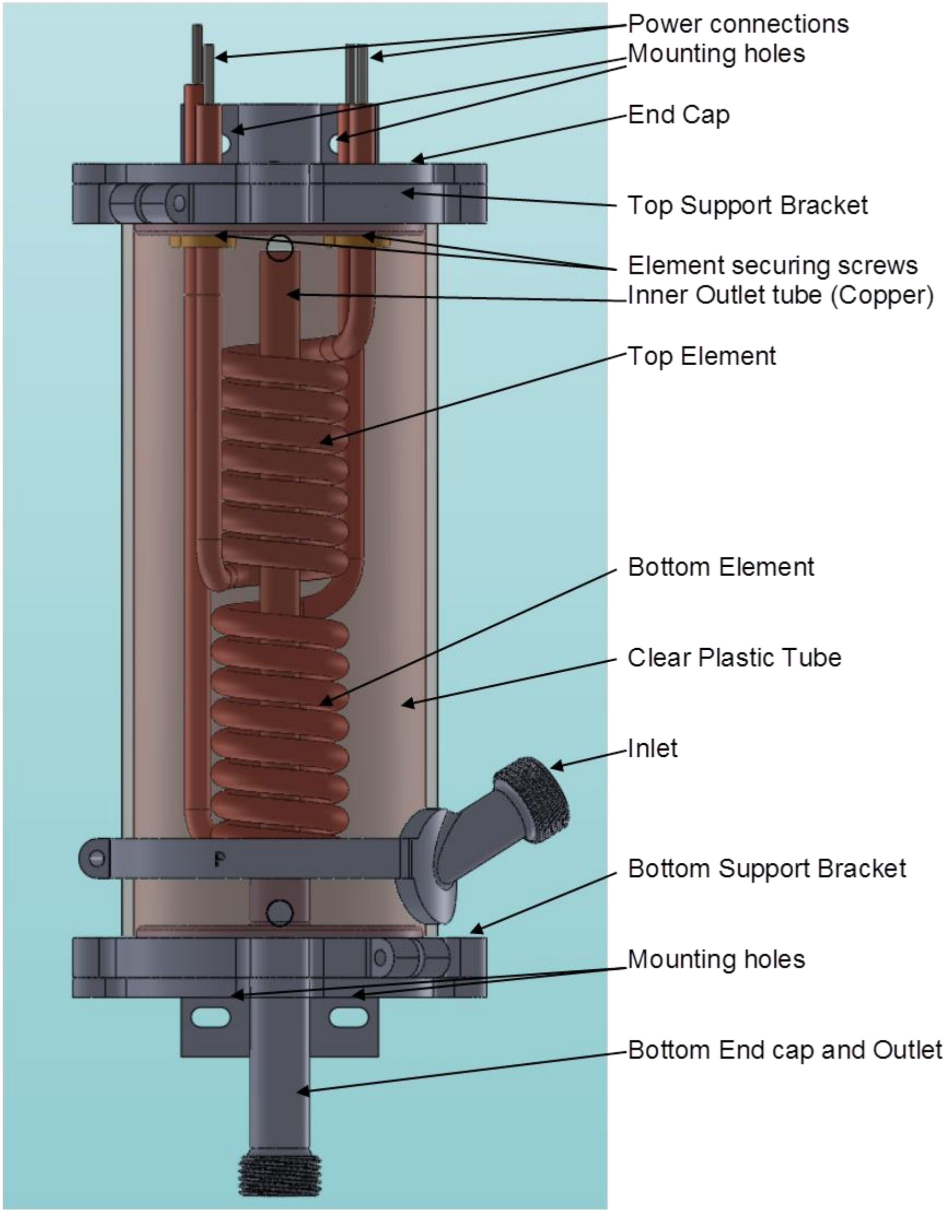

Figure 3-3 Water heating test fixtures

The main heating element consists of two coils with 1970 mm total length and made from nickel chromium, each heating element coil has a resistance of 12.6 Ω, the operation of the heating elements is controlled manually via an on-off switch.

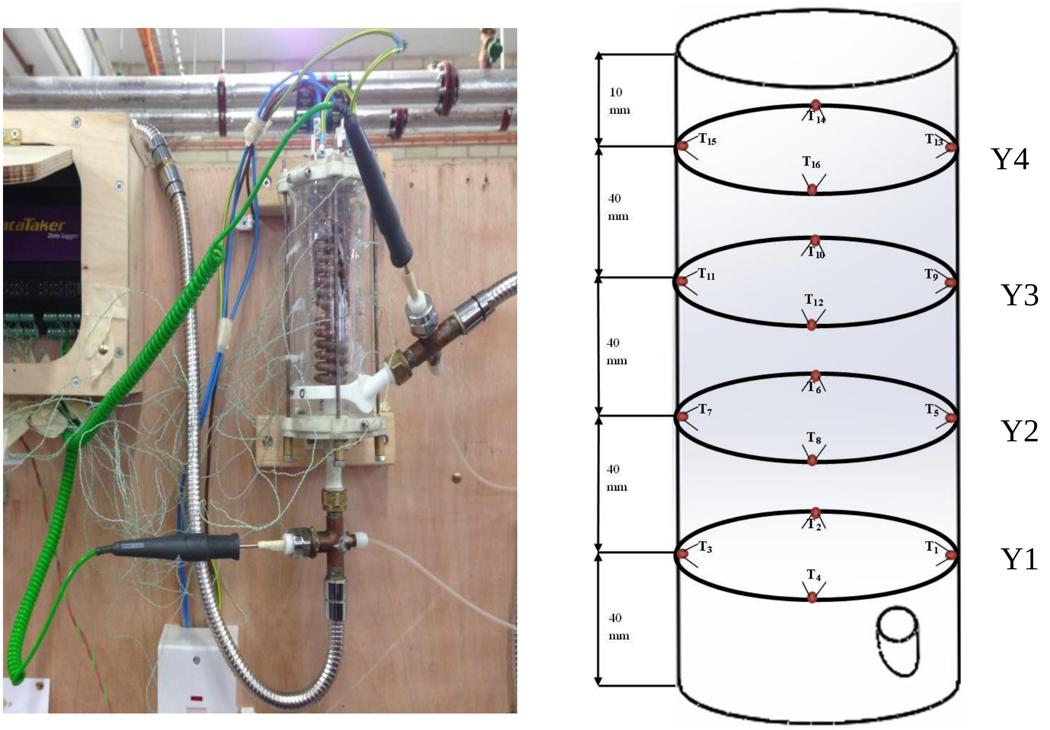

Figure 3-4 A Photo and sketch of the heating tank which indicate the thermocouple locations

The physical dimensions of test section and heating elements coils are listed in the Table 3-1:

Table 3-1. Parameters of the water heater

Parameter	**Value**	**Parameter**	**Value**
Hot Water Tank	0.67 L	Electric Heater Power	7682.5 W
External Tank Height	174.0 mm	Inlet Tube with Diameter	10.0 mm
Internal Tank Diameter	73.2 mm	Outlet Tube with Diameter	10.0 mm
Internal Tank Height	170.0 mm	Upper Heater Volume	3.04 cm^3
Bottom Heater Volume	2.96 cm^3		

The bulk water temperatures at inlet and outlet of the test section were measured by two K-type thermocouples inserted in two holes drilled through the ½” BSP connection at the inlet and outlet.

3.3 Inlet Configurations

The inlet is produced with a variety of inlet angles and is clamped onto the outside of the tube with an o’ring seal. The cold water enters the tank from a horizontal side-inlet at the lateral surface, 15mm above the bottom, while the hot water leaves the tank via a center-outlet located also at the bottom of the tank. Figure 3-5 shows examples for inlet parts with (30° × 45°) and (45° × 0°) inlets.

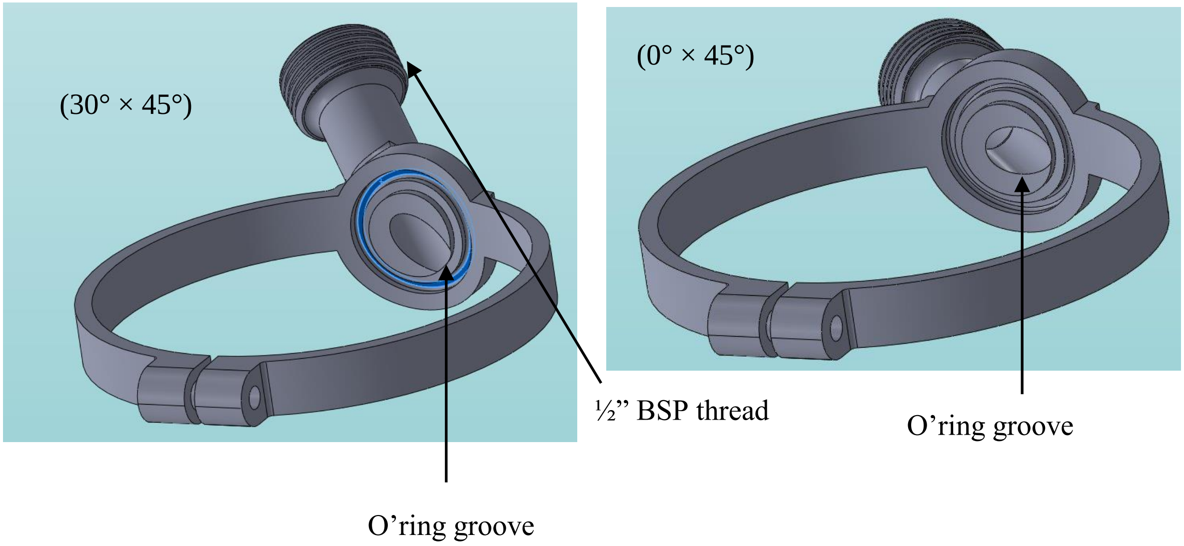

Figure 3-5 Examples of inlet angles part

In this study, tank models utilizing twelve inlet angles are considered. Varied from 0° to 45°, in both the horizontal and vertical direction where inlet angle (15°, 30°) means that it was rotated 15° in the vertical axis and 30° in the horizontal axis as appeared in Figures 3-6 and 3-7.

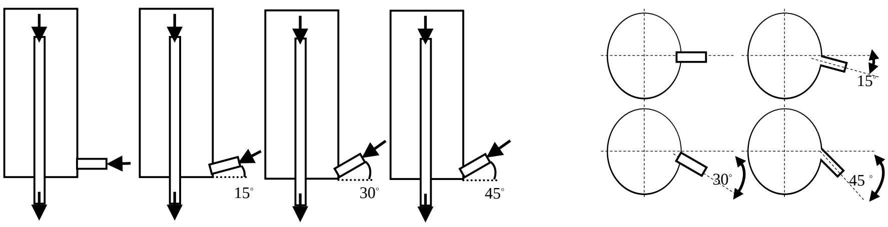

Figure 3-6 Different inlet angles

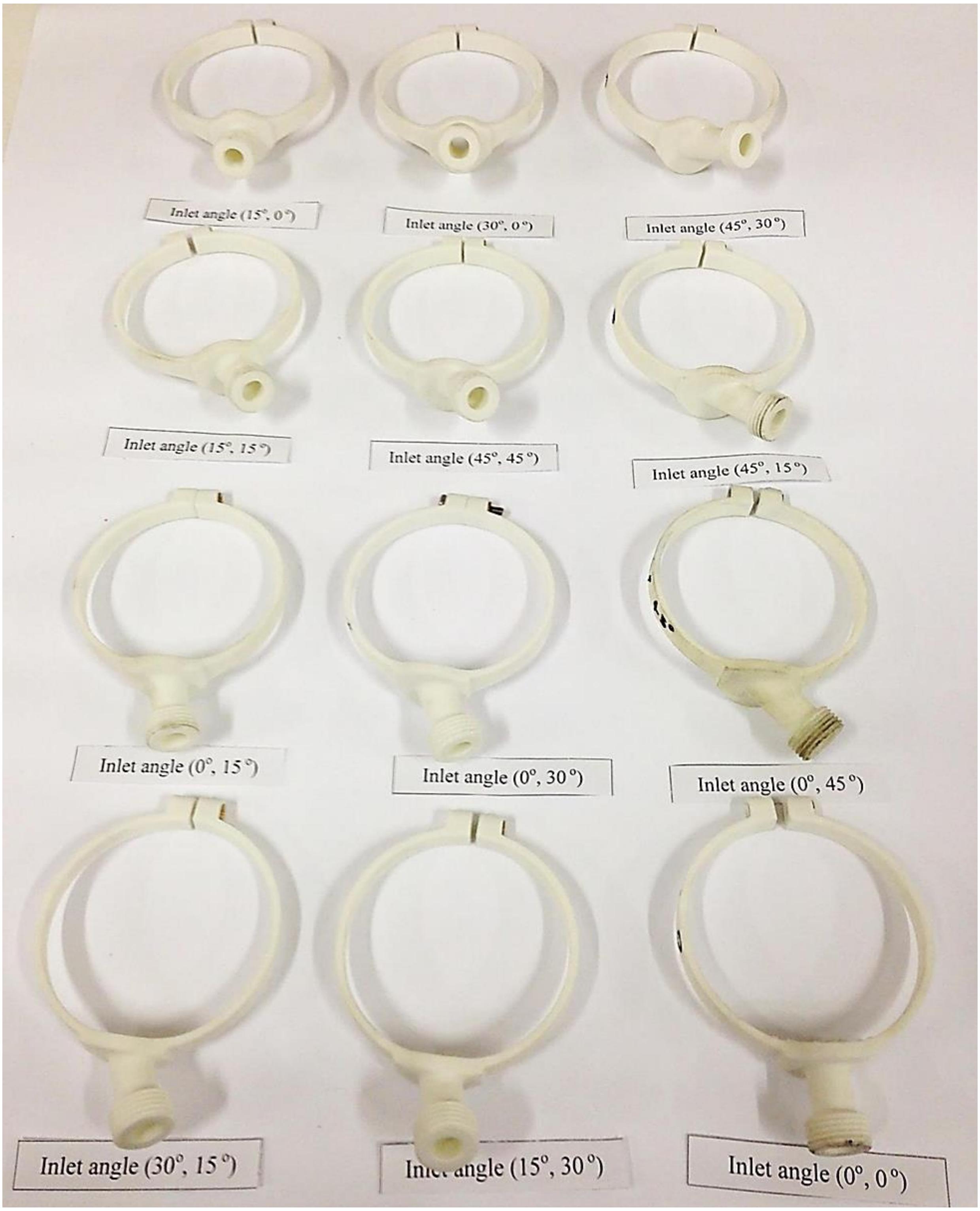

Figure 3-7 Inlet angle configurations

3.4 Procedure and Calculations

3.4.1 Experimental procedure

In this investigation, an experimental program has been performed for twelve different inlets. For each inlet–outlet configuration, experiments have been carried out at four flow rates that were 0.06, 0.08, 0.10 and 0.12 kg/s. Each experiment begins by filling the tank with fresh water. The flow line was properly aligned, the pump was switched on and the whole system was checked against any water leakage. The desired value of the water flow rate is established by means of a previously regulated valve

Then, the heating elements are turned on and the water is heated until its temperature at the outlet section of the tank reaches maximum value, the duration of each test is around 300 seconds. During this time the data acquisition system continuously monitors and records transient water temperatures distributions in the heating tank (T_1, T_2, . . ., T16) as well as the water temperature at the inlet and outlet (T_{inlet} and T_{outlet}), and water flow values from the beginning to the end of the experiment, each experiment was repeated three times to check consistency of the measurement results.

3.5 Validation of experimental data

The temperature difference between the outlet hot water and cold inlet water (ΔT) obtained from the present experimental data is compared with those from the heat transfer equations that computed based on the following equations.

The heat supplied to the heating elements can be calculated from:

$$Q_{elec}=VI \tag{3-1}$$

The heat transferred into the fluid was computed from:

$$Q_f = m^o C_p(\Delta T) \tag{3-2}$$

Where $\Delta T = T_{out} - T_{in}$ (3-3)

At steady state condition, the heat transfer is assumed to be equal heat supplied from the heating elements:

$$Q_{elec} = Q_f \tag{3-4}$$

The temperature difference is estimated by:

$$\Delta T = \frac{VI}{m^o C_P} \tag{3-5}$$

The measured results of temperature difference for plain heater are compared with those obtained from above equations as depicted in Figure 3-8. It is found the measured results are in good agreement with those calculated from heat transfer equations with ± 5% difference. This could be related to the uncertainty of the measurement and heat losses from the heating tank during the testing.

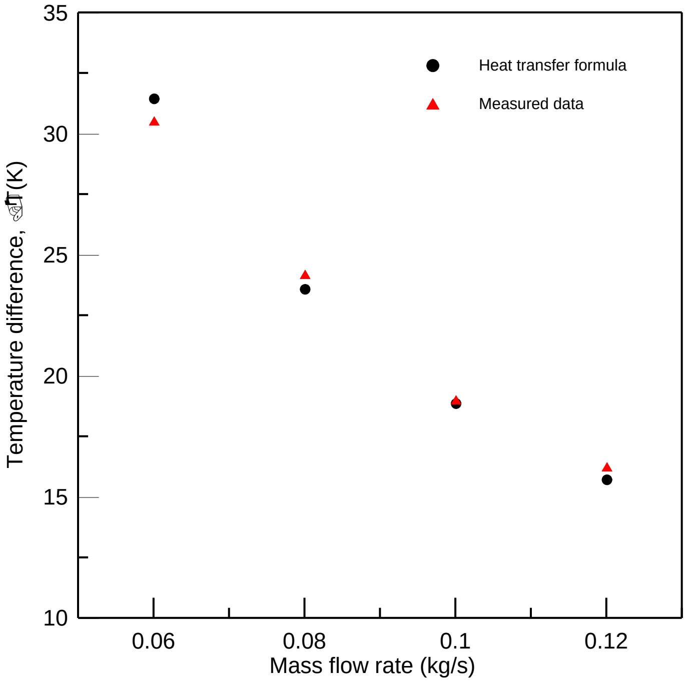

Figure 3-8 Comparison between the measured temperature difference and that calculated from heat transfer equations

Chapter (4)

4. Experimental Results and Discussions

A search of the literature has revealed a number of methods for enhancing the thermal performance of water heating systems. Concerning the present investigations, however, the main purposes of the analysis is the selection of the best inlet angle configuration to promote heater thermal performance, maximize mixing during water heating inside the heating tank and promote the uniform heating of the fluid under different discharge rates. Such ability has the most significant impact on the heater capability of supplying its water capacity at the temperature and rate, which satisfy the needs of the user.

Current national energy policy act standards mandate that all showerheads manufactured in the UK have a maximum flow rate of 6 kg/min. Therefore, for each inlet angle configuration, experiments were carried out for four draw-off flow rates of 0.06, 0.08, 0.10 and 0.12 kg/s to cover a, two heating elements, having a nominal total power of 7682.5 W. Each experiment begins by pumping fresh water through the system. Then, the heating element is turned on and the water is heated for 300 seconds.

4.1. Performance Evaluation Criteria

The first criterion of evaluation is outlet hot water temperature, it is important not only for comfort but also for safety and energy consumption associated with TWHs (Tankless water heaters). This is particularly true when the heated water is not mixed for the end use, for example in a shower, Herrmann et al (Herrmann et al., 1994) concluded that skin sensitivity to water thermal changes is very acute and even more acute during rapid thermal transients and the rate that skin temperature changes influences how readily people can detect the change in temperature. If the temperature changes very slowly, for example at a rate of less than 0.5 °C per minute, then a person can be unaware of a 4-5 °C change in temperature, provided that the temperature of the skin remains within the neutral thermal region of 30-36 °C. If the temperature changes more rapidly, such as at 0.1 °C/s, then small decreases and increases in skin temperature are detected. However, warm and cold thresholds do not decrease any further if the rate at which temperature changes is faster than 0.1 °C/s (Lynette, 2014). In the same time, the disturbance and fluctuation in outlet water temperature increases the difficulty of controlling TWHs. Henze et al., 2009; Russell and Craig, 2006 suggested that TWHs are inappropriate for users who need good temperature stability.

The second criterion of evaluation is behavior of water temperature distribution inside the heating tank; it is desirable for the water flowing within the heating tank to be uniformly heated, as much as possible, by the heating elements. Areas of stagnant flow with the heating tank restrict heat from the nearby part of the heating elements being dissipated evenly/efficiently through to the water. These parts of the heating elements become localized hot spots and can be precipitate premature failure of the heating elements. It is thus desirable to minimize any areas of low water flow rate to avoid such hot spots being formed on the heating elements. In addition decreases the heat losses from the tank to surrounds.

The ability to start-up quickly and to adjust load output in a fast and predictable fashion is a key technology for tankless electric water heaters, meanwhile, the heating elements coils are exposed to greater stresses than ones in the traditional storage tank electric water heater. The heater becomes more efficient if it can reach to the operating conditions quickly. This rapid start-up put tremendous thermal stress on heating coils as the temperature is raised to several hundred degrees in less than minute. So, the heating water temperature variations due to transient events such as start-up and shutdown is important factor should be consider during the designing stage. The thermal stresses have a significant influence on the cyclic creep fatigue life and limit the service life. In materials science, creep is the tendency of a solid material to move slowly or deform permanently under the influence of mechanical stresses. It can occur as a result of long-term exposure to high levels of stress that are still below the yield strength of the material. Creep is more severe in materials that are subjected to heat for long period, and generally increases near their melting point. The rate of deformation is a function of the material properties, exposure time, and exposure temperature. Depending on the magnitude of the applied stress and its duration, the deformation may become so large that a component can no longer perform its function.

In this experimental work, the performance of tankless electric water heater with different inlet ports are compared to determine the one which:

1. Maintains the fluctuations of the outlet water temperature within ±1.0 °C while providing hot water.
2. Heats the flowing water with the heating tank uniformly as much as possible.

4.2. Performance of Inlet Angle Ports

The first significant result obtained concerns the performance of the heater inlet angle configurations. The analysis of the temperature profiles of the draw-off water and water temperature distributions in the tank clearly indicates that different performance depends on inlet angle used.

Figure 4-1 shows the transient temperature profiles of the draw-off water as a function of the time for the twelve inlet port arrangements for water flow rate of 0.06 kg/s (3.6 l/min). It can be observed that outlet water temperature starts rising rapidly in the first 30 seconds and becomes nearly constant when the heater reaches to the steady state, obviously the water outlet temperature depends on the flow rate and input power.

Figurer 4-1.a shows the effect of inlet angle (0^o, 0^o) on the heater thermal performance and outlet water temperature, the results indicate that non uniform temperature distributions inside the heating tank lead to the average water temperature at the top of the tank is higher than the outlet water temperature, in addition the water temperature difference at the top and bottom of the tank around 30 ^oC, meanwhile, the average variation of the outlet water temperature is high and around ± 3 ^oC.

For cold water inlet angle (15^o, 0^o), it can be observed that the temperature difference of water at the top and bottom of the tank has decreased to 15 ^oC, and the fluctuation in outlet water temperature is decreased to ± 2.5^oC, It is also seen that the average water distribution inside heating tank higher than the tank with inlet angle (30^o, 0^o) as shown in Figure 4-1.b.

When the inlet angle is changed to (30^o, 0^o) the average water temperature at all the level in the tank has increased to the level of the outlet water temperature especially at the top of the tank which is highly not desirable as presented in Figure 4-1.c.

For the case of water tank with inlet angle (30^o, 15^o) the water temperature among the tank is lower than the water outlet temperature by approximately 10 ^oC. Meanwhile, the water temperature at the bottom of the heating tank (Y_1) is relatively higher than at the top of the tank as illustrated in Figure 4-1.d.

A significant reduction in water temperature `distributions in heating tanks has been observed for the heating tank with inlet angles of (30^o, 30^o), (30^o, 45^o), (45^o, 15^o), (15^o, 30^o) and (15^o, 15^o) as presented in Figures 4-1 (e, f, g, h and i), also the results indicate that relatively small fluctuation in outlet water temperature and lower average water temperature inside the heating tank during the operation.

For the other cases of heating tank with cold water inlet angles of (0^o, 15^o), (0^o, 30^o) and (0^o, 45^o) can be seen from Figure 4.1(j, k and m), the outlet water temperature almost keeps uniform, especially for the inlet angle (0^o, 45^o) with the maximum fluctuation less than $\pm 0.3^oC$. The most outstanding result is that water in the tank is heated uniformly from bottom to top for these cases. According to the second aspect of criterion, these configurations provide an instantaneous water heater more efficient by direct the fluid flow to swirl or spirally substantially tangentially to the tank wall and minimize areas of stagnant flow and promote uniform heating of fluid flow.

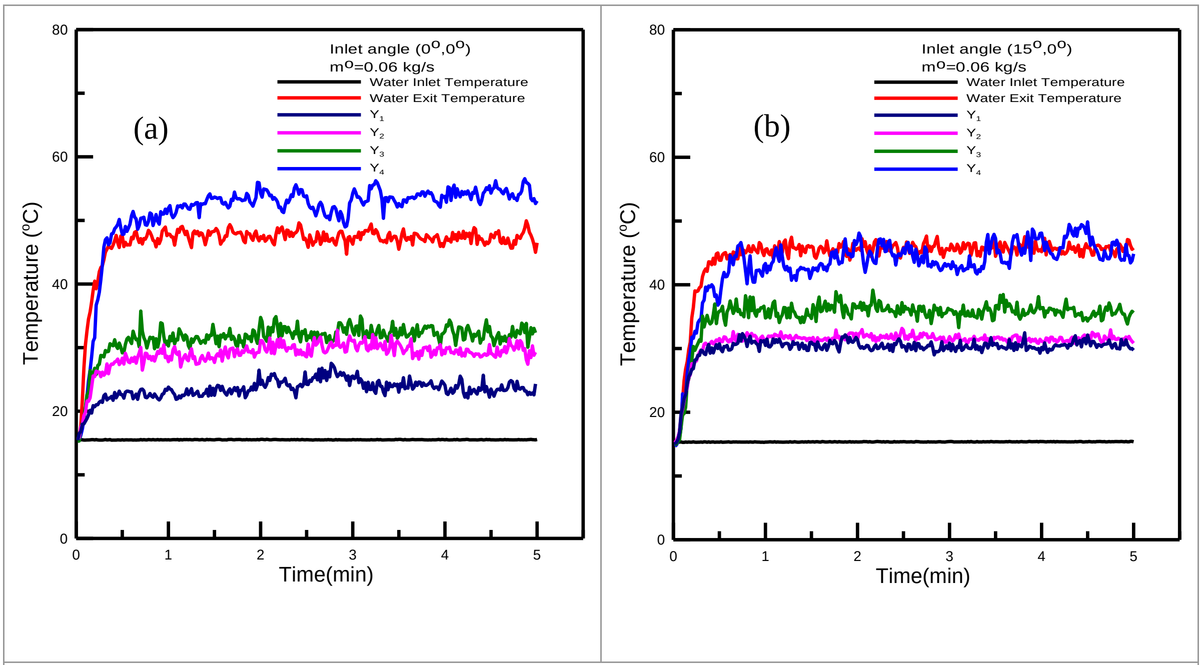

Y_1= 40 mm , **Y2**= 80 mm, **Y_3**= 120 mm and **Y_4**= 160 mm from the bottom of the water tank

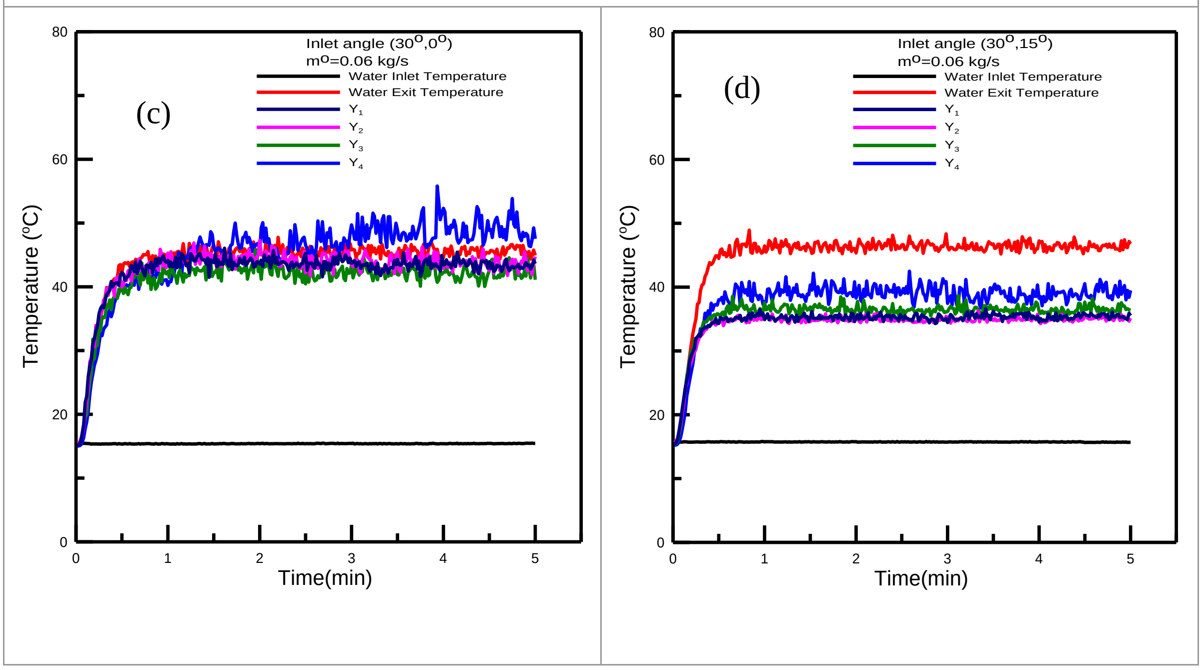

Figure 4-1 Temperature profiles of the draw-off water and temperature distributions of the water along the height of the tank (0.06 kg/s) (continue)

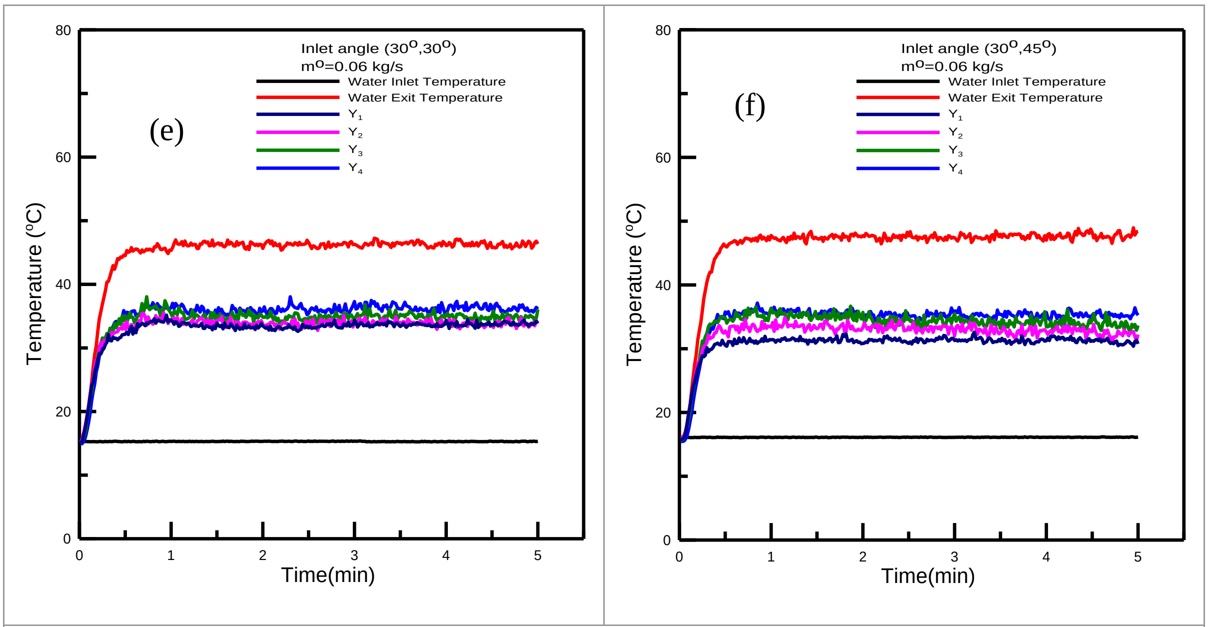

Y$_1$= 40 mm , **Y2**= 80 mm, **Y**$_3$= 120 mm and **Y**$_4$= 160 mm from the bottom of the water tank

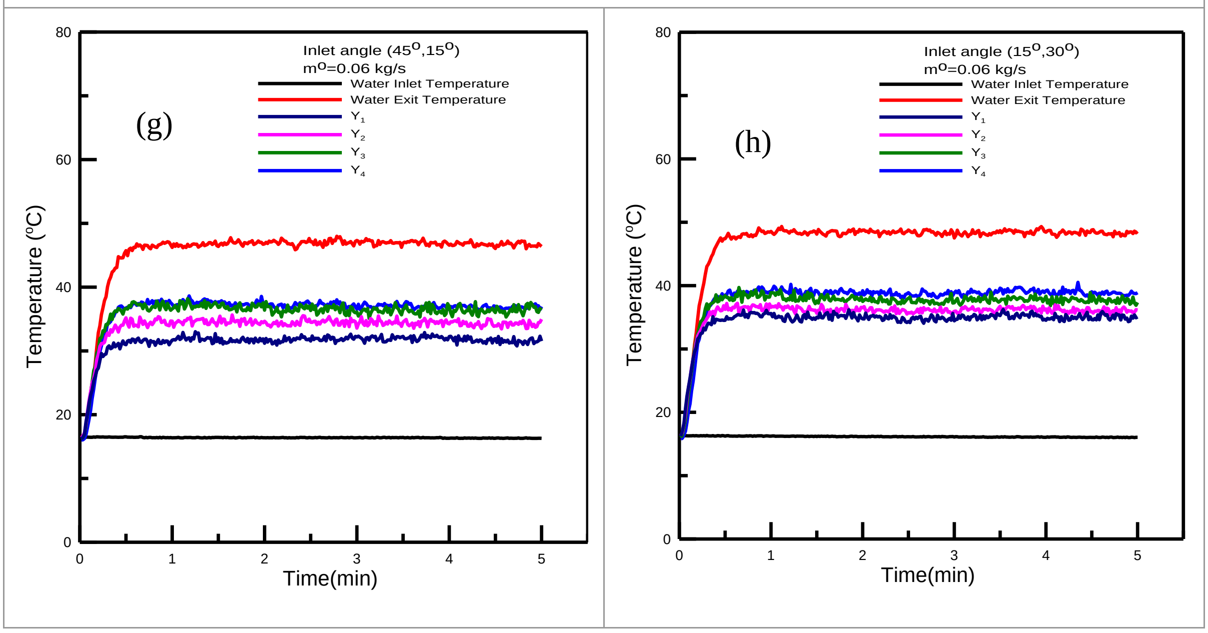

Figure 4-1 Temperature profiles of the draw-off water and temperature distributions of the water along the height of the tank (0.06 kg/s) (continue)

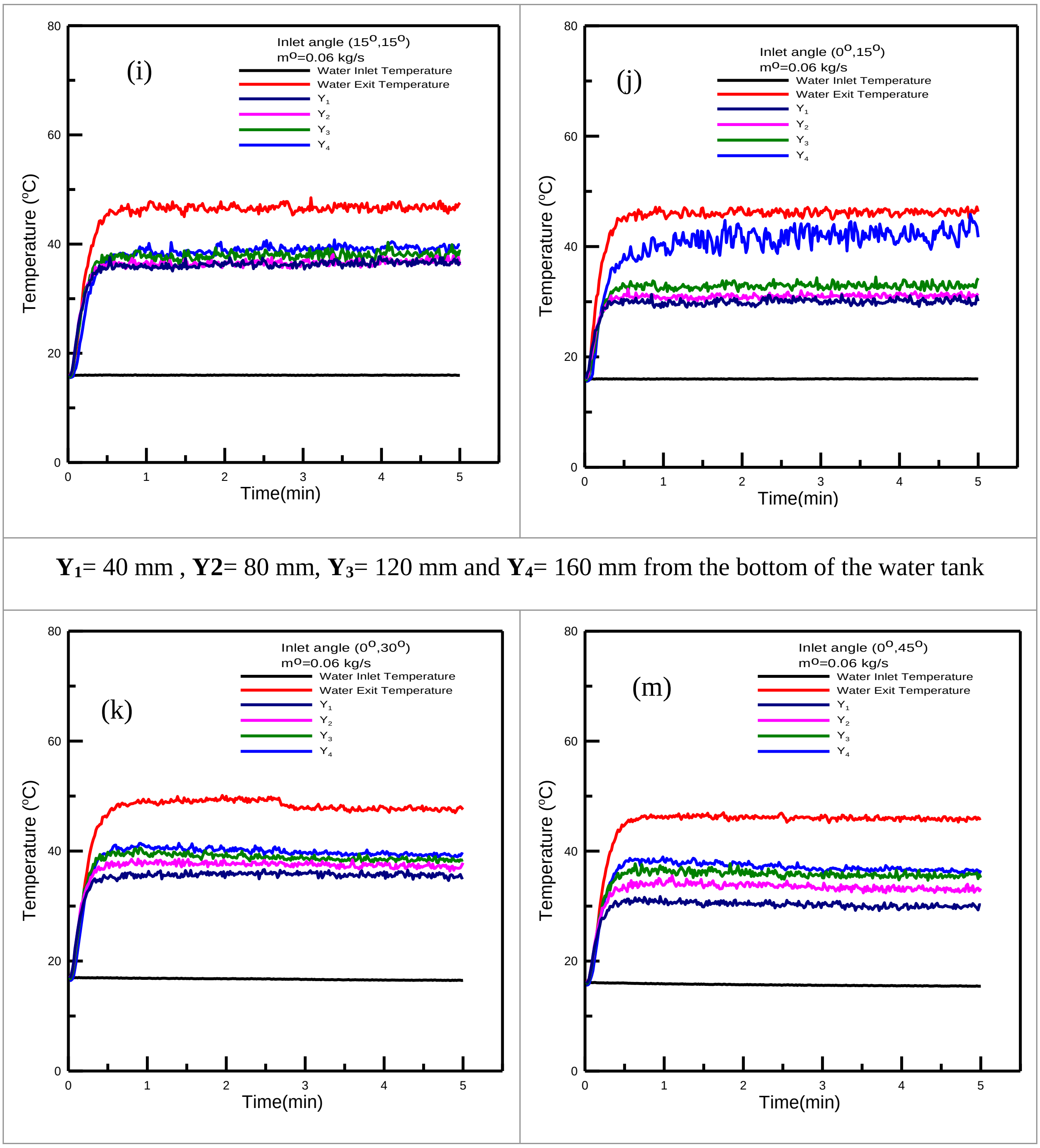

Y$_1$= 40 mm , **Y2**= 80 mm, **Y**$_3$= 120 mm and **Y**$_4$= 160 mm from the bottom of the water tank

Figure 4-1 Temperature profiles of the draw-off water and temperature distributions of the water along the height of the tank (0.06 kg/s)

Figure 4-2 shows that the mean of the transient temperature of the water in the tank during discharging process, these results reflect the impact of inlet angle configurations on the average water temperature in the tank, thus, it confirms that average water temperature decreases with changing inlet angle from vertically inclined configuration to horizontally inclined configuration. This is explained by the fact that there are some locations in tank where the water is very hot and other places where the water is very cold due to poor water distribution.

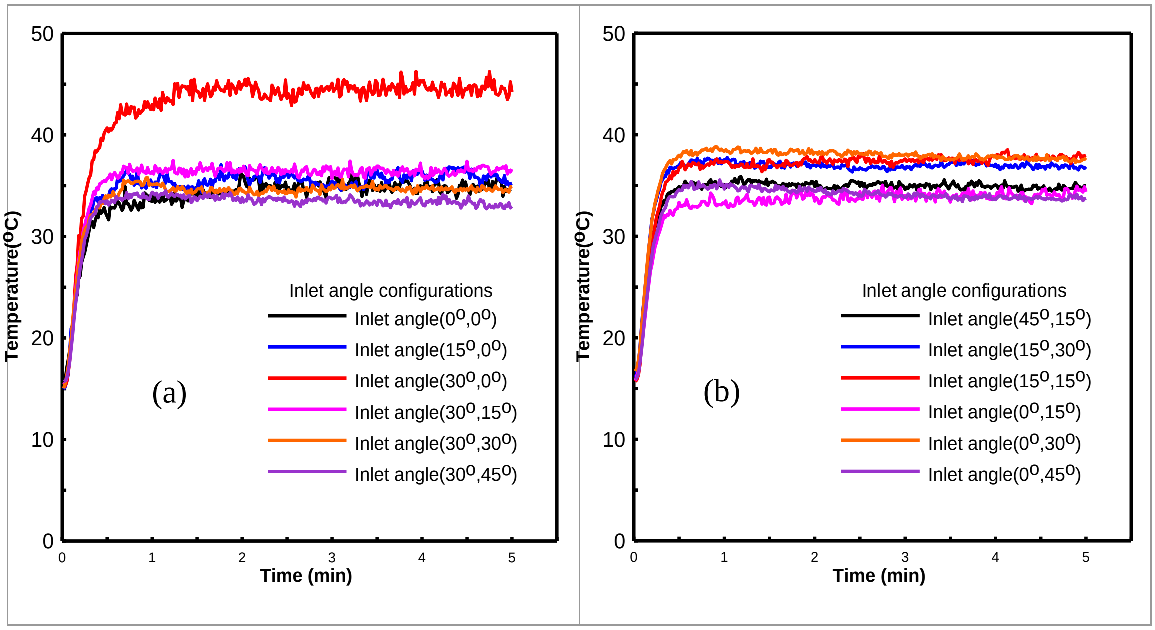

Figure 4-2 Average water temperature in the tank during draw-off (0.06 kg/s)

When water flow rate is increased to 0.08 kg/s, the effect of inlet cold water angle on water temperature in the tank is still significantly clear, especially for the inlet angles of (0º, 0º), (15º, 0º) and (30º, 0º) as displayed in Figures 4-3 (a, b and c).

In the case with the inlet angle of (0º, 0º), it is found that the water heated in the tank is relatively uniform. However, there are high fluctuations in the average water temperature at the top of the heating tank (Y_4) and of the outlet water temperature as indicated in Figure 4-3 a.

For inlet angle of (15º, 0º), it can be seen that the average water temperature$\left(\sum_{i=1}^{i=16} T_i /16\right)$ in the heating tank is slightly higher than for inlet angle of (0º, 0º) and the maximum temperature variation between the top and bottom of the heating tank is around 4ºC as presented in Figure 4-3.b.

Figure 4-3.c shows the water temperature for heating tank with the inlet angle of (15º, 0º), it is clear that the water temperature in the tank at the same level of the outlet temperature.

For inlet angles of (30^o, 30^o), (30^o, 30^o), (30^o, 45^o), (45^o, 15^o), (15^o, 30^o) and (15^o, 15^o) there are significant drop in water temperature in the heating tank. However, the water temperature at different height still has the same value as illustrated in Figure 4-3(d-i), respectively.

For heating tank with horizontally inlet angles of (0^o, 15^o), (0^o, 30^o) and (0^o, 45^o) the outlet water temperature is approximately constant during the operation, As a result, water in the tank is heated gradually as shown in Figures 4-3(j, k and m).

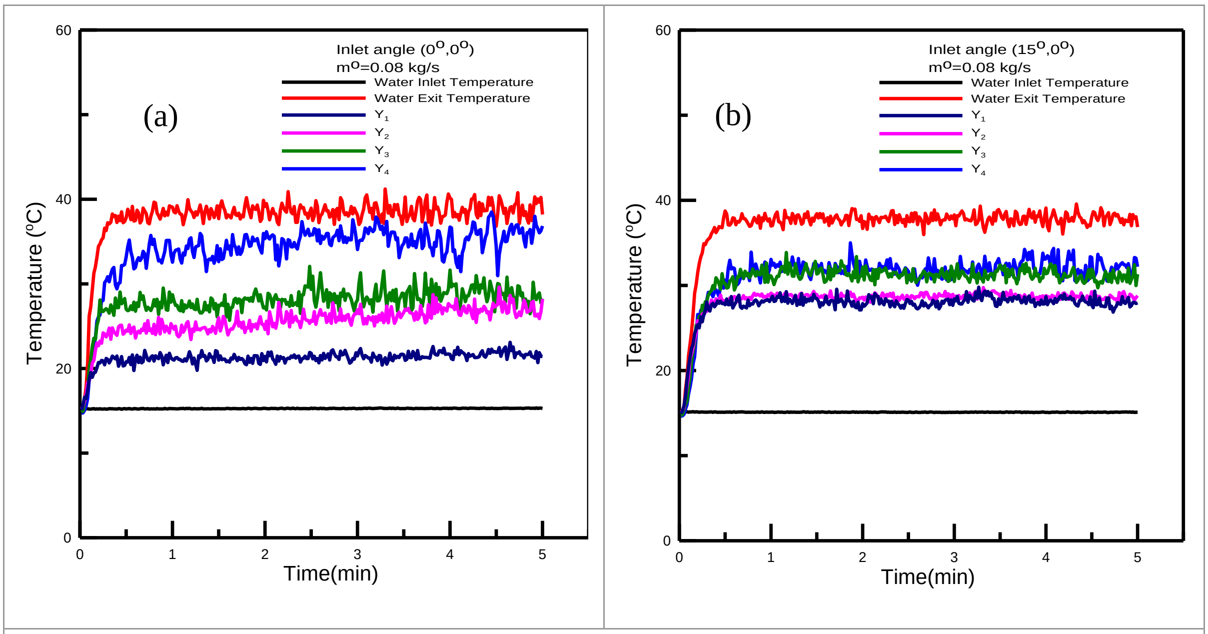

Y_1= 40 mm , **Y2**= 80 mm, **Y_3**= 120 mm and **Y_4**= 160 mm from the bottom of the water tank

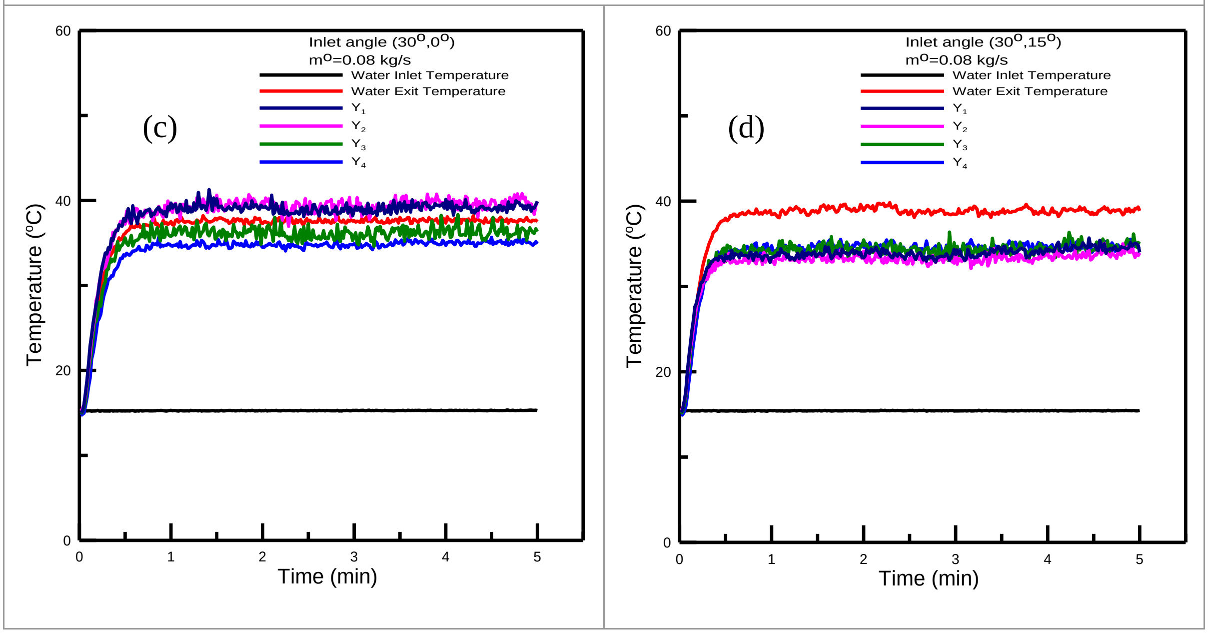

Figure 4-3 Temperature profiles of the draw-off water and temperature distributions of the water along the height of the tank (0.08 kg/s) (continue)

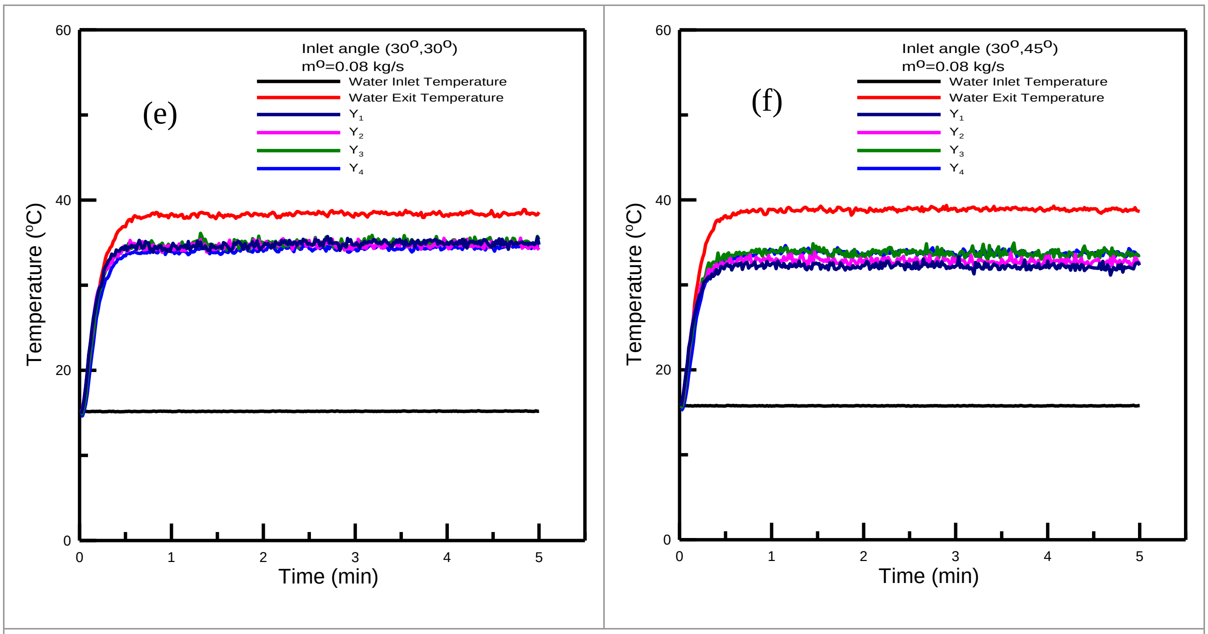

$\mathbf{Y_1}$= 40 mm , **Y2**= 80 mm, $\mathbf{Y_3}$= 120 mm and $\mathbf{Y_4}$= 160 mm from the bottom of the water tank

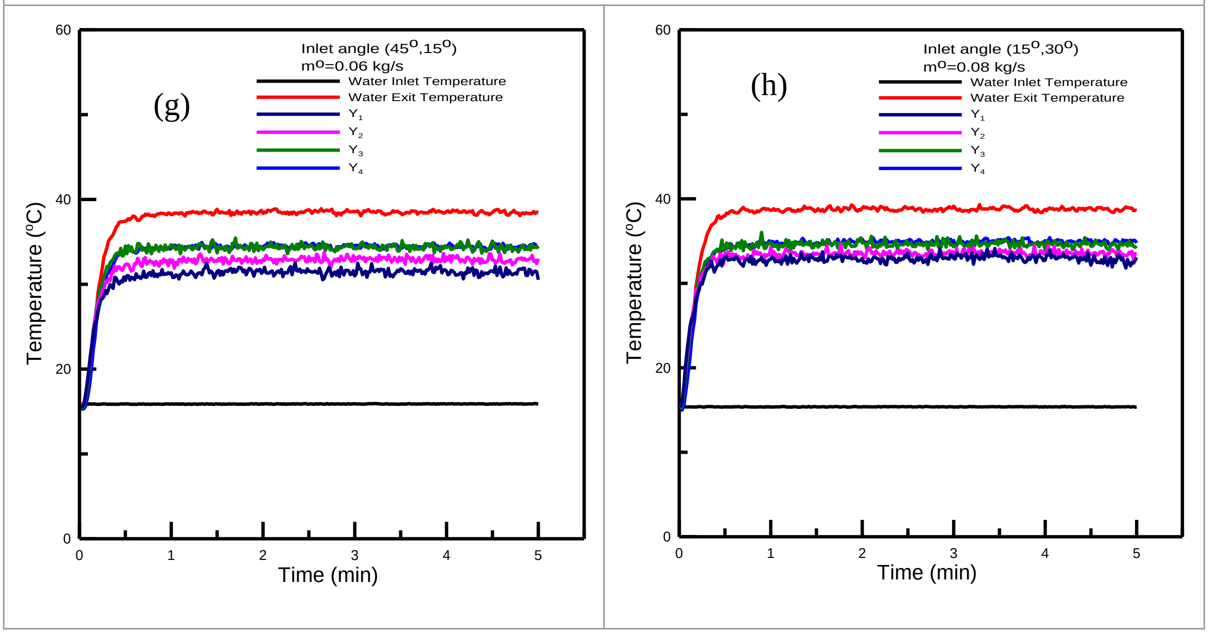

Figure 4-3 Temperature profiles of the draw-off water and temperature distributions of the water along the height of the tank (0.08 kg/s) (continue)

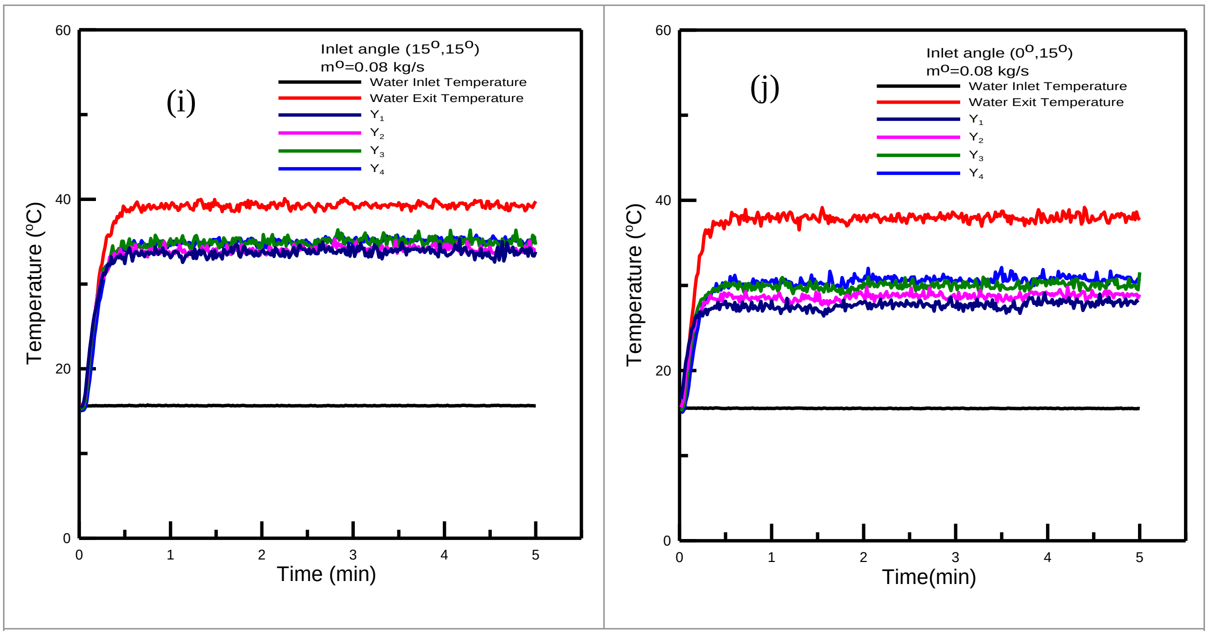

Y_1= 40 mm , **Y2**= 80 mm, **Y_3**= 120 mm and **Y_4**= 160 mm from the bottom of the water tank

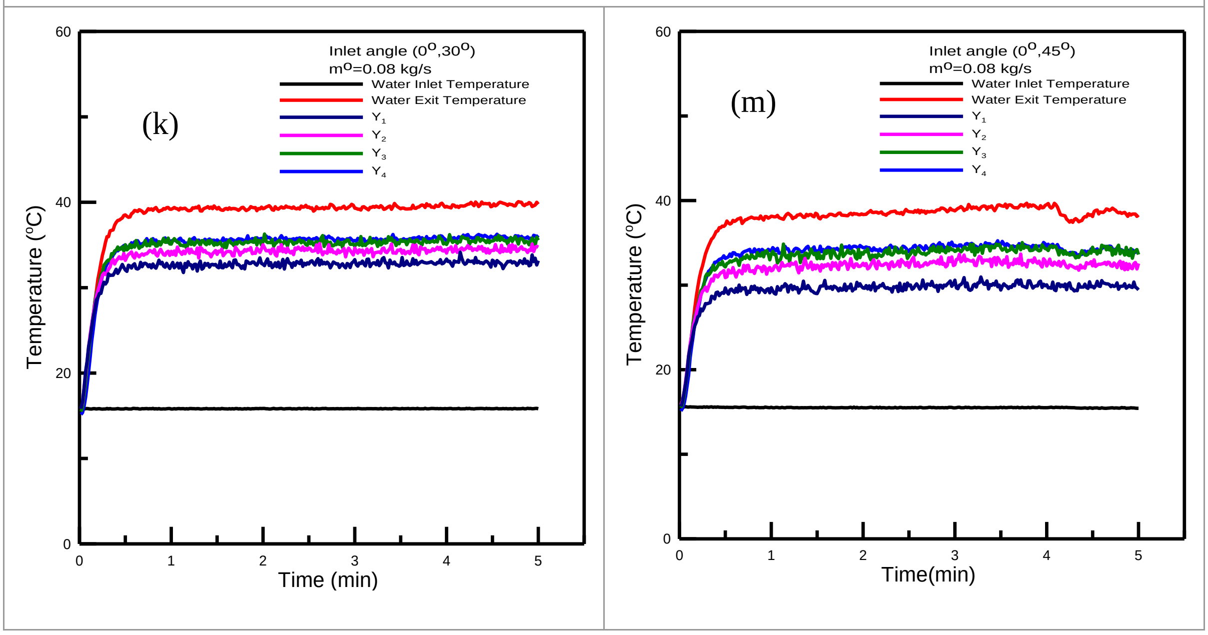

Figure 4-3 Temperature profiles of the draw-off water and temperature distributions of the water along the height of the tank (0.08 kg/s)

Figure 4-4(a) indicates that the heating tank with inlet angle of (30°, 0°) has the highest average transient water temperature in the tank during discharging process, and the heating tank with inlet angle (0°, 15°) has the lowest temperature as shown in Figure 4-4.b

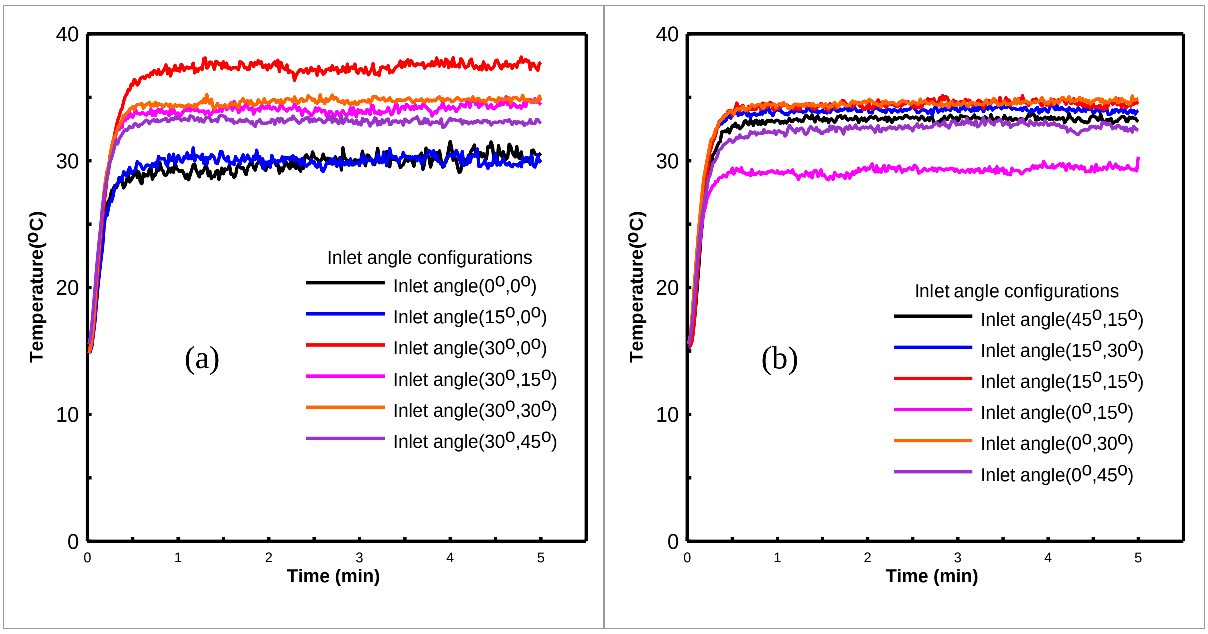

Figure 4-4 Average water temperature in the tank during draw-off (0.08 kg/s)

Figure 4-5 shows the mean of the transient temperature of the water in the tank during the discharging process for m^o=0.10 kg/s. The heater with inlet angles such as (45°, 15°) and (15°, 30°) performs well because of the water outlet temperature is constant during the operation also the inlet cold water is heated gradually as shown in Figures 4-5(g and h).

The results for m^o=0.10 kg/s confirm the previous results for low flow rate that the heater with the inlet angles of (0°, 0°), (15°, 0°) and (30°, 0°) do not perform well as there are relatively high fluctuation on the outlet hot water temperature as shown in Figures 4-5(a, b and c).

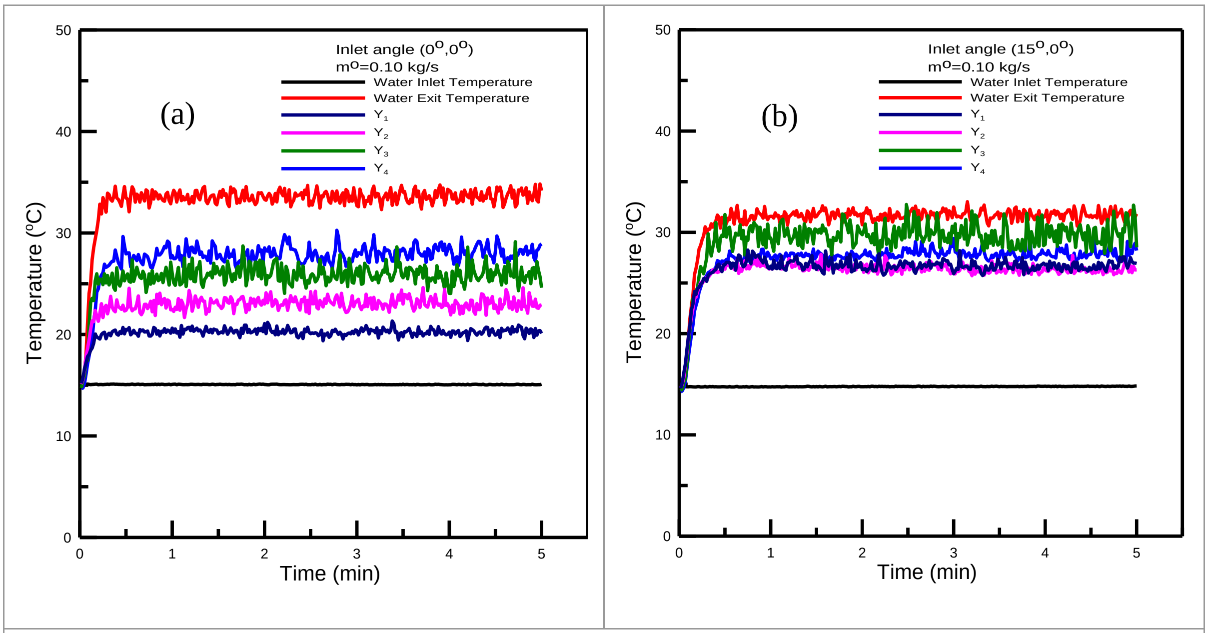

Y_1= 40 mm , **Y2**= 80 mm, **Y_3**= 120 mm and **Y_4**= 160 mm from the bottom of the water tank

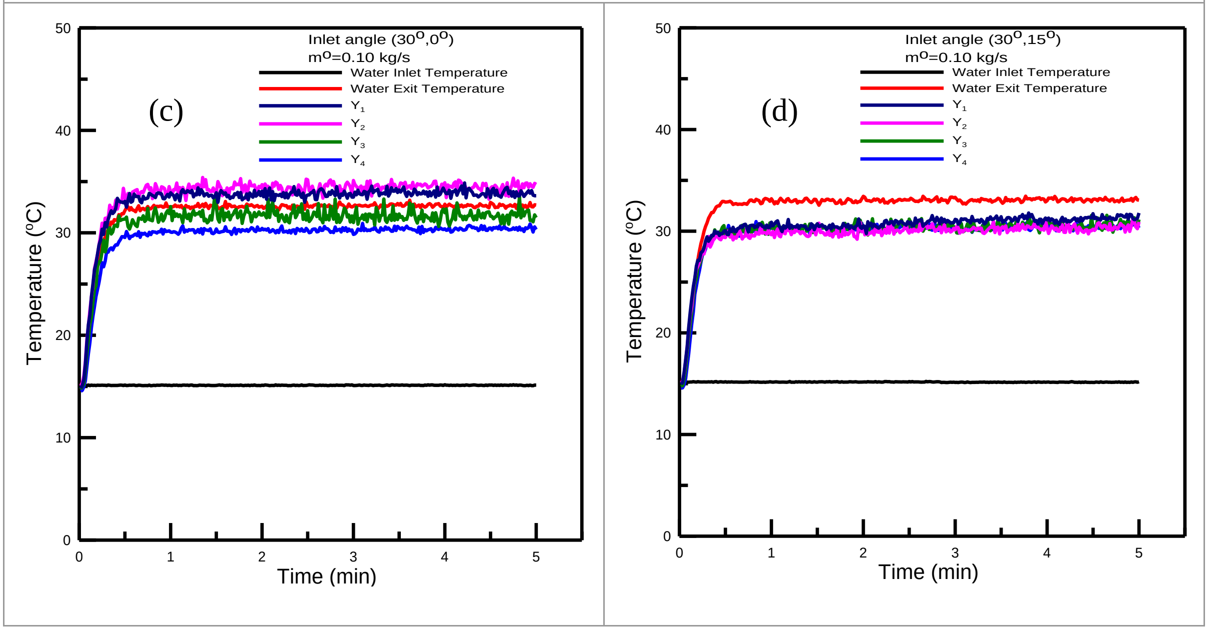

Figure 4-5 Temperature profiles of the draw-off water and temperature distributions of the water along the height of the tank (0.10 kg/s) (continue)

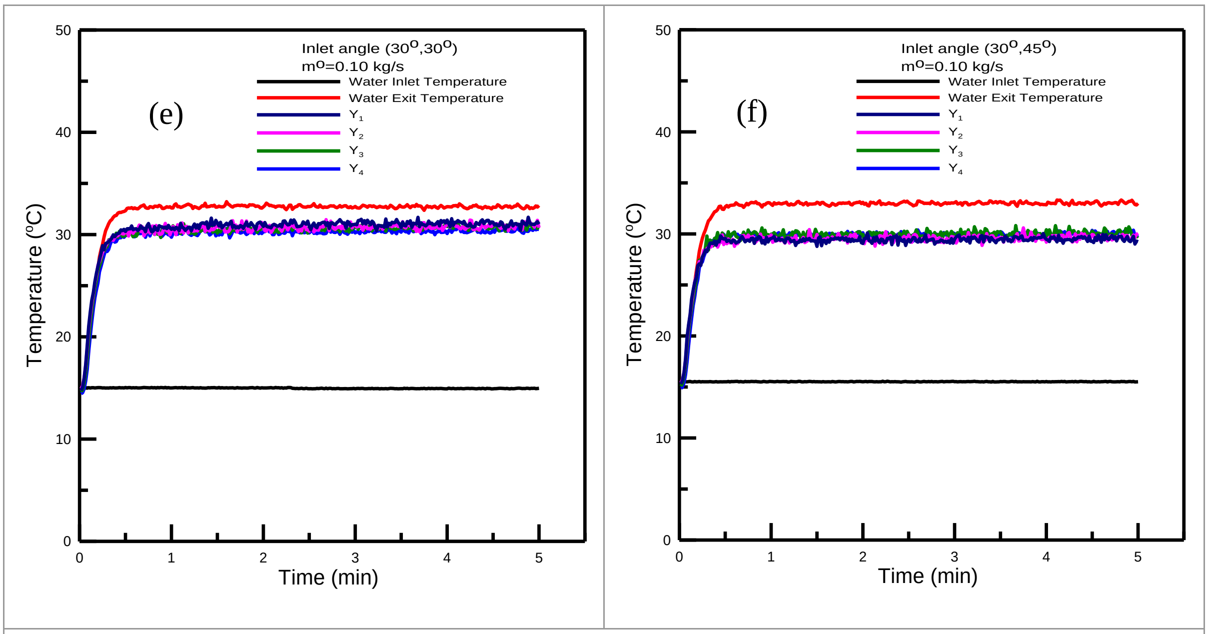

Y_1= 40 mm , **Y2**= 80 mm, **Y_3**= 120 mm and **Y_4**= 160 mm from the bottom of the water tank

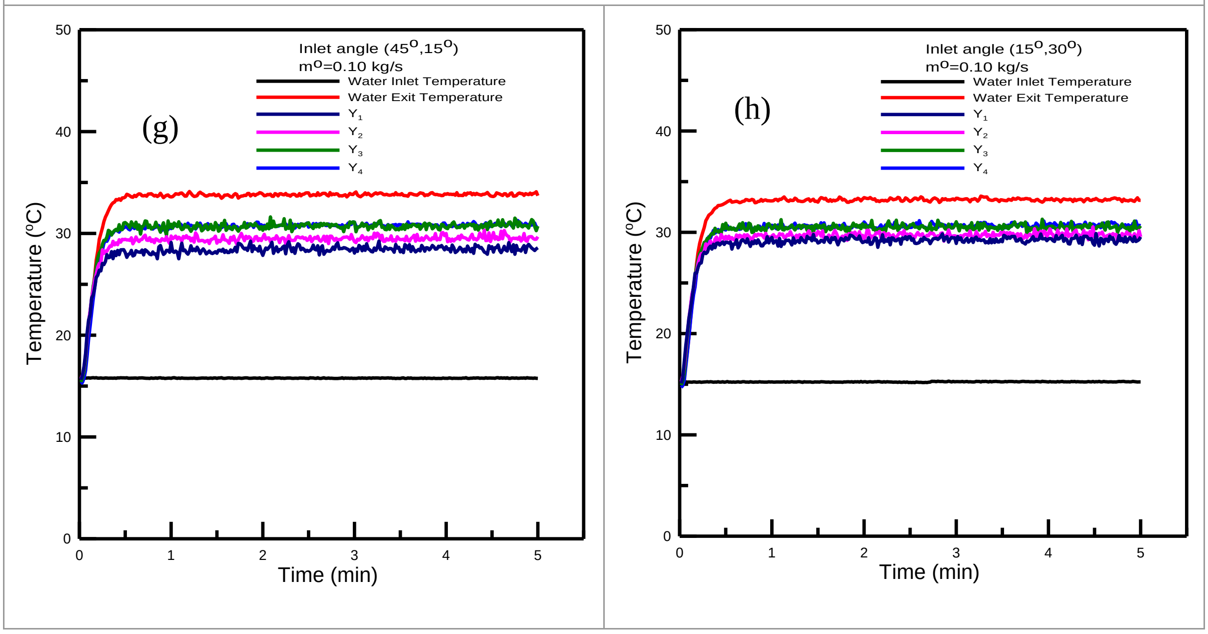

Figure 4-5 Temperature profiles of the draw-off water and temperature distributions of the water along the height of the tank (0.10 kg/s) (continue)

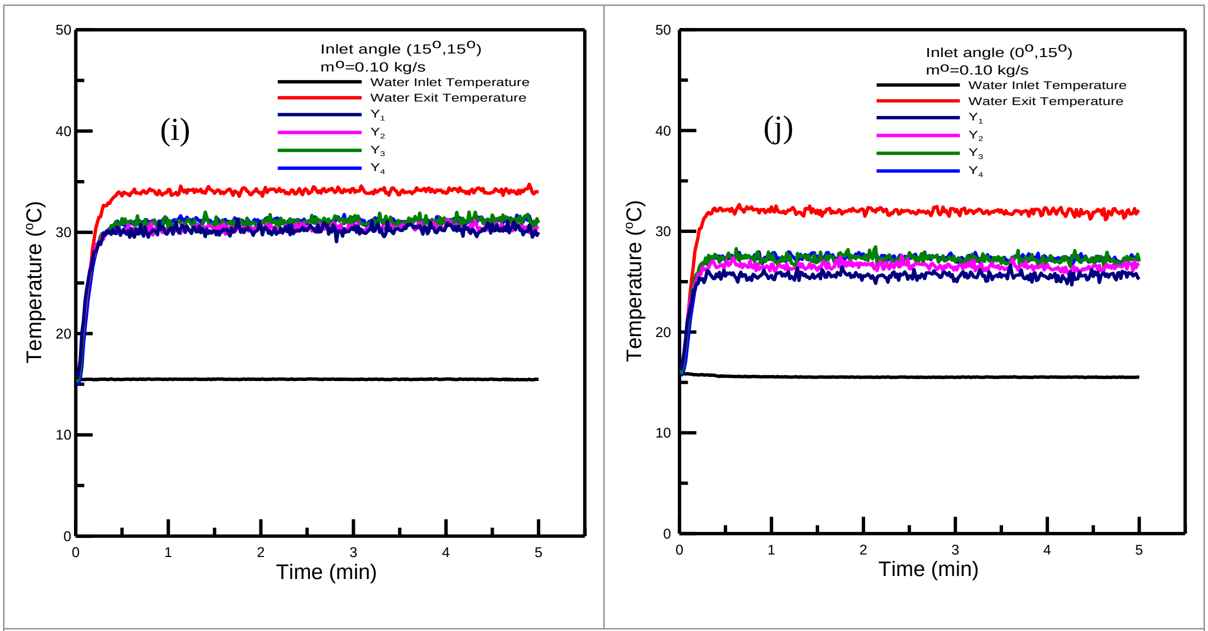

Y_1= 40 mm , **Y2**= 80 mm, **Y_3**= 120 mm and **Y_4**= 160 mm from the bottom of the water tank

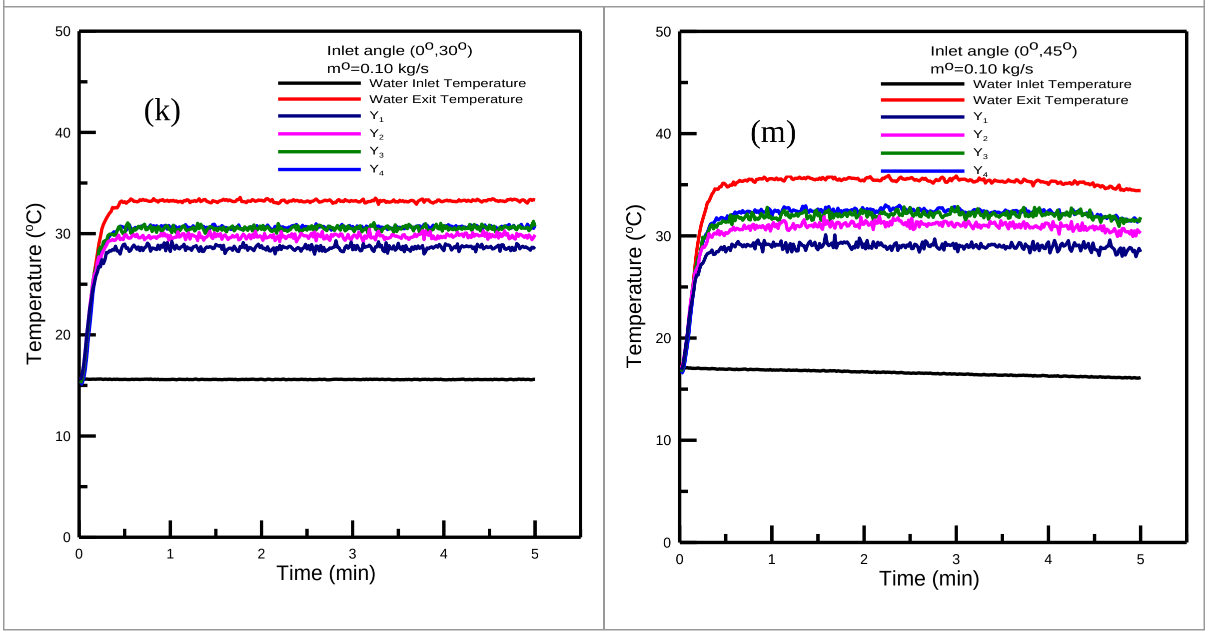

Figure 4-5 Temperature profiles of the draw-off water and temperature distributions of the water along the height of the tank (0.10 kg/s)

Figure 4-6.a shows that, the mean of the transient temperature of the water in the tank during the discharging process for the inlet angle of (30º, 0º) is higher in comparison with the other inlet ports and heating tank with inlet angle (0º, 15º) has the lowest ones as shown in Figure 4-6.b.

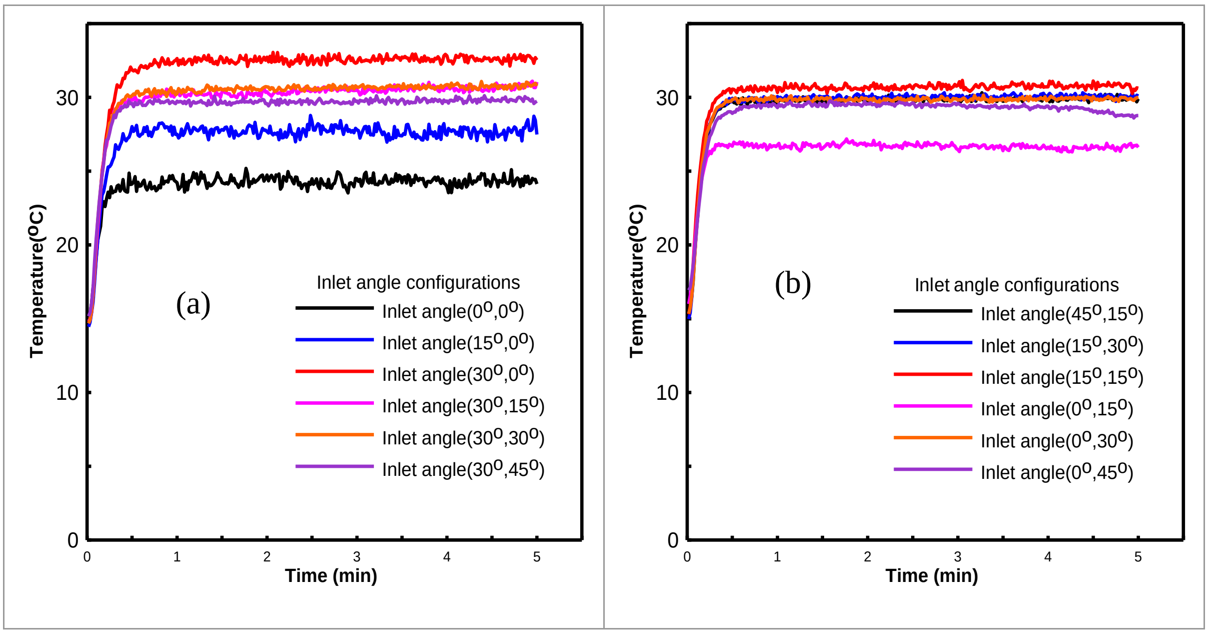

Figure 4-6 Average water temperature in the tank during draw-off (0.10 kg/s)

Finally, The results in Figures 4-7 and 4-8 for mº=0.12 kg/s confirm the previous results again, that the heater with inlet angles of (0º, 0º) and (30º, 0º) provide the worst thermal performance for all of the discharging flow rates, as well as the hot water outlet temperature.

The various discussions above have affirmed the dominant role of cold water inlet design in maximizing mixing inside such small tanks of domestic TEWHs. The above performance characteristics could be explained that the horizontally inclined inlet ports such as (0º, 30º) and (0º, 45º) perform better than vertically inclined ports such as (15º, 0º) and (30º, 0º) because they provide better water mixing which help to releases the heat uniformly from the heating elements, the horizontally inclined inlet ports have a great ability to create swirl flow around the heating elements and increases water mixing in the tank, Therefore, TEWHs equipped with horizontal inclined inlet angles exhibited best thermal performances, and results in an uniform outlet water temperature lead to which have good impact on end use and decreases control complexity.

The above discussed performance characteristics can be summarized to:

1. For horizontally inclined inlet angles, cold water jet momentum effect is stronger than that of vertically inclined inlet jet, because when the jet impinges on the opposite wall the velocities are significantly reduced. The flow diverges in all directions and complex circulation patterns can be observed (Toyoshima and Masaki, 2013).
2. When vertically inclined inlet water jet impinges the bottom wall of the tank, it leads to decrease the water momentum and direct water flow upward. So, the velocity of the jet will fall gradually because the flows are transited from ‘‘the tangential flow jet’’ to ‘‘the impinging jet’’ and leads to decreasing the jet velocity.
3. For horizontally inclined water jet, no short circuiting or stagnant zones are expected due to a large recirculation zone occurs above the jet and leading to homogeneous and efficient distribution of water in the heating tank.
4. The fluctuations in the outlet water temperature is due to the turbulence created by the water inflow are greater when water come through the elbow.
5. Based on the evaluation criteria, it is concluded that tankless heater with horizontal inclined inlet angle has the best performance as the temperature fluctuations of outlet water are less than $\pm 1^oC$ in comparison with the tankless heater with vertical inlet angle which the temperature fluctuations are more than $\pm$ 3^oC and more frequent.

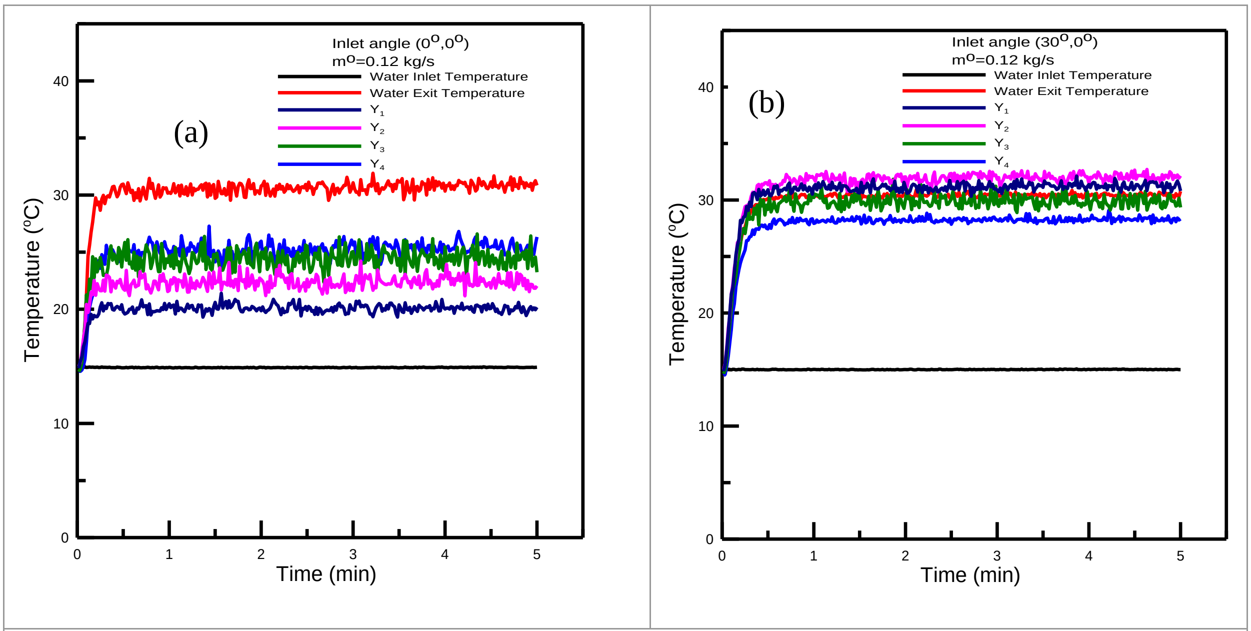

Y_1= 40 mm , **Y2**= 80 mm, **Y_3**= 120 mm and **Y_4**= 160 mm from the bottom of the water tank

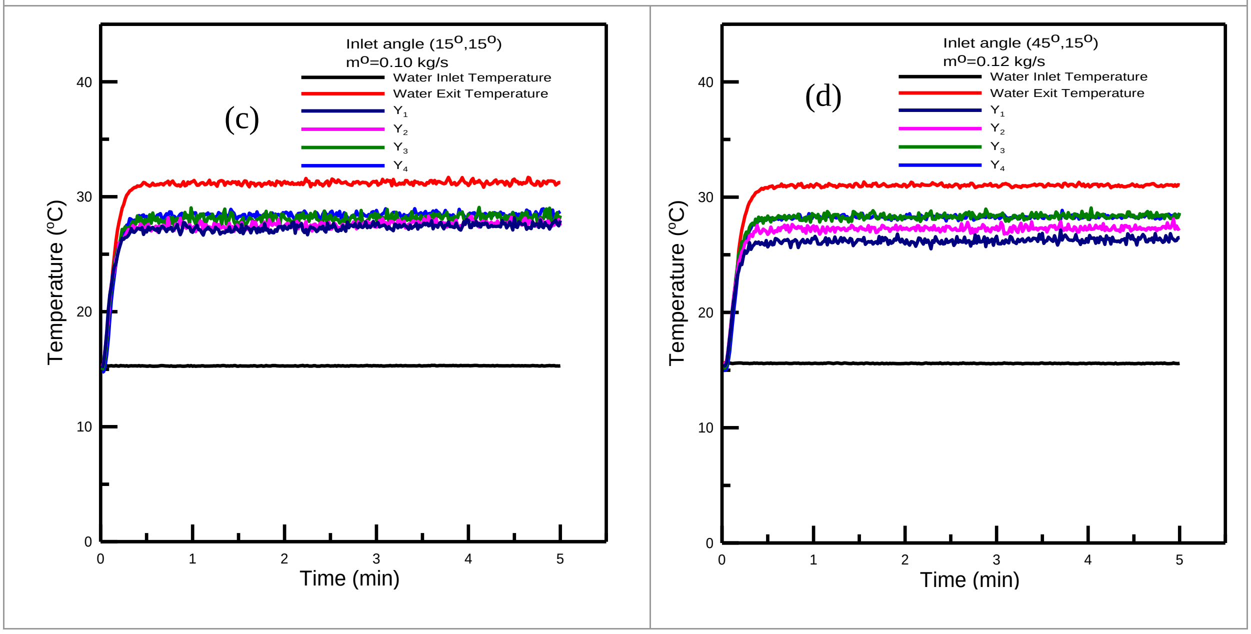

Figure 4-7 Temperature profiles of the draw-off water and temperature distributions of the water along the height of the tank (0.12 kg/s) (continue)

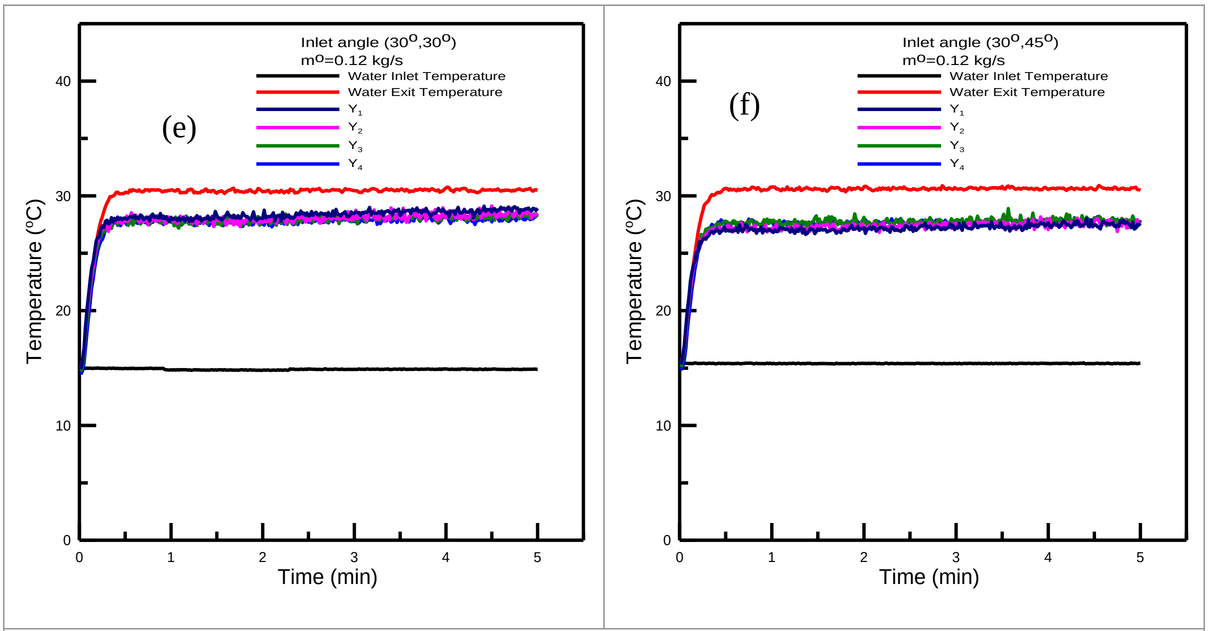

Y_1= 40 mm , **Y2**= 80 mm, **Y_3**= 120 mm and **Y_4**= 160 mm from the bottom of the water tank

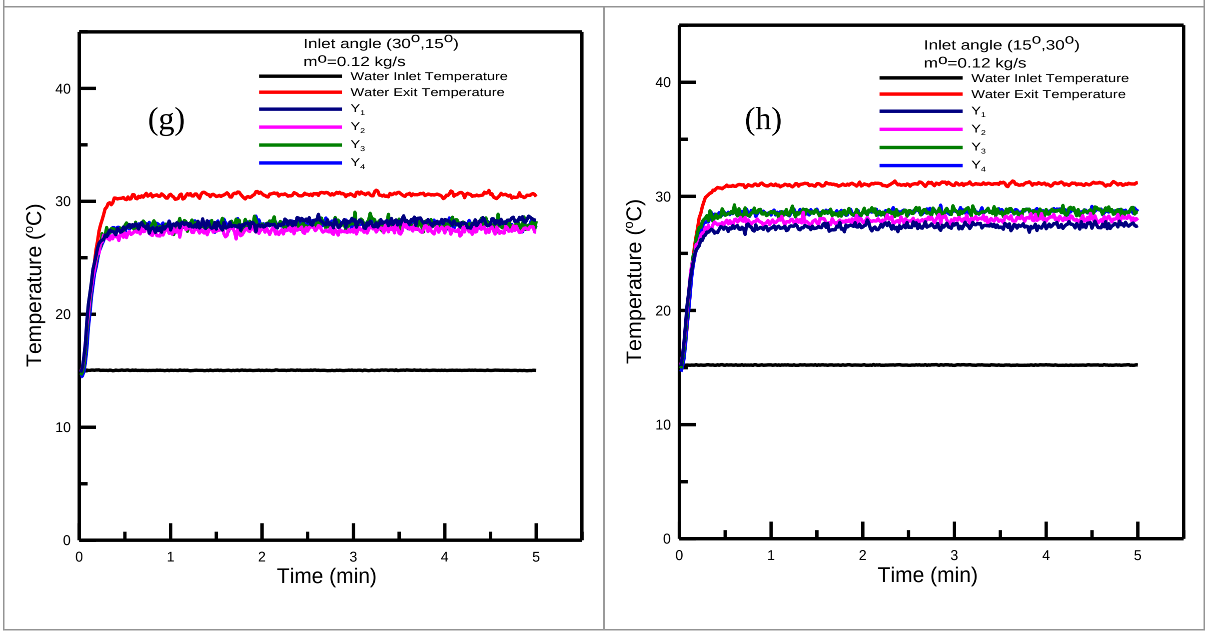

Figure 4-7 Temperature profiles of the draw-off water and temperature distributions of the water along the height of the tank (0.12 kg/s) (continue)

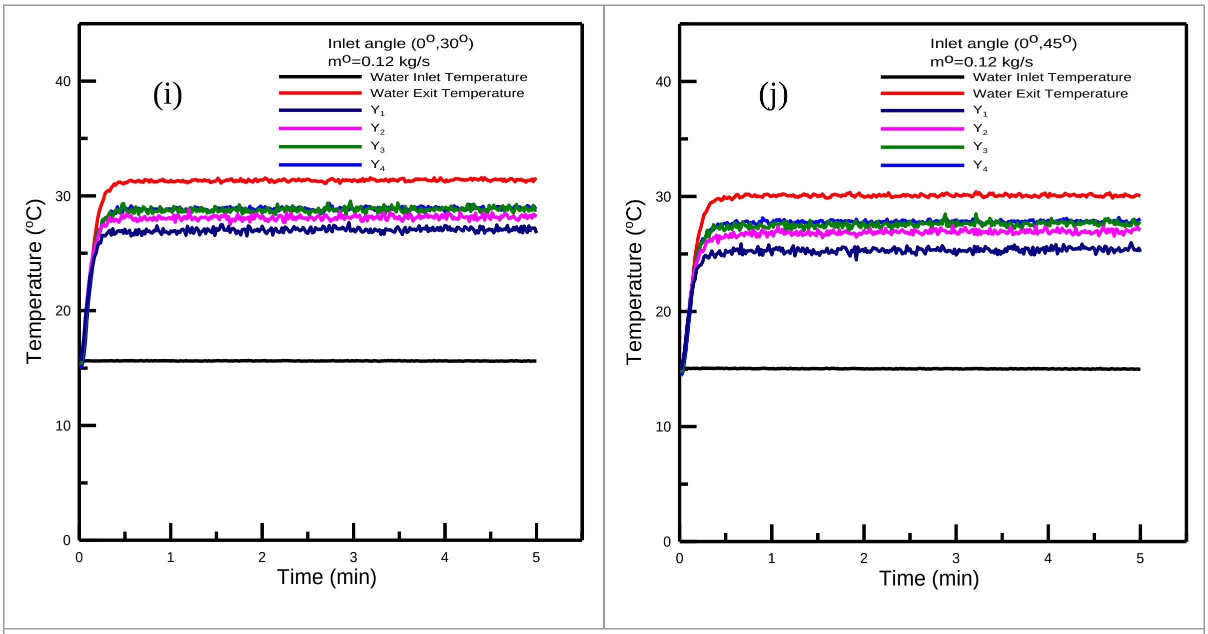

Y_1= 40 mm , **Y2**= 80 mm, **Y_3**= 120 mm and **Y_4**= 160 mm from the bottom of the water tank

Figure 4-7 Temperature profiles of the draw-off water and temperature distributions of the water along the height of the tank (0.12 kg/s)

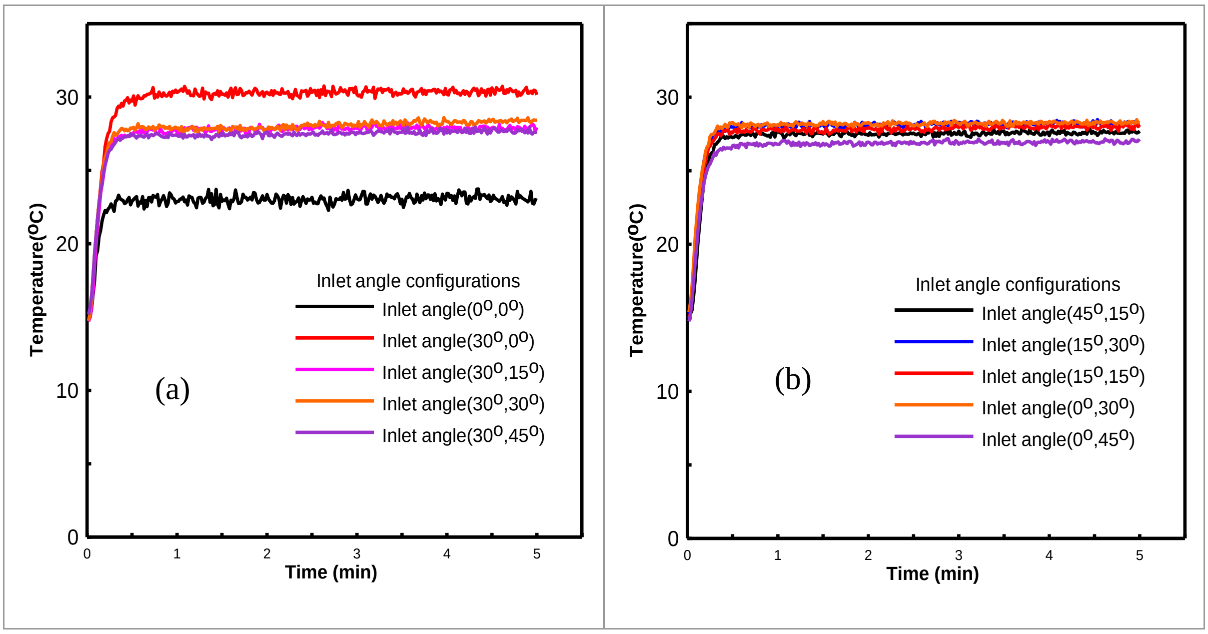

Figure 4-8 Average water temperature in the tank during draw-off (0.12 kg/s)

4.3. Conclusions

Experiments were carried out to investigate the effect of the inlet angles on the thermal performance tankless water heater TWHs. Twelve different inlet geometries were tested four discharge rates of 0.06, 0.08, 0.10 and 0.12 kg/s. The following conclusions can be drawn from the experimental results:

1. Thermal performance of the tankless water heater is quantified in terms of outlet water temperature and transient temperature distribution in the heating tank.
2. The inlet design plays a key role in determining the thermal performance of such type TWHs.
3. The transient temperature-distributions in the tankless water heater during hot water discharging process indicated the effectiveness of the horizontal inlet in promoting thermal stratification inside such small size tanks, this had a direct impact on the heater performance as indicated by the uniform heating values.
4. The two inlet designs of (0^o, 30^o) and (0^o, 45^o) are successful in promoting good thermal performance inside the heating tanks of the TWHs and the outlet hot water is at constant and uniform temperature.
5. The observed differences in the performance with the other inlet angles were due to the variations in mixing intensity produced by each inlet design.
6. The fluctuation on the outlet temperature has dropped by 90% for tankless heater with inlet angle (0^o, 30^o) and (0^o, 45^o).
7. As a result, it is recommended that for use tankless heater with horizontal inclined inlet angle (0^o, 30^o) and (0^o, 45^o) as the fluctuation on the outlet temperature has been dropped by 90% compared to conventional design.

Therefore, it is finally concluded that the horizontally inclined angle port configuration provides the best performance among the various ports arrangements tested and it is recommend for practical use.

Chapter (5)

5. Numerical Simulation

In chapter 4, experiments were carried out to study the effect of inlet angle configuration on the thermal performance of tankless electric water heater, the obtained experimental results confirm that the effect of inlet angle configuration on the water temperature distribution in the heating tank and hot water outlet temperature is substantial, in addition the experimental results have been concluded that cold water horizontally inclined inlet angles performed better than vertically inclined inlet angles.

However, the surface temperatures on the heating element coils are still unknown and there are difficulties to predict it in the experimental work due to the complexity of the water heating system.

In the recent years, CFD (Computational Fluid Dynamics) has become one of the basic methods or approaches that can be employed to solve complex problems in fluid dynamics and heat transfer. There are many advances of CFD, firstly, CFD presents the perfect opportunity to study specific terms in the governing equations in a more details fashion (Tu et al., 2013); secondly, CFD complements experimental and analytical approaches by providing an alternative cost-effective means of simulating real fluid flow. Particularly, CFD substantially reduces the time and costs in design and production compared with experimentally based approaches, furthermore CFD can provide detailed visualization and comprehensive information when compared to the analytical and experimental fluid dynamics.

5.1. CFD Solution Procedure

In this work, commercial CFD package FLUENT has been used for simulation (FLUENT, 2013), FLUENT has capability of analyzing a wide range of fluid flow problems including incompressible and compressible flows, laminar and turbulent flows, viscous and inviscid flows, Newtonian and non-Newtonian flows, single-phase and multi-phase flows, etc. In addition, both steady-state and transient analyses can be performed. Moreover, FLUENT provides solution to heat and mass transfer problems. Conduction and convection can be easily implemented by adding one extra energy equation. Various models are available to simulate more complex phenomena involving radiation. Species transport can be modeled by solving equations, governing convection, diffusion and reaction.

The codes provide a complete CFD analysis, consisting of three main elements:

- Pre-processor
- Solver
- Post-processor

Figure 5-1 presents a framework that illustrates the interconnectivity of three aforementioned elements with the CFD analysis; the functions of these three elements are examined in more details in the subsequent sections.

Figure 5-1 The interconnectivity functions of the three main elements with a CFD analysis framework (Tu et al., 2008)

5.2. Problem Setup-Pre-Process

5.2.1. Creation of geometry

The first step in any CFD analysis is the definition and creation of the geometry of the flow region. A base 3D model was developed to reflect the real dimensions of the heating tank used in the experiment. All the numerical models that have been studied in this chapter are derived from this 3D model to demonstrate the impact of various configuration and operating conditions on the heater thermal performance. This 3D model has been built up based on the following physical dimensions as listed in the Table 5-1:

Table 5-1 Parameters of the water heater

Parameter	Value	Parameter	Value
Hot Water Tank	0.67 L	Electric Heater Power	7682.5 W
External Tank Height	174.0 mm	Inlet Tube Diameter	10.0 mm
Internal Tank Diameter	73.2 mm	Outlet Tube Diameter	10.0 mm
Internal Tube Height	170.0 mm	Inlet Water Temperature	10 $^{\circ}$C
Bottom Heater Volume	2.96 cm^3	Upper Heater Volume	3.04 cm^3

Figure 5-2 provides a schematic view of the water heating tank, the heating tank has an aspect ratio (AR, height/diameter) of 2.38 , the heater geometry has been generated by "Solid works" is reproduced by using “Design Modular” into five computational zones for an adaptive meshing.

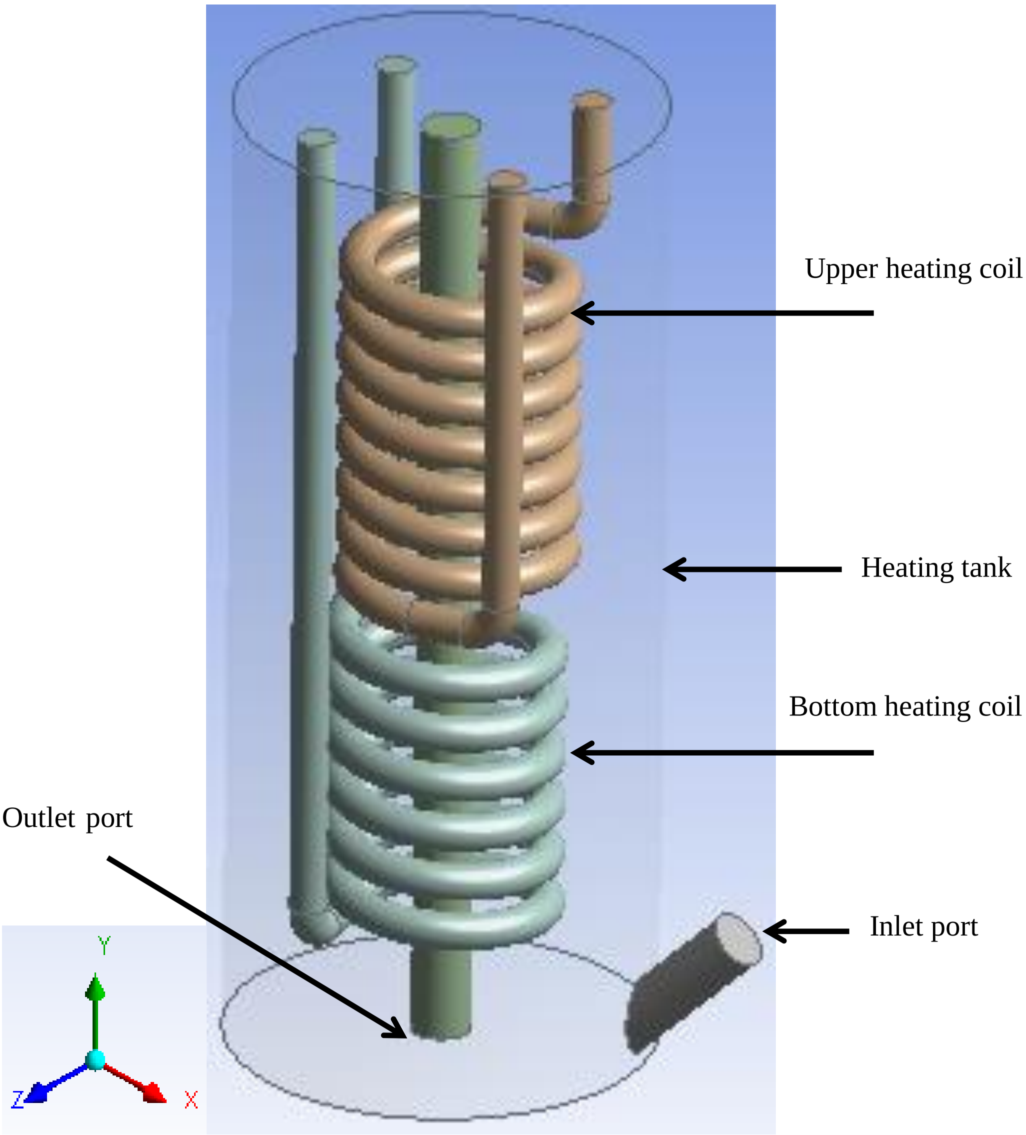

Figure 5-2 Computational domain

In this simulation, tank models utilizing ten inlet angles have been investigated. Varied from 0° to 45°, in both horizontal and vertical directions independently and simultaneously, where inlet angle (15°, 30°) means that it was rotated 15° in the vertical direction and 30° in the horizontal direction as appeared in Figure.5-3.

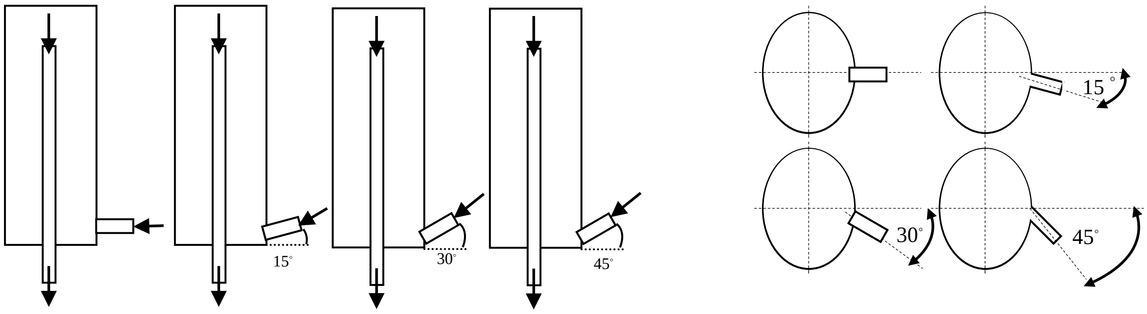

Figure 5-3 Different inlet angles

5.2.2. Mesh generation

The second step, mesh generation, is one of the most important steps in the pre-process stage after the definition of the domain geometry. A high quality mesh is very important for successful numerical simulations.

CFD required the subdivision of the domain into a number of smaller, non-overlapping subdomains in order to solve the flow physics within the domain geometry that has been created. This results in the generation of a mesh (or grid) of cells (elements or control volumes) overlying the whole domain geometry. The essential fluid flows that are described in each of these cells are usually solved numerically, so that the discrete values of the flow properties, such as the velocity, pressure, temperature, and the transport of interest, are determined (Tu et al., 2008).

However, for the 3D simulation, a small change in the size of element will lead a substantial increase in the number of elements. That will results in a significant increase of computational time. In order to balance the accuracy of the simulations and calculations time, an optimum size of mesh need to be chosen.

Due to the complexity of the flow domain, the computational domain has been modeled as five distinct volumes: a large cylinder for the water heater tank, inlet and inner outlet pipes and two helical cylinders for the electric heater coils. This allows the water tank and electric heater coil to be modelled with relatively fine elements, while the inlet / output pipes could have small number of elements. Data are transferred between the two zones by the connective interface. Meshing the five volumes separately allows a dramatic reduction of the amount of the calculating elements in the domain, leading to realistic computational time while maintaining the accuracy of the numerical simulations.

Clustering also plays a very significant role in numerical simulations in heat transfer and fluid flow analysis. In order to increase the accuracy of the results, the channel regions adjacent to the walls were clustered carefully. An inflation method was applied at the heating elements wall, inlet and outlet pipes. The boundary layers on walls of tank, upper and bottom surface are refined by putting several inflation layers. The main tank volume and electric heater coil have been meshed into a combination of unstructured tetrahedral and hybrid elements using the T grid scheme. Considerable time was devoted trying to apply the unstructured tetrahedral and hybrid schemes to this volume due to the fact that it greatly reduces the instances of skewed elements causing inaccurate results. The detailed grid systems of computational domain are presented in Table 5-2 below.

Table 5-2 Details of mesh

Zone	**Cell type**
Upper heating element	Tetrahedral
Bottom heating element	Tetrahedral
Inlet port	Prism with triangular face
Outlet port	Prism with triangular face
Water tank	Mixed

These three different levels of meshing are referred as “Coarse”, “Fine” and “Finer” mesh. The spectral convergence test and computational performance are performed on the three meshes.

The total number of mesh in the computational domain and in these tube zones are listed in Table 5-3 for a “Coarse”, a “Fine” and a “Finer” level mesh. The number of elements in the heating tank is calculated in FLUENT for each mesh. Number of elements for the “Finer” meshes doubles compared to that for the “Coarse” mesh. Number of elements in the heating tank can be increased significantly with a slight increase of element in the fluid and solid regions.

Table 5-3 Number of elements in three different levels of mesh

Mesh	**Num. of elements in total domain**
Coarse	≈ 1.5 million
Fine	≈ 2.5 million
Finer	≈ 3.0 million

The mesh structure near the heating elements region, at the interface and in the inlet regions is displayed in Figure 5-4.

A grid independence test was carried out to determine the optimal number of cells to use for the CFD simulations and has been concluded that the fine mesh is sufficient to satisfy the spectral convergence. Fine mesh is used to perform the simulations to obtain the results presented in the next sections for various flow conditions.

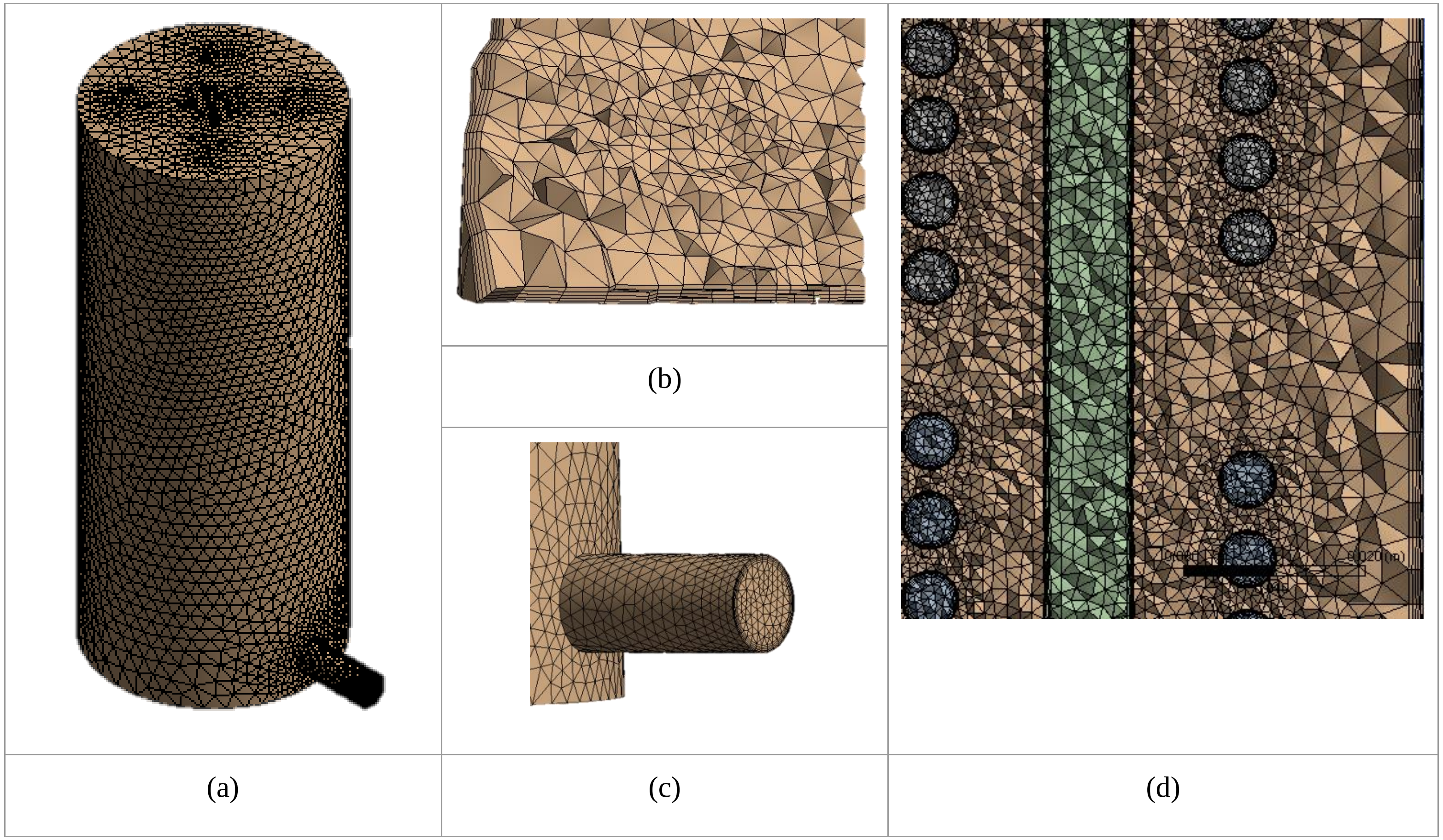

Figure 5-4 Mesh structure (a) Mesh structure of the computational domain, (b) near the tank wall, and (c) in the inlet and (d) at the interface

5.2.3. Selection of physics and fluid properties

Many industrial CFD flow problems may require solutions for very complex physical flow process such as heat transfer in fluid flow, it is important that setting up the flow physics is also accompanied by ascertaining what fluid is used with the flow domain. Therefore, the appropriate properties need to be assigned to correctly define the particular fluid in the pre-process step.

5.2.4. Specification of boundary conditions

It is important to define boundary conditions that mimic the real physical representation of the fluid flow in a solvable CFD problem.

This step deals with the specification of permissible boundary conditions that are available for impending simulation, evidently, where inflow and outflow boundaries exist with the flow domain, appropriate boundary conditions also need to be assigned for external stationary solid wall boundaries that border the flow geometry and the surrounding walls of possible internal obstacles with the flow domain. The boundary conditions used in this simulation are demonstrated in Figure 5-5.

The full set of boundary conditions imposed on the flow field and the thermal boundary conditions are listed in Table 5-4.

5.3. Mathematical Model and Numerical Methods

In this investigation a three-dimensional numerical simulation of the conjugate heat transfer was conducted using the CFD code FLUENT 13. The modeling was carried out in order to predict and explain the experimental observations. The CFD modeling involves numerical solutions of the conservation equations for mass, momentum and energy. These equations for incompressible flows can be written as follows.

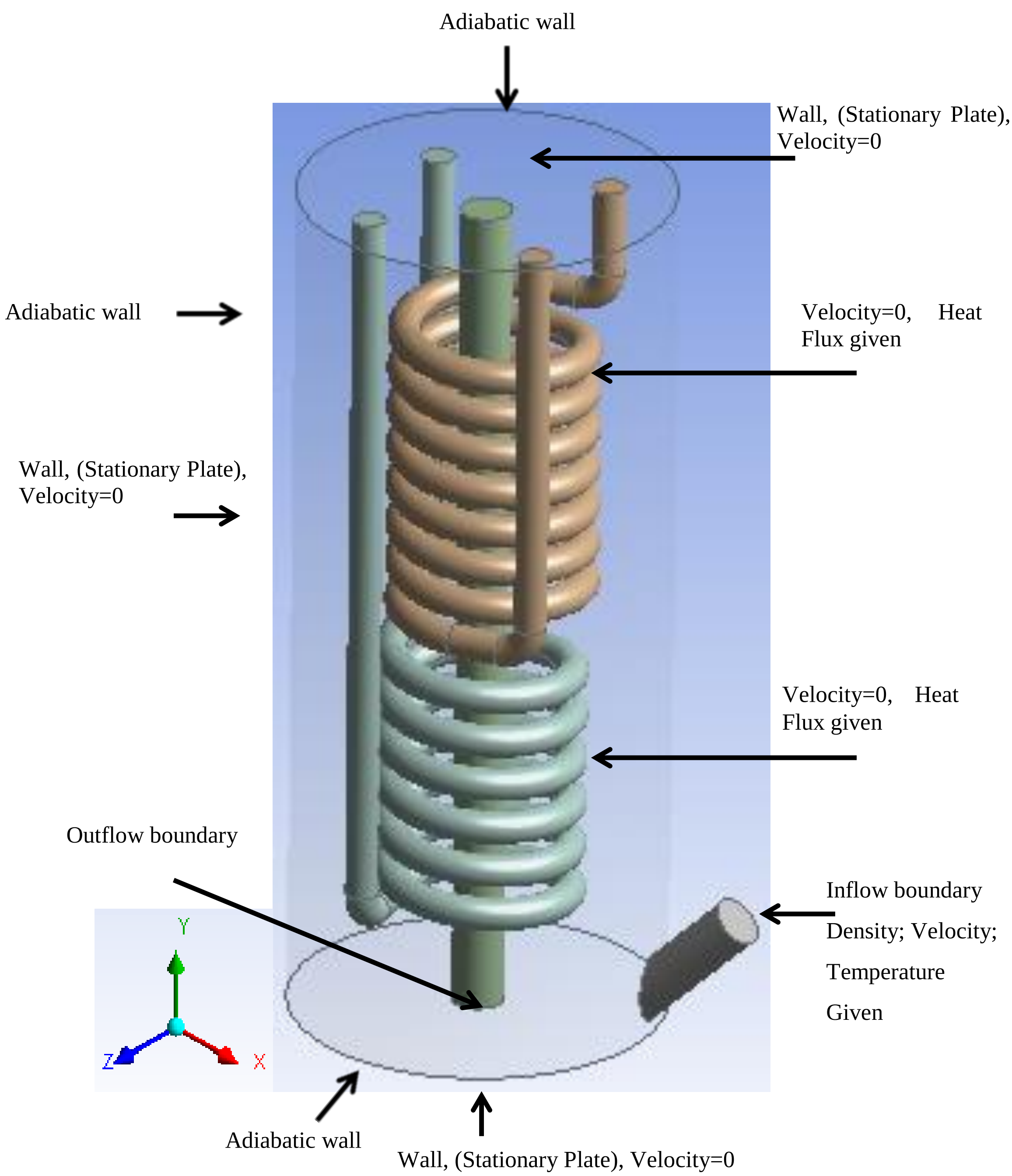

Figure 5-5 Boundary conditions for computational domain

5.3.1. Governing equations

Mass conservation:

$$\frac{\partial \rho}{\partial t} + \nabla.(\rho \vec{u}) = 0 \tag{5-1}$$

Momentum conservation:

$$\frac{\partial (\rho \vec{u})}{\partial t} + \nabla.(\rho \vec{u}\vec{u}) = \rho g - \nabla P + \nabla.(\bar{\tau}) \tag{5-2}$$

Energy conservation

$$\frac{\partial (\rho e)}{\partial t} + \nabla.(\vec{u}(\rho e + P)) = \nabla.(k_{eff}\nabla T + (\bar{\bar{\tau}}_{eff}.\vec{u})) \tag{5-3}$$

Where

$$\bar{\bar{\tau}} = \mu\left((\nabla\vec{u} + \nabla\vec{u}^{T}) - \frac{2}{3}\nabla.\vec{u}I\right) \tag{5-4}$$

In the case of turbulent flow, the random nature of flow precludes computations based on a complete description of the motion of all the fluid particles. Turbulent flows are characterized by fluctuating velocity fields. These fluctuations mix the transported quantities such as momentum and energy and can be of small scale and high frequency. Therefore, turbulent flows are too computationally expensive to be simulated directly in practical calculations.

On the other hand, the instantaneous exact governing Equations. (5-1) – (5-4) can be averaged in time and in space or otherwise manipulated to remove these small scales, resulting in a modified set of equations that are computationally easier to solve. However, the modified equations contain additional unknown variables and additional turbulence equations are needed to determine these variables in terms of known quantities. In the present study, the

RNG ((Versteeg and Malalasekera, 1995) version of *k–ε* turbulence model (Yakhot and Orszag,1986) with enhanced wall functions for the near wall treatment were used to model the turbulent flow regime. The following equations were used for this purpose:

$$\mu_{eff} = \mu + \mu_t, \;\; \mu_t = \rho C_\mu \frac{k^2}{\varepsilon} \tag{5-5}$$

$$\frac{\partial(\rho k)}{\partial t} + \frac{\partial}{x_i}(\rho k u_i) = \frac{\partial}{x_i}\left[\frac{\mu_{eff}}{\sigma_k}\frac{\partial k}{\partial x_i}\right] + \mu_t\left(\frac{\partial u_i}{\partial x_j} + \frac{\partial u_j}{\partial x_i}\right)\frac{\partial u_i}{\partial x_j} - \rho\varepsilon \tag{5-6}$$

$$\frac{\partial(\rho \varepsilon)}{\partial t} + \frac{\partial}{x_i}(\rho \varepsilon u_i) = \frac{\partial}{x_i}\left[\frac{\mu_{eff}}{\sigma_\varepsilon}\frac{\partial \varepsilon}{\partial x_i}\right] + C_{1\varepsilon}\frac{\varepsilon}{k}\mu_t\left(\frac{\partial u_i}{\partial x_j} + \frac{\partial u_j}{\partial x_i}\right)\frac{\partial u_i}{\partial x_j} - C_{2\varepsilon}\rho\frac{\varepsilon^2}{k} - \alpha\rho\frac{\varepsilon^2}{k} \tag{5-7}$$

$$\propto = C_\mu \eta^3 \frac{1-\frac{\eta}{\eta_0}}{1+\beta\eta^3} \; and \; \eta = E\frac{k}{\varepsilon}, \;\; E^2 = 2E_{ij}E_{ij}, E_{ij} = 0.5\left(\frac{\partial u_i}{\partial x_j} + \frac{\partial u_j}{\partial x_i}\right) \tag{5-8}$$

C_μ, $C_{1\varepsilon}$, and $C_{2\varepsilon}$ are the model constants, and σ_k and σ_ε are the turbulent Prandtl numbers for k and ε, respectively. These constants have the following default values (Launder &Spalding 1972):

C_μ= 0.09, $C_{1\varepsilon}$= 1.44, $C_{2\varepsilon}$= 1.92, σ_k =1.0, and σ_ε=1.3

It should be noted here that the RNG *k–ε* model shows fundamental improvements over the standard *k–ε* model (Launder and Spalding, 1974), since the effects on turbulence of strong streamline curvature, vortices and swirl effect are better taken in account, thus enhancing the final solution accuracy (Habchi and Harion, 2014).

5.3.2. Initialization and solution control

5.3.2.1.Boundary conditions

In order to simulate the conditions observed in the experiments, specific boundary conditions must be provided to the model to begin with, including inlet velocity and temperature, heat flux through the wall, the full set of boundary conditions imposed on the flow field and the thermal boundary conditions imposed on the temperature field are listed in Table 5-4.

Table 5-4 Boundary conditions for flow and heat transfer simulations

	Flow Simulation	Heat Transfer Simulation
Inlet	Uniform velocity, v=**0.764** and **1.27** m/s.	Uniform temperature at 283K
Outlet	Outlet flow, $\frac{\partial u}{\partial x} = 0$	$\frac{\partial T}{\partial x} = 0$
Wall of the tank	Standard no slip wall on no penetration	Adiabatic wall, q"=0 Watt/m^2
Heating element coils	Standard no slip wall on no penetration	**7682.5 W** is considered uniformly distributed on the surface of the heating elements

5.3.2.2.Solution procedure and solver setting

The solver used for the flow computation is the CFD code Fluent, which is based on cell-centered finite volume discretization. The flow equations are solved sequentially with double precision and a second-order upwind scheme for spatial discretization of the convective terms (Warming and Beam, 1976). The diffusion terms are central differenced and second-order accurate. Pressure–velocity coupling is achieved by the SIMPLE algorithm (Patankar,1980).The flow in the near-wall region is solved by a two-layer approach in which the near-wall region is divided into a viscous sub-layer and a turbulent region. These two regions are delimited by the turbulent wall Reynolds number based on the distance normal to the wall y, which is defined as $Re_w = \rho y\sqrt{k}/\mu$. In the viscous sub-layer, for $Re_w < 200$, the one-equation model of (Wolfshtein, 1969) is used, where only the continuity, momentum and turbulent kinetic energy transport equations are solved (Equations (5-2) and (5-3)), and the turbulent dissipation rate ε is related to the turbulence kinetic energy k by an empirical formula defined by Chen and Patel (Chen and Patel, 1988). This approach requires estimation of the wall-adjacent cell size corresponding to an ideal dimensionless wall distance y_c^+ of no more than 4, ensuring that the viscous sub-layer is meshed. Therefore, the size of the cells near the wall region is refined using the tool provided in Fluent, thus refining the near-wall cells for which y_c^+.

The conduction within the heating elements coils is taken into account by solving the heat conduction equation in a solid. Copper was chosen as the material for the heating elements coils.

The working fluid is water, with physical properties assumed independent of temperature, for the simulations, inlet turbulence parameters, such as the inlet kinetic energy and inlet turbulence intensity must be assigned. The turbulence intensity (I_T) is defined as the ratio of the root-mean-square of the velocity fluctuations (u'), to the mean flow velocity, (u_{avg}). The turbulent length scale (L_T) is a physical quantity related to the size of the large eddies that contain the energy in turbulent flows. Also it is a measure of the size of the turbulent eddies that are not resolved. For fully developed turbulent flow these parameters can be obtained as:

$$I_T = \frac{\grave{u}}{u} = 0.016\ \mathrm{Re}^{-\frac{1}{8}} \tag{5-9}$$

$$L_T = 0.07\ D \tag{5-10}$$

The prerequisite processes in the solution procedures that have implications for computational solution is presented in Figure 5-6.

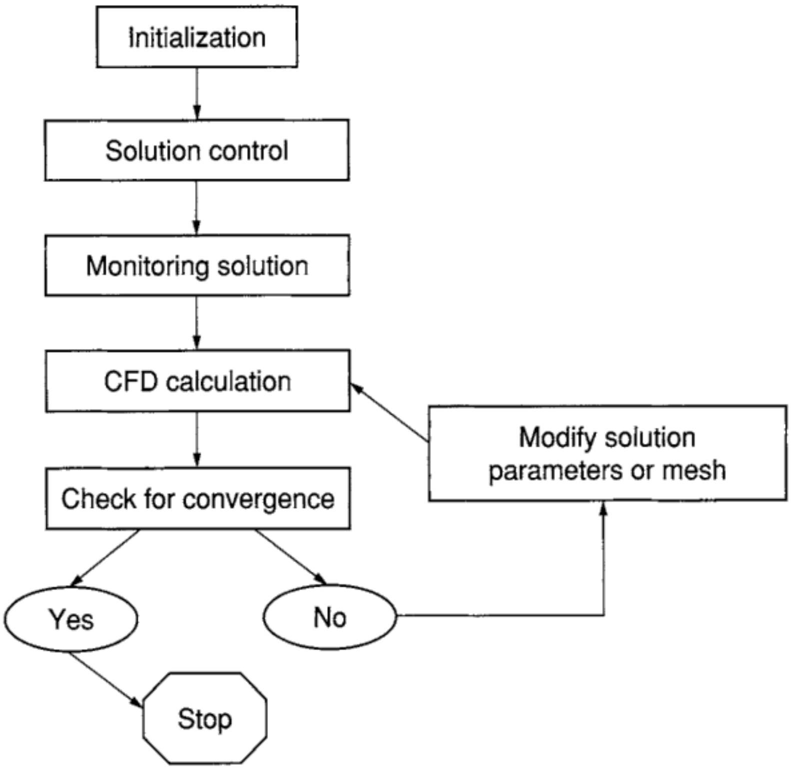

Figure 5-6. An overview of the solution procedure

5.3.2.3.Monitoring convergence

The residual value 10^{-6} is set as the convergence criterion for the solutions of the flow and energy equations in the Equations (5-1) to (5-4) and (5-6). Beyond this value no significant changes were observed in the velocity, temperature fields and turbulence quantities. To ensure that the simulating solution is convergence, the monitor of the residual for the continuity and energy are as shown in Figure 5-7, the final number of iterations was 5000.

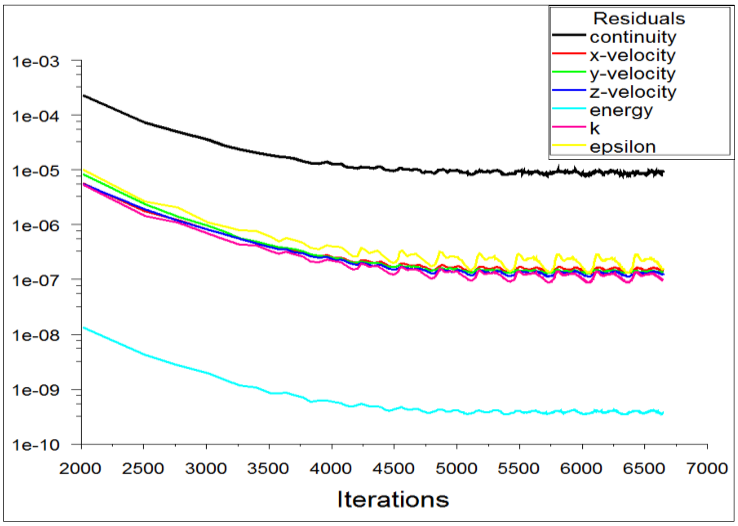

Figure 5-7 Residuals for iterations in the modelling

5.4. Verification of the Numerical Simulation with Experimental Results

The validity of CFD model is assessed by the comparison with the results from the experimental work. The obtained numerical results of outlet water temperature against time are compared with the experimental results, for different mass flow rate m^o=0.06 kg/s and 0.10 kg/s at different inlet angles (0^o, 0^o) and (0^o, 30^o) as shown in Figures 5-8 and 5-9, respectively. A good overall agreement between CFD prediction and experimental data is observed, which are within less than10% of discrepancy. The difference between the present numerical results and the experimental data is slightly high particularly for mass for m^o = 0.06 kg/s and inlet angle (0^o, 0^o). This is believed to be due to experimental uncertainty and flow disturbance .This numerical model was then used for further analyses of different inlet angle configuration of water heating tank

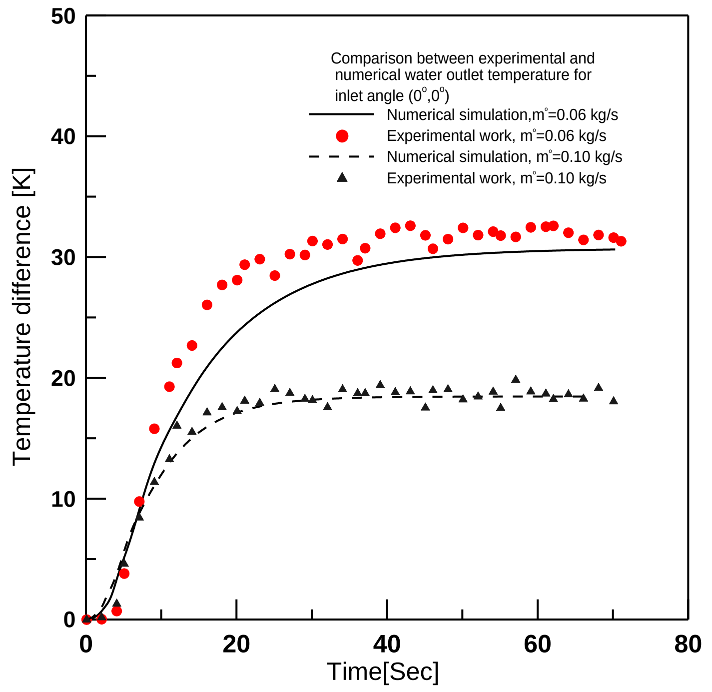

Figure 5-8 Simulated and measured water outlet temperature profiles for inlet angle (0º, 0º)

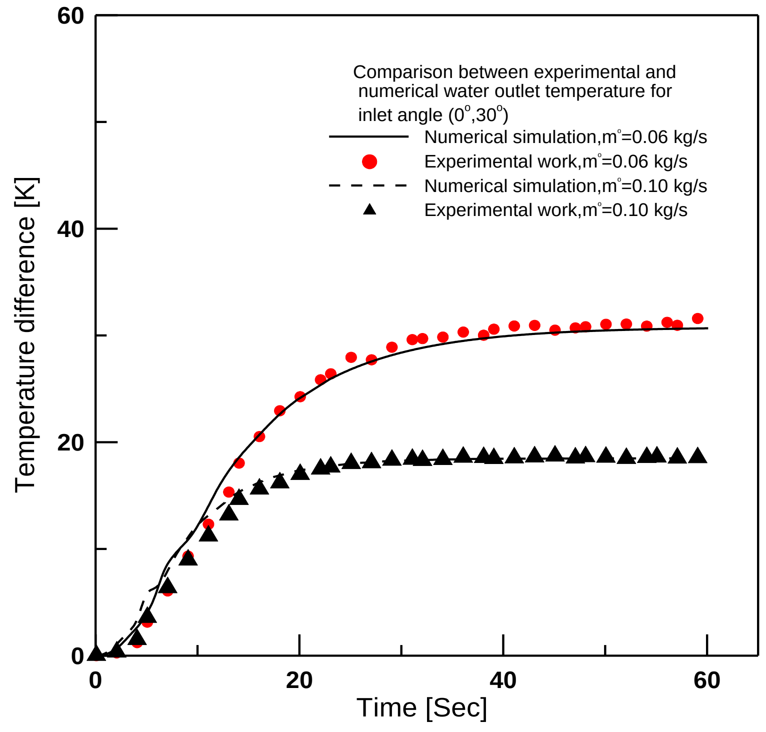

Figure 5-9 Simulated and measured water outlet temperature profiles for inlet angle (0º, 30º)

5.5. Results and Discussion of the Numerical Results

5.5.1. Effect of the inlet angle configurations

Ten different water heating tank configurations have been simulated to study the effect of cold water inlet angles on heat transfer and thermal performance of an instantaneous Tankless electric water heater.

Surface temperature distribution contours at the upper and bottom electric heating elements for m^o=0.06 kg/s and ten simulated cases are shown in Figure 5-10. The results show that the heating elements surface temperature changes with the variation of the tank inlet angle configuration; however, there are some cases where the heating elements are not symmetrically loaded. It is evident that the highest surface temperature distribution of the heating element is the tank with the inlet angle of (45°, 0°), because there are hotspot areas located at the top of the upper heater which increase the failure rate and reduce the durability of the heater. Furthermore water heating tank with the inlet angles of (30°, 0°), (0^o, 15^o) and (0°, 0°) provide the lowest temperature compared case of tank with inlet angle (45°, 0°). The most of the hotspot areas have been located on the upper heating element coil. The best heaters' surface temperature distributions are for the inlet angles of (0°, 45°) and (0°, 30°). As the heating elements temperature are almost constant and uniform and at a relative lower temperature will decrease the possibilities of the heater failure and also reduce the load of the heating elements.

Figure 5-11, shows water temperature contour distributions inside the heating tank at different horizontal sections alone the y direction (y= 0.04, 0.07, 0.10, 0.13 and 0.16 m) from the bottom. It is clear that the water is heated uniformly at all the cross sections in heating tank with inlet angles of (0°, 30°) and (0°, 45°). But for the others inlet angle configuration the water temperatures are not heated uniformly and there are some locations where water temperature higher than exiting water temperature, thus leading the electric heating coil working under thermal stress which increases the possibility of failure.

Figure 5-12, presents the water temperature distribution through the vertical cross section at the middle of the heater tank for different inlet angle configurations. The temperature distributions are quite different for various inlet angles. When the cold water enters the tank with the inlet angle of (0°, 0°), it is clear that the cold water hits the opposite side of the tank and flows up immediately to the top of the tank without creating any severe mixing, therefore, there are locations where the water temperature increases heavily due to the poor water circulation around the heating elements. As the heating elements temperature increase results in the non-uniform water temperature distribution. The other inlet angles have better uniform water temperature distributions in the vertical direction owing to the improved water distribution around the heating elements especially for horizontally inclined inlet angle configurations, where is nothing obstructing the inlet flow and there is a significant uniform temperature distribution in the tank.

In Figure 5-13, the velocity streamlines of water within the heating tank with different inlet angles are presented. It is obviously that the velocity streamlines change with the alteration of the inlet angles. For (0°, 0°) inlet angle, the cold water is supplied directly to the other side of the tank inducing the degradation of the flow energy, after that the cold water flows up to the top of the tank along on side, resulting in the poor water distribution around and through the heating elements coils. Therefore, the surface temperature of the heating elements is the worse one and non-uniform as detailed in Figures 5-10, 5-11 and 5-12.

Similar situation happened for the tank with inlet angles of (15°,0°) , (30°,0°) and (45°,0°) where the cold water hits the bottom of the tank before flows up which also produces the poor water distributions around the heating elements and induces the hotspots on the surface of the heating elements are displayed in Figure 5-11. When the jets are oriented vertically, jet flows conform well to the general flow field in the tank, transforming the most of the jet flow energy into the fluid thermal energy. With the jet angle increasing, more jet flow energy is dissipated because the jet strikes the tank bottom within a relatively short distance. In addition, the jet flow crosses the streamlines of the fluid at an angle.

When the inlet pipes start to be inclined at both the horizontally and vertically directions such as the (15°,15°), (30°,30°) and (45°,45°), there are a little enhancements of the water distributions around the heating elements but still are poor as the inlet cold water hits the bottom of the tank. When the inlet pipes inclined by the angles of (0°, 15°), (0°, 30°) and (0°, 45°), a good water distribution around heating elements is observed. This is because these angles produce swirl flows strengthening the heat transfer rate inside the water; in addition it is enhancing the heat transfer from the heating element to the water as the water stream is forced to move in the tangential direction rather than axial and radial directions.

To sum up, it should be emphasized that the intensity of the swirl is enhanced when the inlet angle inclined increases in the horizontal direction which produced tangential velocity (Karagoz and Kaya, 2007).

When the water flow rate has increased to 0.1 kg/s, the contours of temperature distribution of electric heating elements are shown in Figure 5-14. Two very interesting findings differ from the mass flow rate of 0.06 kg/s. The hotspots on the surface of heating element only occur for the inlet angle of (0°, 0°) and there are non-uniform temperature distribution on the surface of the heating elements except for inlet angles of (0°,30°) and (0°,45°). There are three reasons causing these: Firstly, the velocity of the inlet cold water is high enough to carry the thermal energy released from the heating element away within the other angles except (0°, 0°); Secondly; the high speed flows induce the uneven water distribution resulting in the non-uniform surface temperatures of the heating elements except for inlet angles of (0°,30°) and (0°,45°); Thirdly, the water distribution around the heating element at the angle of (0°, 0°) is not good enough, and some dead regions induced by the high speed turbulent current. Therefore, for the flow rate of 0.10 kg/s, both of the (0°,30°) and (0°,45°) inlet angles can provide uniform surface temperature on heating elements , improve the energy efficiency of heating system and protect the element coils from thermal stress.

Figures 5-15 and 5-16 confirm the previous analysis about the Figure 5-11 and Figure 5-12, that for the tank with inlet angles of (0°, 30°) and (0°, 45°), the cold water is heated uniformly because of the even water distribution inside the tank owing to the swirl flow induced by the inlet angles . Figure 5-17 expresses the streamlines of the velocity for inlet angles of (0°, 0°), (15°, 0°), (30°, 0°) and (45°, 0°) hitting the other side of the tank and trending to the top of the tank, which leads the poor water distribution. However, for the inlet angles of (0°, 15°), (0°, 30°) (0°, 45°), (15°, 15°), (30°, 30°) and (45°, 45°) the water flows hit the bottom of the tanks and gradually flow from the bottom to the top, which induce the uniform water distributions. These angles produce swirl flows around the heating elements and increase the heat transfer rate form the heating element to the water resulting in a shorter heating time.

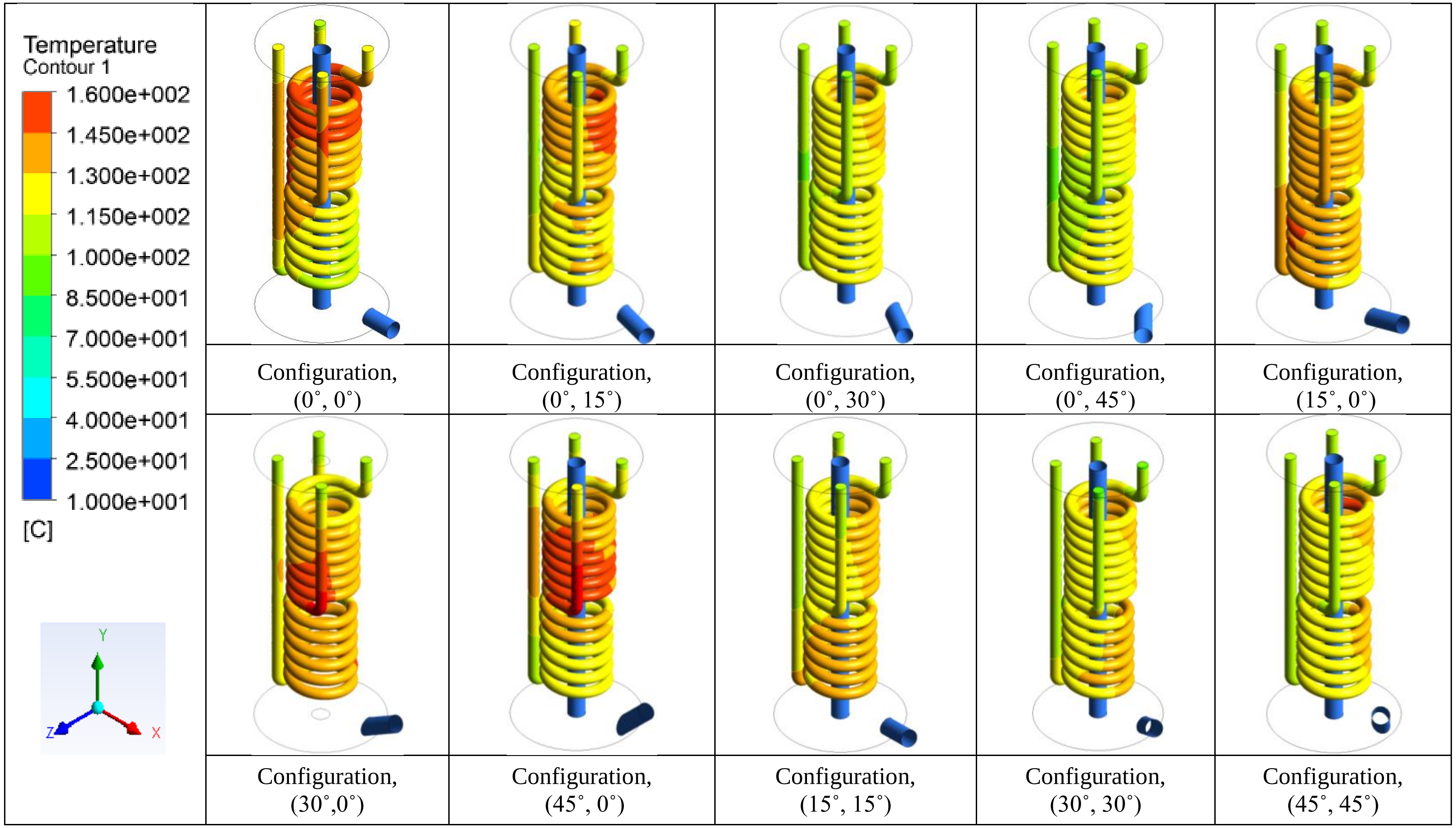

Figure 5-10 Surface temperature distributions at the upper and bottom heater coils (m˚=0.06 kg/s)

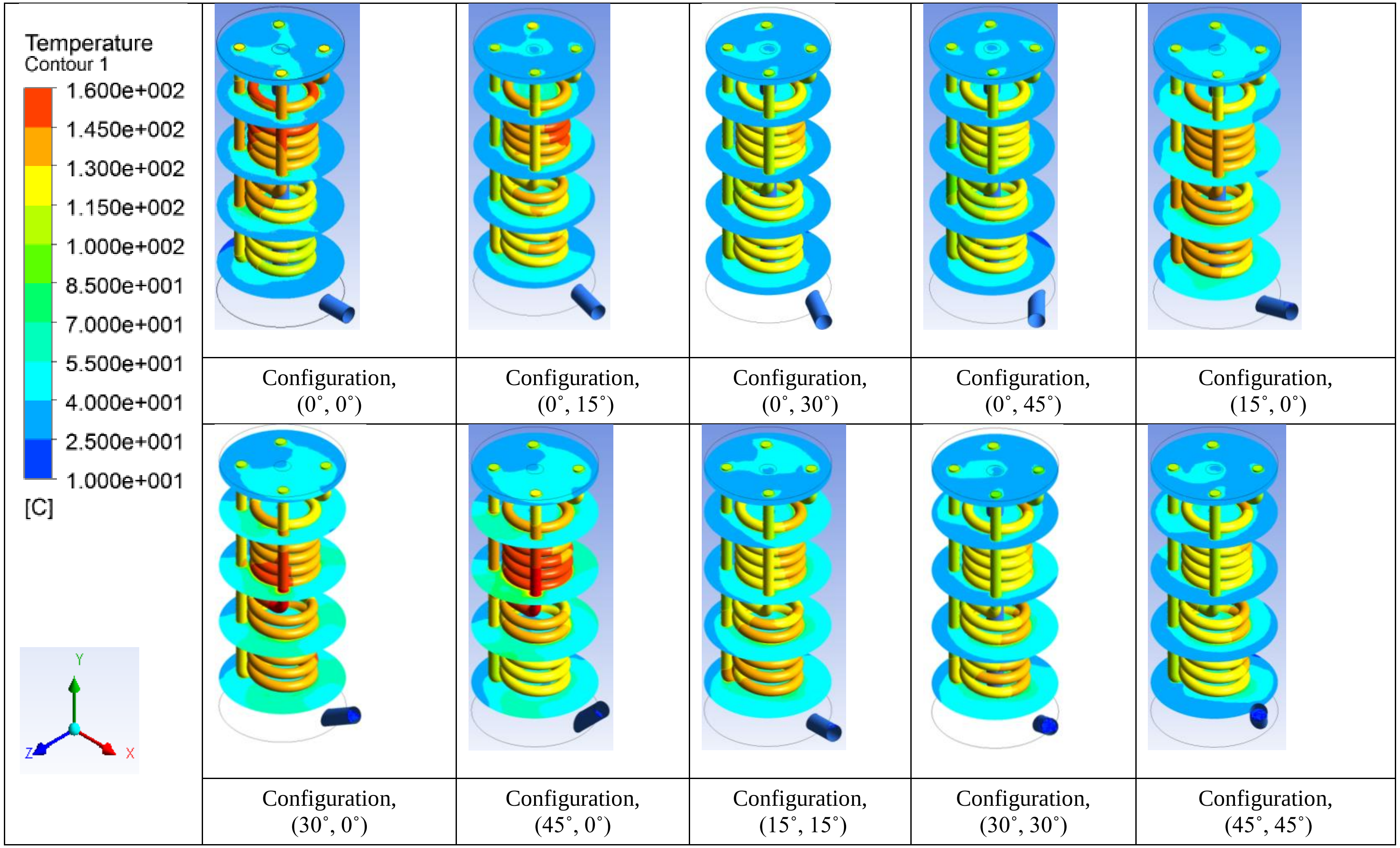

Figure 5-11 Water temperatures contour through different horizontal cross sections (m˚=0.06 kg/s)

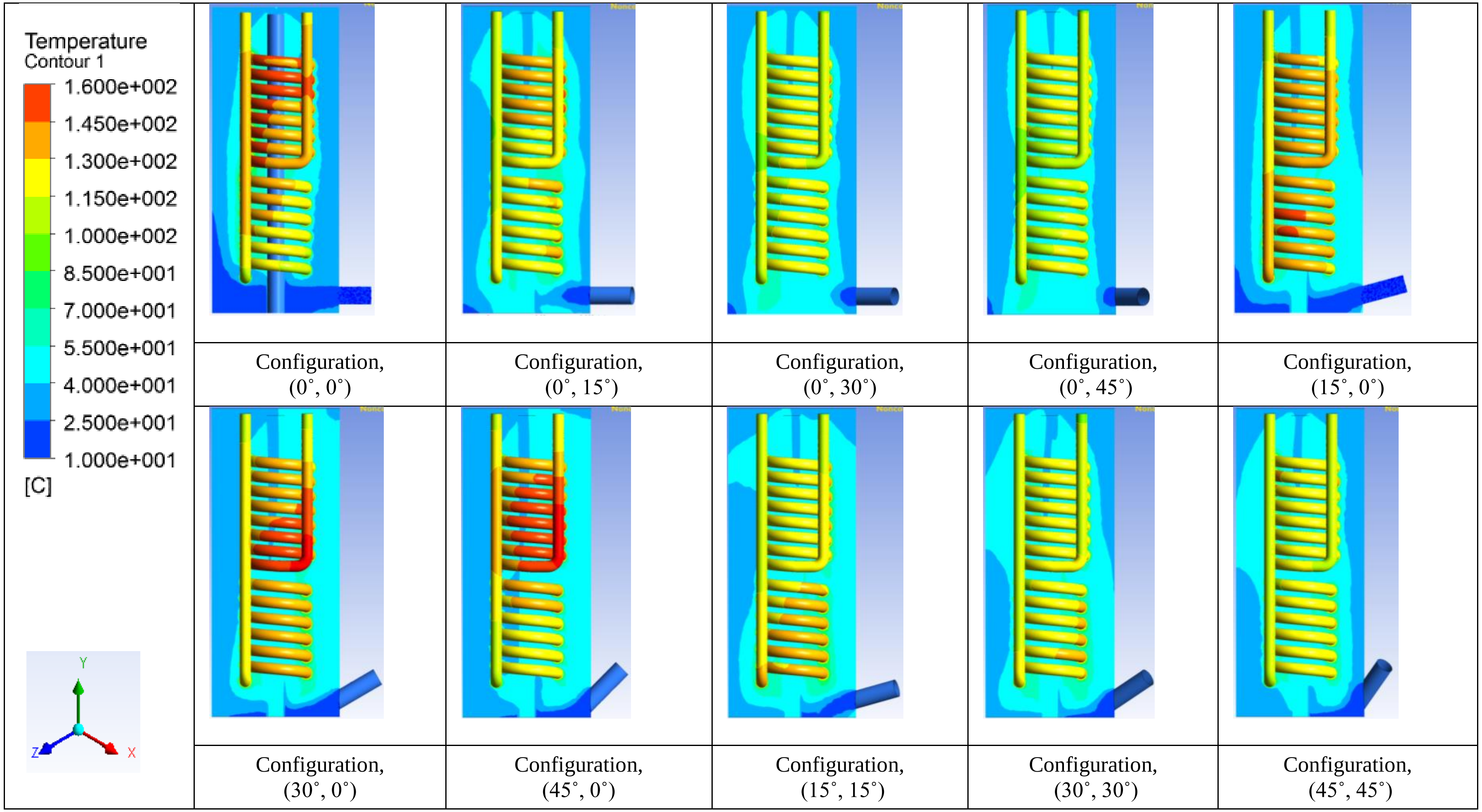

Figure 5-12 Fluid temperatures contour thought the vertical cross section (m˚=0.06 kg/s)

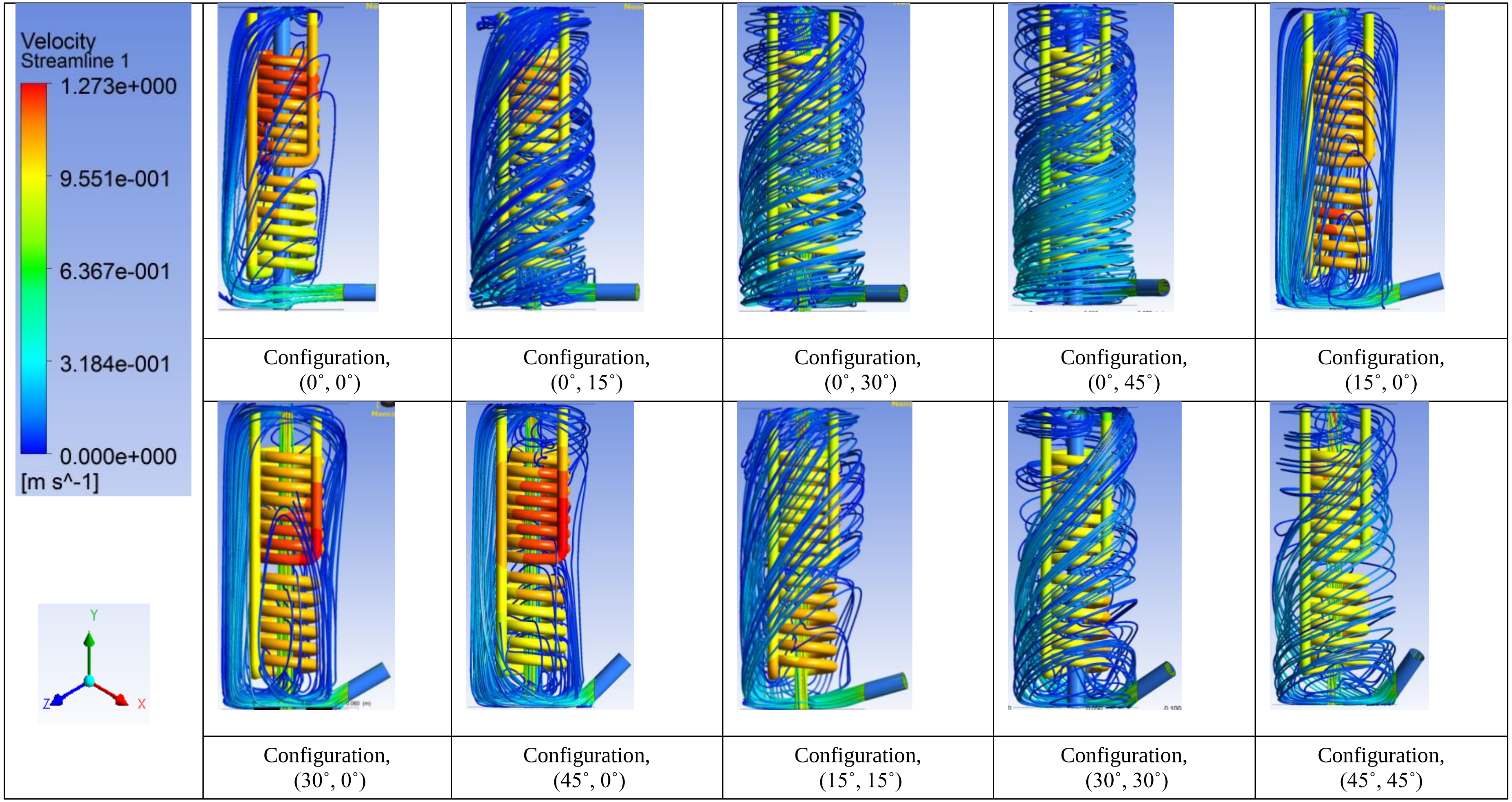

Figure 5-13 Calculated flow fields for different inlet angles (m˚=0.06 kg/s)

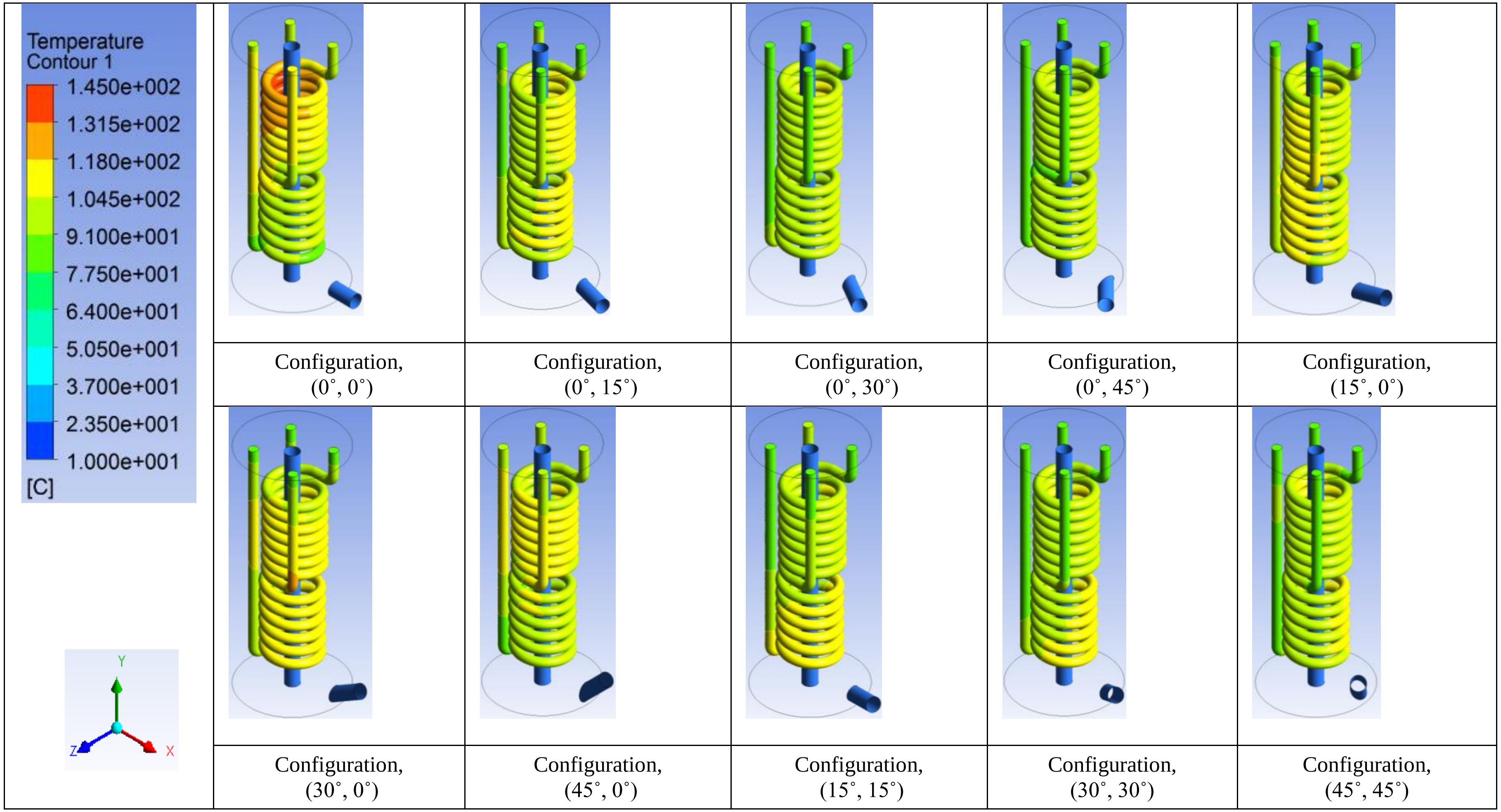

Figure 5-14 Surface temperature distributions of the upper and bottom heater coils (m˚=0.10 kg/s)

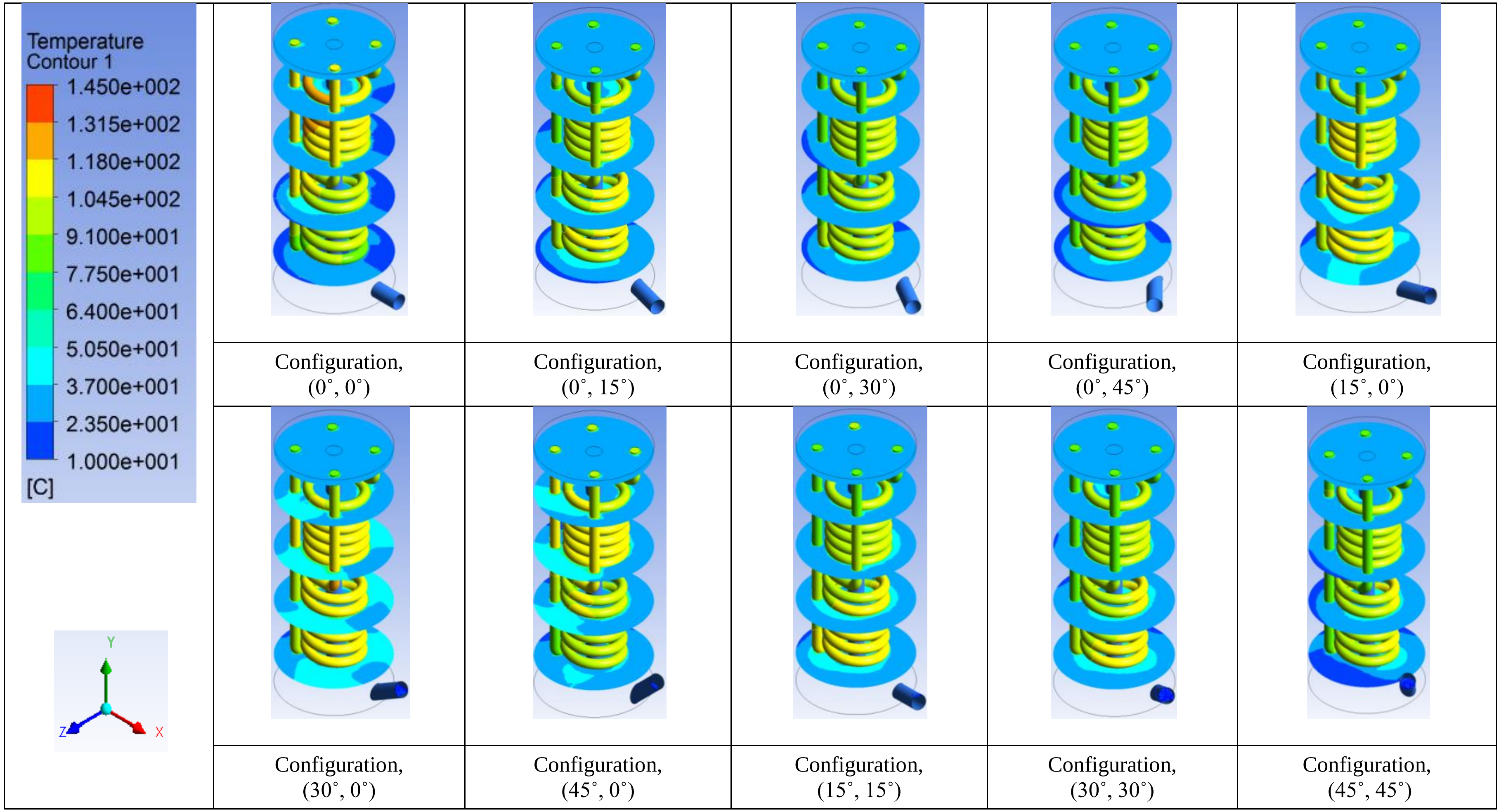

Figure 5-15 Water temperatures contour through different horizontal cross sections (m°=0.10 kg/s)

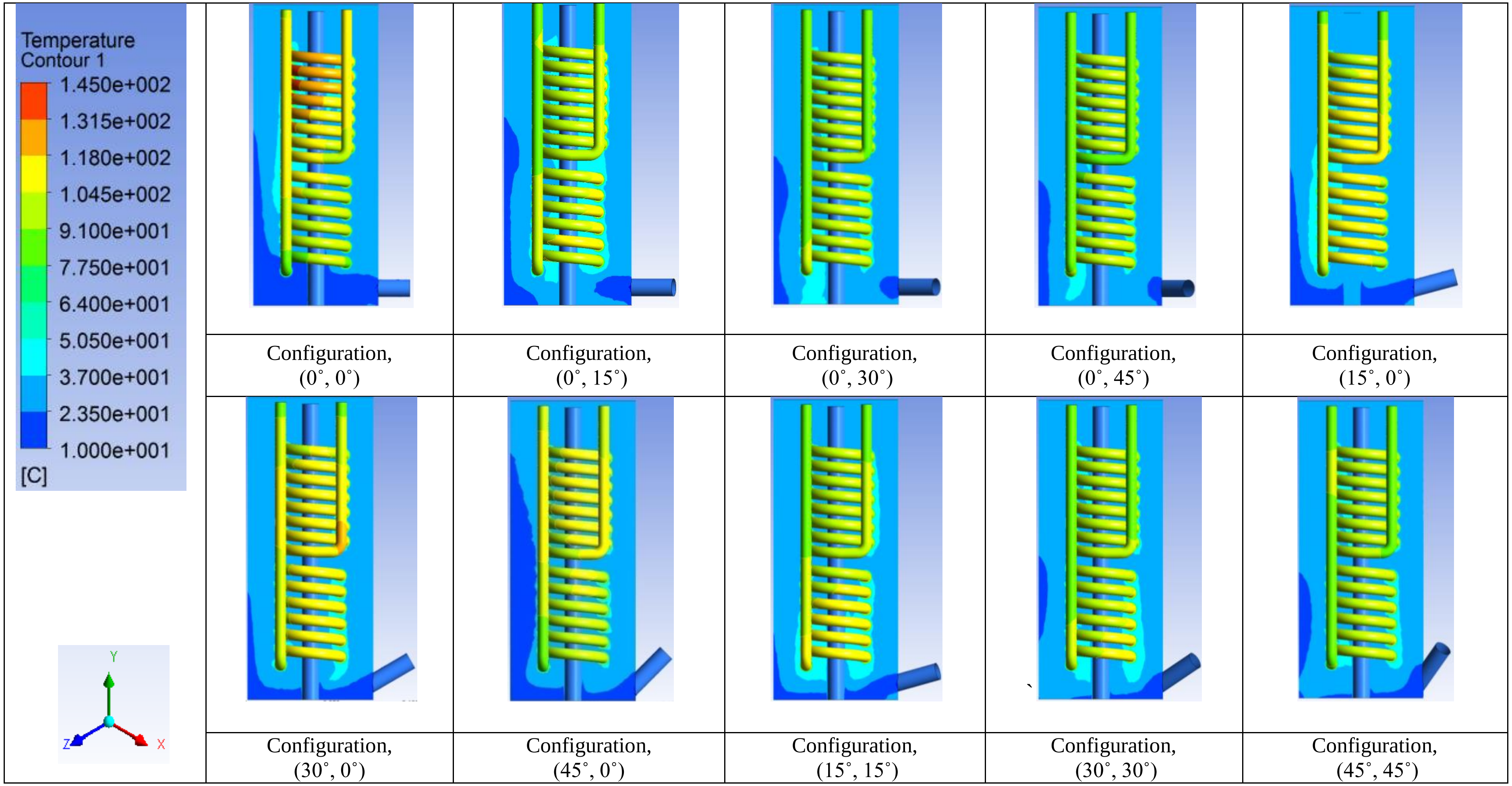

Figure 5-16 Fluid temperatures contour thought vertical cross section (m˚=0.10 kg/s)

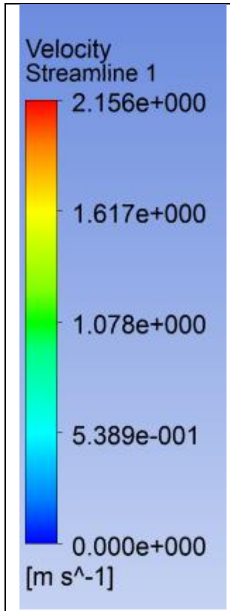	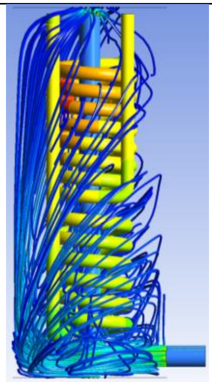	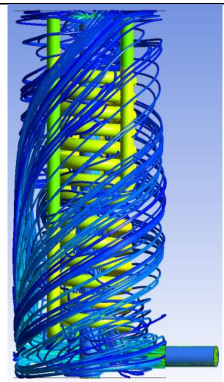	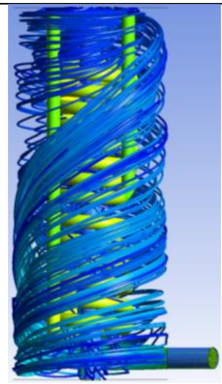	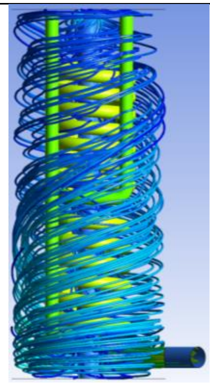	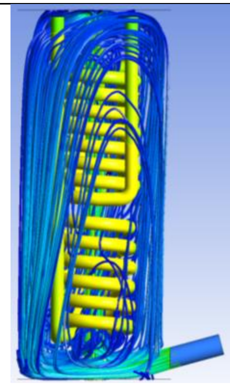
	Configuration, (0˚, 0˚)	Configuration, (0˚, 15˚)	Configuration, (0˚, 30˚)	Configuration, (0˚, 45˚)	Configuration, (15˚, 0˚)
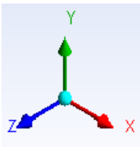	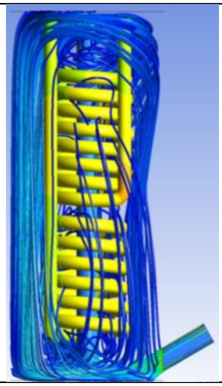	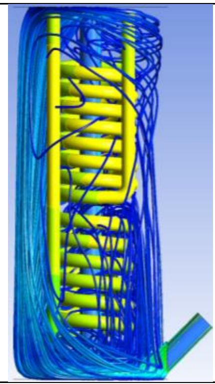	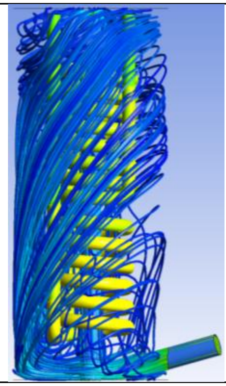	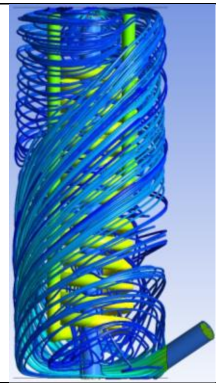	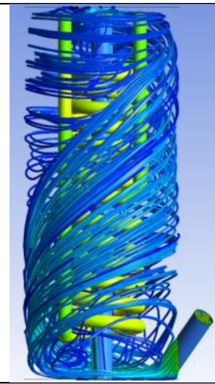
	Configuration, (30˚, 0˚)	Configuration, (45˚, 0˚)	Configuration, (15˚, 15˚)	Configuration, (30˚, 30˚)	Configuration, (45˚, 45˚)

Figure 5-17 Calculated flow fields for different inlet angles (m˚=0.10 kg/s)

Figure 5-18 represents the maximum temperature of the upper and bottom heater coils with different inlet angles configuration for m˚= 0.06 kg/s. This diagram indicates that, the angle of (45°, 0°) has the maximum average temperature around 166.4^{o}C for the upper heater coil and (15°, 0°) has the maximum average temperature around 147.25^{o}C for the bottom heater coil. It is desired to keep the surface temperature of the heating element as low as possible to avoid the hotspots and excess thermal stresses. With the same criteria, the inlet angles of (0°, 30°) and (0°, 45°) have the lowest maximum surface temperature.

When the water mass flow rate has increased to m˚= 0.10 kg/s, as shown in Figure 5-19, the highest heating element surface temperature was reached by the configuration with the inlet angle of (0°, 0°) for both the upper and bottom heater coil, but inlet angles of (0°, 30°) and (0°, 45°) still induce the lowest maximum surface temperature of the heating elements.

Figure 5-20 illustrates the water average temperature along the 'H' vertical direction at the mass flow rate of m˚= 0.06 kg/s. These curves indicate the change trend of the water average temperature inside the heating tank, it can be seen that the configurations with inlet angles of (0°, 30°) and (0°, 45°) provide the approximately constant value around 30^{o}C which means that the heating processes take place uniformly inside the tank and the thermal performance of the heating system is improved. For the other angles the average temperature of the water inside the tank fluctuates from one location to another.

The similar trend of the uniform and constant heating process inside the tanks with inlet angles of (0°, 30°) and (0°, 45°) are found as displayed in Figure 5-21 for the mass flow rate of m˚= 0.10 kg/s.

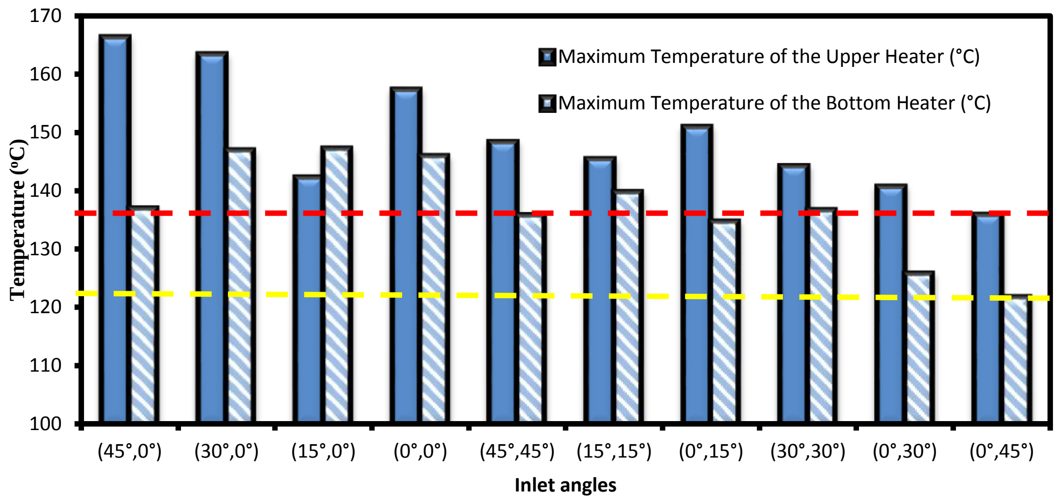

Figure 5-18 Maximum temperature at the bottom and upper heater surface for different inlet angles (m°=0.06 kg/s)

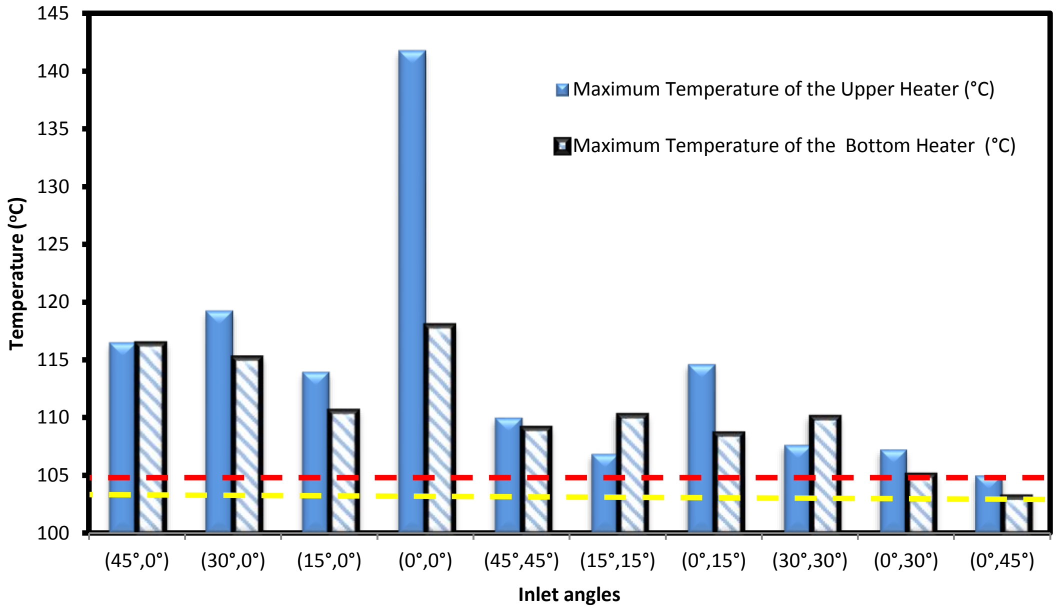

Figure 5-19 Maximum temperature at the bottom and upper heater surface for different inlet angles (m°=0.10 kg/s)

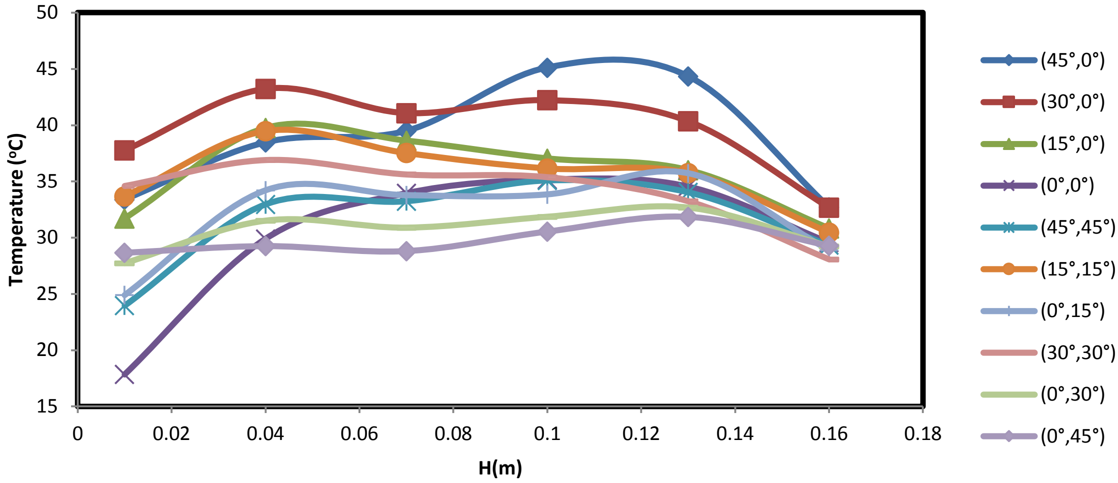

Figure 5-20 Average water temperature distribution for different tank configuration (m°=0.06 kg/s)

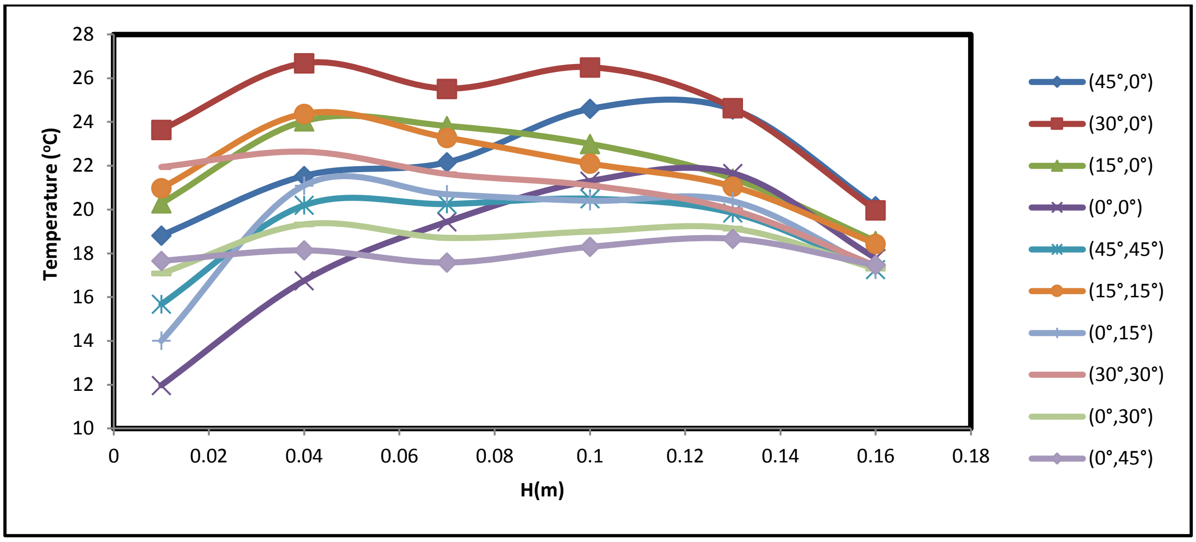

Figure 5-21 Average water temperature distribution for different tank configuration (m°=0.10 kg/s)

5.5.2. Effect of heating element and tank geometrical structures

In the previous section, the influence of inlet angles on thermal performance of instantaneous electric water heater have been studied, the results have showed that tank inlet angle configuration has significant impact on the heater performance.

Also, poor water distributions within the heater tanks increase the surface temperature of the heating coils and the possibility of failure. To avoid this problem it is important to introduce swirl flows within the heating tank. This will increase the heat transfer from the heating elements coils to the water, leading to longer durability of the heater coils and fewer hotspots occurred at the surface of the heater coil. Therefore, the objective of this part is to find the best method of water heating and replace the less efficient systems. This section mainly focuses on two important parameters to evaluate the efficiency and performance of instant heater:

1- The structure of the heating elements coils.
2- The shape and the size of the heating tanks.

Different models of instant electric water heated have been simulated by the computational fluid dynamics (CFD) as shown in Figure 5-22. These models have different structure such as, the heating elements coils have external or internal ends legs; different shape of water tanks with different internal diameter of 58, 66, and 73.2 mm, respectively; the cold water enters the tank directly from different positions (top and bottom) and the inlet angle inclined by angle 45^{o} to the horizontal direction. In all cases the inlet and outlet diameter are fixed at d =10 mm.

The volume of each heating element coils are fixed and equal to $3.0x10^{-5}$ m^3 for the both structure of the heating elements coils with internal or external legs; the diameter of the cross section of the heating elements coils equal to d_{coil} = 6.4 mm; the total power of each heating element coil equal to 3841.27 W; and the constant water discharge flows rate are 0.06 and 0.10 kg/sec (3.6 L/min and 6 L/min) with the inlet water temperature at $10^{o}C$.

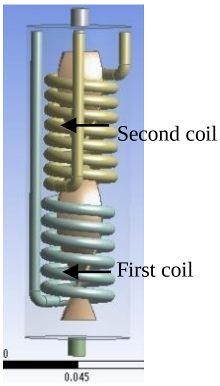

(a) Tank heater with D= 58 mm and twisted tape

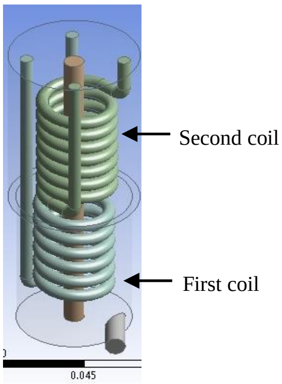

(b) Tank heater bottom D= 58 mm and Top D= 66 mm, with inlet angle (0º, 45º)

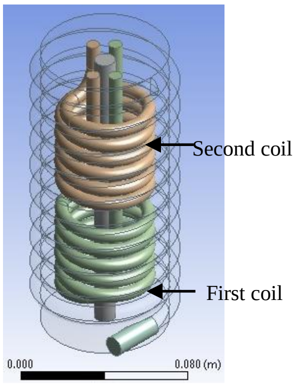

(c) heating elements with internal legs and tank wall grooves D=73.2 mm, with inlet angle (0º,45 º)

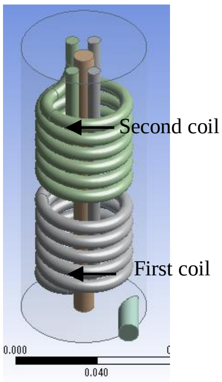

(d) Heater with internal legs and tank D=62 mm, with inlet angle (0º,45 º)

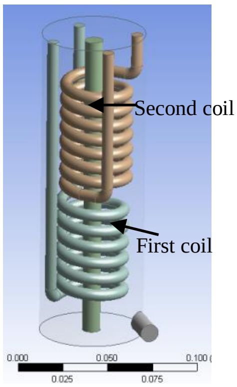

(e) Tank heater D=58 mm with inlet angle (0º,45 º)

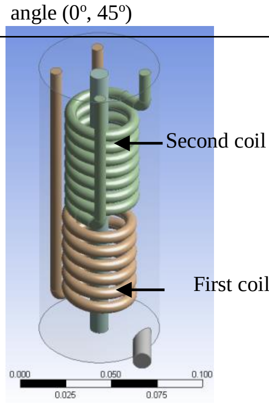

(f) Tank heater D=66 mm with inlet angle (0º,45 º)

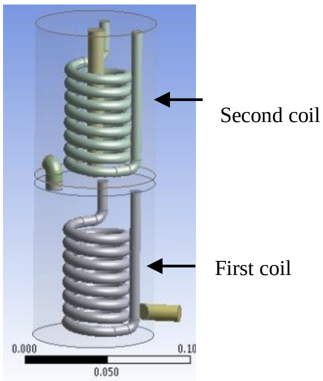

(g) Two tank s with D=73.2 mm, with inlet angle (0º,45 º)

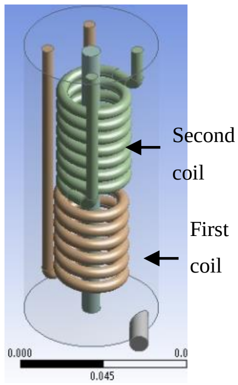

(h) Tank with D=73.2 mm with inlet angle (0º, 45º)

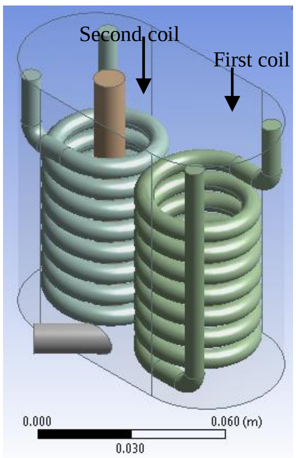

(i) Vertical oval tank with inlet angle (0º,45 º), D=50 mm

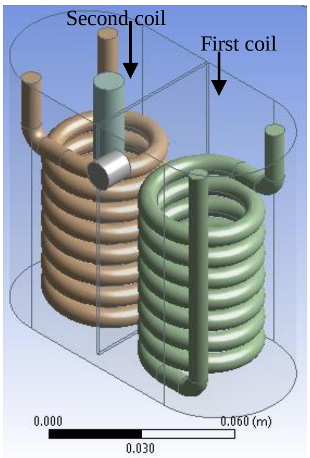

(j) Vertical oval tank with internal separation wall and inlet angle (0º,0º), D=50 mm

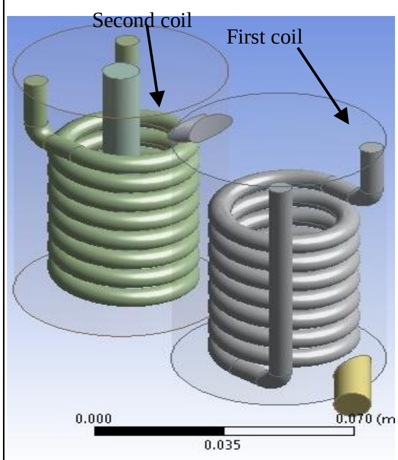

(k) Two tank s with D=58 mm, H=90 mm with inlet angle (0º, 45º)

Figure 5-22 Geometrical details of the heater coils and tanks

5.5.2.1.Proposed eleven configurations

In this section, eleven tanks utilizing two different structures of heating elements coils, (one with external legs and the others with internal legs), and different shapes of the tank have been simulated.

a. Cylindrical tank with internal diameter D= 58.0 mm, height H=174.0 mm, and twisted tape inserted.
b. Two cylindrical tanks with internal diameters, D= 58.0 and D= 66.0 mm.
c. Heating elements with internal legs and tank wall grooves D=73.2 mm.
d. Cylindrical tank with internal diameter, D= 62.0 mm and height, H=155.0 mm.
e. Cylindrical tank with internal diameter, D= 58.0 mm and height, H=174.0 mm.
f. Cylindrical tank with internal diameter, D= 66.0 mm and height, H=174.0 mm.
g. Two cylindrical tanks with internal diameter, D= 73.2 mm, H=174 mm and inlet angle of (0^o, 45^o).
h. Cylindrical tank with internal diameter D= 73.2 mm and height H=174.0 mm and inlet angle of (0^o, 45^o).
i. Vertical oval tank and height, H=90.0 mm, D= 50 mm and inlet angle of (0^o, 45^o).
j. Vertical oval tank and height, H=90.0 mm, D=50 mm. and internal separation wall.
k. Two cylindrical tanks with internal diameter, D= 58.0 mm, H=90 mm and join angle of (0^o, 45^o).

5.5.2.2.Thermal profiles of the heating element coils

The surface temperature distribution of the heating elements coils are obtained and shown in Figures 5-23 and 5-24. For the mass flow rate at m°=0.06 and 0.10 kg/s, the surface temperature of the heating elements coils is depending on the tank shapes, inlet positions/angles and structures of the heating elements coils. In Figure 5-23, for the mass flow rate at m°=0.06 kg/s, in general, the heating coil surface temperature increases with the decreasing of the tank diameter. This is because the reduction of the tank diameter obstacle the flow and reduce the intensity of swirl flow around the heating elements coils, which influences the flow structure inside the tank such as the models e and f. On the other hand to avoid the high thermal stresses loading on the heating elements coils, a new designs have been created, tank wall with grooves (model c) and split the cylindrical tank into two volumes with joint (models of b, g and k), these configurations are helping the flow to swirl and provide a symmetrical flow distribution along the heating elements coils. As a result, the inlet cold water diffuses inside the tank and causes the mixing flow on the top layers. The heating tanks with oval cross section (models i and j) have higher temperature on the second heating elements coils because of the poor water distribution around it. The two tanks configuration with D=58 mm (model k) has a relatively uniform temperature distribution on the first heating element coil because the inlet angle inclined with an angle of 45^o to horizontal direction, which generates swirl flows around the heating coils, because the intensity of the swirl flow decrease with the height of the tank, so we locking for configuration to recover the kinetic energy of the flow, using this principle, two tanks with internal diameter 73.2 mm (model g) was simulated, this model produces uniform temperature distribution on the surface of the heating elements coils, the only difference between this model and two tanks with diameter 58 mm (model k) is that bigger internal diameter helps the flow to swirl around the heating elements coils without any obstacles, and in this model heating elements coils relatively at low uniform temperature which helps to a void heating elements thermal stresses and failures.

When the water flow rate is increased to $\dot{m} = 0.10$ kg/s as shown in Figure 5-24 there are a quite different on the surface temperature of the heating elements coils because the velocity of the flow relatively high which able to overcome the obstacles and provided good water distribution around the heating elements coils and high heat transfer from the heating elements coils to the cold water, in the case of (model h) heating tank with inlet angle of (0^o, 45^o) and internal diameter of (D=73.2 mm. It can be seen that heating element coils have uniform and lower surface temperature, In contrast heating tanks with oval cross section (models i and j) have the second heating element coil at relatively high temperature which the possibility of heater failures increase.

Figures 5-25 and 5-26 show the temperature distribution couture of the heating water in the center of the tank for $\dot{m} = 0.06$ and 0.10 kg/s, it is clear that the degree of mixing the water in the tank depends on the tank’s shape, heating elements coils structure, position of the inlet and outlet water ports. The temperature distribution in the tank is quite different for all shapes.

As shown in Figure 5-25, for the models of (e), (f) and (h) with the same inlet angle of (0^o, 45^o), but different tank diameter D=58, 66 and 73.2 mm, the temperature distribution of water approximately is uniform around the heating elements coils. The model of (d) which contains heating elements coils with internal legs, leads the heating water slightly higher in the middle of the tank, on the contrary, for oval cross section tanks models (i) and (j), there are non-uniform heating distribution which is not acceptable. The same behavior of water temperature distribution for high mass flow rate $\dot{m} = 0.10\ kg/s$ is presented in Figure 5-26.

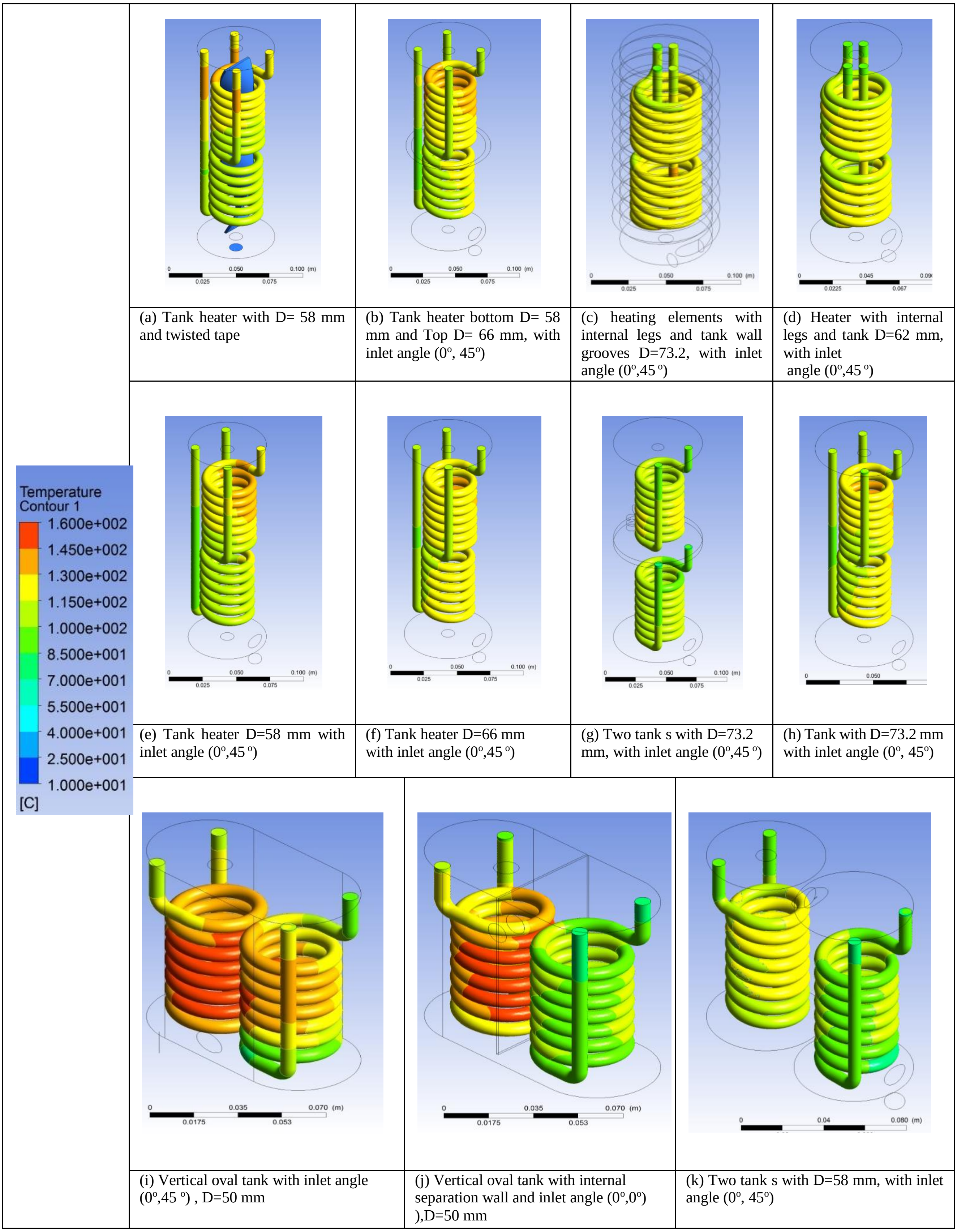

(a) Tank heater with D= 58 mm and twisted tape

(b) Tank heater bottom D= 58 mm and Top D= 66 mm, with inlet angle (0º, 45º)

(c) heating elements with internal legs and tank wall grooves D=73.2, with inlet angle (0º,45º)

(d) Heater with internal legs and tank D=62 mm, with inlet angle (0º,45º)

(e) Tank heater D=58 mm with inlet angle (0º,45º)

(f) Tank heater D=66 mm with inlet angle (0º,45º)

(g) Two tank s with D=73.2 mm, with inlet angle (0º,45º)

(h) Tank with D=73.2 mm with inlet angle (0º, 45º)

(i) Vertical oval tank with inlet angle (0º,45º) , D=50 mm

(j) Vertical oval tank with internal separation wall and inlet angle (0º,0º)),D=50 mm

(k) Two tank s with D=58 mm, with inlet angle (0º, 45º)

Figure 5-23 Solid temperature distribution of heater elements coils for m°=0.06 kg/s

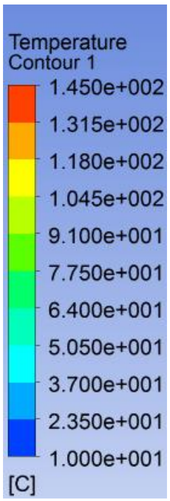

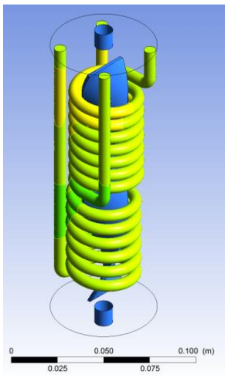

(a) Tank heater with D= 58 mm and twisted tape

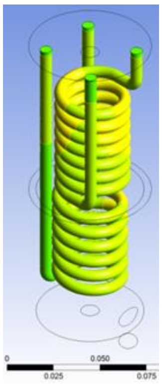

(b) Tank heater bottom D= 58 mm and Top D= 66 mm, with inlet angle (0º, 45º)

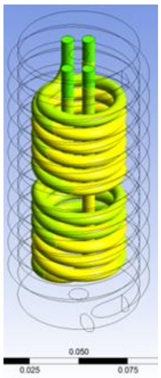

(c) heating elements with internal legs and tank wall grooves D=73.2, with inlet angle (0º,45 º)

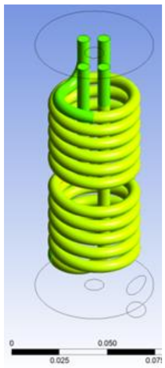

(d) Heater with internal legs and tank D=62 mm, with inlet angle (0º,45 º)

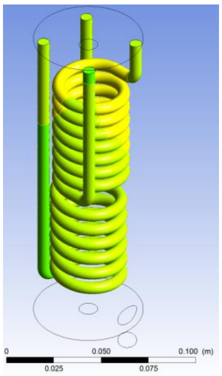

(e) Tank heater D=58 mm with inlet angle (0º,45 º)

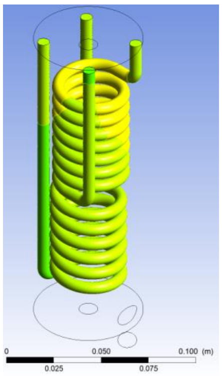

(f) Tank heater D=66 mm with inlet angle (0º,45 º)

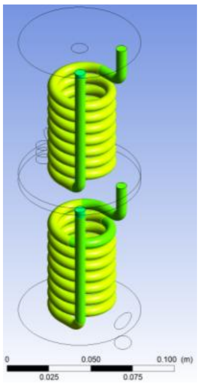

(g) Two tank s with D=73.2 mm, with inlet angle (0º,45 º)

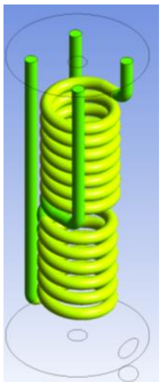

(h) Tank with D=73.2 mm with inlet angle (0º, 45º)

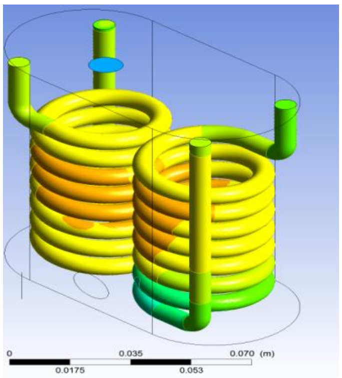

(i) Vertical oval tank with inlet angle (0º,45 º)) , D=50 mm

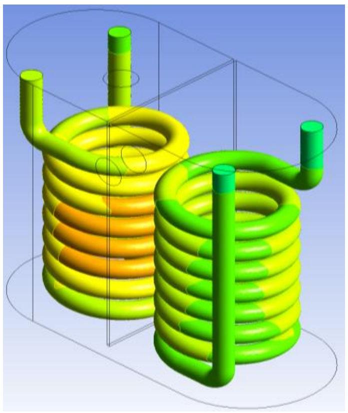

(j) Vertical oval tank with internal separation wall and inlet angle (0º,0º)) , D=50 mm

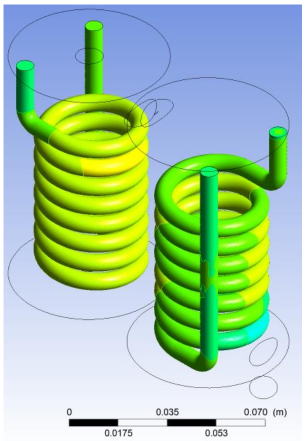

(k) Two tank s with D=58 mm, H=90 mm with inlet angle (0º, 45º)

Figure 5-24 Solid temperature distribution of heater elements coils for m°=0.10 kg/s

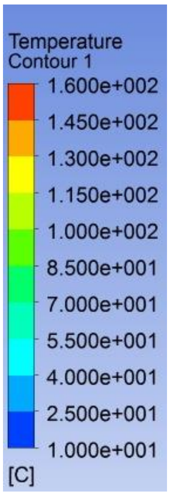

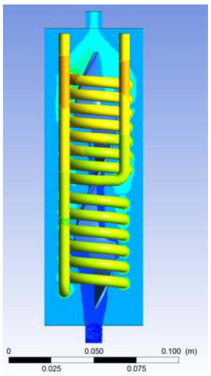

(a) Tank heater with D= 58 mm and twisted tape

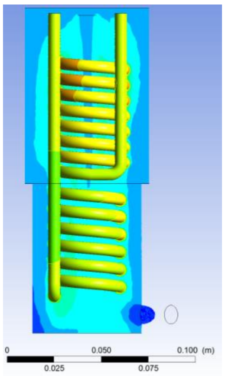

(b) Tank heater bottom D= 58 mm and Top D= 66 mm, with inlet angle (0º, 45º)

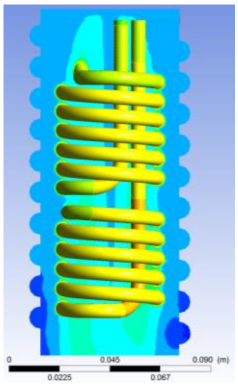

(c) heating elements with internal legs and tank wall grooves D=73.2, with inlet angle (0º,45º)

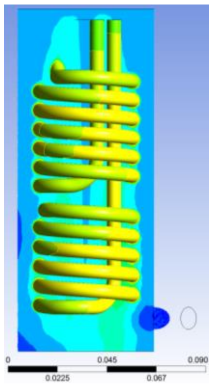

(d) Heater with internal legs and tank D=62 mm, with inlet angle (0º,45º)

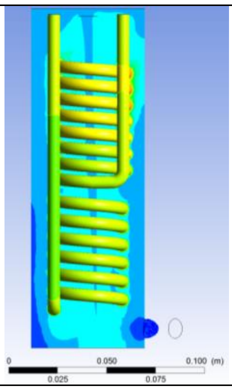

(e) Tank heater D=58 mm with inlet angle (0º,45º)

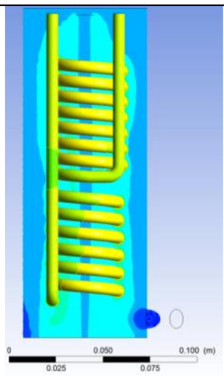

(f) Tank heater D=66 mm with inlet angle (0º,45º)

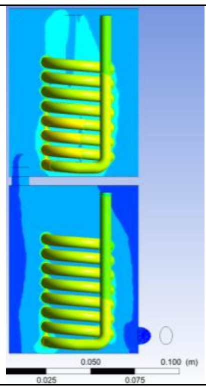

(g) Two tank s with D=73.2 mm, with inlet angle (0º,45º)

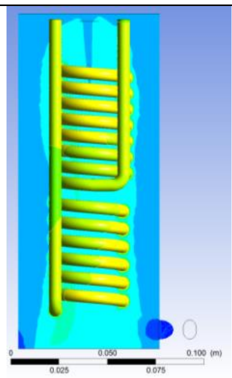

(h) Tank with D=73.2 mm with inlet angle (0º, 45º)

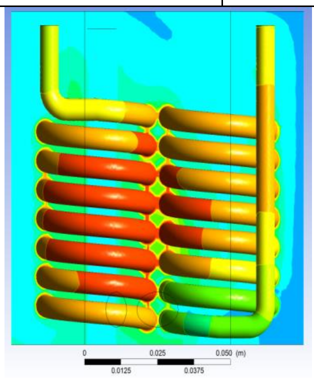

(i) Vertical oval tank with inlet angle (0º,45º),) , D=50 mm

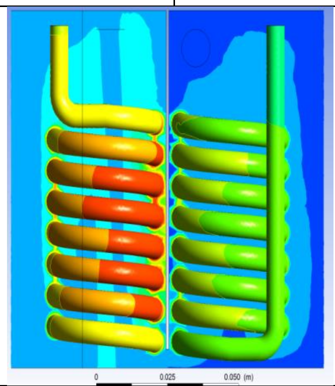

(j)Vertical oval tank with internal separation wall and inlet angle (0º,0º)) , D=50 mm

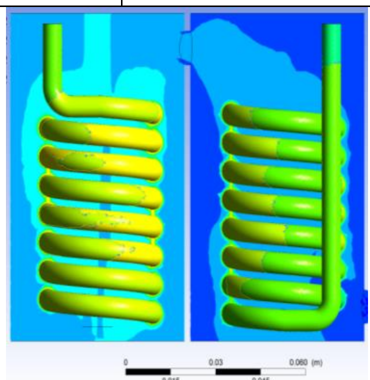

(k) Two tank s with D=58 mm, H=90 mm with inlet angle (0º, 45º)

Figure 5-25 Temperature distribution in the tank centre for m°=0.06 kg/s

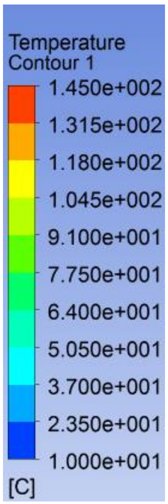

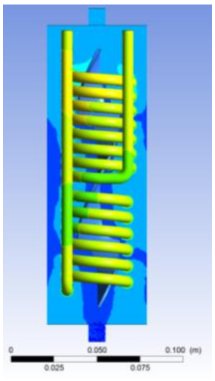	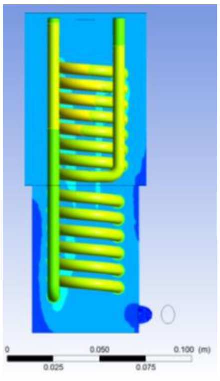	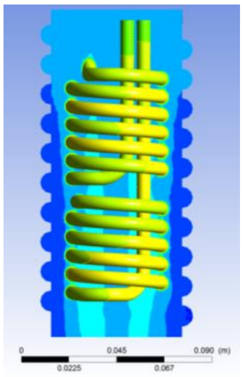	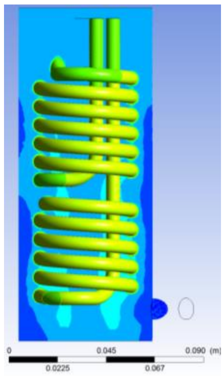
(a) Tank heater with D= 58 mm and twisted tape	(b) Tank heater bottom D= 58 mm and Top D= 66 mm, with inlet angle (0°, 45°)	(c) heating elements with internal legs and tank wall grooves D=73.2, with inlet angle (0°,45°)	(d) Heater with internal legs and tank D=62 mm, with inlet angle (0°,45°)
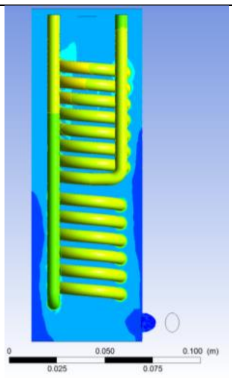	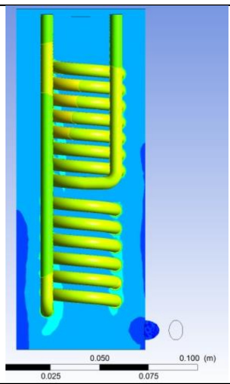	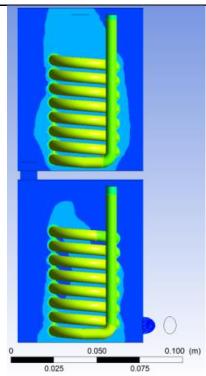	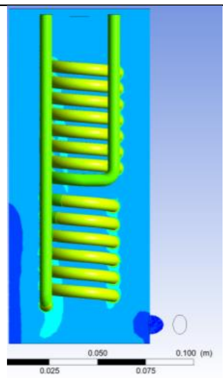
(e) Tank heater D=58 mm with inlet angle (0°,45°)	(f) Tank heater D=66 mm with inlet angle (0°,45°)	(g) Two tank s with D=73.2 mm, with inlet angle (0°,45°)	(h) Tank with D=73.2 mm with inlet angle (0°, 45°)
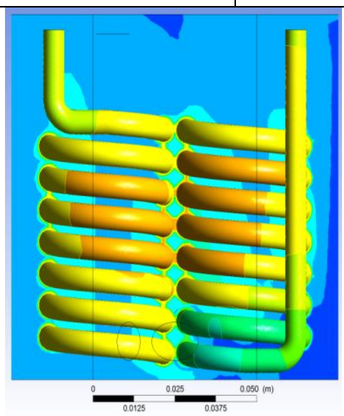	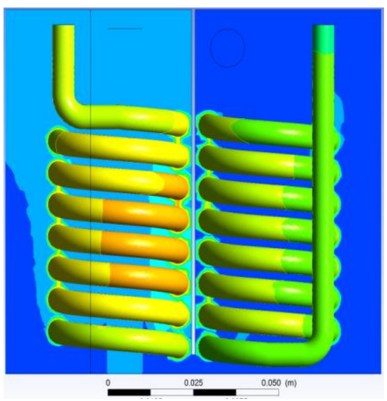	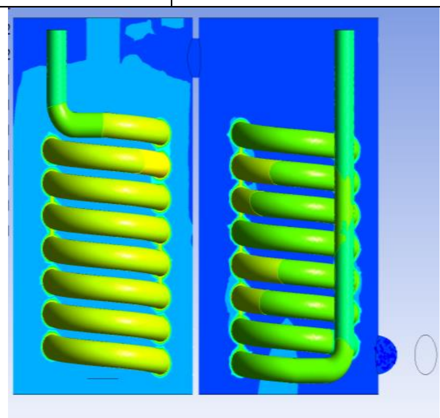	
(i) Vertical oval tank with inlet angle (0°,45°)) , D=50 mm	(j) Vertical oval tank with internal separation wall and inlet angle (0°,0°)) , D=50 mm	(k) Two tank s with D=58 mm, H=90 mm with inlet angle (0°, 45°)	

Figure 5-26 Temperature distribution in the tank centre for m°=0.10 kg/s

Figures 5-27 and 5-28 show the stream traces colored by velocity magnitude (where yellow, green and blue indicate high, medium and low velocities), it is clear that for different flow rates $\dot{m} = 0.06$ and 0.10 kg/s, the velocity stream is identical but it changes by changing the heating tank geometry, it is obvious that for all tank geometries with inclined inlet angle the intensity of swirl flow is high and the fluid distribute uniformly around the heating elements coils which leads to efficient heat transfer from the heating elements coils to the heating water, However, for the case of tank helical grooves on its inward facing surface of the annular wall (model c) and tank with internal legs heating elements coils (model d), the intensity of swirl flow increased because no obstacles disturb the flow and the grooves guide the flow to the top. Also moreover leading homogenous and efficient distribution of the water in the tank and the better heat transfer between the heating elements coils and water will be created, leading the surface temperature reduce of the heating elements coils. For the case of two connected tank the joint tube (model g), as can be seen, the connected joint tube is helping to continue the swirl flow till the top of the tank as a result no short circuiting or stagnant zone are expected.

In the case of tank with oval cross section, models (i) and (j), we can see non uniform fluid flow distribution among the heating tank and around the heating elements coils due to the geometry of the tank. In to summary, the degree of swirl flow decreases with the decrease of the tank diameter.

There are practical interest to determine the maximum temperature of the heating element coils, because that will give the indication of the performance and efficiency of the heater, the particular variation is presented in Figures 5-29 and 5-30 for bottom and upper heating elements coils for the mass flow rate of $\dot{m} = 0.06$ and 0.1 kg/s.

As shown in Figure 5-29 for the mass flow rate of $\dot{m} = 0.06$ kg/s, generally, the maximum temperature of each heater coils changes with the variation of the tank geometry and structure of heating elements coils. There are hot spots at both the heater element coils in the tank with oval cross section (model i) that owing to the poor water distribution around the heating elements coils as displayed in Figure 5-27. For the tank with the oval cross section and separation in the middle such as the model (j), the temperature of the first heating element is low because of the inlet cold water facing the heating elements coil all time, but for the other geometries the maximum temperature of the element coils are varying from 143 to 105 ^oC . Similarly for the high mass flow rate of $\dot{m} = 0.1\ kg/s$, as shown in Figure 5-30, the hot spots appear in the oval cross section tank within the models (i) and (j). On the other side the heater coils for tank with internal diameter of 73.2 mm and angle of (0^o, 45^o) as model (h), the maximum temperature reaches to around 105.0 ^oC . This temperature is perfect for the operation of the water heater and increases the performance of the heating.

5.5.2.3. Pressure drop

One of the most important parameter impacts on the performance of the heating is the pressure drop; certainly, with increasing the obstructions the pressure drop will be aggravated. Figures 5-31 and 5-32 present the pressure drop inside different tank geometries for the flow rate of m^o=0.06 and 0.1 kg/s, respectively.

As shown in Figure 5-31 the highest pressure drop occurs within the model with two heating coils with the diameter of 73.2 mm (model g) because the joint throat the flow and the pressure drop reaches to 1800 Pa. The second highest pressure drop is the model two tanks for with internal diameter 58 mm (model k). For the rest of the models the pressure drop approximately the same and is around 900 Pa except the model with twisted tape, which pressured drop is reached to 500 Pa.

When the mass flow rate is increased to m^o=0.1 kg/s, similar trend for the pressure drop his similar trend is shown in Figure 5-32, the pressured drop reached to highest value(5000 Pa) for model (g) and lowest pressure drop is for model (a) (1444Pa).

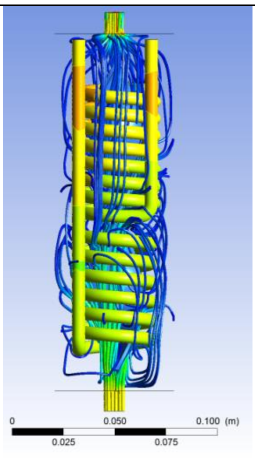

(a) Tank heater with D= 58 mm and twisted tape

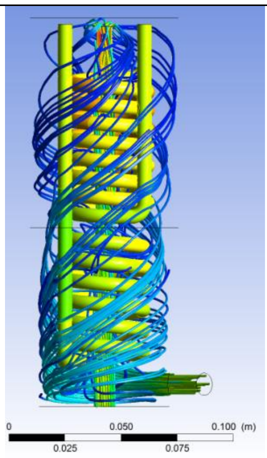

(b) Tank heater bottom D= 58 mm and Top D= 66 mm, with inlet angle (0°, 45°)

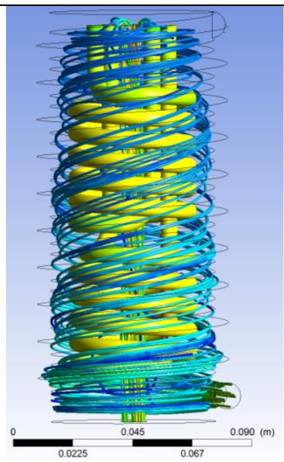

(c) heating elements with internal legs and tank wall grooves D=73.2 mm, with inlet angle (0°,45°)

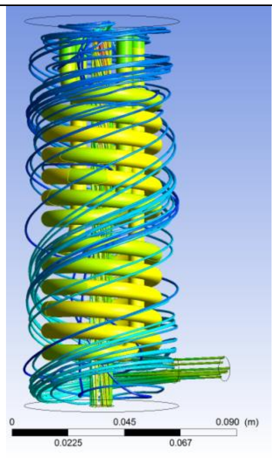

(d) Heater with internal legs and tank D=62 mm, with inlet angle (0°,45°)

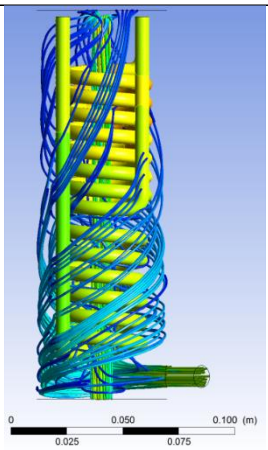

(e) Tank heater D=58 mm with inlet angle (0°,45°)

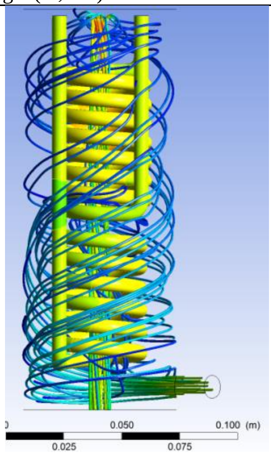

(f) Tank heater D=66 mm with inlet angle (0°,45°)

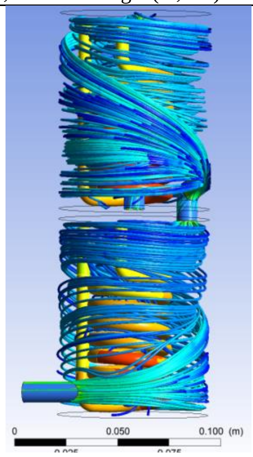

(g) Two tanks with D=73.2 mm, with inlet angle (0°,45°)

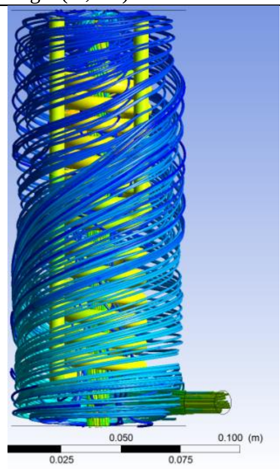

(h) Tank with D=73.2 mm with inlet angle (0°, 45°)

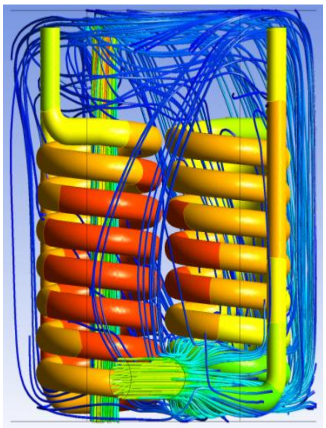

(i) Vertical oval tank inlet angle (0°,45°)

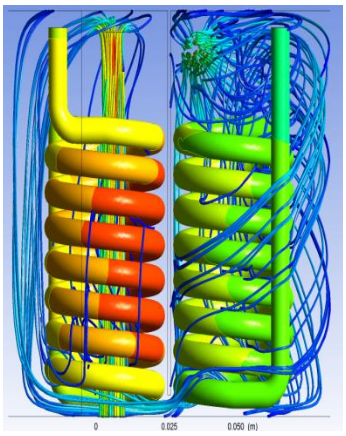

(j) Vertical oval tank internal separation wall and inlet angle (0°,0°)

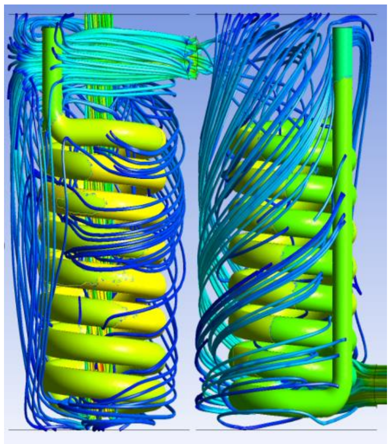

(k) Two tank s with D=58 mm, H=90 mm with inlet angle (0°, 45°)

Figure 5-27 Simulated three dimensional flow field for m°=0.06 kg/s

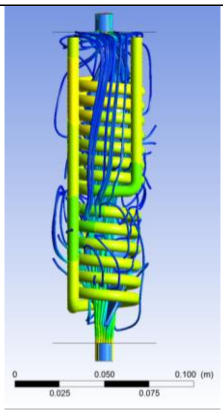

(a) Tank heater with D= 58 mm and twisted tape

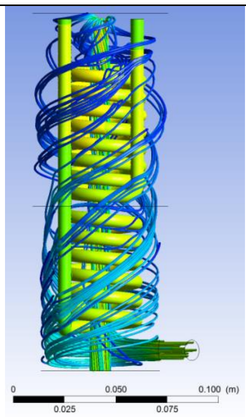

(b) Tank heater bottom D= 58 mm and Top D= 66 mm, with inlet angle (0°, 45°)

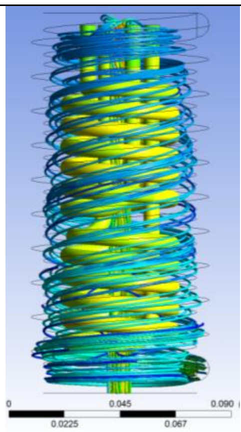

(c) heating elements with internal legs and tank wall grooves D=73.2mm, with inlet angle (0°,45°)

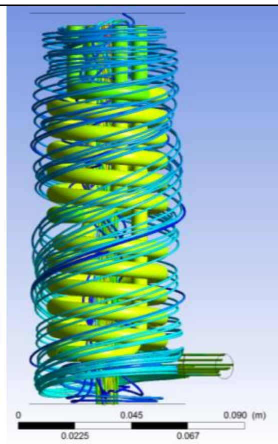

(d) Heater with internal legs and tank D=62 mm, with inlet angle (0°,45°)

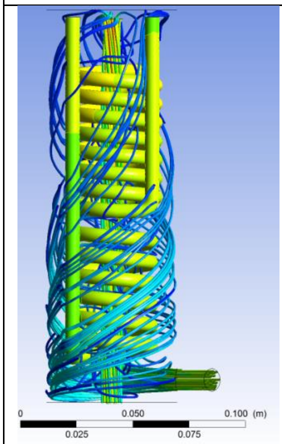

(e) Tank heater D=58 mm with inlet angle (0°,45°)

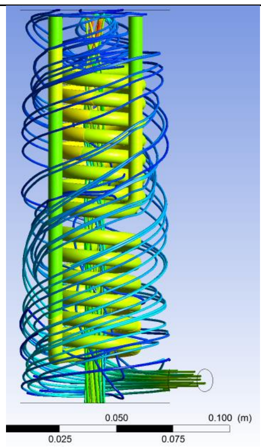

(f) Tank heater D=66 mm with inlet angle (0°,45°)

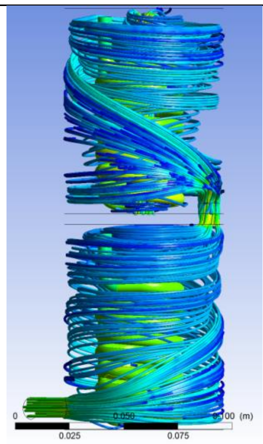

(g) Two tanks with D=73.2 mm, with inlet angle (0°,45°)

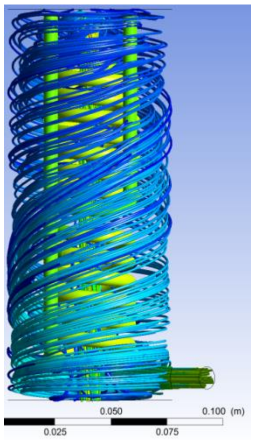

(h) Tank with D=73.2 mm with inlet angle (0°, 45°)

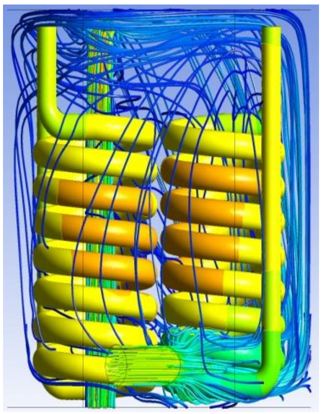

(i) Vertical oval tank with inlet angle (0°,45°)

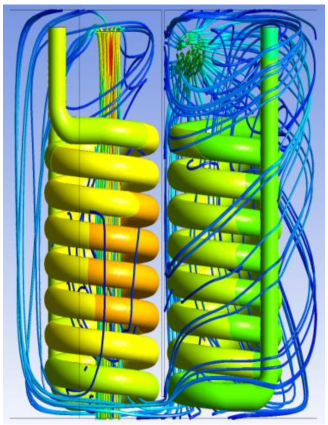

(j) Vertical oval tank with internal separation wall and inlet angle (0°,0°)

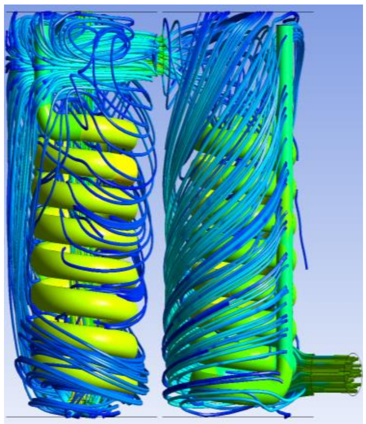

(k) Two tank s with D=58 mm, H=90 mm with inlet angle (0°, 45°)

Figure 5-28 Simulated three dimensional flow field for m°=0.10 kg/s

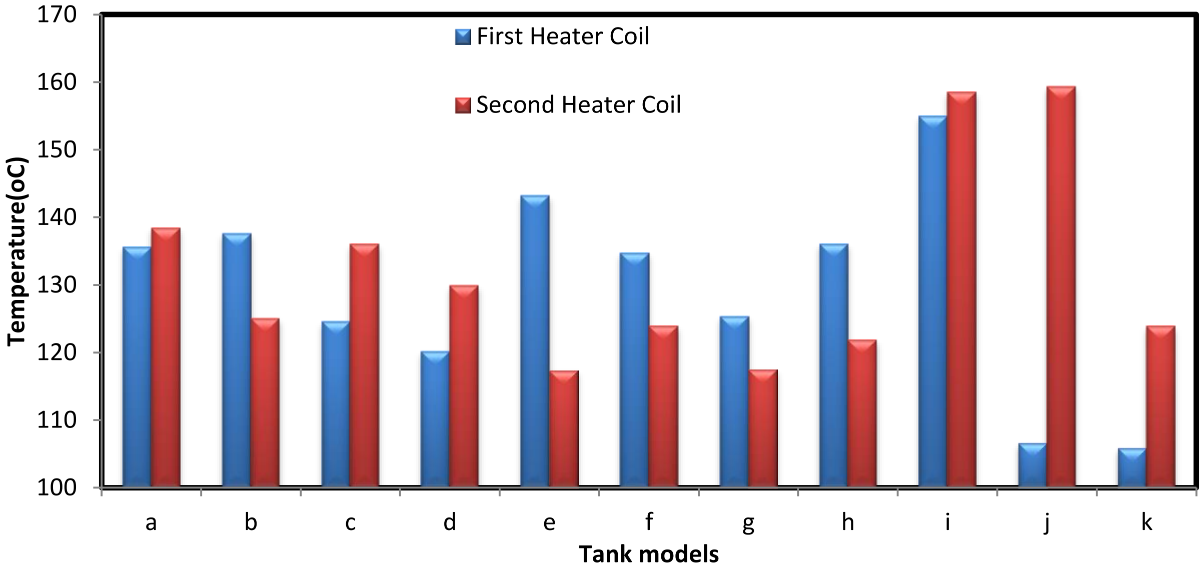

Figure 5-29 The maximum temperature of the heating elements coils for various tank configurations (m°=0.06 kg/s)

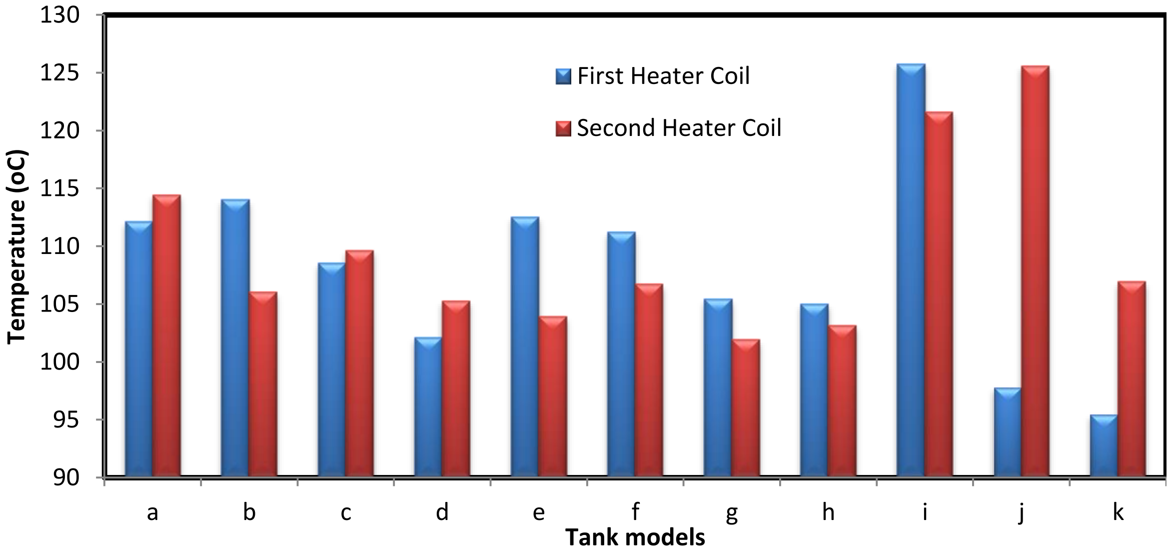

Figure 5-30 The maximum temperature of the heating elements coils for various tank configurations (m°=0.10 kg/s)

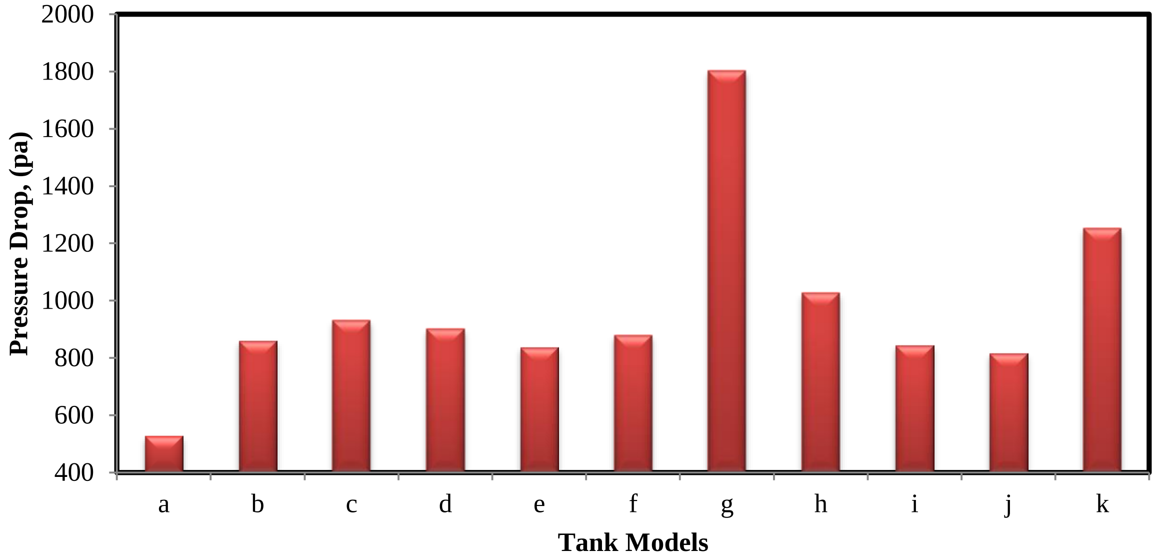

Figure 5-31 Pressure Drop inside the tank for different tank configurations (m^o=0.06 kg/s)

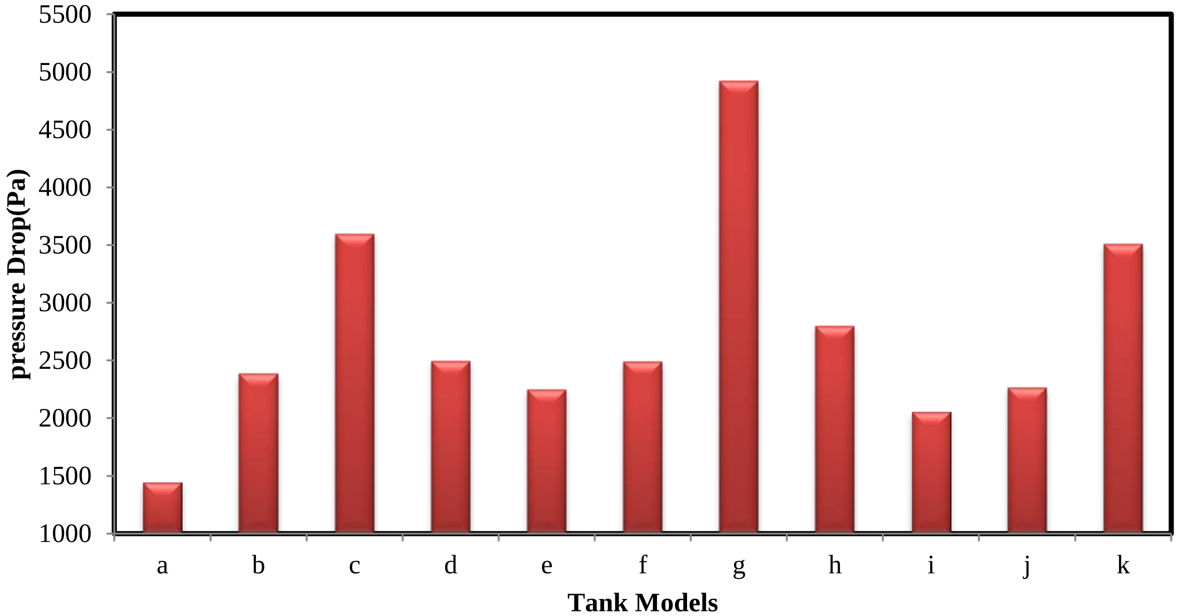

Figure 5-32 Pressure Drop inside the tank for different tank configurations (m^o=0.10 kg/s)

5.6. Conclusion

The 3D model for an instantaneous electric water heaters were applied to investigate the influence of several design on flow mixing inside water heating tank, The key parameters considered in this work were geometrical factors such as aspect ratios based on the variation of the tank diameter or height with a fixed height or fixed diameter, respectively, water inlet/outlet port positions, angles; heater coil structures and operating conditions such as the water loading flow rate. Different computation test cases were run to systematically analyze their effects on the system performance. Flow behaviour, heater thermal performance have been analysed.

The present results have not only confirmed some observations reported in experimental studies, but also provided an envelope for the optimum design parameters when the operating conditions and geometrical factors are varied for performance enhancement.

The fluid motion and the thermal profiles in the electric water heater have been simulated for two mass flows m^o=0.06 and 0.10 kg/s within this study. The CFD model was validated against the experimental data. Good agreement between the numerical results and the experiments was found.

It was shown that using horizontally inclined angles at the inlet provides better thermal performance compared to using the origin inlet and vertically inclined inlet angles. The heating tanks with inlet angles of (0°, 30°) and (0°, 45°) represent the best thermal performance. This means these tanks supplying hot water at higher temperature rather than tanks with the others inlets angles; also they have great influence on reducing the average surface temperature of the electric heater coils and decrease the failure rate of the electric heater; they reduce the heating load on the electric coil and are more likely to improve their durability. For the inlet angle of (0^o, 0^o), the water flows horizontally hitting another side of the water tank inducing the water flows directly to the top and less swirl flows. For the inlet angles oriented in the vertical level, some of the water flows upwards along the heating tank after hitting the tank wall and some flows downwards along the heating tank towards the tank bottom.

In the second part of the study, eleven different shapes of the heating tank were produced including two different shapes of heating elements coils (external and internal legs) both of them have the same power rating, length, the heating tank diameter are varied from 58, 66 to 73.2 mm, with different inlet angles from top, bottom, tangential and inclined by (0^o, 45^o) to vertical to ensure that produce swirl flow.

The numerical results demonstrates that changing the heating elements coils structure and heating tank geometry have a significant impact on reducing the maximum surface temperature of the heating element and favourable uniform water distribution in the heating tank. In addition, temperature distribution indicates that the new shape of heating element coil is likely to improve the heating efficiency and reduce the occurrence of failures.

From the comparison of the results the following conclusions are drawn:

1. The shape of the tank affects the mixing and circulation of water inside the tank. There are obstructions on the flow direction; the inlet kinetic energy is dissipated.
2. The structures of the heating elements coils have a strong influence on abstracting the inlet flow and the maximum surface temperature of the heating elements coils.
3. The use of guiding pipe such as two tanks with joint will advance re-circulating the flow around the heating elements coils. Therefore, the use of guiding entrance improves the circulation efficiency and the models (d and g) have been proposed for construction.
4. Modification of the heating elements coils structure and geometry of the tank could be significant benefit, since distribution of fluid temperature is more uniform and favourable , Moreover, reduced loading of the heating elements coils which has a much lower maximum temperature and this more like to improve the heater durability.
5. The maximum surface temperature of heating elements for tankless heater with inlet angle (0^o, 45^o) have been dropped by approximately 18% in comparison with other tankless heater with vertical inlet angles.
6. The pressure drop for tankless heater with baffle has increased by approximately 100 % in compression with other studied designs.
7. Tankless heater with twisted tapes has the minimum pressure drop.
8. Oval Vertical Tankless Heater with internal separation wall and inlet angle (0^o, 0^o) has the worth design as the maximum temperature of the heating elements is increased by 25%.

9. The Numerical simulation results also indicate that the degree of mixing decreased with the reduction in heating tank diameter.

Chapter (6)

6. Thermal Management of Residual Heat in Storage Water Tank

Temperature is one of the most significant factors impacting both the thermal performance and life cycle of tankless water heater. Therefore it is necessary to develop effective thermal management techniques to ensure sufficiently low operating temperature for reliability, durability and user comfort. Shower temperature higher or less than 41^{o}C could cause discomfort to users (McNabola and Shields, 2013); (Wong et al., 2010). Water temperature in the heating tank can be increased to 62^{o}C after the heating system being switched off due to the high thermal inertia within the heating element coils, at the same time this kind of heat will be lost to the atmosphere surrounding as shown in Figure 6-1.

Figure 6-1 Depiction of temperature - time profile during overshoot of electric water heating system (Triton Showers, 2014)

Hence, this work aims at examining experimentally the effect of using Phase Change Material (PCM) for thermal management of tankless water heater.

Experiments have been performed on a heating water container prototype that designed and constructed to assess the effect of presence of PCM on transient thermal performance of the water heating system.

6.1. Experimental Setup

Figure 6-2 shows a schematic diagram of the experimental facility used in this work. It consists of a hot water tank surround by PCM and enclosed by insulation material (thermal conductivity of 0.037 W/m K) to minimize the thermal losses, thermocouples and a data acquisition system.

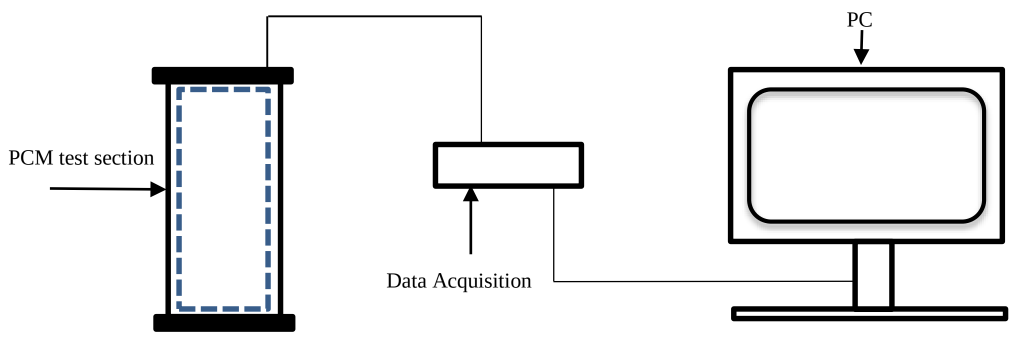

Figure 6-2 Schematic diagram of experimental setup

In this present study, a vertical arrangement of water tank unit as shown in Figure 6-3 was examined. The annular space between the copper tube and the outer shell was filled with PCM.

Figure 6-3 Proposed water heating system with the thermal storage arrangement

The Perspex cylinder is 200 mm long and has OD =102 mm and ID = 95 mm. A copper tube passes through the container center; the copper tube has OD = 76 mm and ID= 73 mm. Water is stored in the copper tube.

Four tubes with internal diameter of 2 mm and height of 5 cm are connected at the top of the Perspex cylinder to ensure the PCM in the annular gap between the copper tube and the Perspex tube are connected to the atmosphere.

During the charge mode testing, hot water at a constant temperature was injected into the tank, which was initially filled with air.

Three T-type temperature probes with the diameter of 1 mm were installed in the water storage tank to measure the vertical temperature distribution at an interval of 50 mm (T_1, T_2 and T_3). The vertical probes inserted into the storage tank through the opening at the top of the tank and supported by Plexiglas cylinder with a diameter of 2 mm.

Another three T-type thermocouples probe (T_4, T_5 and T_6) were used to measure the external wall temperature of the storage tank at an equal distance of 50 mm, all thermocouples were fixed using epoxy resin with high thermal conductivity. The temperatures of the PCM are also measured by four T-type thermocouple probes at different locations, (T_7, T_8, T_9 and T_{10}).The probes are inserted in suitable openings in the Perspex cylinder and these openings are sealed with araldite epoxy. The thermocouples' locations are detailed in Figure 6-4. The Perspex cylinder is covered by over 40 mm thick wool glass to provide sufficient thermal insulation to stop the significant heat loses to the environment. PCM was solid in the container under the room temperature. All thermocouples probes were thoroughly calibrated by a constant temperature water bath, and the accuracy is around ±0.2 ºC. Temperatures were measured at an interval of 1 second during the whole experiment.

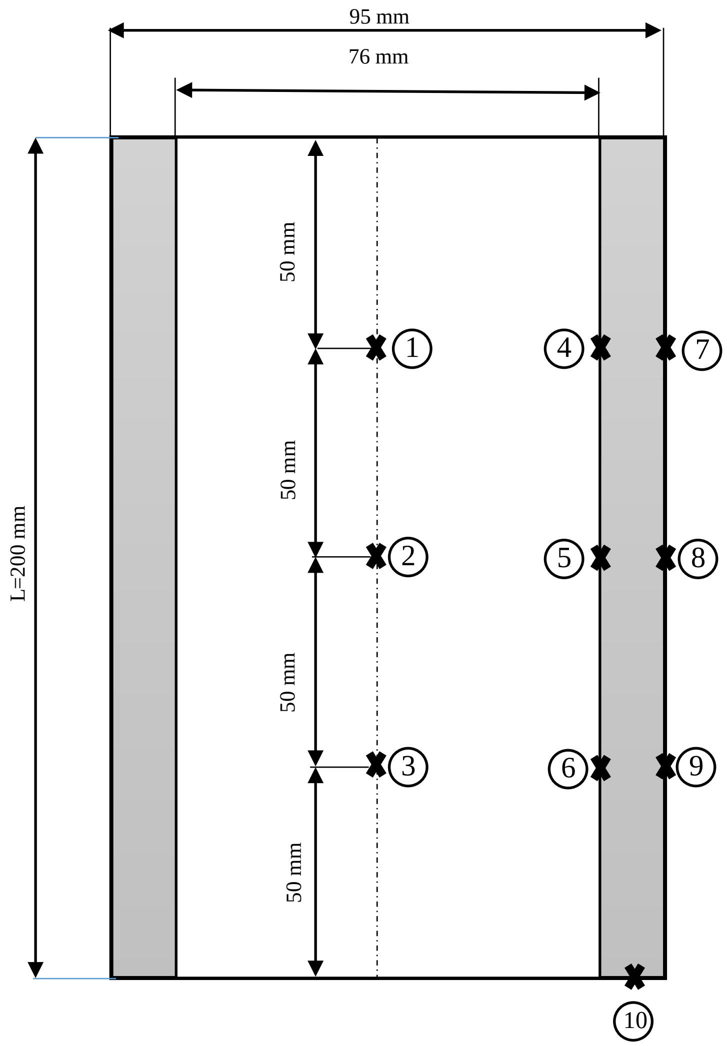

Figure 6-4 Schematic arrangement of thermocouples

6.2. PCM selection

In the present study, the commercial paraffin RT42 (RUBITHERM® R, 2014) is used as the latent heat energy storage material. Because of that RT42 is chemically stable, non-poisonous and non-corrosive over a long storage period that displays a promising stable performance through the phase change cycles. Table 6-1 depicts the thermophysical properties of RT42.

Table 6-1 Thermophysical properties of RT42

Properties	Values
Melting Temperature	38/43 ^oC
Density(solid/liquid)	880/760 kg/m^3
Kinematics Viscosity	$3.42x10^{-3}$ m^2/s
Specific Heat (solid/liquid)	2400/1800 J/kg K
Thermal Conductivity (solid/liquid)	0.2/0.15 W/m K
Latent Heat of Fusion	179 kJ/kg
Thermal Expansion Coefficient	0.0005 K^{-1}

6.3. Results and Discussion

The objective of this work is to investigate the performance of the PCM to store the residual heat in the electric shower, during shut down of an electric shower, after the user has finished showering, the flow of water into the heating tank and the heating elements must be turned off. Once the flow of water into the heating tank had stopped, the heating elements will continue to heat the water therein. This can result in the volume of water in the heating tank reaching unsafe temperatures (i.e. water temperatures which could potentially harm a user who next uses the electric shower). This is because, if the electric shower is turned on before the water in the chamber has had time to cool, the over-heated volume of hot water will be outputted immediately through the shower rose onto the user. Based on the previous experimental measurements, it is recommended that the comfortable and acceptable water temperature of the shower runs around 41-42^{o}C and after switched off the remained water's temperature reaches to around 60^{o}C.

Several tests were carried out within the experimental rig. The experiments were started by heating the water inside the tank to a temperature range of 59-81^{o}C, and then leave the tank to cool down until 40-45 ^{o}C to study the effect of PCM on the thermal performance of the tank. Table 6-2 shows the initial temperatures of the stored water and PCM in each run.

Table 6-2 Initial conditions of the stored water and PCM

Stored water temperature	PCM initial temperature
59.5 ^{o}C	21.4 ^{o}C
64.0 ^{o}C	18.4 ^{o}C
64.0 ^{o}C	31.2 ^{o}C
80.4 ^{o}C(extreme condition)	27.1 ^{o}C

Figure 6-5 illustrates the temperature distribution along the central vertical axis of the hot water tank, the water was initially heated to 59.5^{o}C and the PCM was 21.4^{o}C. It can be observed that the water temperatures decreased rapidly from 59.5 ^{o}C to 44 ^{o}C within the first 30 min, from 30 to 130 min the water temperature decreased at a lower rate from 44 ^{o}C to 40 ^{o}C. This shows a clear advantage of using PCM to keep the water at an acceptable temperature for shower for long time. This is due to the PCM has released the stored heat back to the stored water (Mahmoud et al., 2013), it is also seen that during phase change period (Δt_2) the water temperature is 3-4^{o}C higher than the melting temperature of the PCM.

Figure 6-6 shows the temperature variation during the melting process of the PCM. It can be seen that the PCM temperature was increased linearly in the first 35 min and reached the melting temperature 38 ^{o}C at which stage the PCM is undergoing phase change and therefore it is absorbing large amounts of heat without increasing its temperature until the end of the experiment. Also it is clear that the temperature of T_{10} is lower thanT_7, T_8 and T_9 that because point T_{10} is at the bottom of the PCM container and during the melting process, the melting front moves regularly downward along the container with a vessel shape. This particular shape is due to a natural convective flow, which appears after a pure conduction mode as soon as a sufficient layer of PCM is melted (Longeon et al., 2013).

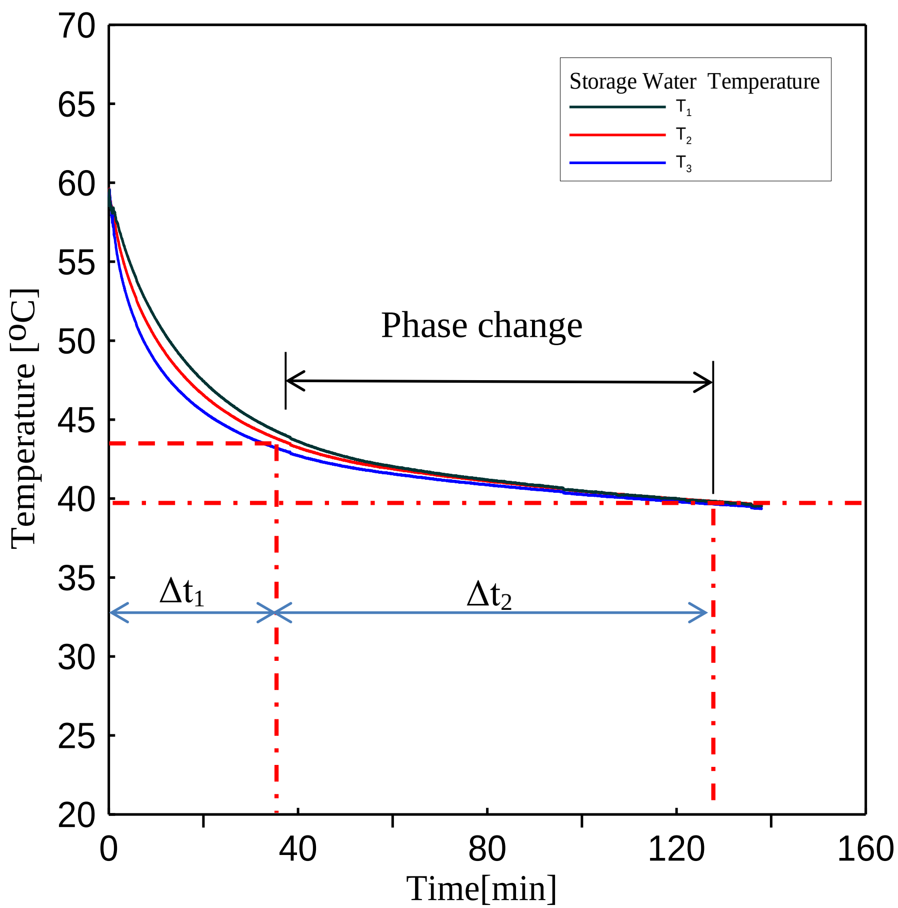

Figure 6-5 Temperature distribution along the central vertical axis of the hot water tank, T (water) $_{initial}$ =59.5°C

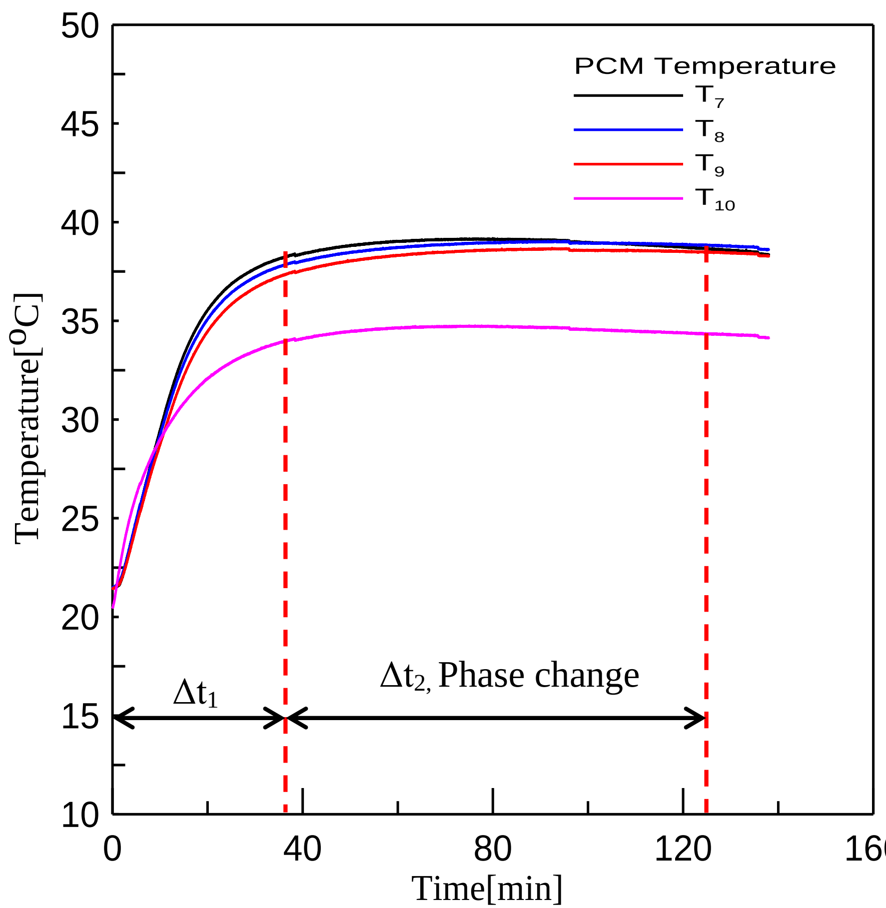

Figure 6-6 PCM temperature distribution, T (PCM) $_{initial}$= 21.4 °C

The experimental results show good agreement with the numerical simulation carried by (Longeonet al., 2013) as that shown in Figure 6-7. During charging process the temperature maps show the PCM first melts over its whole thickness at the top of the tank and not at the bottom. This is due to the following successive steps:

1. First a thin vertical layer of PCM melts along the inner tube from the bottom to the top. A natural convective flow moving upward along the inner tube intensifies the heat exchange.
2. This hot fluid arrives at the top and enables the melting of the upper PCM layer.
3. Finally, the remaining external solid PCM melts from the top due to the natural recirculation effect.

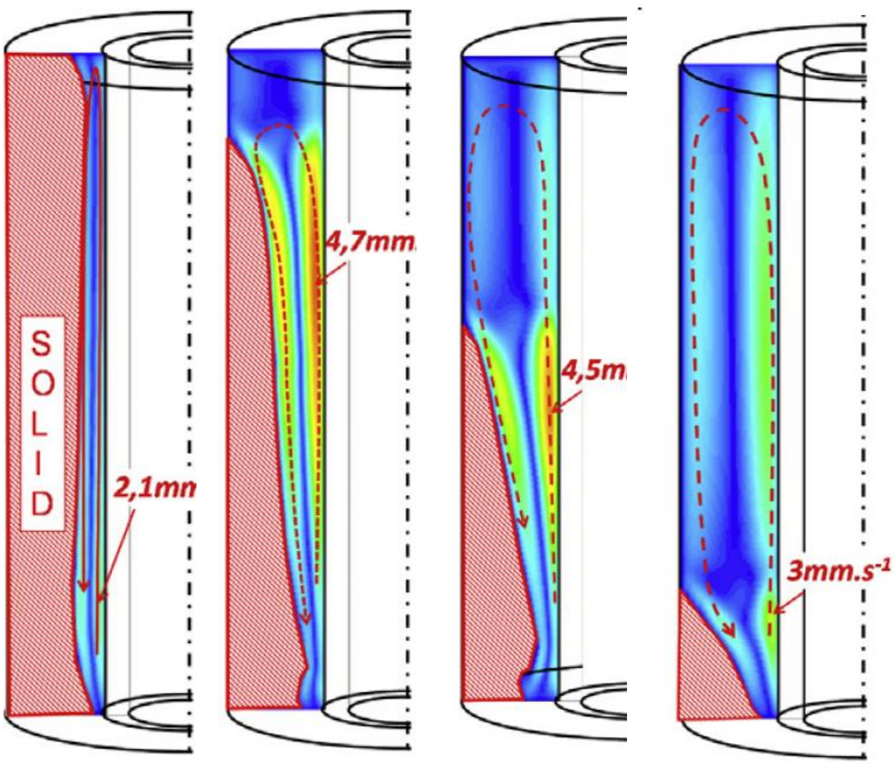

Figure 6-7 Numerical velocities magnitude in the PCM melting during charge

Figure 6-8 shows that, the heat exchange between the stored water and PCM is relatively high at the beginning of the experiment due to high temperature difference between the hot water and the cold PCM, after 42 min the heat exchange gets effectiveness then gradually reduces over the phase change process.

The most valuable result is the capability of the electric water heating system incorporating with phase change materials kept the stored water temperature constant or decreased more slowly than the stored water with no interaction with the PCM for long period, this leads to enhance the overall thermal performance of the heating system.

Figure 6-9 shows that when the PCM initial temperature was 31.4 ^{o}C, it can be figured out that, stored water temperature has reached to 42^{o}C after 120 min, from 42^{o}C to 40 ^{o}C in 180 min and from 40 ^{o}C to 33 ^{o}C in 500 min also it is clear that PCM temperature profiles and stored water temperature difference profiles for three repetitions of a charge process respectively which shows a good repeatability for the experimental study.

When the initial temperature of the stored water was about 80.4 ^{o}C as shown in Figure 6-10, the three curves of water temperature share the same behavior. First, all the stored water temperatures fall down to the phase change temperature(40^{o}c) and PCM temperature has increased sharply in the first 45 min and reached to about 54^{o}C as shown in Figure 6-11. This because the amount of heat in the stored water is relatively high and the PCM is not able to absorb this amount of heat gradually due to the lack of the heat capacity of this volume of PCM and the stored water temperature has reached to 45^{o}C after 180 min.

6.4. Conclusion

Experimental investigation were carried out to observe the advantage of using PCM in thermal energy storage system, four experiments had been carried out using different initial temperature for the stored water and the PCM. The experimental findings indicate that, the use of PCM helps to stabilize the system temperature to an allowable working temperature of 40 ^{o}C and extends the usage time. The findings indicate that the melting time of the solid PCM is still a problem that needs to be resolved. The time for the PCM completely melting is still long due to the poor thermal conductivity of PCM. Briefly the results show that inclusion of a PCM in water tanks for domestic hot-water supply is a very promising technology. It would allow the user to have hot-water for long period of time even without exterior energy supply. Additionally, further studies should focus on optimized latent thermal energy storage with heat transfer enhancement methods. Among them, several finned tubes and thermal conductivity improvement based on graphite foam could be tested and compared.

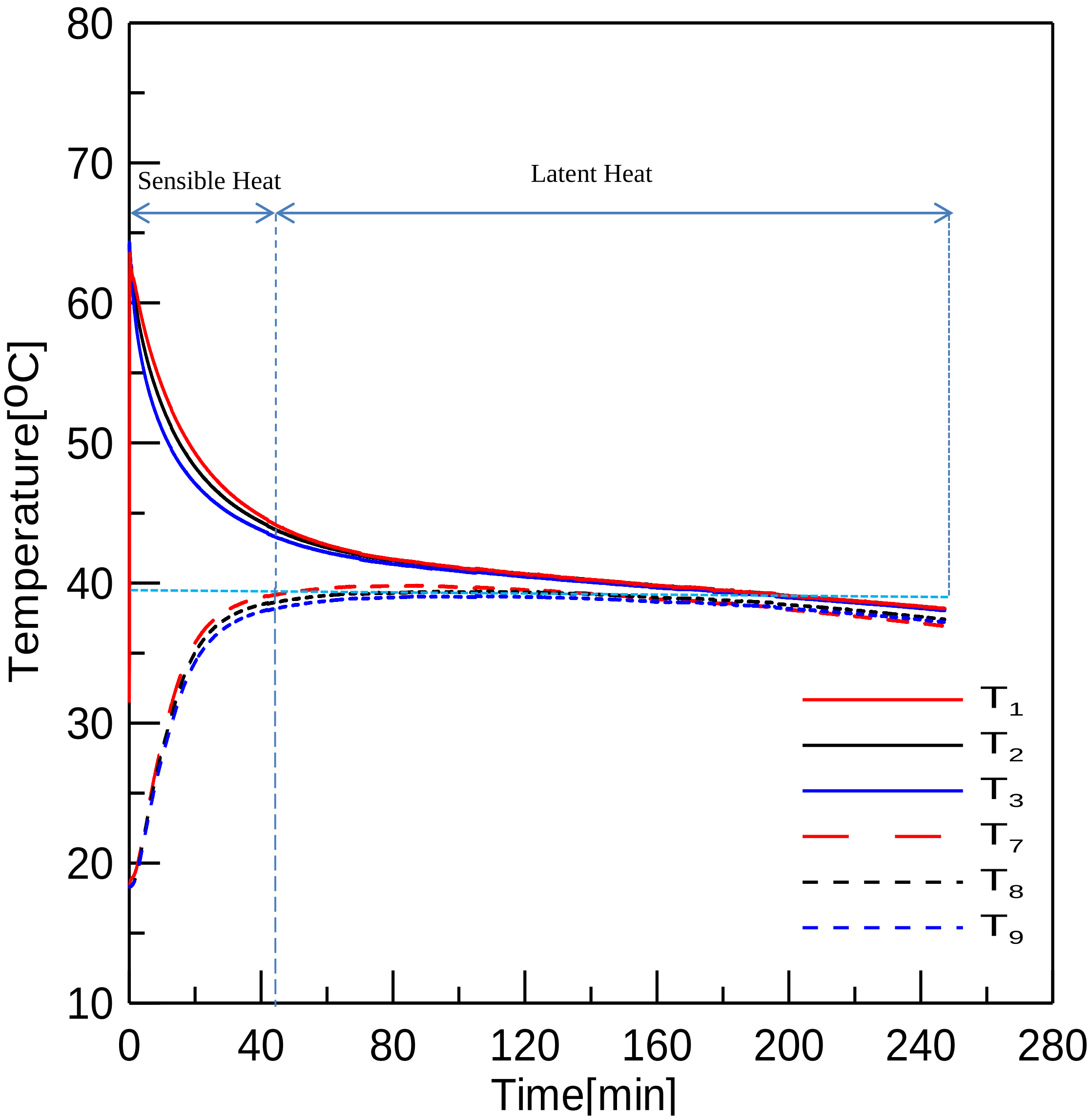

Figure 6-8 Temperature distribution along the central vertical axis of the hot water tank, T (water) $_{initial}$ =64 ^{o}C and PCM temperature distribution, T (PCM) $_{initial}$= 21.4 ^{o}C

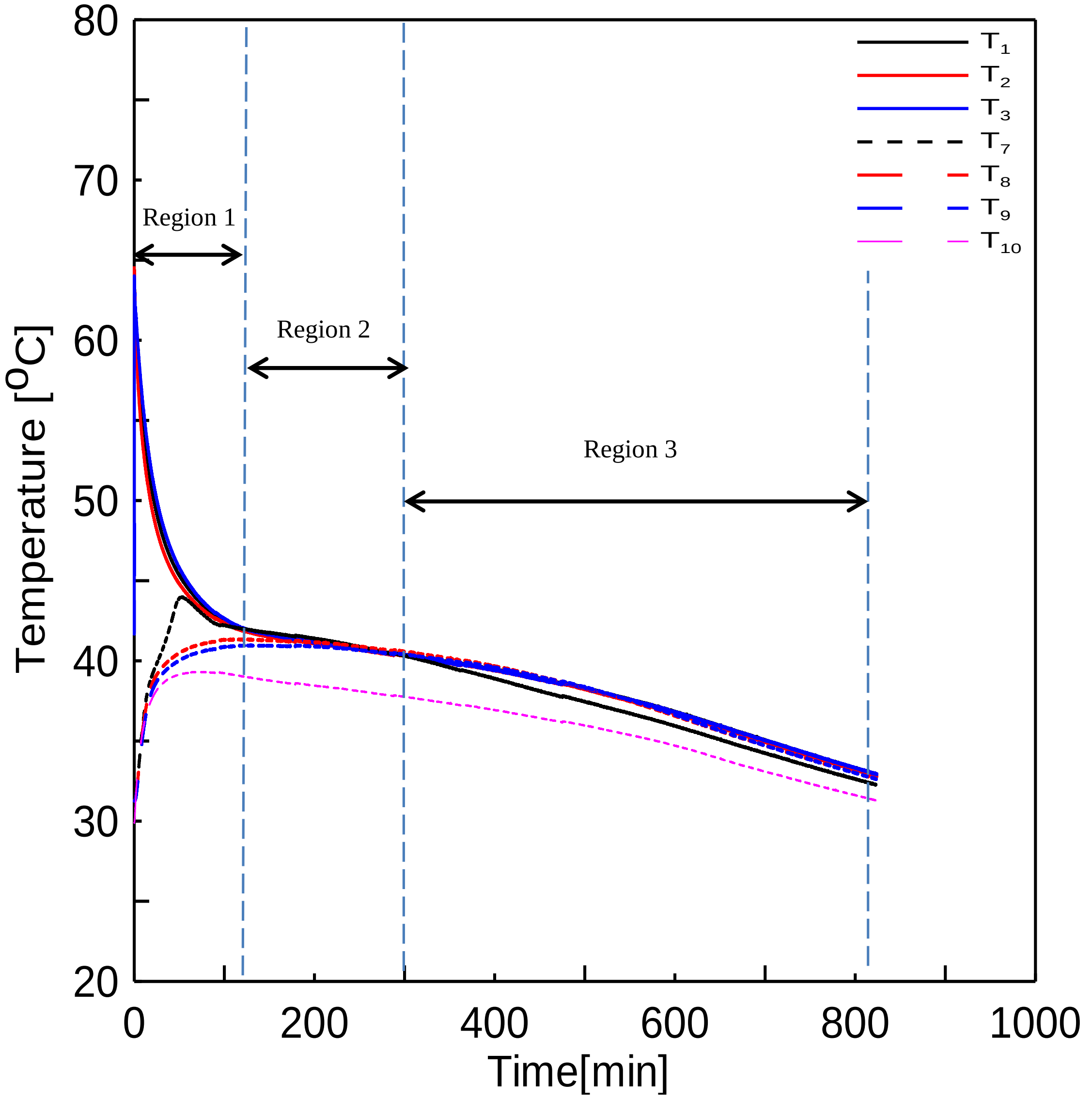

Figure 6-9 Temperature distribution along the central vertical axis of the hot water tank, T (water) $_{initial}$ =64 °C and PCM temperature distribution, T (PCM) $_{initial}$= 31.2 °C

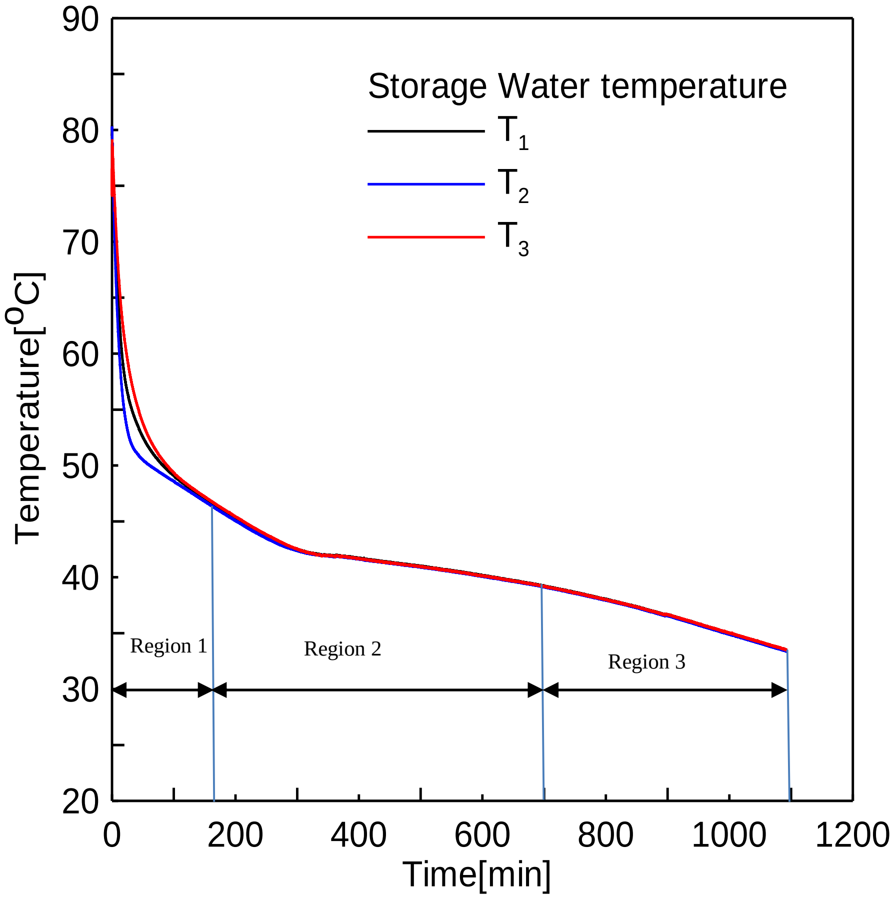

Figure 6-10 Temperature distribution along the central vertical axis of the hot water tank, T (water) $_{initial}$ =80.4 °C

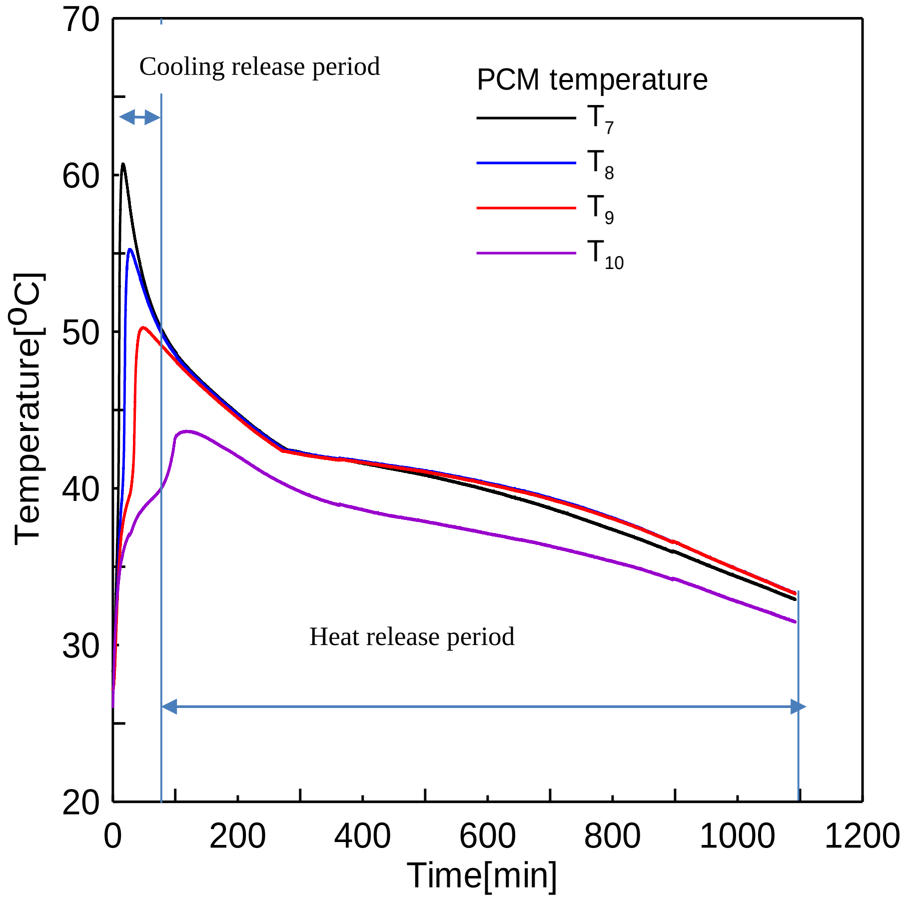

Figure 6-11 PCM temperature distribution, T (PCM) $_{initial}$= 27.1 °C

Chapter (7)

7. Performance Analysis of an Ohmic Heating for Water Heating

Ohmic heating is an innovative electro-heating method for water heating, involves the passage of alternative electric through the water, thus generating internal energy as the result of electric resistance causing temperature rise (Icier, 2012) the uniform heat generation results in uniform temperature distribution.

From the previous works which have been done, it can be concluded that there are large number of potential future applications exist for Ohmic heating, including its use in water heating. On the other side, research is needed on the methods for measurements and design of testing equipment.

The objective of the present work is to evaluate the thermal performance of Ohmic heating system based on different parameters such as voltage gradient, electrical conductivity, heating rate and electrode materials.

7.1.Experimental Setup

7.1.1.Design of the Ohmic heating unit

Ohmic heating experimental apparatus were conducted in a laboratory scale. Ohmic heating system consists of power supply, a data logger system, an isolating variable transformer, Ohmic heating unit, thermocouples and PC. A schematic diagram of the Ohmic heating equipment is presented in Figure 7-1.

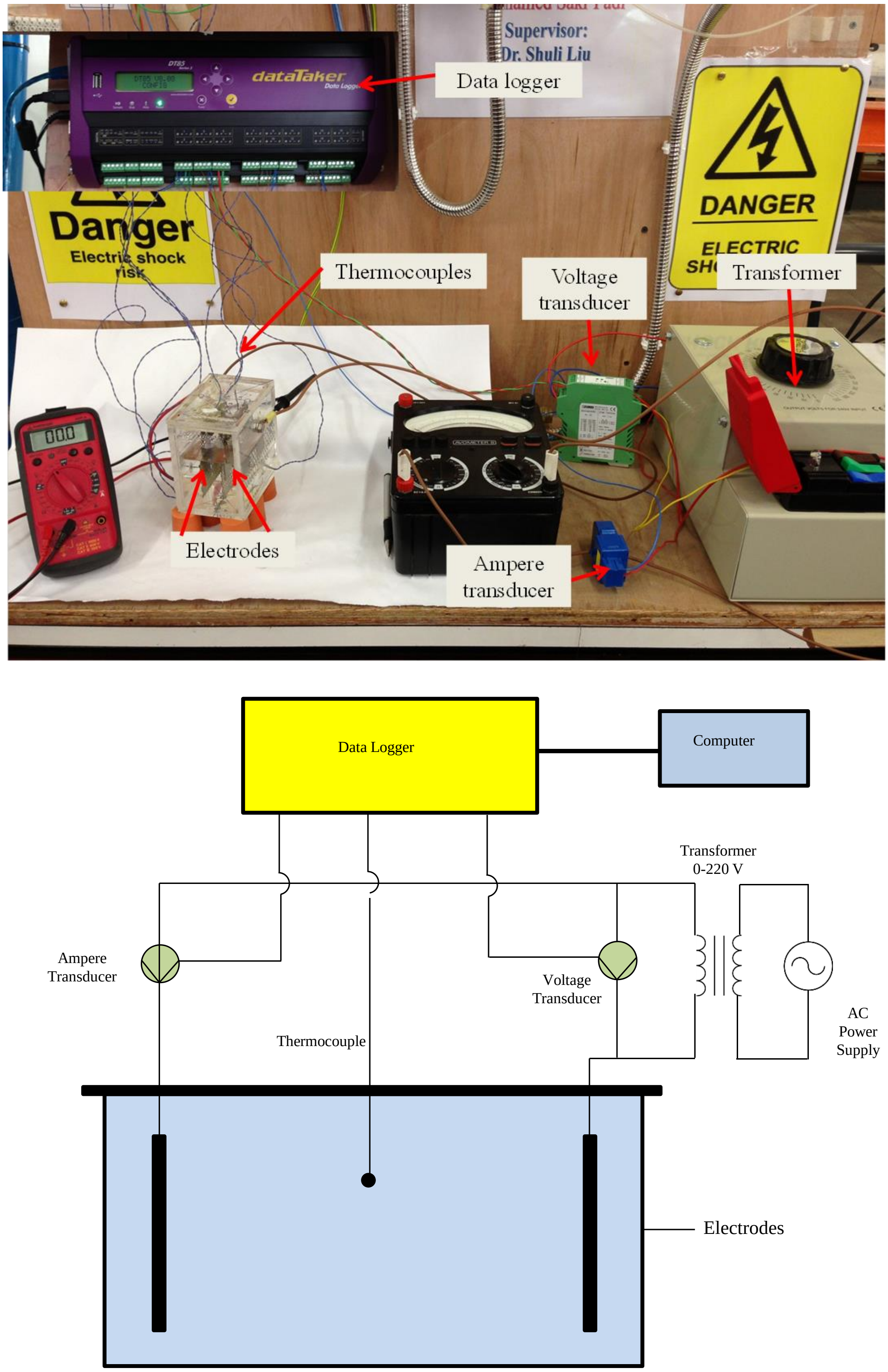

Figure 7-1 Testing rig and schematic diagram of the static Ohmic heating system

7.1.2. Power supply system

The power supply system includes a manual voltage regulator ranging from 0 to 240 V (RS, United Kingdom). The power supply was connected to the main power supply, using alternative current (AC) and 60 Hz frequency.

7.1.3. Ohmic heating unit

The Ohmic heating chamber was designed and made from Perspex glass with dimensions 60×100×100 mm^3; the total volume of water is 0.36 liters; two rectangular sheet platinized-titanium electrodes were used as shown in Figure 7-2. The electrodes were purchased from Schloetter Co Ltd, United Kingdom. The platinised titanium electrodes consist of a titanium base in the form of sheet with a thin coating of platinum between 2 to 5 microns thick. Platinised titanium electrodes have a lot of advantages such as, long operating life, maintenance-free, economical due to low platinum requirements, high dimensional stability and load resistance, good current distribution, high corrosion resistance and low weigh. Electrodes were inserted from the top opening in the middle of the chamber, the details of the heating chamber and electrodes locations are shown in Figure 7-3. The gap between the electrodes was controlled by nut and threaded bars on the cell wall, the distance can be adjusted.

A major challenge for performance evaluation is monitoring the water temperature during the heating process. However, the use of thermocouple probes in an Ohmic heating environment can lead to problems such as electrical discharges and signal perturbations inside the heating device (Zell et al., 2009), so the thermocouple probe must be selected appropriately to permit quick response time while being resistant to withstand repeated use. There must have appropriate internal insulation to eliminate the risk of electrical interference and to protect the data logger.

Water temperature was continuously recorded during the experiments by measuring the temperatures at different locations in the test unit. Four thermocouples Teflon coated (to prevent interference from the electric field), rigid, T-type (Omega engineering Inc, UK), were fixed perpendicularly along the cell a shown in Figure 7-4 to measure water temperature at different section in the test cell.

The insulated thermocouple probes were calibrated to check the rapid respond for the temperature reading, the selected thermocouples have been calibrated with k-type thermocouples in order to check it rapid time response for use in Ohmic heating system, as shown in Figure 7-5, the insulated thermocouples have good time response and there is no electrical interferences occurred due to the presence of a thermocouples probe in the Ohmic cell also each insulated thermocouple has an accuracy of ±0.2 ^{o}C over the temperature range 10-90 ^{o}C. An overall accuracy of ±0.3 ^{o}C is generally accepted for uncelebrated commercial thermometers which are in line with the results presented above (Anon, 1981).

7.1.4. Data logger system

The data logger system monitors and recorders the measurements data related to the electric current, temperature and voltage as a function of time. Data was measured and recorded at constant time one second interval. The data logger (DT85 Series 3 Data Logger, Victoria, Australia) linked to a computer to store data. The data logger was connected by voltage transducer and current transducer to be able measures both AC current voltage and temperature; data were logged at 1 second time interval.

7.2. Test Procedure

7.2.1. Electrical conductivity

The EC, electrical conductivity (σ, s/m) can be determined from the current and voltage data from the following equation (Zellet al., 2009; Zhu et al., 2010; Assiry, 2011).

$$\sigma = \frac{I}{V}\frac{X}{A} \tag{7.1}$$

The ratio of (X/A) is known as the cell contact of the Ohmic heating, where X is the gap between the two electrodes (m), A is the electrodes cross section area (m^2), V is the voltage (Volt) and I is the current in (Amp).

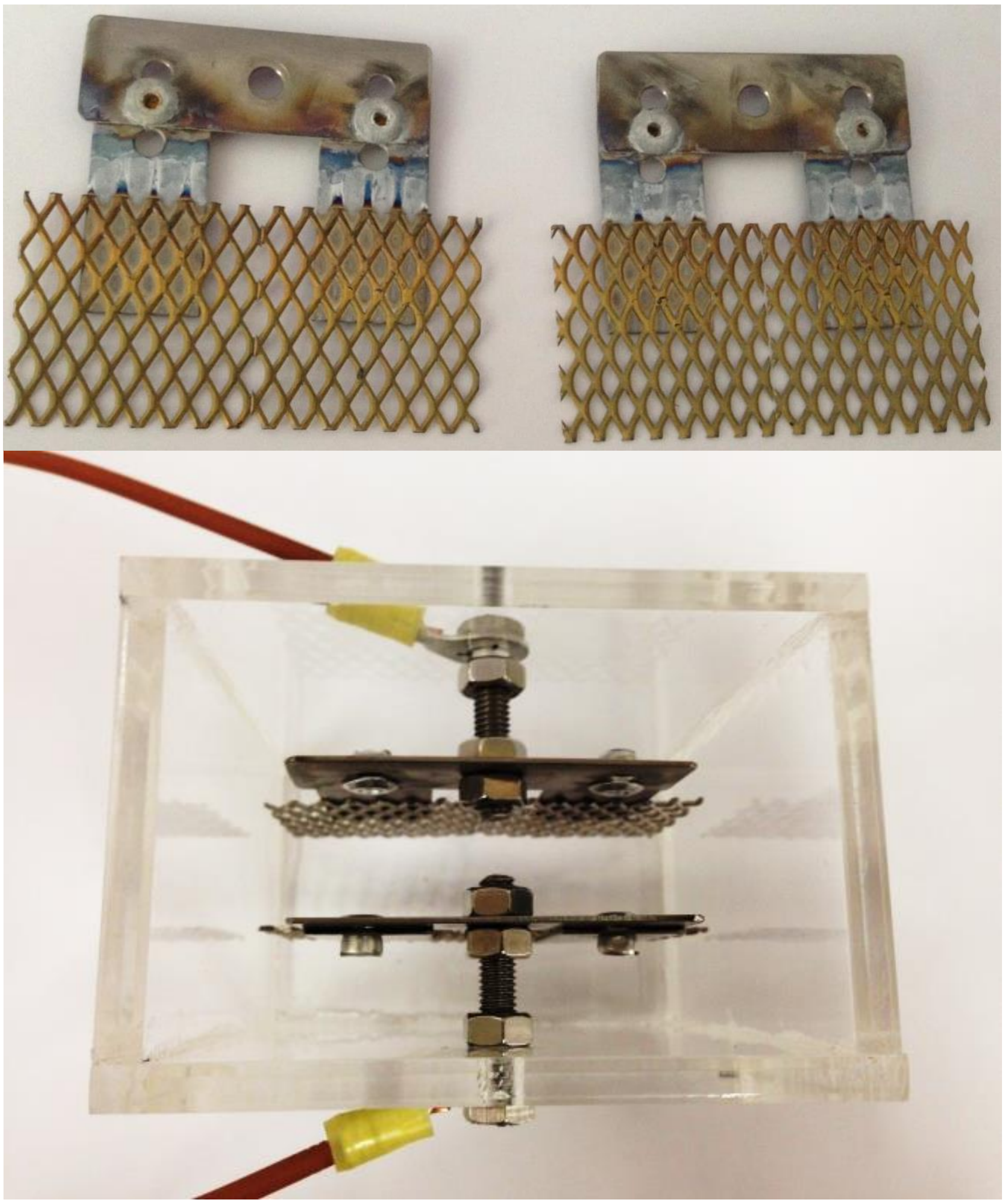

Figure 7-2 Photograph of the platinized-titanium mesh electrodes

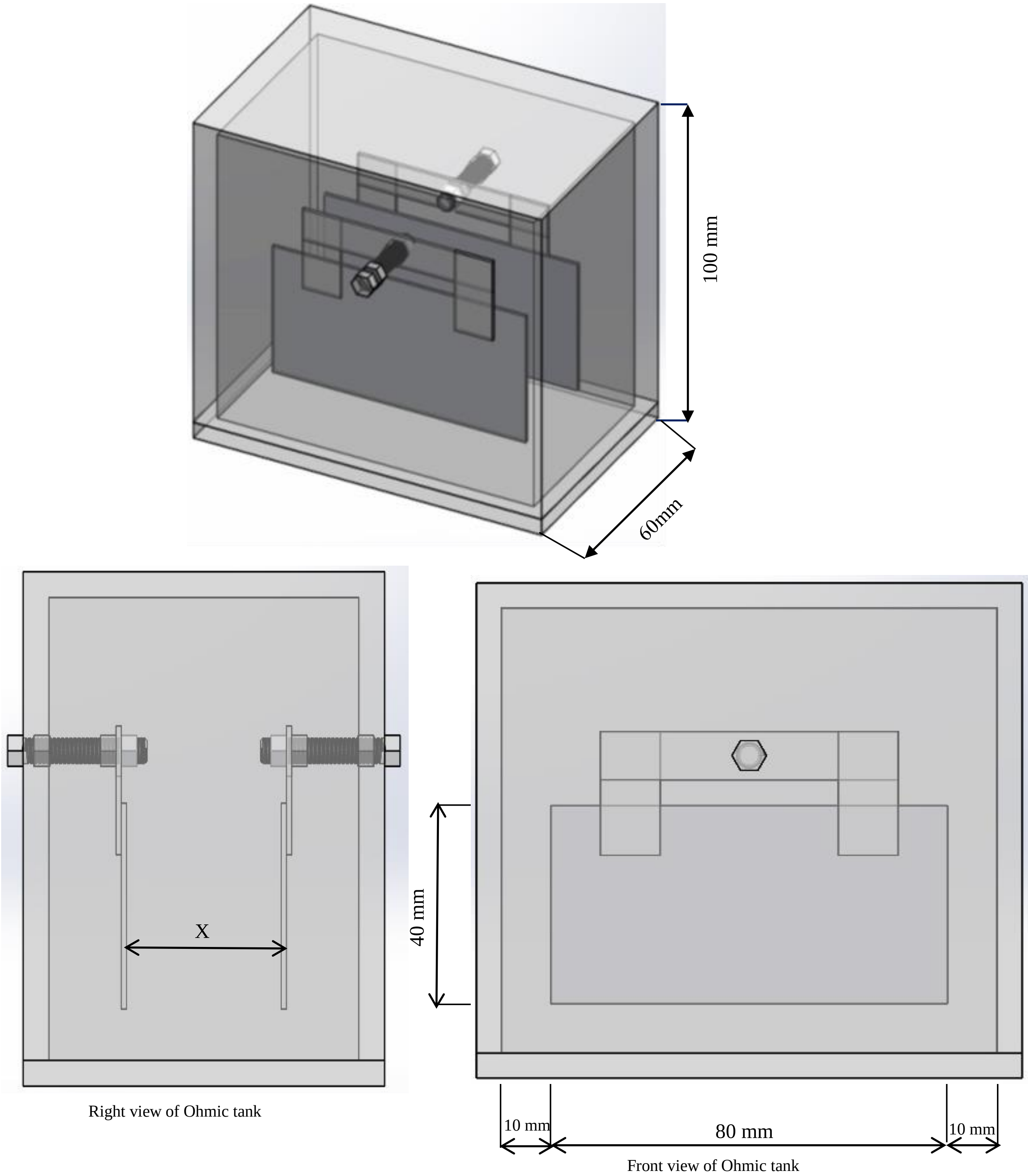

Figure 7-3 Schematic diagram of the electrodes location in the Ohmic cell

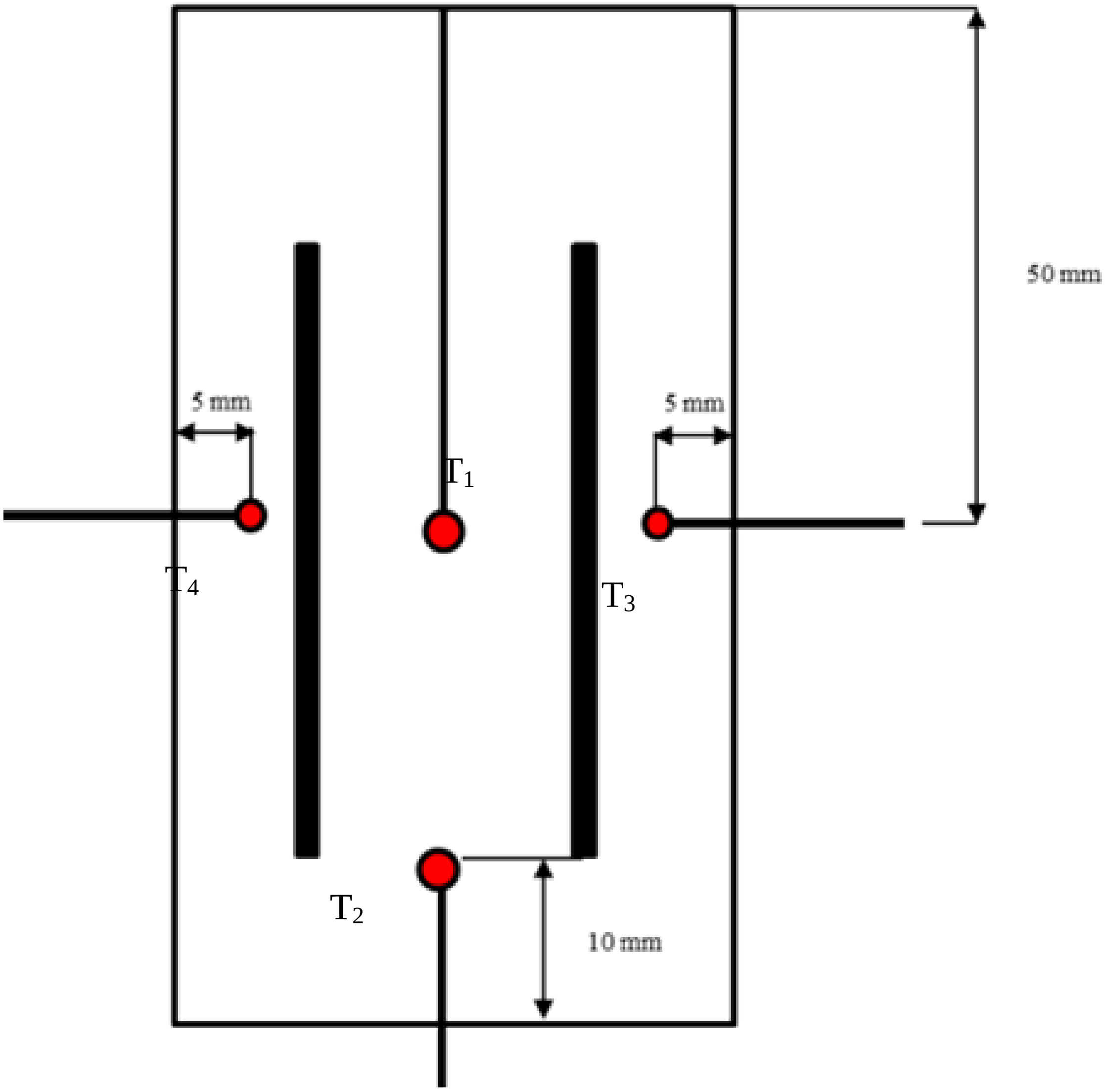

Figure 7-4 Configuration of temperature probes

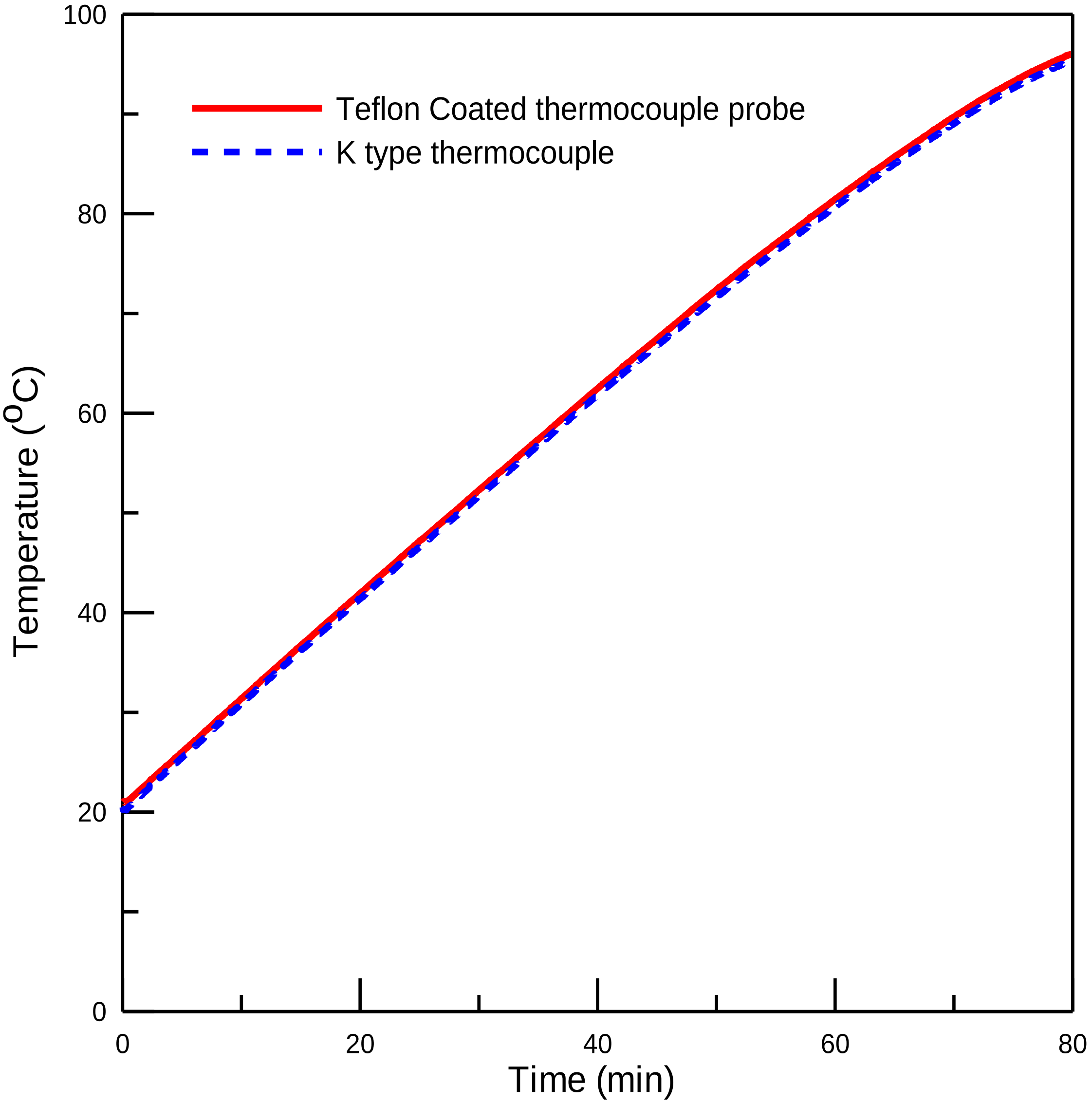

Figure 7-5 Time–temperature profiles of water temperature measured with coated and K-type thermocouple

7.2.2. Energy efficiency measurement

The performance of Ohmic heating system under different modes is defined by energy given to the system and the heat taken up by water, which has been calculated by using the voltage, current and temperature values. The temperature has been recorded during the heating experiments and the energy losses to the surround are neglected.

$$E_{input} = \Sigma(\Delta VIt) \tag{7.2}$$

$$Q_{absorbed} = m\, C_p(\, T_f - T_i) \tag{7.3}$$

The average water temperature at any time is calculated by:

$$T(\tau) = \frac{\sum_{i=1}^{n} T_i(\tau)}{n}, n = 4 \tag{7.4}$$

Total energy given to the system should be equal to the total energy absorbed to heat up the water. System performance coefficient is defined as:

$$\text{System Performance Coefficient(SPC)} = \frac{\text{Energy uyilized to heat water}}{\text{Total input energy}} \times 100 \tag{7.5}$$

Errors and uncertainties in experiments could occur from the instrument selection, condition, observation, and reading. The uncertainty analysis was performed using the method described by Holman (Holman, 2011). The details of the experimental uncertainty analysis are given in the appendix (E).

7.3. Results and discussions

7.3.1. Heating rate

The objective is to study the water heating performance during Ohmic heating. Heat is generated in the water due to passing the electric current through the heating system, water was initially at room temperature at 18^{o}C and heated up to 95^{o}C, the amount of heat generated within the water sample is depended on its electric conductivity which keeps varying during the heating process. The gaps between electrodes were X=23, 28, 34 and 38 mm and the applied voltages were 100, 150 and 200 Volt.

Water temperature distributions during the Ohmic heating cell for different applied voltage and gap between the electrodes are shown in Figures 7-6, 7-7 and 7-8. It can be clearly seen that the average water temperature is increased approximately linearly with time, the water temperature (T_1) in the middle of the electrodes are higher than at the bottom (T_2) and behind the electrodes (T_3, T_4) due to affect varying electric field strength for the same applied voltage and the heating time is increased with increasing electrodes gap. For the same gap between the electrodes, the heating time is decreased with the increase of the applied voltage.

Figure 7-6 shows that, for applied voltage, V=100 Volt, the heating time to increase water temperature from 20 ^{o}C to 85 ^{o}C is 850 s for X=23 mm; 900 s for X=28 mm; 1200 s for X=34 mm and 1400 s for X=38 mm.

When the applied voltage increased to 150 Volt, the heat time to raise the water temperature from 18 ^{o}C to 80 ^{o}C is 330 s for X=23 mm, 400 s for X=28 mm, 430 s for X=430 mm and 670 s for X= 38 mm as shown in Figure 7-7.

For applied voltage, V= 200 Volt, the heating time to raise the water temperature from 21 ^{o}C to 70 ^{o}C, is 150 s for X=23 mm, 165 s for X=28 mm, 190 s for X=34 mm and 230 s for X=38 mm as shown in Figure 7-8.

It is noticed that there are difficulty of reading water temperature during ohmic heating due to appearing steam bubbles which effect thermocouples reading.

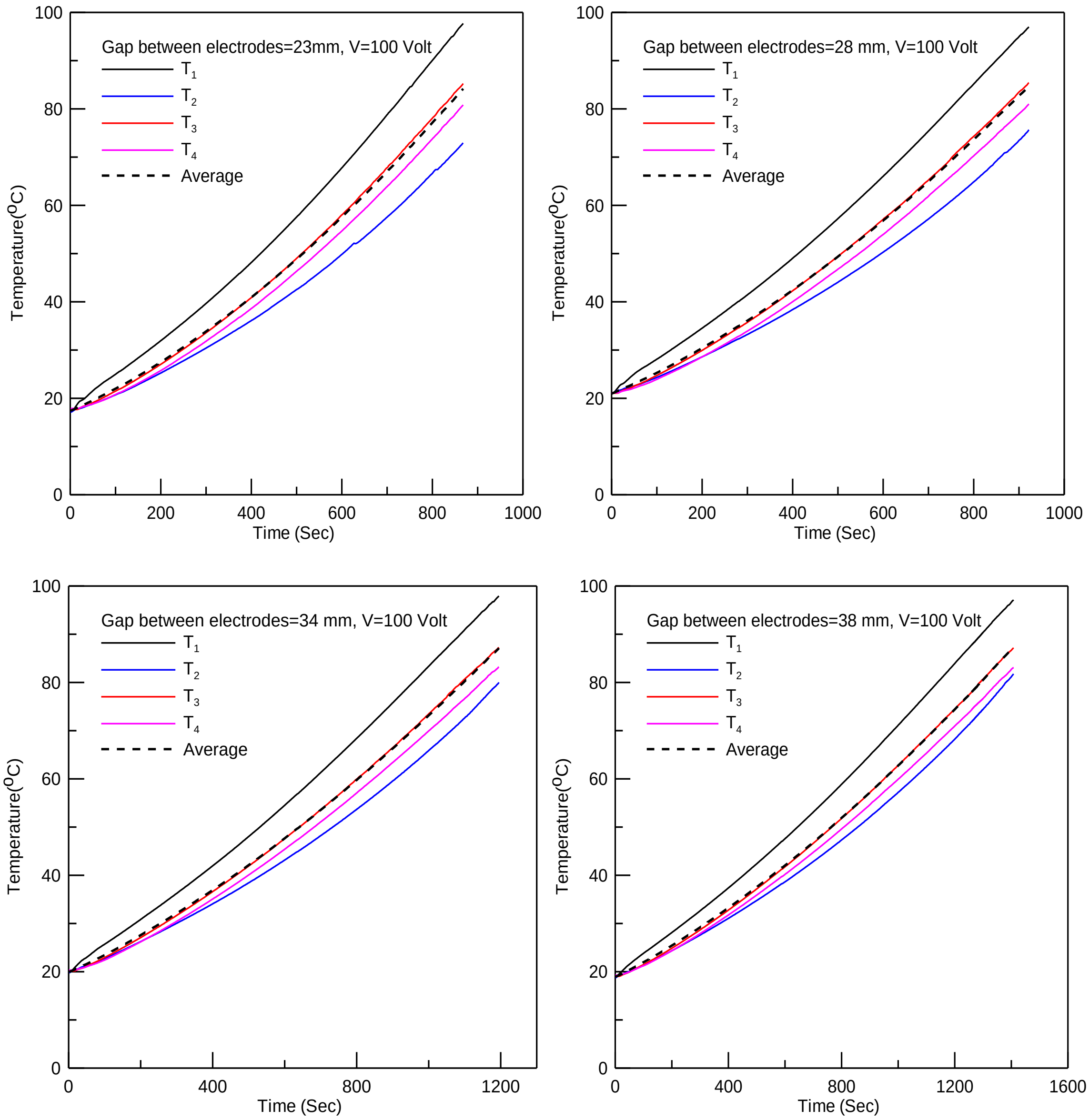

Figure 7-6 Time-temperature profiles of Ohmic heating for V=100 V and X=23, 28, 34 and 38 mm

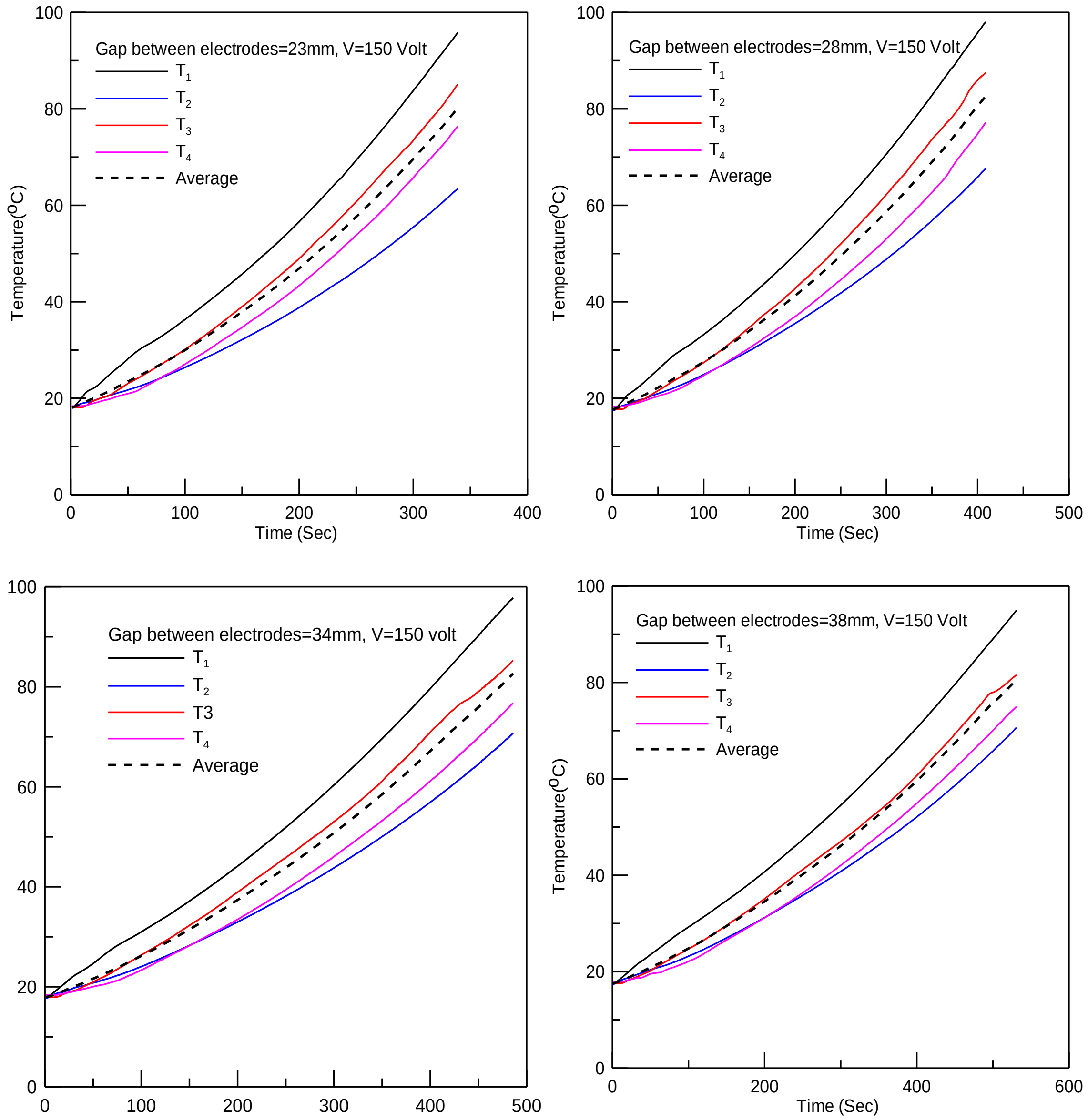

Figure 7-7 Time-temperature profiles of Ohmic heating for V=150 V and X=23, 28, 34 and 38 mm

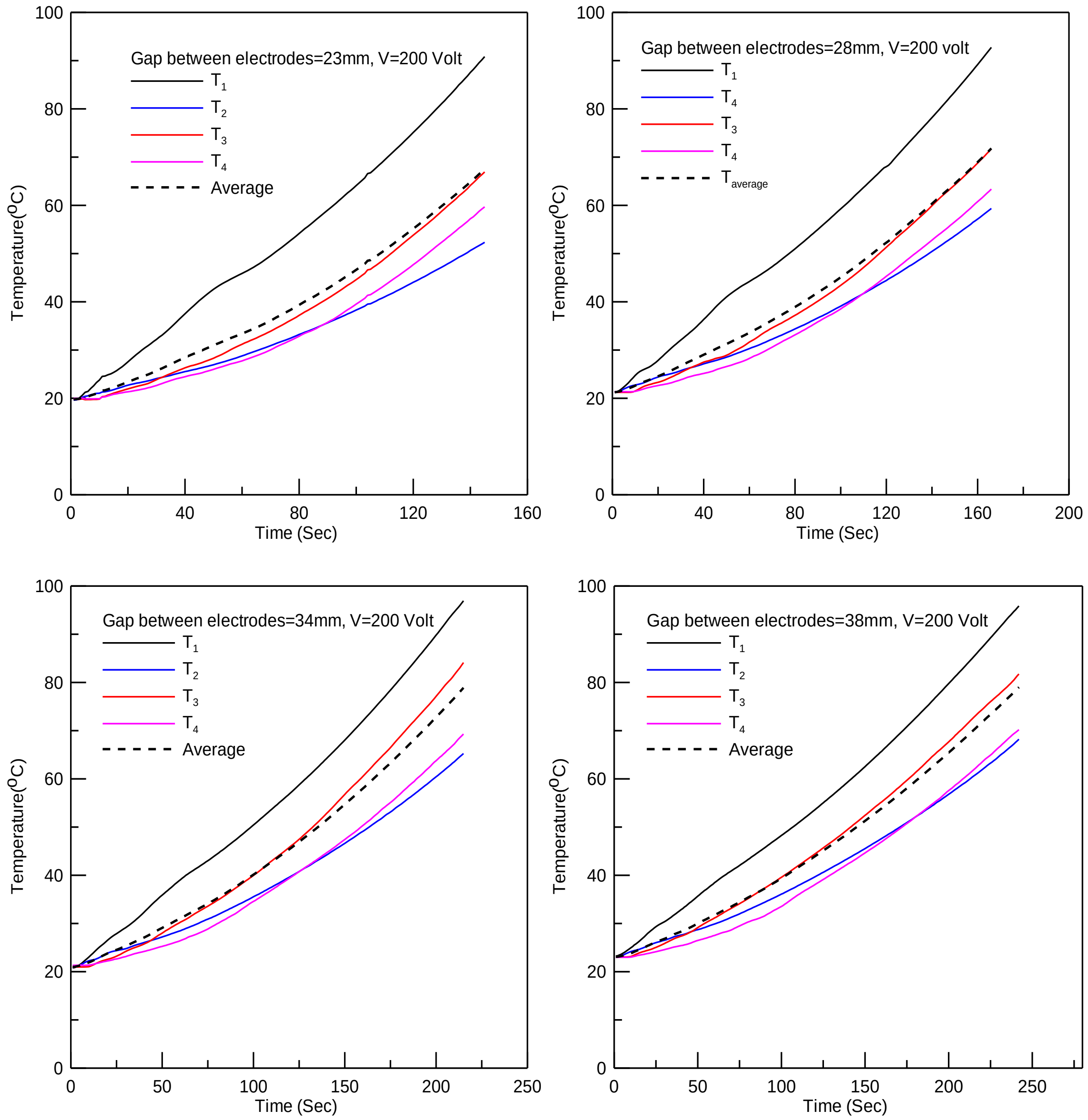

Figure 7-8 Time-temperature profiles of Ohmic heating for V=200 V and X=23, 28, 34 and 38 mm

The amount of passing current to heat up water for different applied voltage are illustrated in Figures 7-9, 7-10 and 7-11. It can be clearly seen that the amount of electric passing current is increased as the temperature increases, meanwhile, the electrical passing current through the heating sample is increased with increase of voltage gradient and this induced the heat generation faster (Sakr and Liu, 2014; Darvishi et al., 2013; Nguyen et al., 2013; 3 Icier ,2012; Assiry, 2011).

For applied voltage V= 100 Volt, the electric current passing has increased from 0.67 to 2.19 Amp in 868 s for X=23 mm; from 0.67 to 1.94 Amp in 922 s for X=28 mm; from 0.53 to 1.606 Amp in 1195 s for X=34 mm and from 0.43 to 1.38 Amp in 1408 s for X=38 mm as shown in Figure 7-9.

Figure 7-10 shows that, for V=150 Volt, the passing electric current has increased from 1.05 to 3.25 Amp in 339 s for X=23 mm, 0.916 to 2.885 Amp in 409 s for X=28 mm, from 0.75 to 2.45 Amp 486 s for X=34 mm and from 0.79 to 2.21 Amp on 531 Sec for X=38 mm.

For applied voltage V= 200 Volt, the passing current has changed from 1.689 to 4.59 Amp in 145 s for X=23 mm, from 1.5424 to 4.24 Amp in 166 s for X=28 mm, from 1.2678 to 3.6187 Amp in 215 s for X=34 mm and from 1.1189 to 3.0656 Amp in 242 s for X=38 mm as shown in Figure 7-11.

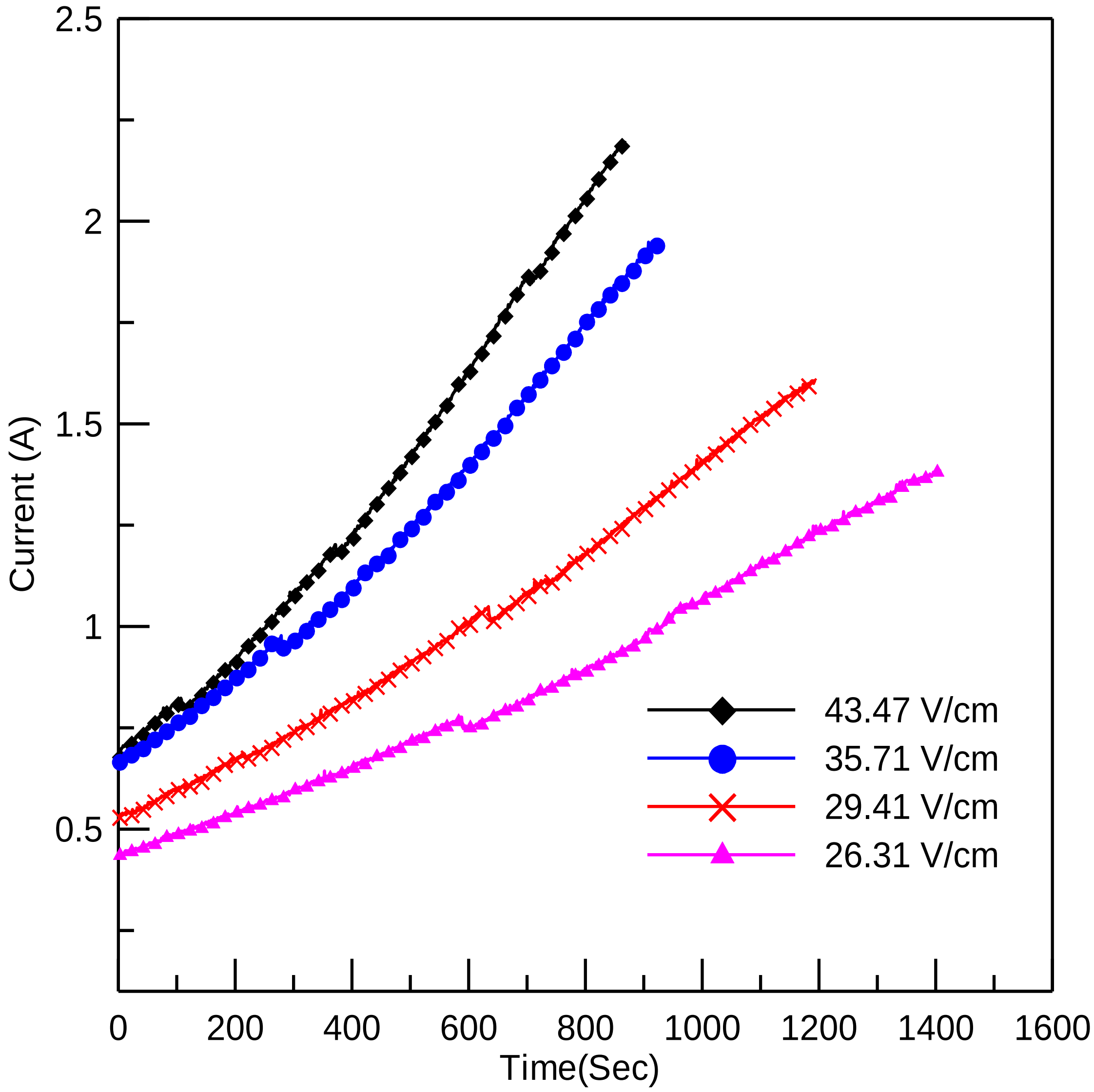

Figure 7-9 Changes in electric current passing under different voltage gradients, V= 100 Volt

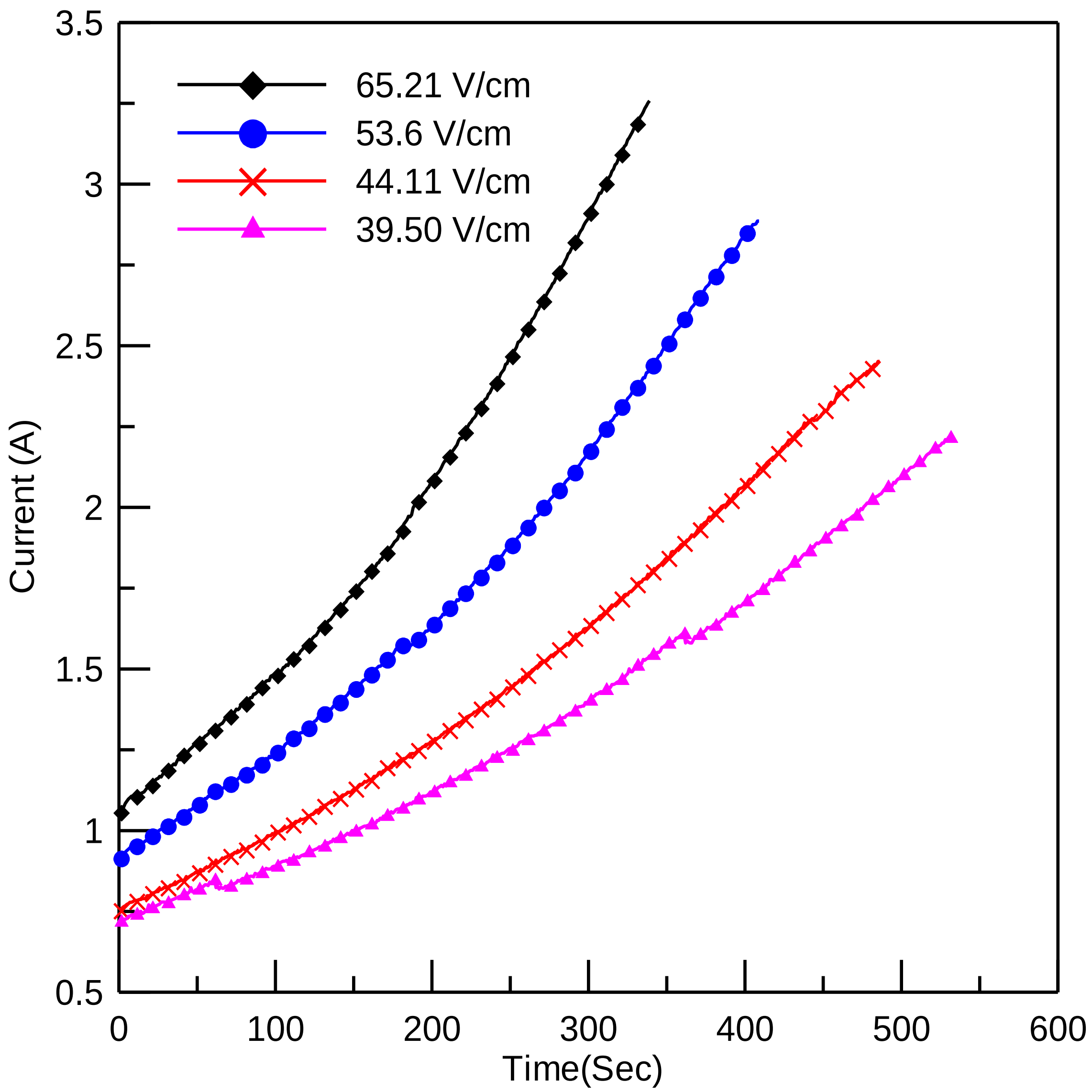

Figure 7-10 Changes in electric current passing under different voltage gradients, V=150 Volt

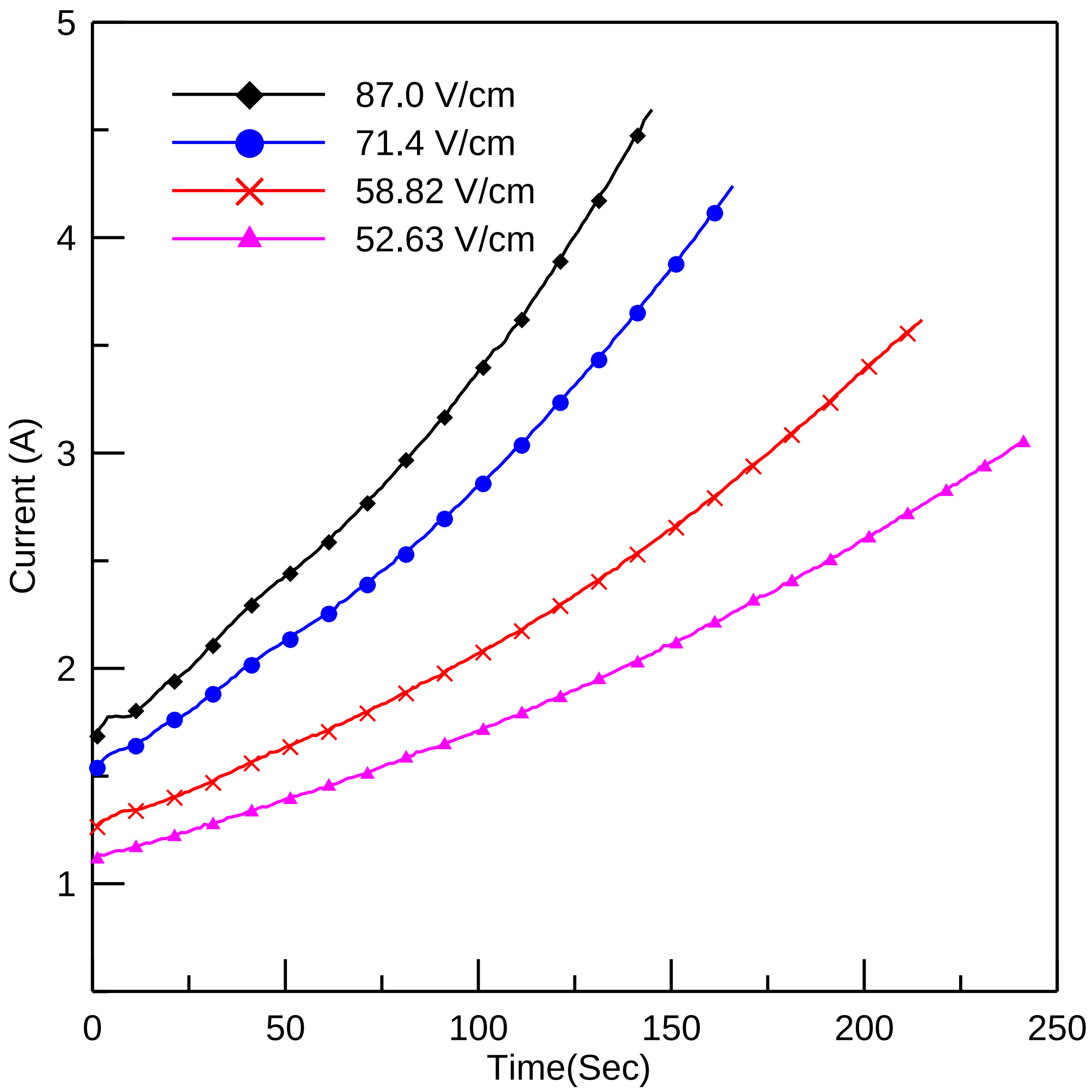

Figure 7-11 Changes in electric current passing under different voltage gradients, V=200 Volt

Table 7-1 shows the summarize of electric passing current gradient for different applied voltage and electrodes gaps, (Amp/s)

Table 7-1 Summarize of passed current gradient for different applied voltages and electrodes gaps, (Amp/s)

	V=100 Volt	**V=150 Volt**	**V=200 Volt**
X=23 mm	0.00175	0.006	0.020
X=28 mm	0.00137	0.0048	0.016
X=34 mm	0.00090	0.00354	0.011
X=38 mm	0.00067	0.0026	0.008

The effect of the voltage gradients on the Ohmic heating time were found significant as shown in Figures 7-12, 7-13 and 7-14. For different voltage gradient (26 to 87 V/cm), it is apparent that the heating time is decreased as the voltage gradient increases, this because the electric energy generated during the heating process is dependent on both the electric current passing through the simple and the voltage gradient. As a result of this the heating time was decreased due to higher energy generation rate at high voltage gradients, also It should be noted that the water temperature profile is approximately linearly with the heating time.

As shown in Figure 7-12, for voltage gradient varies from 26.31 to 43.47 V/cm. It can be seen from the graph that to heat up the water from 20 ^oC to 85 ^oC, the heating time is 850 s for the voltage gradient of 43.47 V/cm; when the voltage gradient decreased to 35.71 V/cm, the heating time is increased by 8 %, and increased by 37.6 % for the voltage gradient of 29.41 V/cm and further increased by 58.8 % when the voltage gradient dropped to 26.31 V/cm.

For applied voltage of 150 Volt, the heating time to raise the water temperature from 18^oC to 80 ^oC is 340 s for voltage gradient of 65.21 V/cm, when voltage gradient decreased to 53.60 V/cm, the heating time is increased by 17.6 %, by 38.23 % for voltage gradient of 44.11 V/cm and by 55.9 % for voltage gradient of 39.50V/cm as illustrated by in the Figure 7-13.

For relatively high voltage gradients, as shown in Figure 7-14, to heat up the water from 21°C to 67 °C, the heating time is 141 s for voltage gradient of 87 V/cm, when the voltage gradient decreased to 71.4 V/cm the heating time is increased by 10 % and increased by 27.65 % for voltage gradient of 58.8 V/cm and 56 % for voltage gradient of 52.6V/cm.

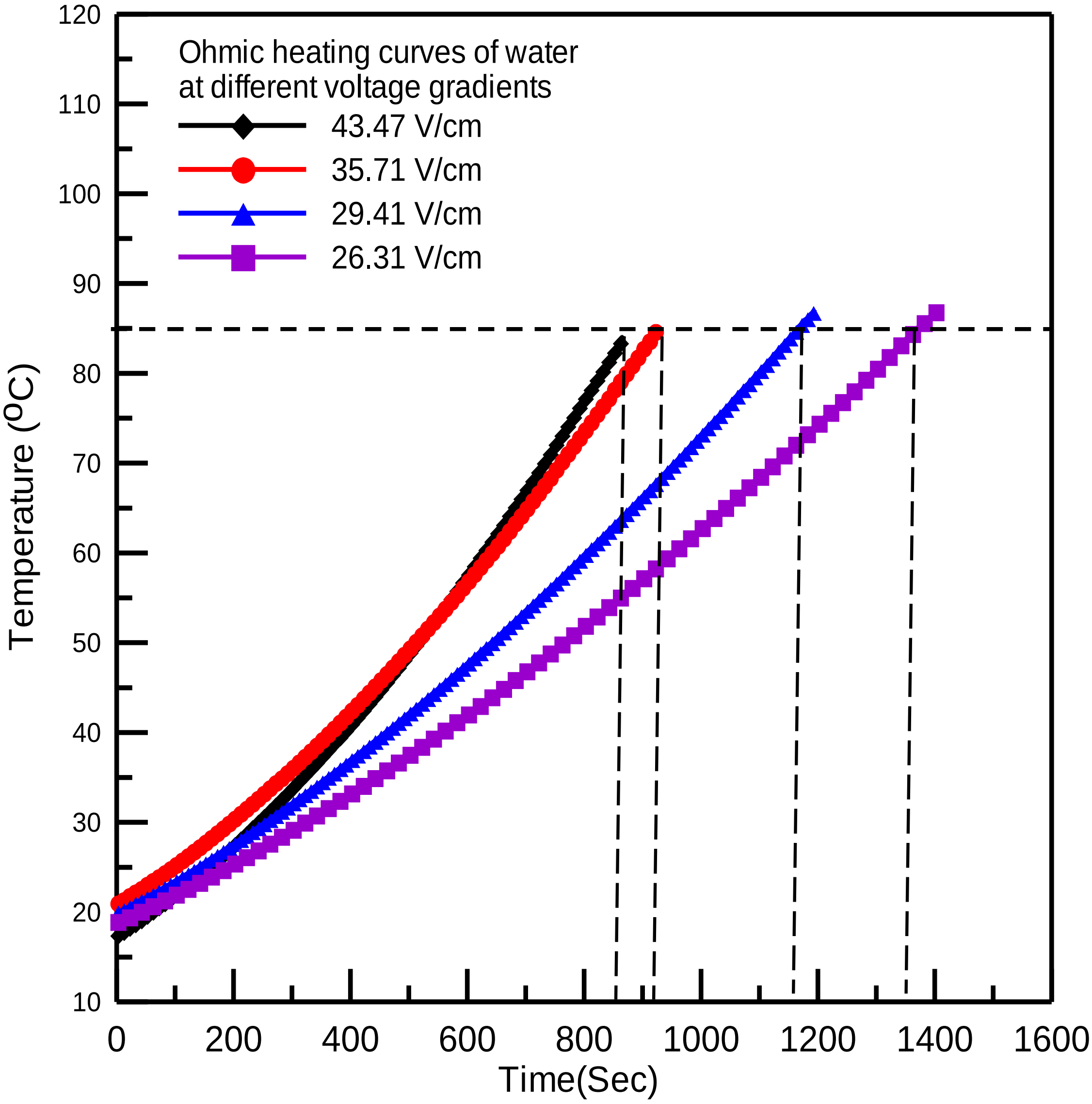

Figure 7-12 Ohmic heating curve of water at different voltage gradients, V=100 Volt

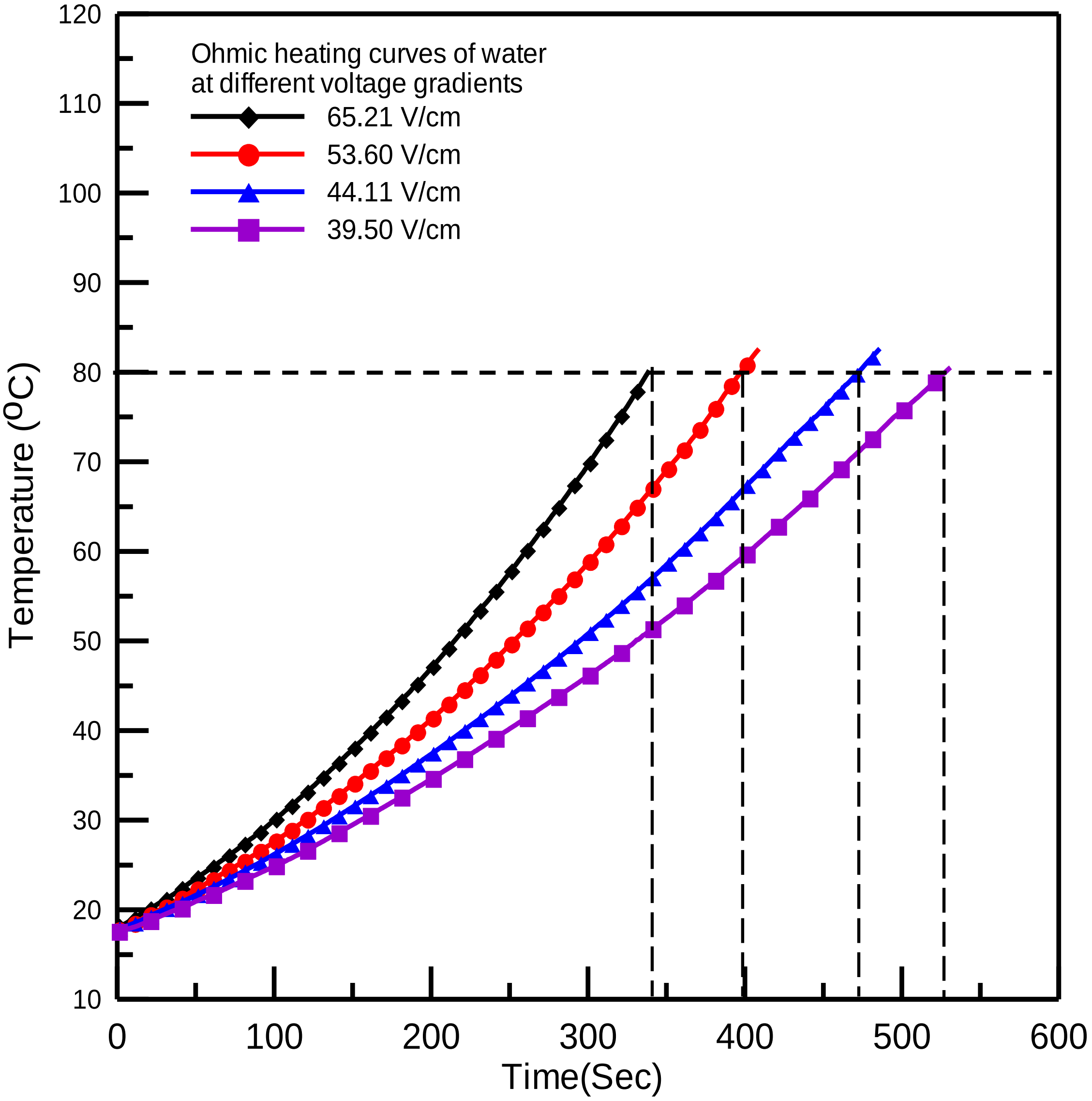

Figure 7-13 Ohmic heating curve of water at different voltage gradients, V=150 Volt

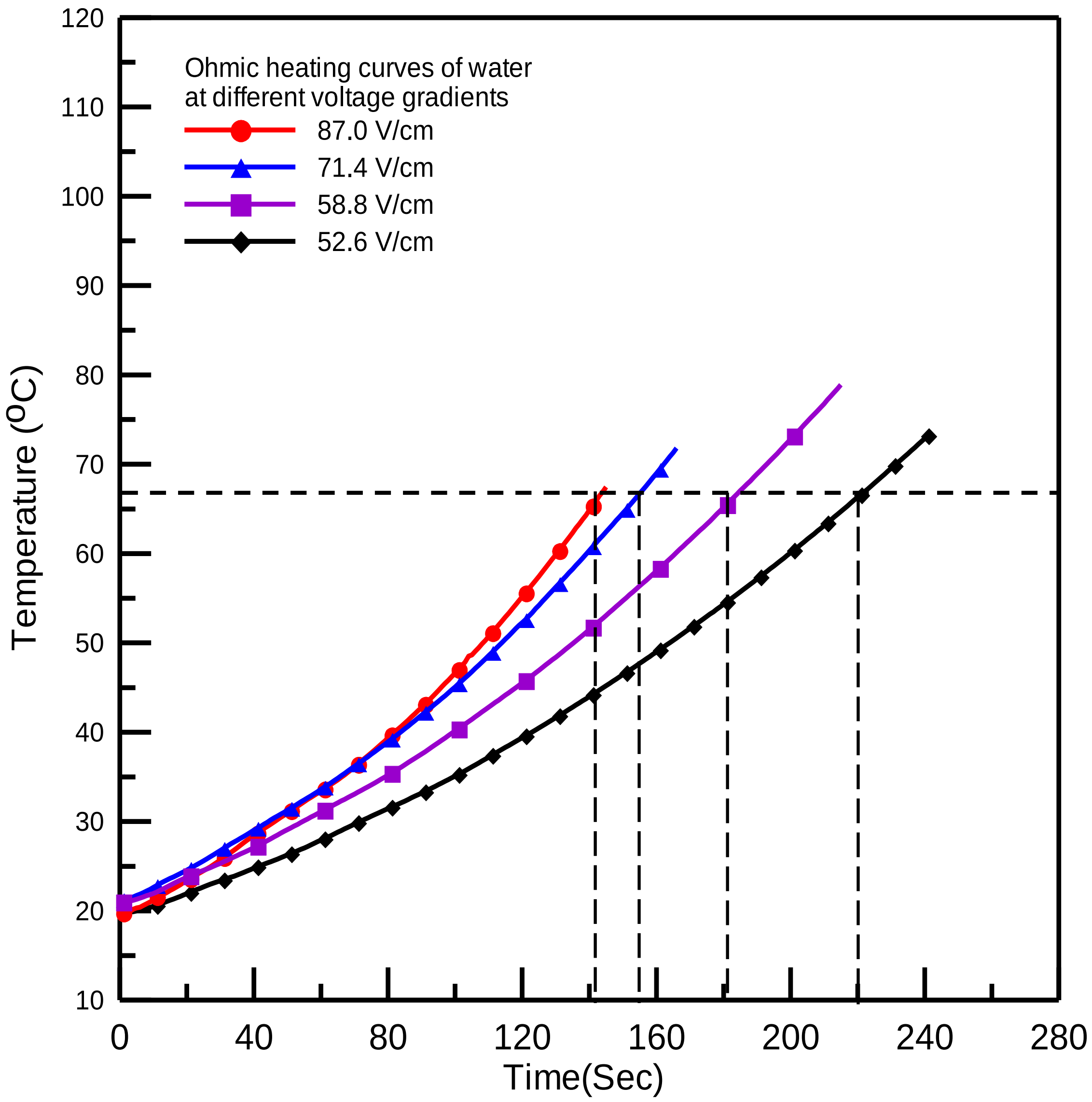

Figure 7-14 Ohmic heating curve of water at different voltage gradients, V=200 Volt

Table 7-2 summarize the heat rate for different voltage gradients, it is clear that the heating rates were varied from 0.04 to 0.31 ^{o}C/s depend on the voltage gradient. It can be concluded that, applying Ohmic heating method in water heating should consider the advantage of this high heating rate. Traditional heating of water in boilers or tanks generally involves the use of electric heating elements in the boiler section. Due to increase thickness of the scaling material outside the heating coils, the overall heat transfer coefficient decreases. Thus cleaning of the heating coils and in some cases the replacement of the tubes is necessary. In addition, some tubes suffered considerable corrosion and erosion–corrosion in service resulting in substantial reduction in wall thickness (Assiry et al., 2010). Heat is transferred across traditional heater due to the temperature difference between the heating coils and the water whereas Ohmic heating uses electricity to generate heat within the water in which there is no heat transfer limitations. The advantages of this method are more rapid, uniform and immediate water heating.

Table 7-2 Summarize of heat rate for different voltage gradients

Applied voltage	X (mm)	heating rate (°C/s)	heating rate (°C/min)
V=100 Volt	23	0.0768	4.608
	28	0.069	4.14
	34	0.0561	3.366
	38	0.0485	2.91
V=150 Volt	23	0.183	10.98
	28	0.158	9.48
	34	0.133	7.98
	38	0.1185	7.11
V=200 Volt	23	0.221	13.26
	28	0.328	19.68
	34	0.3044	18.264
	38	0.269	16.14

7.3.2. Electric conductivity

The most critical property affecting Ohmic heating rate is water electrical conductivity and it is function mainly of water dissolved ionic species. The variation of electric conductivity of water sample with temperature for different velocity gradient are shown in Figures 7-15, 7-16 and 7-17. These Figures illustrate that there is a linear relation between the electrical conductivity and temperature for the values obtained with the Ohmic heater.

It is clear that the electrical conductivity increases with temperature. For voltage gradient between 26.31 to 43.47 V/cm, it is obvious that the electric conductivity at voltage gradient of 43.47 V/cm was lower than that at 26.31, 29.41 or 35.47 V/cm especially at high temperature as shown in Figure 7-15.

For medium voltage gradient between 39.50 to 65.21 V/cm, it found that there is small variation in electric conductivity for temperature below than 50 ^{o}C, when temperature increased the variation is increased as shown in Figure 7-16. Similar effects of voltage gradient on electrical conductivity is shown in Figure 7-17 for relative high voltage gradient, however, no significant difference in electrical conductivity of the sample was observed below 50^{o}C.

Icier and Ilicali (Icier and Ilicali, 2005) reported that, the electric conductivity is increased with temperature because the drag for moment of ions was reduced, Zhu et al (Zhu et al., 2010) assumed that is most satisfactory for products which having values in a range of 0.01 – 10 S/m, and the optimum efficiency in the range of 0.1–1.0 S/m.

Ohmic heating curves were presented using linear model to fit the electrical conductivity data of water samples.

$$\sigma=\sigma_o+n.T \qquad (7.6)$$

The statistical empirical relations constants (σ_o and n) and coefficients of determinations (R^2) are shown in Table 7-3, in all cases, the R^2 values for the models were greater the acceptable R^2 value 0.9985 indicating a good fit. The temperature factor range (n) varies from (0.0130 to 0.0242 (S cm^{-1} ^{o}C^{-1})). So the linear model may be assumed to represent the electrical conductivity of water during the Ohmic heating. The linear model has been proposed by previous researcher for different liquid during Ohmic heating (Zell et al., 2011; Darvishi et al., 2013; Assiry et al., 2010 and Assiry, 2011).

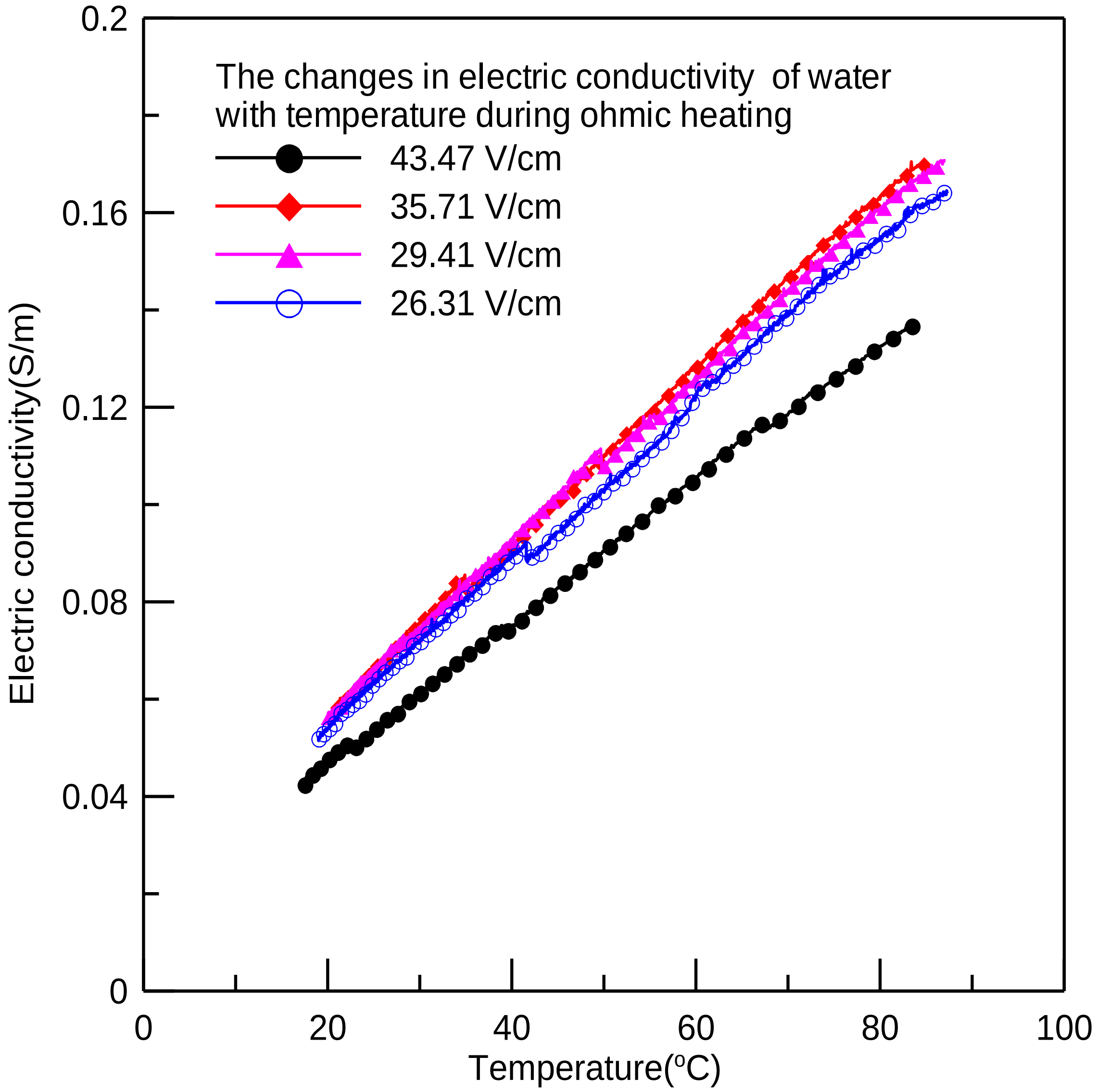

Figure 7-15 Changes in electrical conductivity of water with temperature during Ohmic heating, (Voltage=100 V)

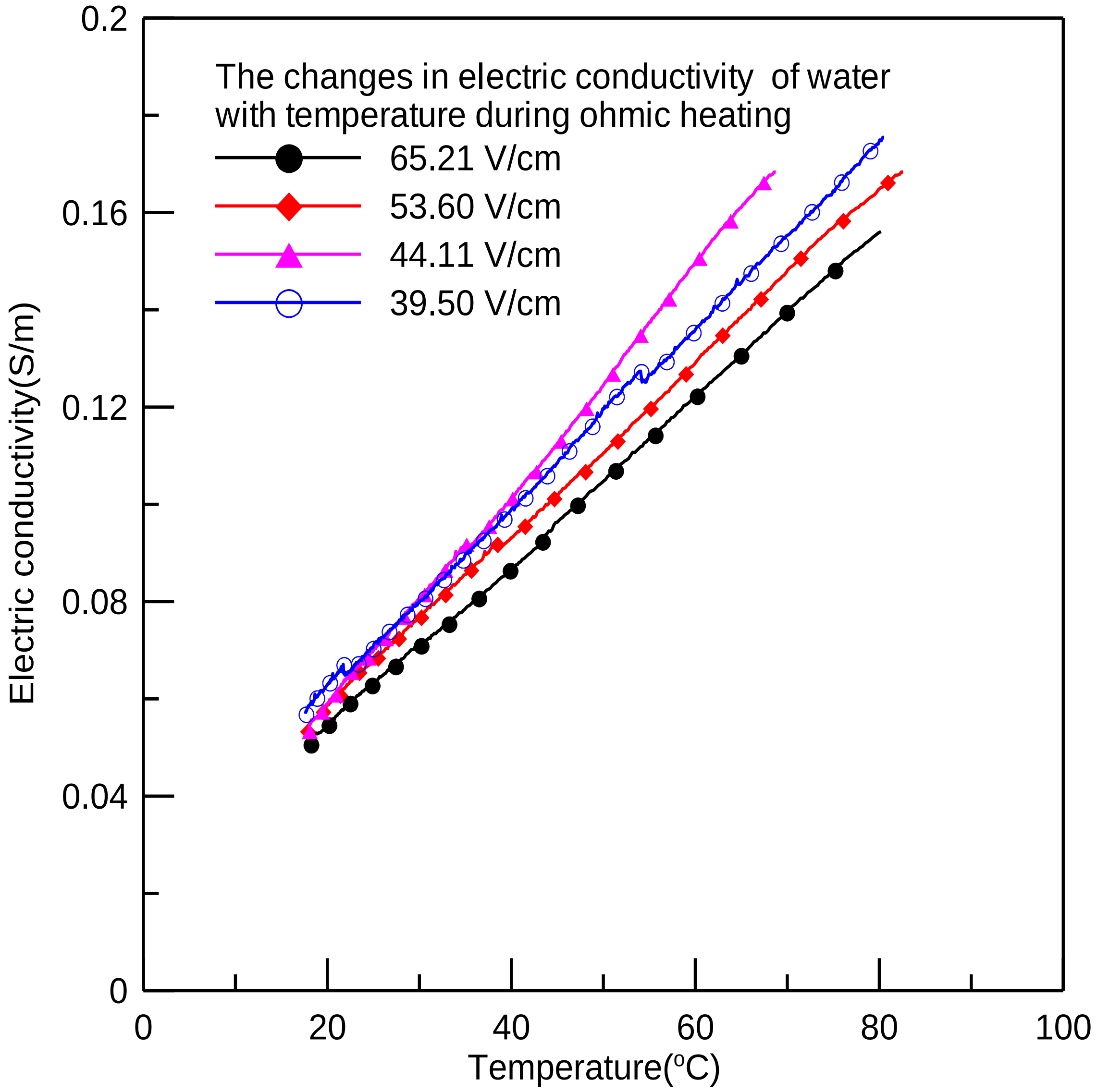

Figure 7-16 Changes in electrical conductivity of water with temperature during Ohmic heating, (Voltage=150 V)

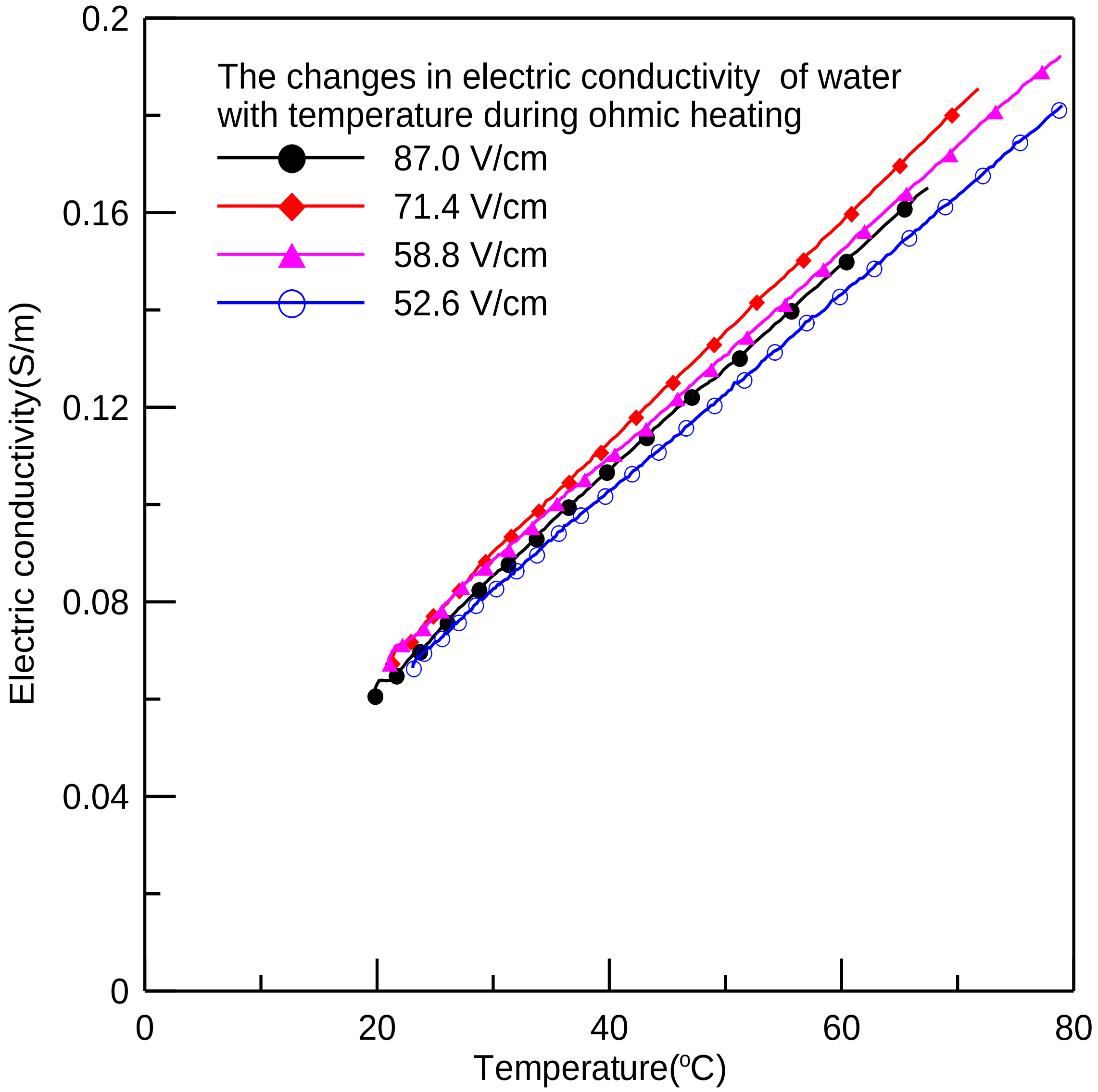

Figure 7-17 Changes in electrical conductivity of water with temperature during Ohmic heating, (Voltage=200 V)

Table 7-3 Results of statistical analysis on the modelling of electrical conductivity with temperature of water

Model	Voltage gradient (V/cm)	Parameters		R^2
		σ_o	n	
$\sigma=\sigma_o+n.T$	87.00	0.0022	0.0196	0.9995
	71.40	0.0023	0.0205	0.9998
	62.21	0.0017	0.0201	0.9995
	58.80	0.0021	0.0242	0.9999
	53.60	0.0018	0.0232	0.9996
	52.60	0.0020	0.0211	0.9999
	44.11	0.0023	0.0130	0.9985
	43.47	0.0014	0.0183	0.9993
	39.50	0.0019	0.0244	0.9995
	35.71	0.0018	0.0216	0.9994
	29.41	0.0017	0.0236	0.9993
	26.31	0.0017	0.0213	0.9986

Figures 7-18, 7-19 and 7-20 show the amount of electric power consumption during Ohmic heating testing; in general it is clear that, the amount of electric power consumption is increased with the increase of voltage gradient due to the decrease in the water resistance, however, the heating time is decreased with the increase of the electrical power consumption.

Figure 7-18 shows that the maximum electric power is 230 W for voltage gradient 43.47 V/cm, when voltage gradient is increased to 65.21V/cm, the maximum electrical power consumption increases to 480 W as shown in Figure 7-19. For higher voltage gradient 87 V/cm, the electrical power consumption is increased to 900 W as shown in Figure 7-20.

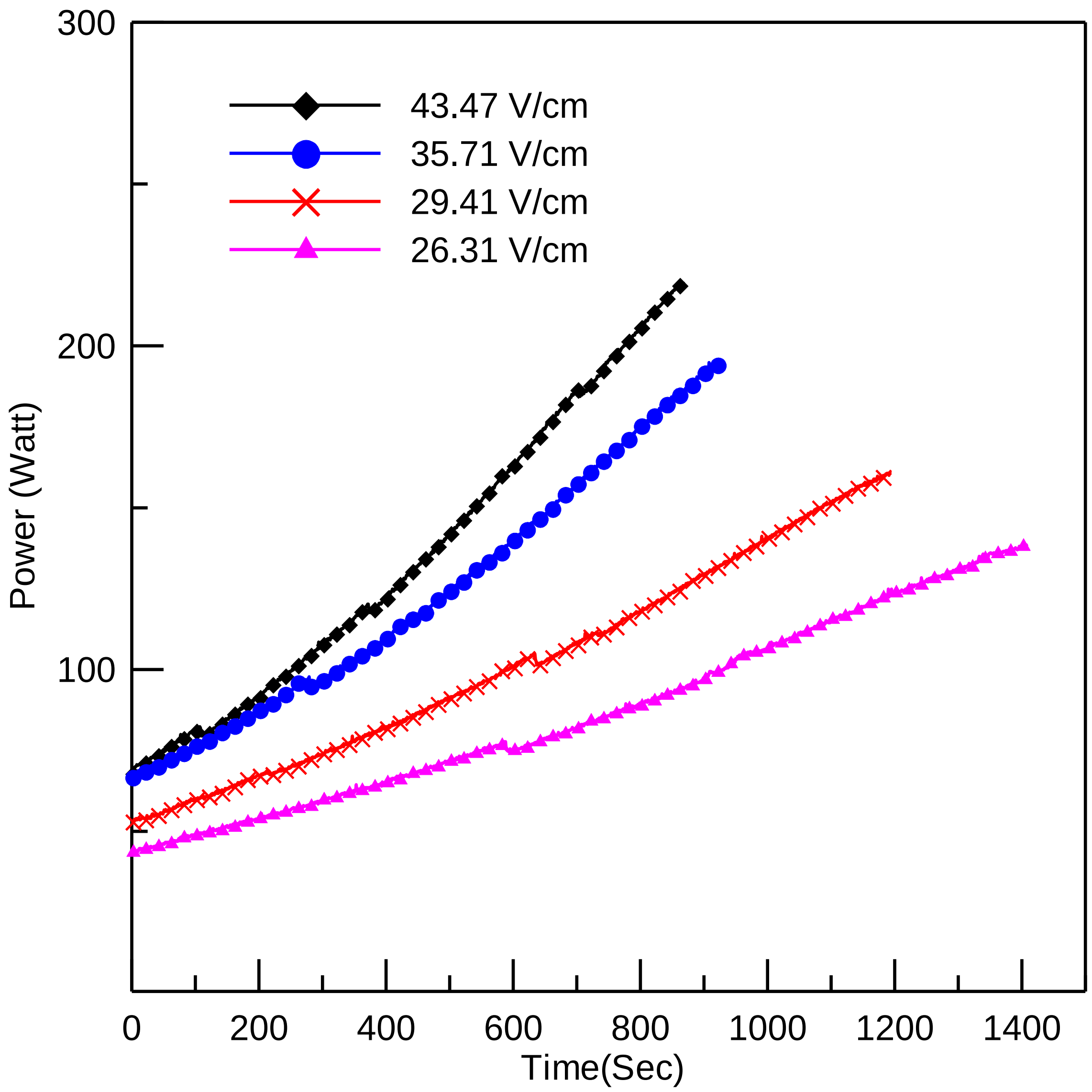

Figure 7-18 Power consumption as a function of time for different voltage gradient, V=100 Volt

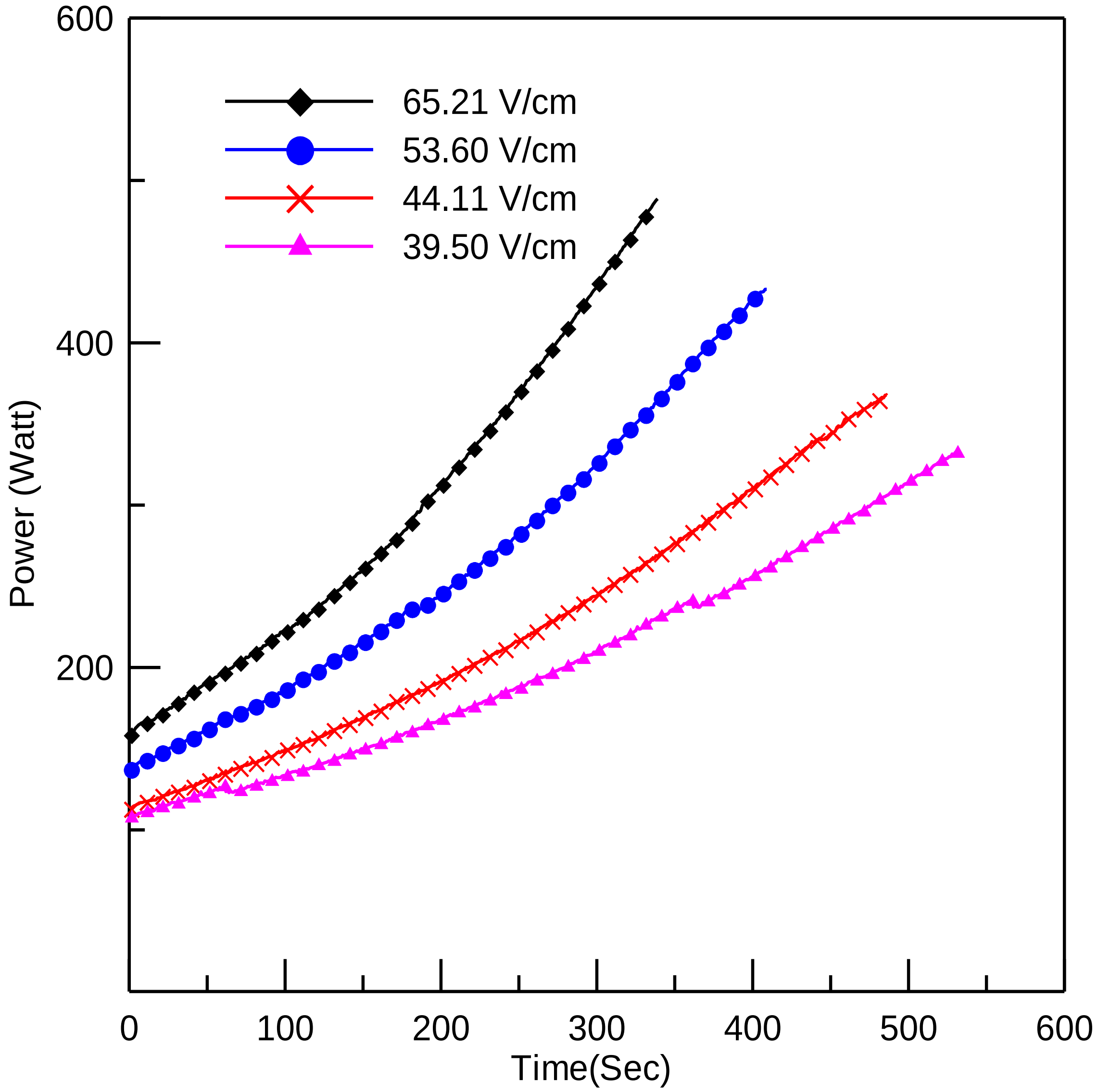

Figure 7-19 Power consumption as a function of time for different voltage gradient, V=150 Volt

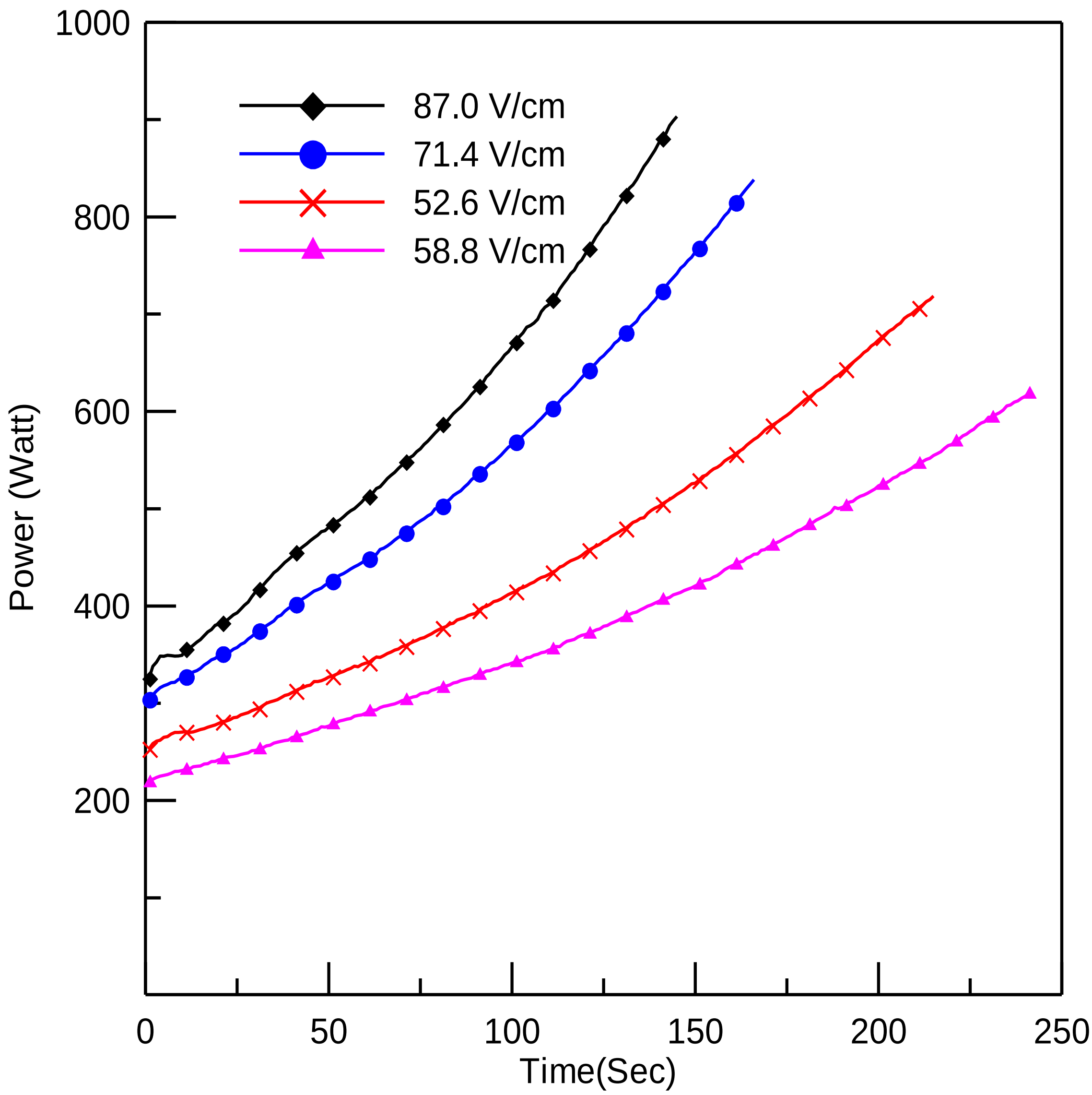

Figure 7-20 Power consumption as a function of time for different voltage gradient, V=200 Volt

7.3.3. System performance analysis

The heat taken by the water samples and the electrical energies given to the system were calculated out of experimental data, and the system performance coefficient, SPC for each Ohmic heating experiment is determined through equations 7-2, 7-3 and 7-4. The calculated SPC values for each heating experiment are shown in Table 7-4. The results indicated that the system performance coefficients strongly depend on the applied voltage gradient. The highest SPC 86.45% was obtained under the voltage gradient of 62.21 V/cm and the lowest 77.25 % under the voltage gradient of 29.41 V/cm.

At low voltage gradients, it is clear that the SPCs perform slightly better than higher ones because that the conservation of electrical energy into thermal heat was larger. The energy losses take approximately 15-23 % of the energy given to the system. Heat transfer area was also small, for this reason the energy losses to the surroundings by convection was small and they could be neglected without any loss in accuracy; so at higher voltage gradients, the difference between the energy given to the system and energy taken by the water can be explained partly by these losses, However, at low voltage gradients the energy losses mentioned above is only a small portion of the total energy losses (Darvishi et al., 2013).

The energy losses can be mostly explained by the energies used for the purposes of physical, chemical and electrochemical changes during heating (Icier and Ilicali, 2005; Assiry et al., 2003; Zhao et al., 1999). It is rather difficult to comment on the exact nature of this loss. These reactions are not beneficial and further study must be conducted on the effects of them on food. In conclusion, SPCs can be used to determine the system performance of Ohmic heaters.

Table 7-4 System performance analysis for different voltage gradient during Ohmic heating

Voltage (V)	P(w)	E_{input} (J)	$T_{initial}$ (°C)	T_{final} (°C)	Time (s)	SPC
87.00	83685.53	66305.79	19.76	67.44	145	79.23
71.40	88634.91	70283.86	21.25	71.79	166	79.30
62.21	99792.44	86273.55	18.14	80.19	339	86.45
58.80	96767.68	80516.84	20.99	78.89	215	83.21
53.60	106278.2	90143.33	17.78	82.60	409	84.82
52.60	93912.22	74331.39	19.76	73.22	241	79.15
44.11	108955.7	89946.39	17.95	82.64	486	82.55
43.47	116714	92762.95	17.46	84.17	868	79.48
39.50	106940.9	87500.45	17.60	80.53	531	81.82
35.71	113625.6	88607.56	21.03	84.75	922	77.98
29.41	120807.3	93328.92	20.00	87.12	1195	77.25
26.31	121418.8	95016.99	18.96	87.29	1408	78.26

7.4. A case study

7.4.1. Effect of electrode materials

As mentioned in the literature review direct Ohmic heating (Joule's heating) is a technology to warm up the fluids using an electric energy where electric current is passed through a material which gets heated by virtue of its electrical resistance.

Advantages over conventional indirect heating methods are speed and uniformity of heating. On the other side, the direct Ohmic heating of liquid has some problems, for example corrosion and deposits creation on electrodes (fouling). This section concentrates upon the effects of material and surface properties of electrodes, in addition, evaluates the influence of electrodes material (graphite electrodes), electric current density (at constant frequency 60 Hz) and temperature (in a limited temperature range 19 –95 ^{o}C), upon the Ohmic heating thermal performance.

The most important electrolytic problems are the contamination of heating sample (especially food) with metal ions migrated from electrodes and the resulting electrochemical reaction products. This contamination could be either toxic (carcinogenic) or bring undesired taste and colouring to processed food (Amatore et al., 1998).

Platinised titanium electrodes have been used in the Ohmic heater unit in section 7.1.3, the electrode sizes are 80 mm in length and 40 mm in width, and the distance between the electrodes varies from 23 mm to 38 mm.

The graphite electrodes which have been used in the experimental work have different electrical resistivity. Electrical resistivity (also known as resistivity, specific electrical resistance, or volume resistivity) quantifies how strongly a given material opposes the flow of electric current. A low resistivity indicates a material that readily allows the movement of electric charge. Resistivity is commonly represented by the ρ.

The SI unit of electrical resistivity is the ohm.metre (Ω.m) although other units like ohm.centimetre (Ω.cm) are also in use. As an example, if a 1 m × 1 m × 1 m solid cube of material has sheet contacts on two opposite faces, and the resistance between these contacts is 1 Ω, then the resistivity of the material is 1 Ω.m. In these experiments, five pair of graphite electrodes were used, the resistivity varied from 10 to 660 $\mu\ \Omega.m$. Figures 7-21 and 7-22 show the photographs of the graphite electrodes.

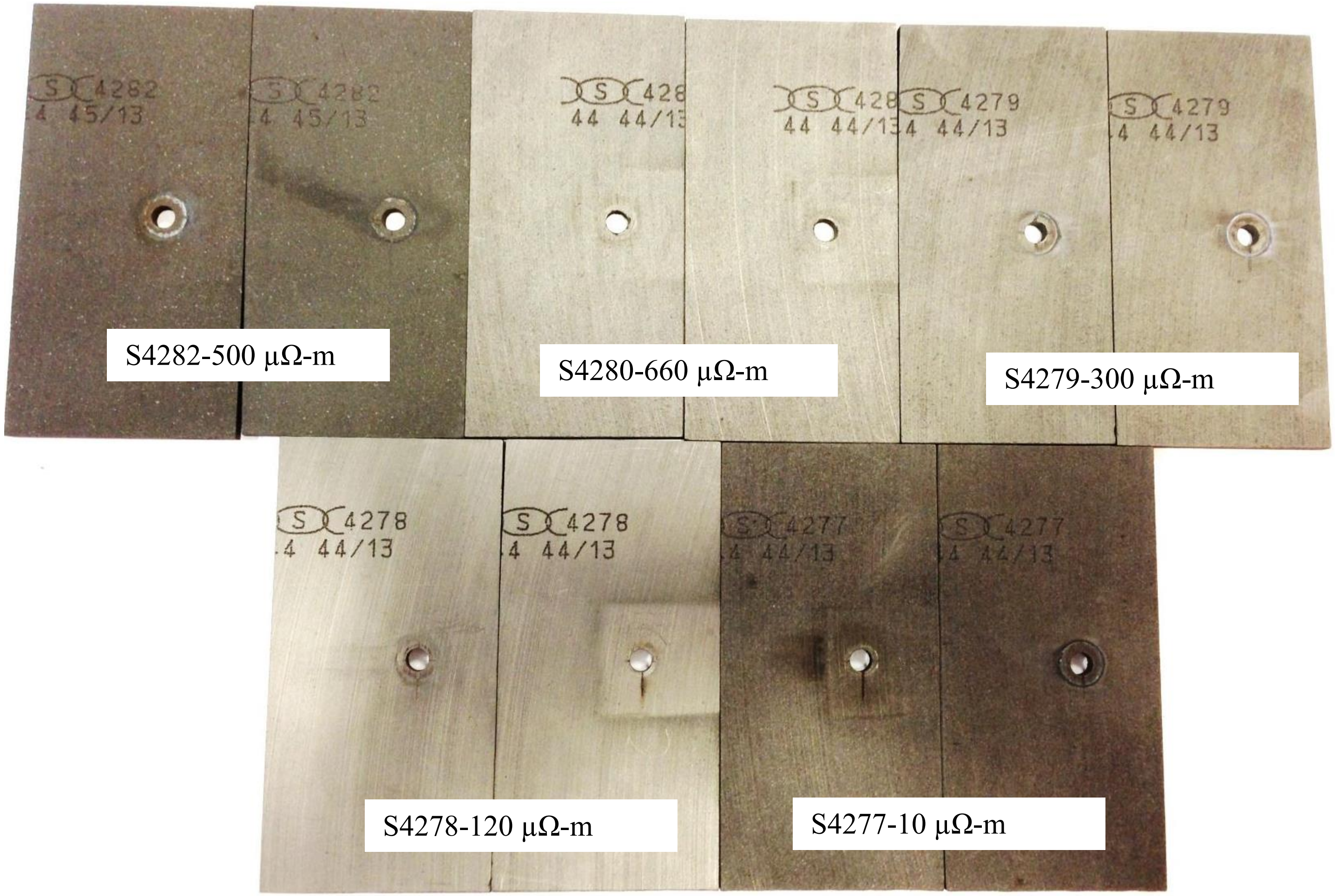

Figure 7-21 Different graphite electrodes

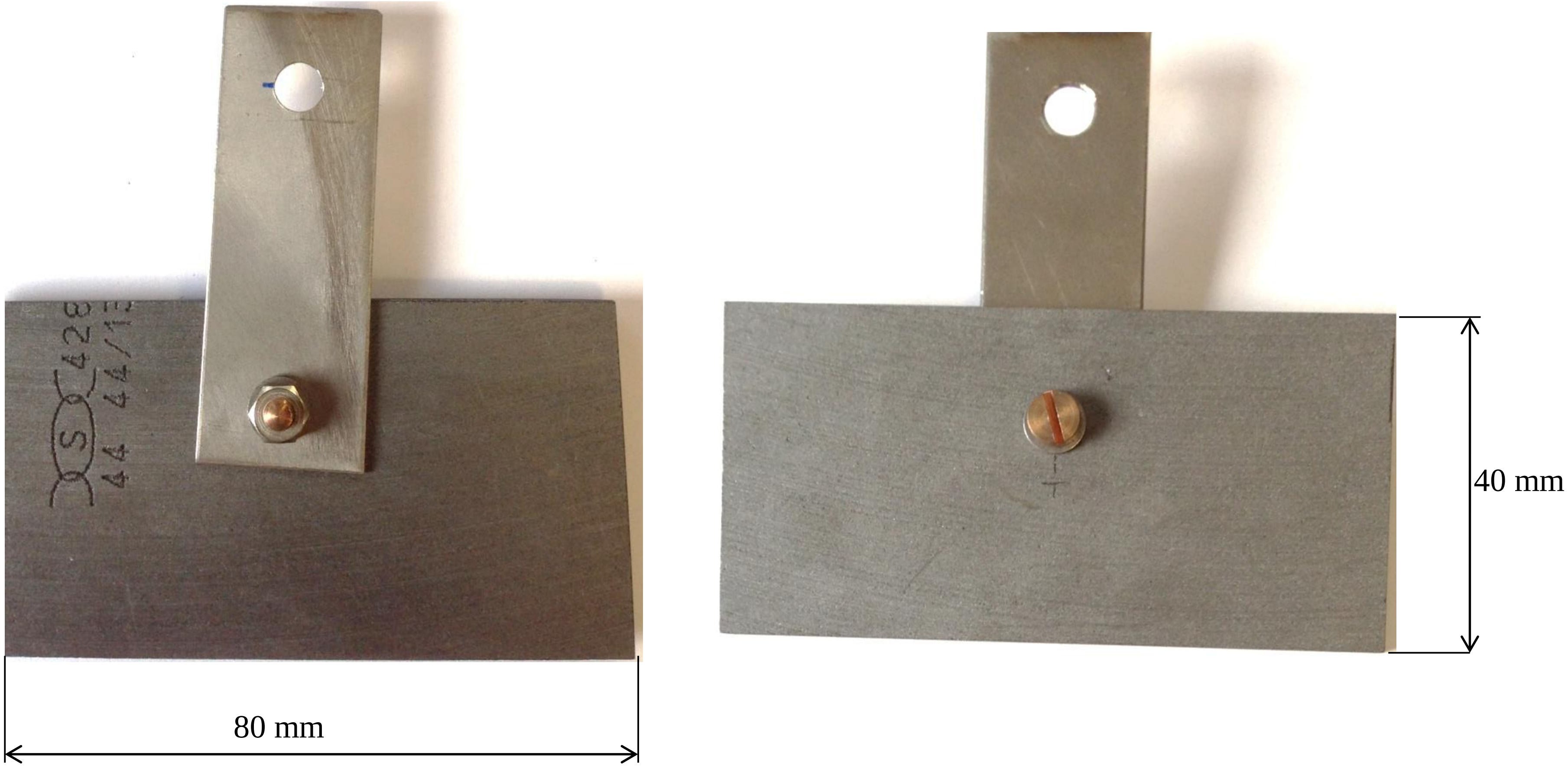

Figure 7-22 Dimensions of the graphite electrode

7.4.2. Experimental procedure

For each experimental run, water volume of 324 mL was loaded in the Ohmic heater, the sample was heated to 95 °C using alternating current of 60 Hz at applied voltages of 100, 150 and 200 V, and different electrodes gabs of 23, 28, 34, 38 mm corresponding to electrical field strengths of 26.31, 29.41, 35.71, 43.47, 39.47, 44.11, 53.57, 65.21, 62.6, 58.8, 71.4 and 87.00 (V/cm). Temperature, voltage and current data were recorded on a data logger at 1.0 second intervals.

7.4.3. Effect of electrode materials on the heating rates

Figures 7-23 to 7-27 show the variation of average water temperature for different voltage gradient and different graphite electrodes types; In general, it is clear that, Ohmic heating times are dependent on the voltage gradient. As the voltage gradient increases, the heat generation per unit time increases, and hence the heating time demanded to reach the prescribed temperature decreases.

Figure 7-23 indicates that for electrode No S4277 which has lowest resistivity (10 µ Ohm-m), under constant applied voltage. It is clear that as the voltage gradient decreases, the heating time increases. The heating time to raise the water temperature from 20 to 80 ^{o}C is 1050s for voltage gradient of 43.47 V/cm, and then it is increased to 1180s, 1425s and 1650s for voltage gradients of 35.57, 29.41 and 26.31 V/cm respectively.

For the applied voltage V=150 Volt, the heating time is decreased from 660 s (voltage gradient of 39.47 V/cm) to 590, 480 and 400 s for applied voltage gradients of 44.11, 53.57 and 66.21 respectively.

For applied voltage 200 volt, a sharp decrease in the heating has been noticed for voltage gradient 87 V/cm and the heating time to raise the water has decreased to 240 s and 360 s for voltage gradient equalling to 52.6 V/cm.

Figure 7-24 shows that for electrode No S4278 which has resistivity equalling to 120 µ Ohm-m, the heating time is decreased by 50-100 s for electrode gaps X= 34 mm and 38 mm for any applied voltage, for other electrodes gap there is no such significant difference has been observed.

The same trend with slight difference has been observed for other electrode types as presented in Figures 7.25, 7.26 and 7.27.

Figures 7-28, 7-29, 7-30, 7-31 and 7-32 show the amount of passing current through the heating water for different voltage gradient and different electrode types, in general, the amount of passing current is increased as the temperature and time increase, in the same time, the passing current through the heating sample is increased with the increase of voltage gradient and this induces faster heat generation.

To sum up, it should be noted that when the gap between the electrodes is decreased, the heating sample resistance is decreased, so the passing current will increase based on Ohm’s law.

7.4.4. Comparison between mesh platinised titanium and graphite electrodes

Platinum coated titanium mesh electrodes are very expensive, and are not suitable for production large scale due to the economical factor; the price of the platinised titanium electrodes which have been used in this experiment is £ 200.00, on the other side, the price of the graphite electrodes is very cheap, less than £ 1.00.

Figure 7-33 shows the time temperature profiles of water during Ohmic heating for various electrode materials and voltage gradients.

It is very clear that, for any voltage gradient, the water heating time using titanium electrodes is less than using graphite electrodes; the difference is slightly small at the begin of the heating process until 100 s, after 100 s the difference is increased.

However, it is obvious that, the difference in heating time can be as high as 500 s for low voltage gradient of 26.31 V/cm, but for high voltage gradient of 52.63 V/cm the difference decreased to 100 s for voltage gradient.

Figure 7-34 shows changes in electric current passed with different voltage gradient during Ohmic heating for mesh and graphite electrodes under different voltage gradients, the results are consistent with previous discussions, that the current passed with mesh electrode is higher than the graphite one, which is lead to faster heating. Also the difference in electric passing current between the mesh and graphite electrodes is high for high voltage gradient and small for low voltage gradient.

However, for any voltage gradient, the effect of graphite electrode types is not significant; the deviation in the passing current is very small and around 0.2 Ampere. To sum up, the significant result which has been observed during the testing that, the graphite electrodes change the water color, which is not desirable, especially if the heated water will be used for domestic purpose.

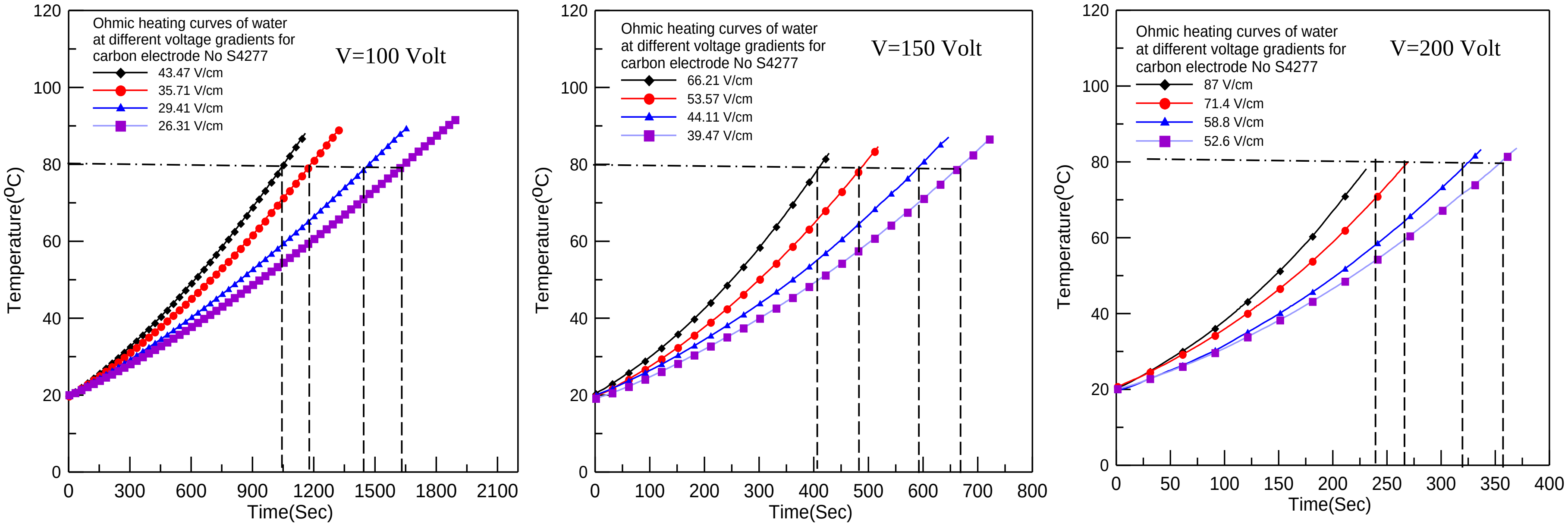

Figure 7-23 Ohmic heating curve of water at different voltage gradients, Electrode No S4277

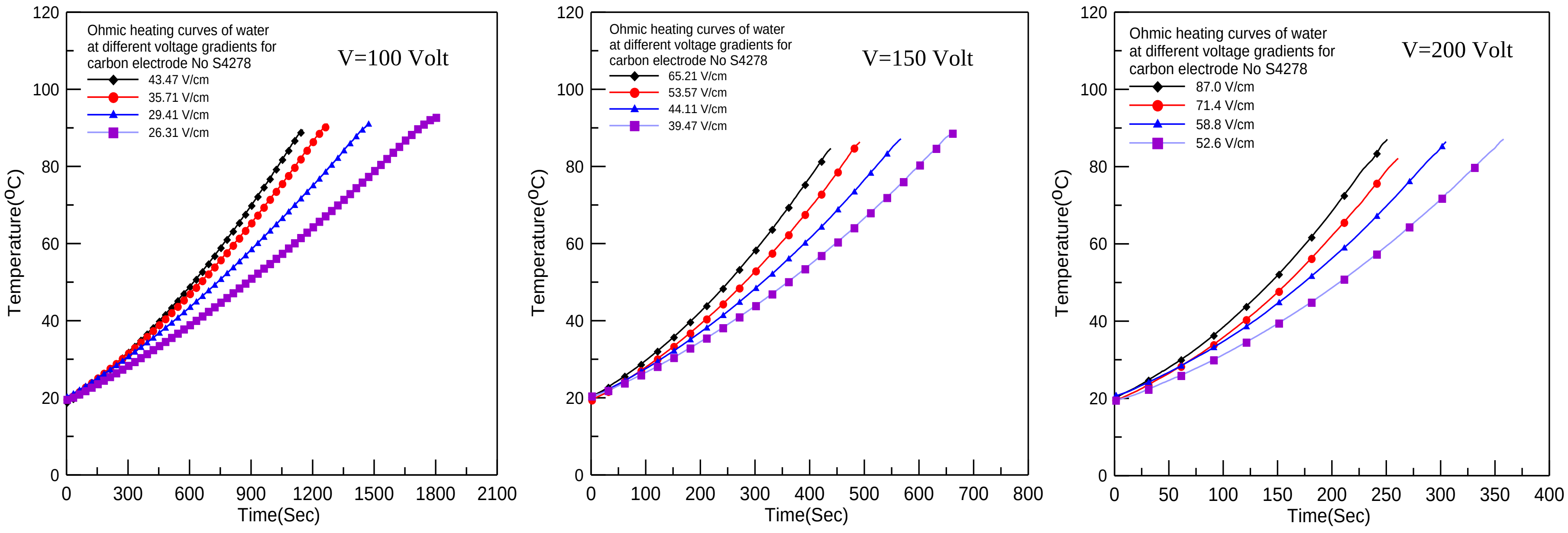

Figure 7-24 Ohmic heating curve of water at different voltage gradients, Electrodes No S4278

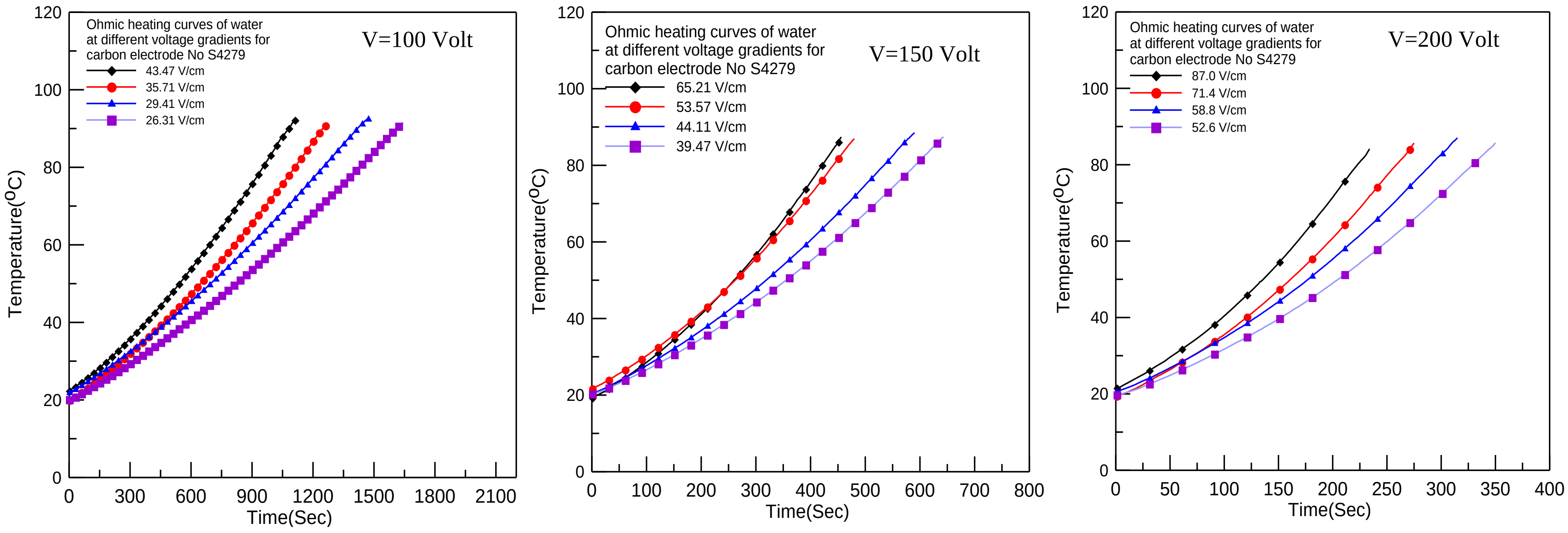

Figure 7-25 Ohmic heating curve of water at different voltage gradients, Electrode No S4279

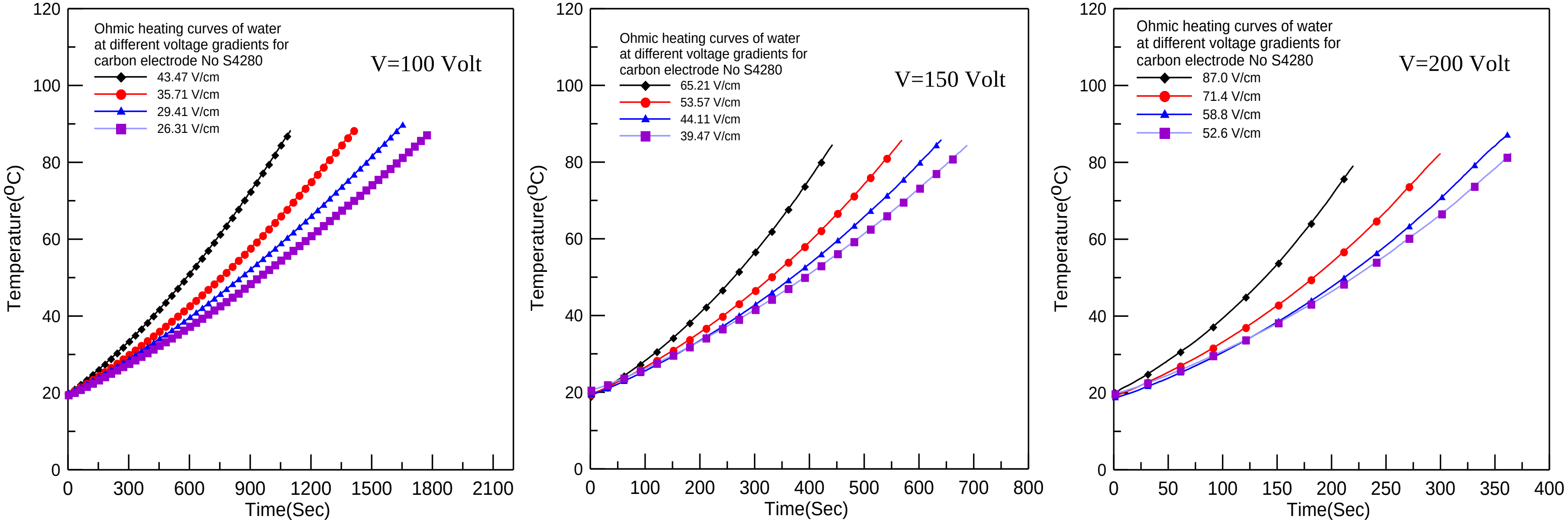

Figure 7-26 Ohmic heating curve of water at different voltage gradients, Electrode No S4280

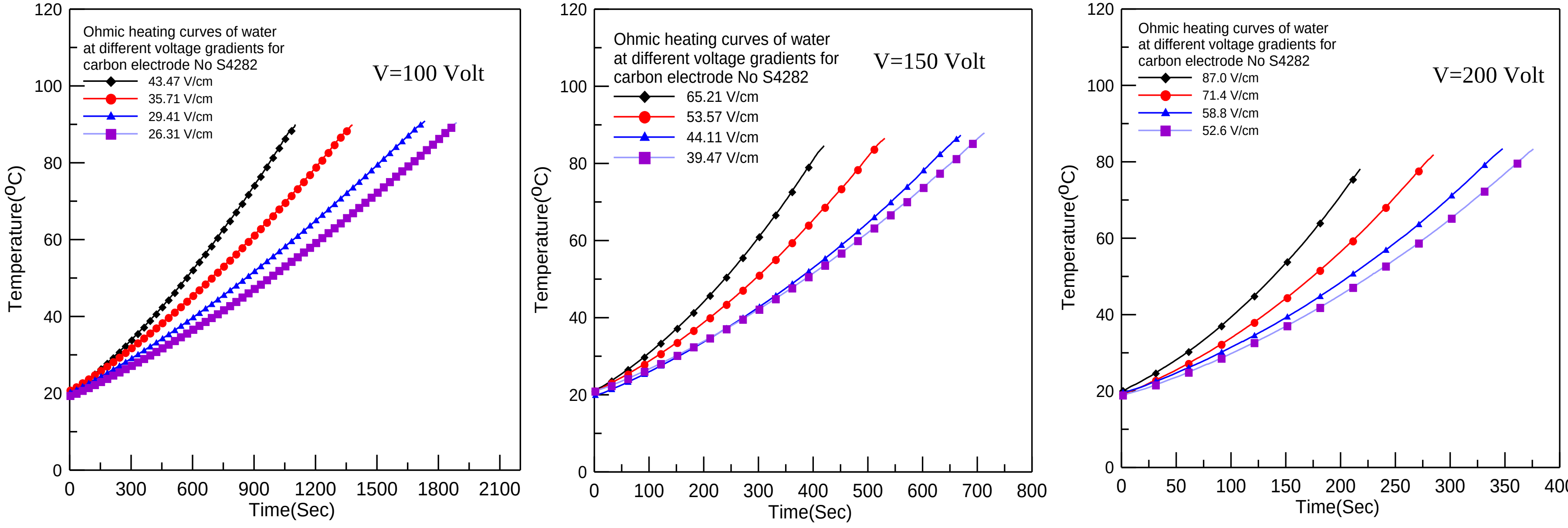

Figure 7-27 Ohmic heating curve of water at different voltage gradients, Electrode No S4282

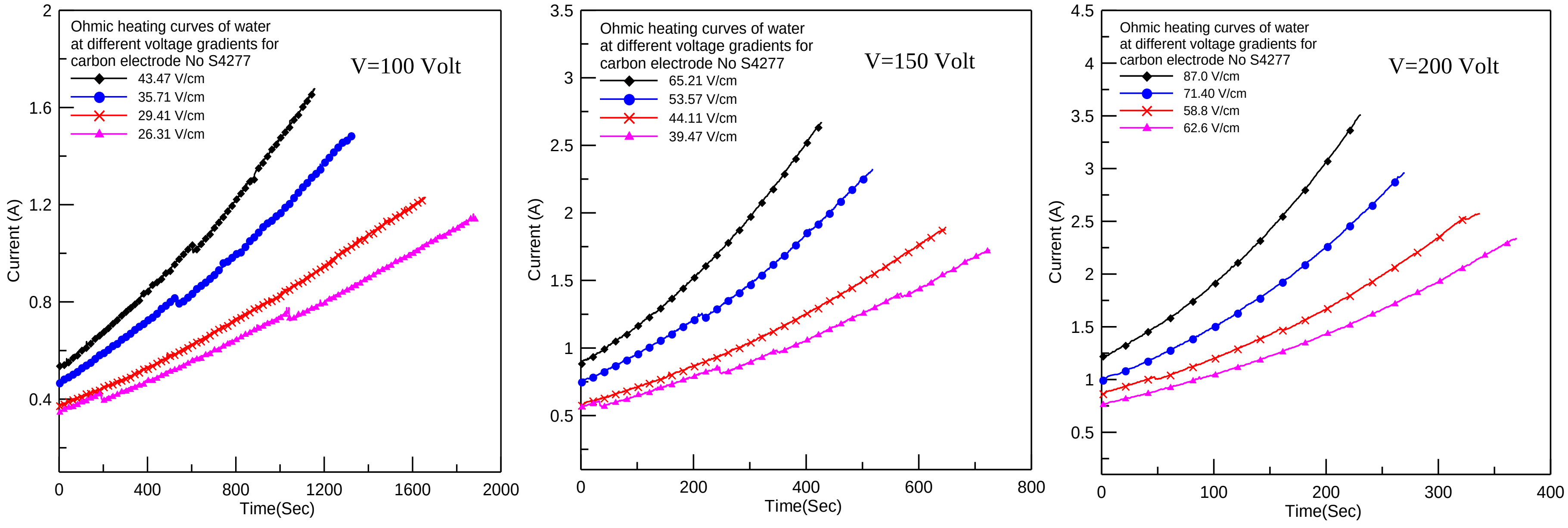

Figure 7-28 Changes in electric passing current for different voltage gradient during Ohmic heating, Electrode No S4277

.

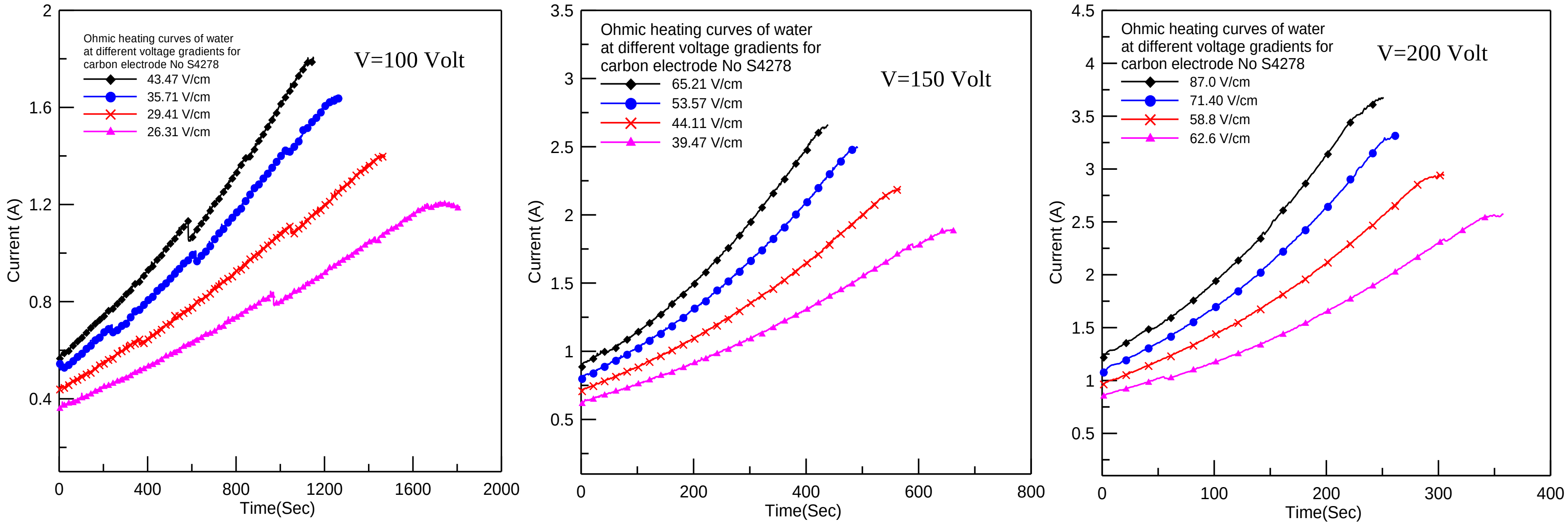

Figure 7-29 Changes in electric passing current for different voltage gradient during Ohmic heating, Electrode No S4278

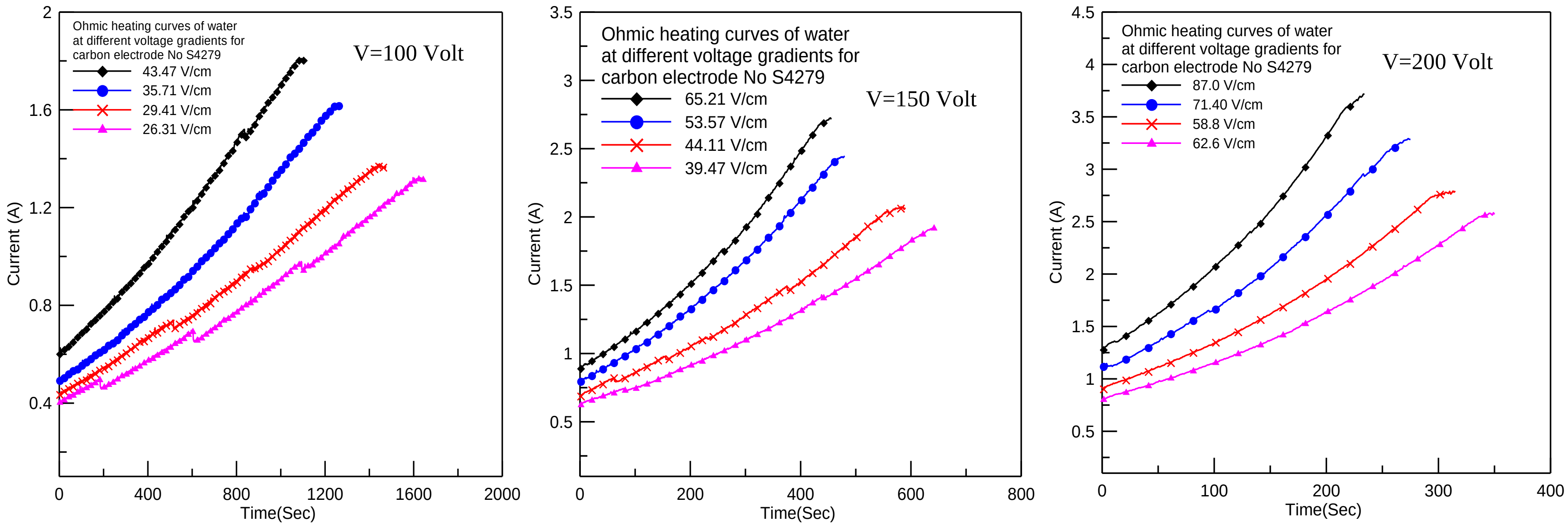

Figure 7-30 Changes in electric passing current for different voltage gradient during Ohmic heating, Electrode No S4279

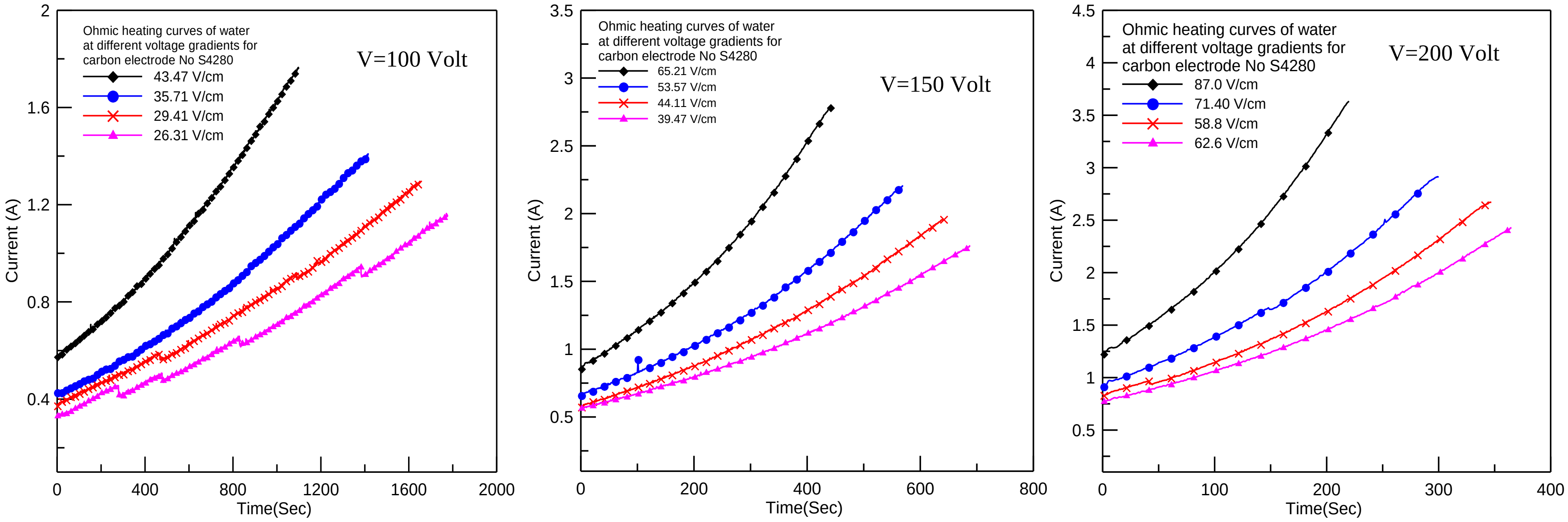

Figure 7-31 Changes in electric passing current for different voltage gradient during Ohmic heating, Electrode No S4280

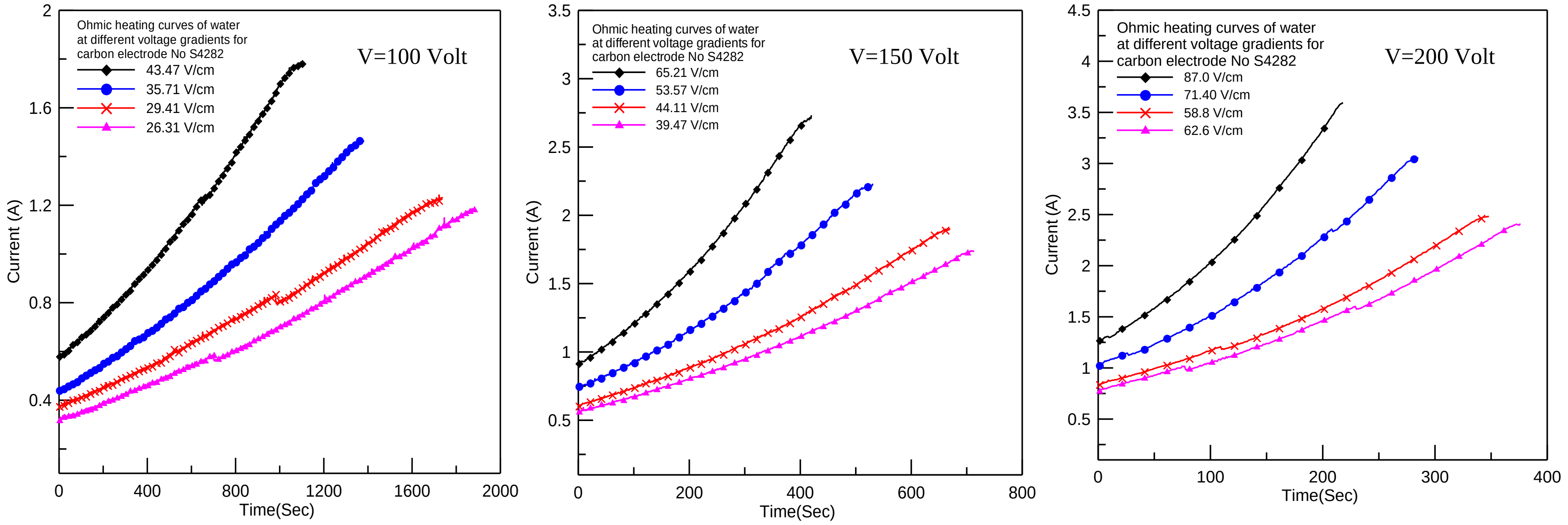

Figure 7-32 Changes in electric passing current for different voltage gradient during Ohmic heating, Electrode No S4282

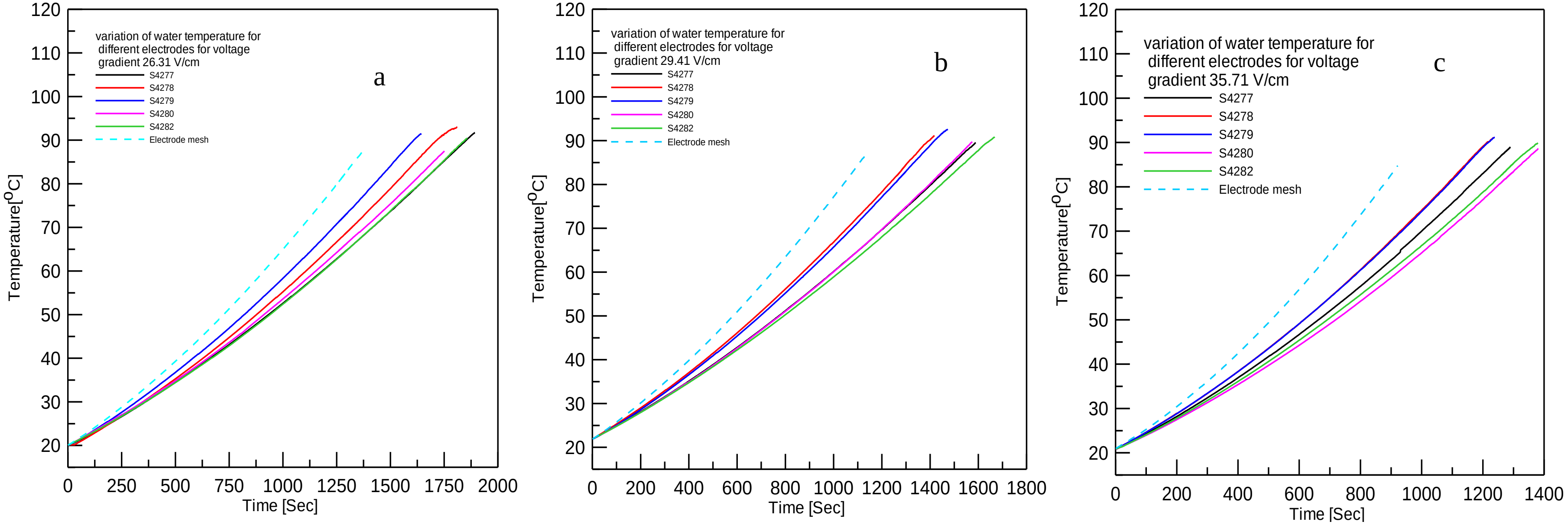

Figure 7-33 Time temperature profiles of water during Ohmic heating for various electrode materials and voltage gradients

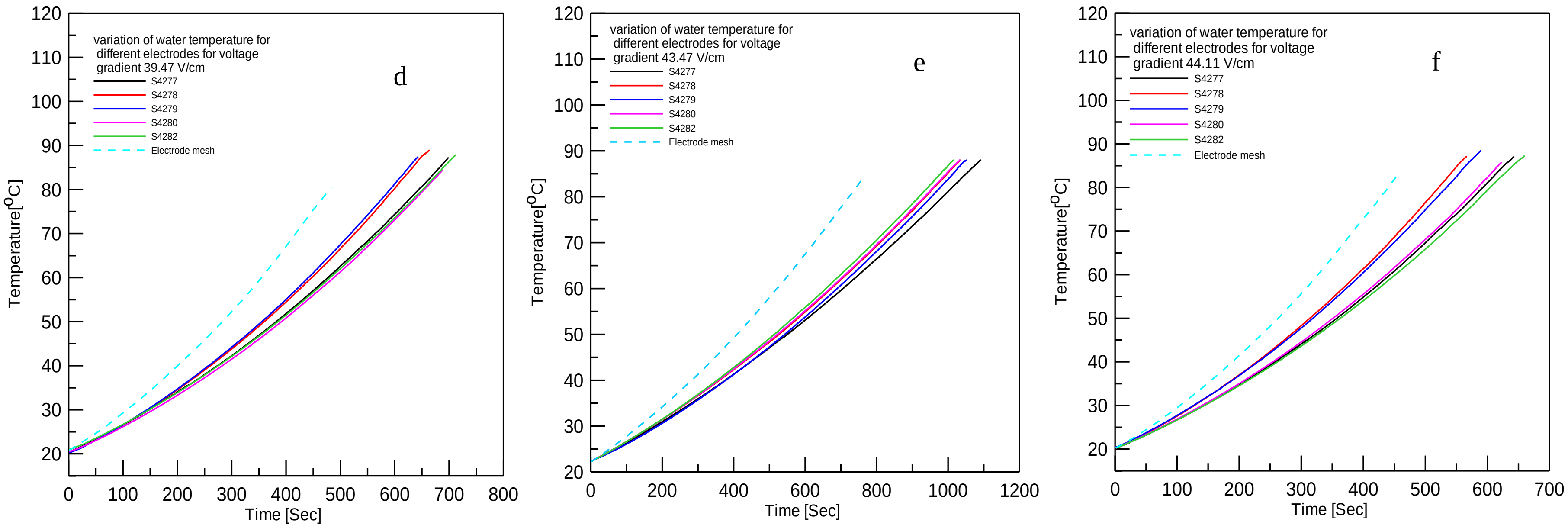

Figure 7-33 Time temperature profiles of water during Ohmic heating for various electrode materials and voltage gradients

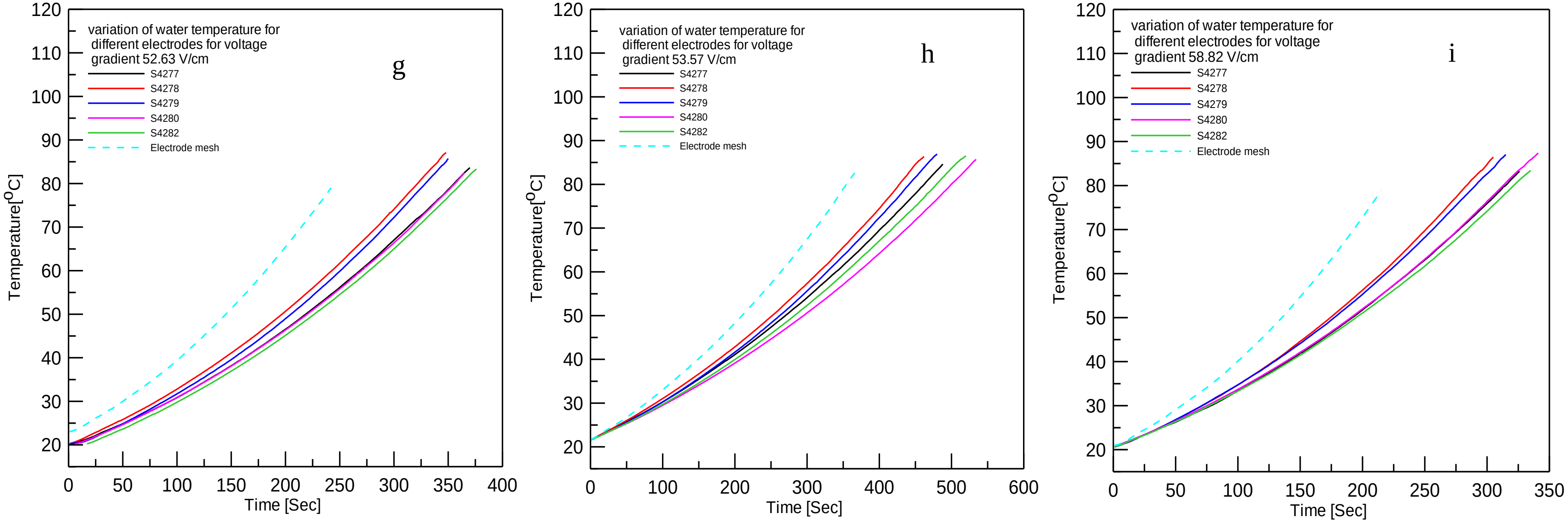

Figure 7-33 Time temperature profiles of water during Ohmic heating for various electrode materials and voltage gradients

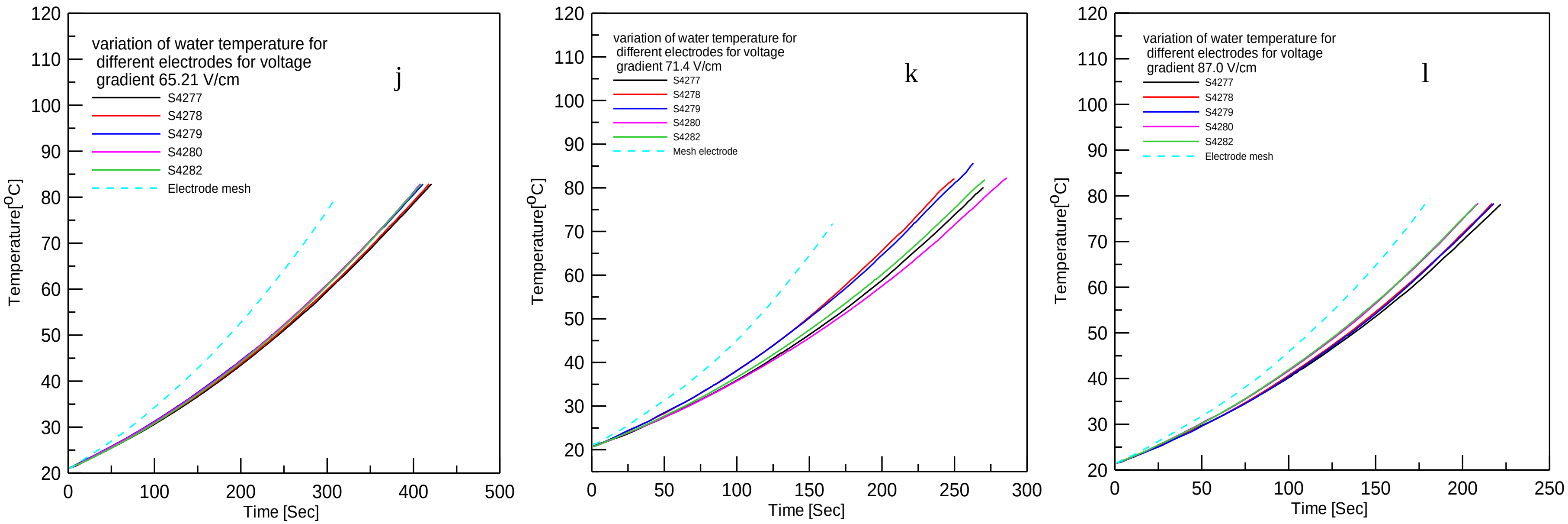

Figure 7-33 Time temperature profiles of water during Ohmic heating for various electrode materials and voltage gradients

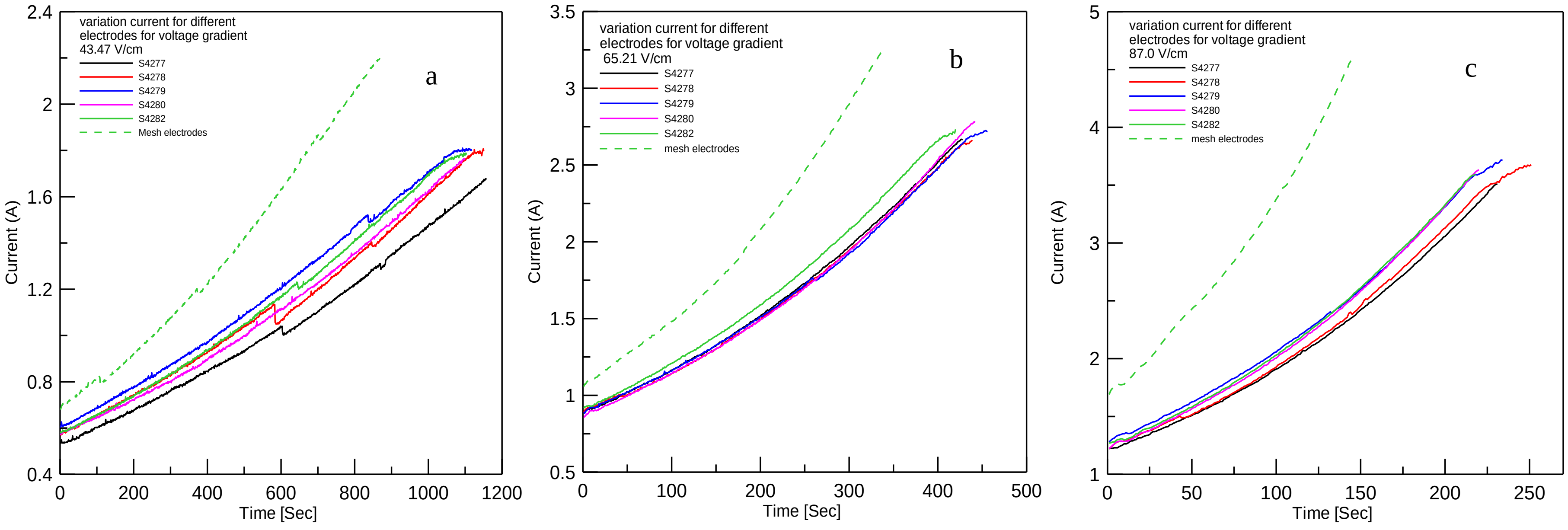

Figure 7-34 Changes in electric current passed during Ohmic heating for various electrode materials and voltage gradients

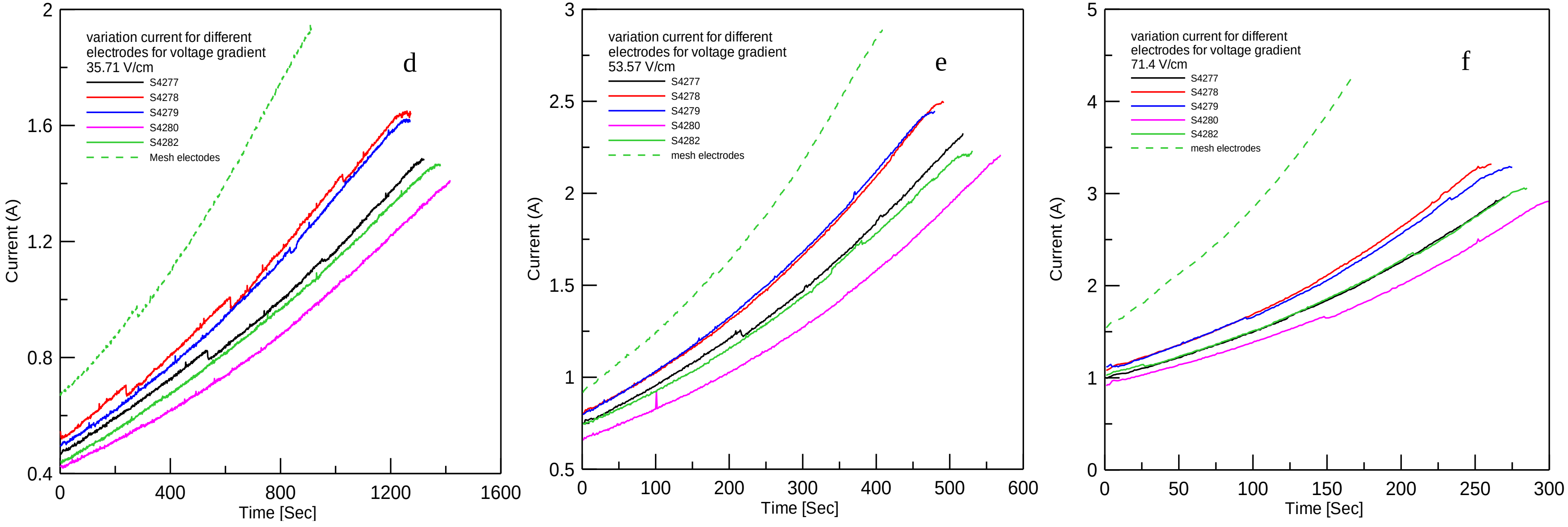

Figure 7-34 Changes in electric current passed during Ohmic heating for various electrode materials and voltage gradients

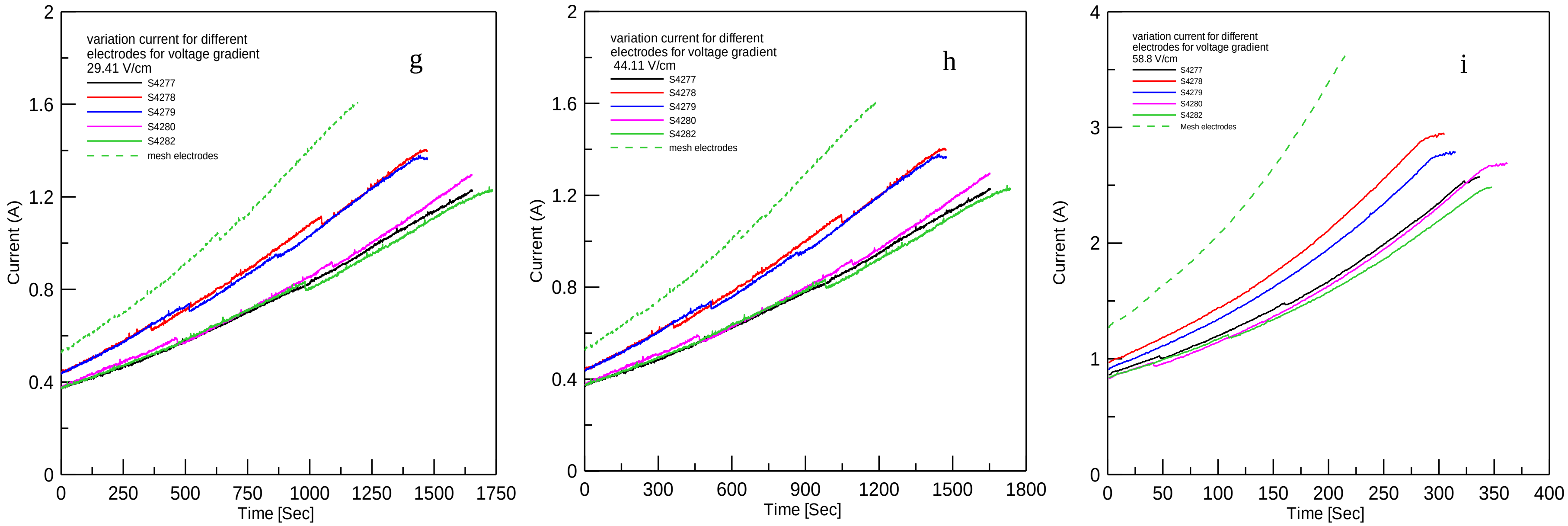

Figure 7-34 Changes in electric current passed during Ohmic heating for various electrode materials and voltage gradients

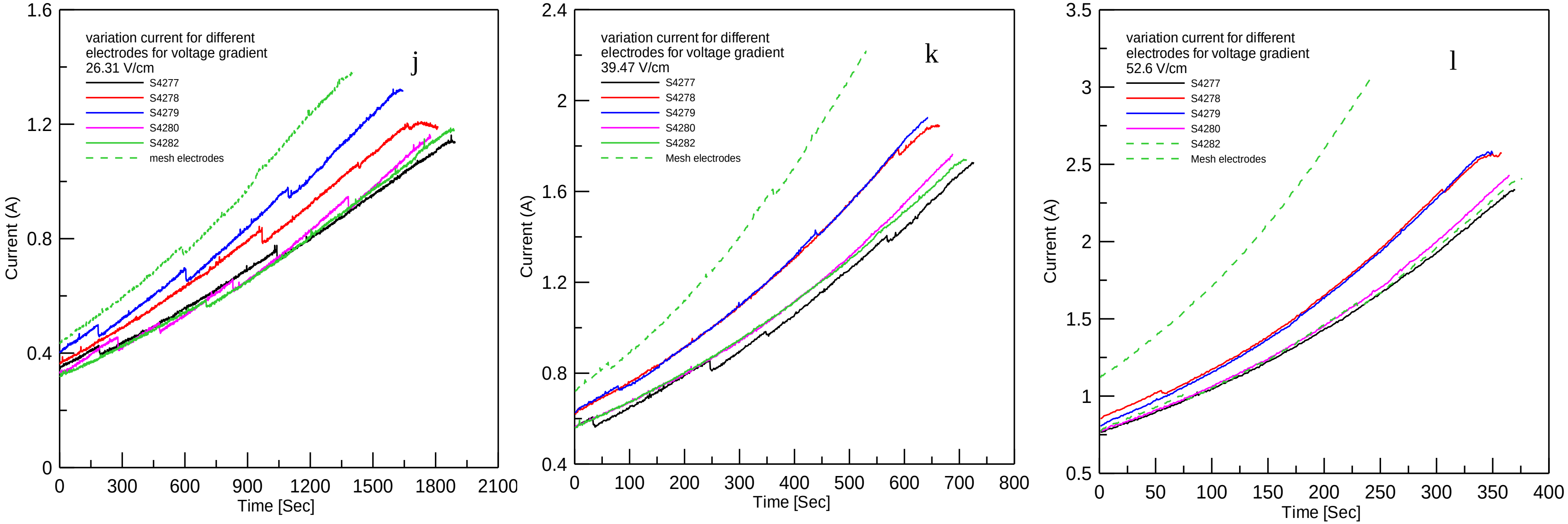

Figure 7-34 Changes in electric current passed during Ohmic heating for various electrode materials and voltage gradients

7.4.5. Effect of electrodes surface area

In this section the effect of electrodes surface area on Ohmic heating performance has been studied, 50 mm x 50 mm solid electrodes were used as shown in Figure 7-35; Platinised titanium electrodes consist of a titanium base, in the form of expanded metal with a thin coating of platinum between 2 to 5 microns thick. The titanium used is 99.5% pure titanium as established by ASTM (American Society of Metal).

The Ohmic heating testing chamber is designed and made from Perspex glass with dimensions of 60×90×100 mm^3, the total volume of the water is 0.42 liter, at the initial room temperature of 18 ^oC and has been heated to 95 ^oC. The amount of heat generation within water sample depends on its electric conductivity which varies during the heating process. The gaps between the electrodes were X=23, 28, 34 and 38 mm, the applied voltages were 100, 150 and 200 Volt.

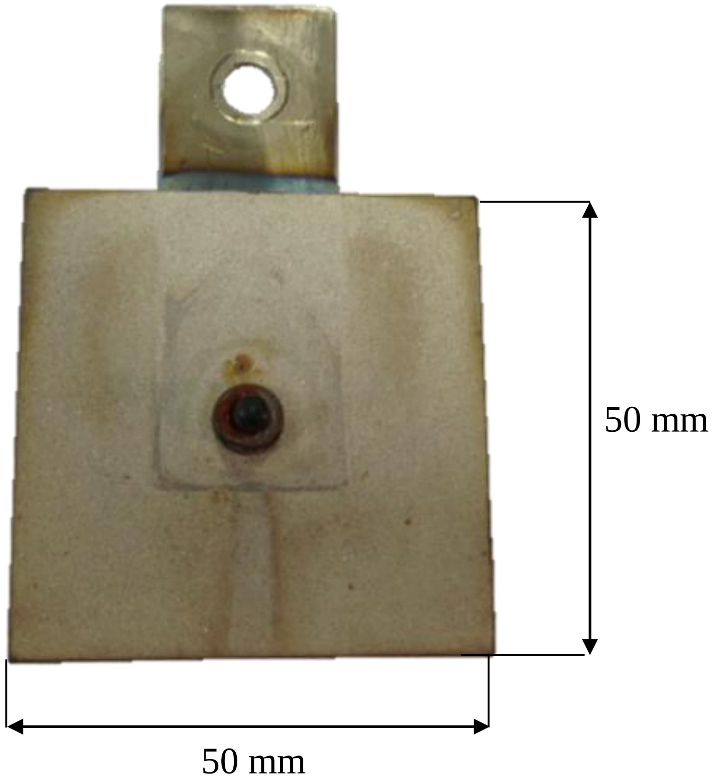

Figure 7-35 Photograph of the platinized-titanium solid electrodes

Figure 3-36 shows the Ohmic heating curve of water at different voltage gradients for coated solid electrodes, it is clear that, the heating time is decreased with voltage gradient increases.

The heating time to raise the water temperature from 20 to 80 ^{o}C is 1700 s under the voltage gradient of 26.3 V/cm and decreased to 1400s, 120s and 1050s for the voltage gradient of 29.41, 35.71 and 43.47 V/cm respectively.

For applied voltage, V= 150 Volt, the heating time is significantly decreased; it is decreased to 440 s for voltage gradient 65.21 V/cm.

For high applied voltage, V= 200 Volt, the heating time is sharply decreased to 250 s for voltage gradient 87 V/cm, and has reached to 365 s for voltage gradient 52.8 V/cm.

Table 7-5 summarize the heat rate for different voltage gradients, it is clear that, the heating rates were varied from 2.1 to 14.4 ^{o}C/min depend on the voltage gradient.

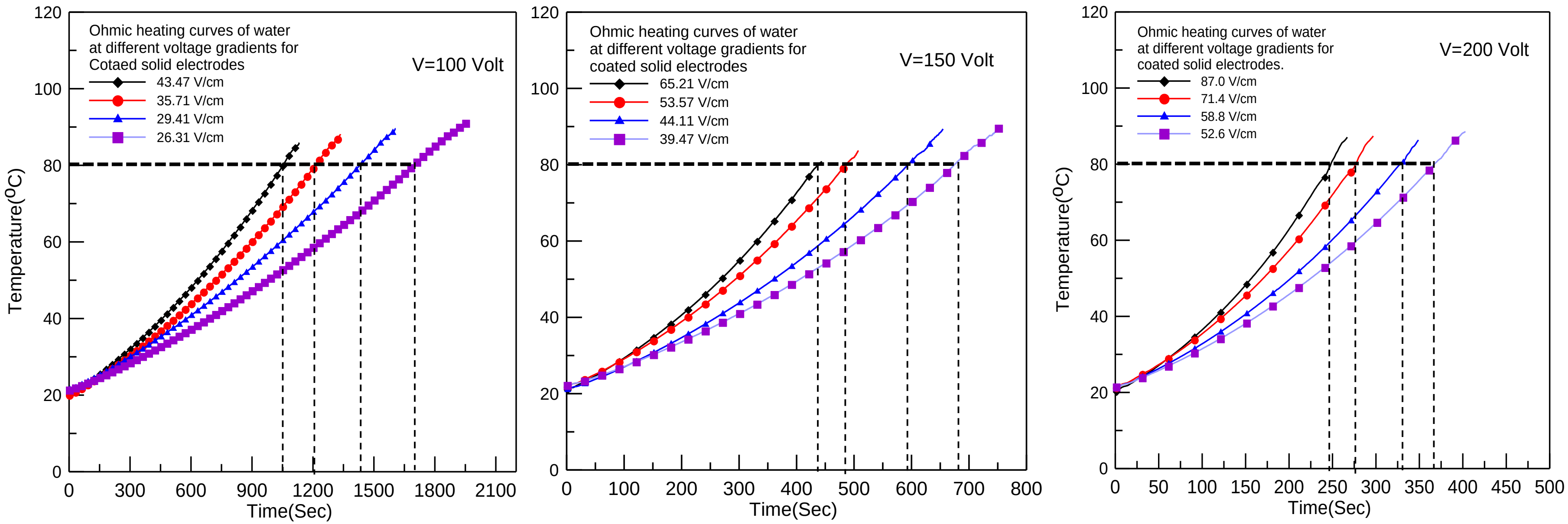

Figure 7-36 Ohmic heating curve of water at different voltage gradients for coated solid electrodes

Table 7-5 Summarize of heat rate for different voltage gradients for solid electrodes

Applied voltage	X (mm)	heating rate (ºC/s)	heating rate (ºC/min)
V=100 Volt	23	0.057	3.42
	28	0.050	3
	34	0.0428	2.568
	38	0.035	2.1
V=150 Volt	23	0.136	8.16
	28	0.122	7.32
	34	0.101	6.06
	38	0.089	5.34
V=200 Volt	23	0.240	14.4
	28	0.2181	13.086
	34	0.1818	10.908
	38	0.164	9.84

Figure 7-37 shows the comparison of heat rate between the mesh and solid electrodes per surface area and mass of heating water , It would seem clear that the heating rate is increased with voltage gradient increases; however, the heating rate for mesh electrodes is slight higher than solid one, the maximum heating rate for the mesh electrodes is 1.7 ^{o}C/min.cm^{2}.kg at voltage gradient 71.43 V/cm^{2} and the maximum heating rate for solid electrodes is 1.37 ^{o}C/min.cm^{2}.kg for voltage gradient 87 V/cm.

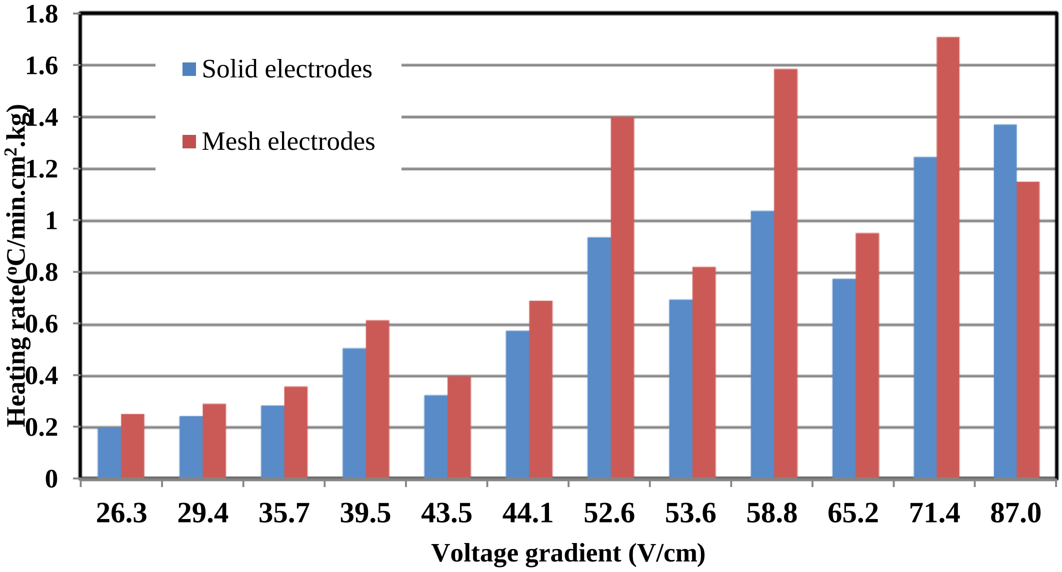

Figure 7-37 comparison between heat rate for mesh and solid electrodes

Figure 7-38 shows the amount of current passing to heat water for different voltage gradient, in general, the amount of passing current is increased as the temperature increases, in the same time, the current passing through the heating sample is increased with increase of voltage gradient and this induced the heat generation faster. For applied voltage V= 100 Volt, the passing current has changed from 0.67 to 2.02 Amp in 1130 s for X=23 mm, from 0.57 to 1.75 Amp in 1336 s for X=28 mm, from 0.49 to 1.49 Amp in 1607 s for X=34 and from 0.37 to 1.25 in 1968 s for X=38.

For V=150 Volt, the passing electric current has changed from 1.02 to 3.04 Amp in 444 s for X=23 mm, 0.905 to 2.708 Amp in 508 s for X=28 mm, from 0.72 to 2.3 Amp 655 s for X=34 mm and from 0.65 to 1.93 on 754 s for X=38.

For applied voltage V= 200 Volt, the passing current has changed from 1.38 to 4.00 Amp in 267 s for X=23 mm, from 1.22 to 3.62 Amp in 297 s for X=28 mm, from 1.006 to 3.01 Amp in 349 s for X=34 and from 0.918 to 2.73 in 403 s for X=38.

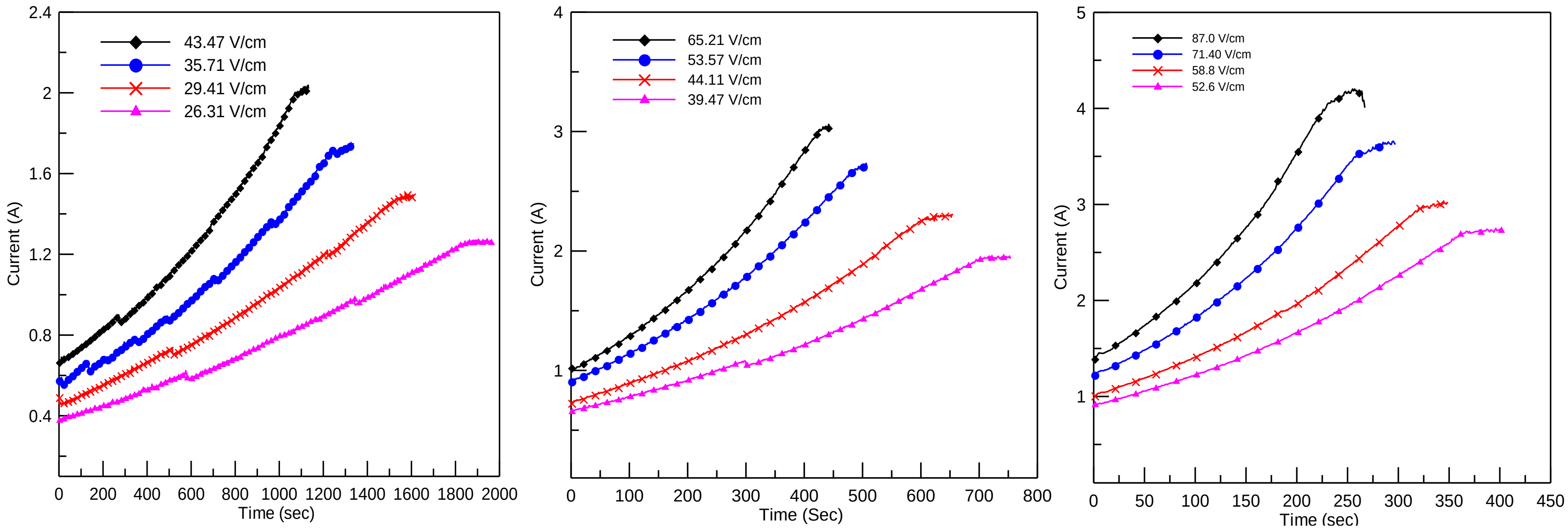

Figure 7-38 Changes in electric current passed with different voltage gradient during Ohmic heating for solid electrodes

7.5. Conclusions

Ohmic heating is an excellent novel alternative water heating technique that shows very promising future in both industry and domestic applications such as pre-treatment for water removal and water desalination. Uniform heating process, less heating time, lower capital cost, and better energy efficiency compared to the other electro heating methods.

The aims from this study were to design, build and evaluate the thermal performance of an Ohmic heating apparatus in bench scale for water heating. It can be concluded from the experimental results that.

1. The electric conductivity values having an increasing trend with increasing the water temperature.
2. Ohmic heating are dependent on the voltage gradient used. As the heating time was decreased with the voltage gradient increase.
3. The system performance coefficients for water were in the range of 77.25 to 86.4%.
4. The results showed that the linear model was found to be the most suitable model to describe the electrical conductivity curve of the Ohmic heating process of water.
5. The results show that as the voltage gradient increased the role of energy losses increased, in other words SPC values decreased.
6. The effect of graphite electrode's resistivity is not significant on Ohmic heating performance.
7. The heating rate for mesh electrodes is higher than graphite electrodes for any voltage gradient.
8. A graphite electrode is the best choice based on the economical aspect.
9. The graphite electrodes have bad effect on change water color.
10. The maximum heating rate for the mesh electrodes is 1.7 $^{o}C/min.cm^{2}.kg$ at voltage gradient 71.43 V/cm^{2}
11. The maximum heating rate for solid electrodes is 1.37 $^{o}C/min.cm^{2}.kg$ for voltage gradient 87 V/cm. In general comprehensive understandings of the process as

well as the energy efficiency are necessary to ensure the applicability of this method in economic sense.

Chapter (8)

8. Conclusions and Recommendations

8.1. Conclusions

The aims of this research are the improvement of the thermal performance of the instantaneous electric water heating systems and investigation for an alternative new water heating methods. These aims are successfully achieved by carrying out the objectives presented in Chapter (1). The main findings from the research will be highlighted in this chapter.

8.1.1 Effect of inlet angle configurations

According to the literature review it is clear that the configuration and shape of the cold water inlet angle, hot water outlet location, heating tank shapes and geometries have significant impact of the water heating systems performance in general, so the experimental and numerical simulation were carried out to investigate the effect of these parameters on thermal performance instantaneous electric water shower.

8.1.1.1 Experimental results

Experiments were carried out to investigate the effect of inlet angle configuration on the thermal performance of instantaneous electric water heater. Twelve different inlet geometries were tested under four discharge rates 0.06, 0.08, 0.10 and 0.12 kg/s. The following conclusions can be drawn from the experimental results:

- Cold water inlet angle configuration plays a key role in determining the thermal performance of such type TEWHs (Tankless electric water heaters).
- Cold water inlet angles (0^o, 30^o) and (0^o, 45^o) were successful in promoting good thermal performance inside the heating tanks of the TEWHs and the outlet hot water keeps at constant and uniform temperature.

8.1.1.2 Numerical results

The 3D model for instantaneous electric water heaters were applied to predict flow mixing in the heating tank, various modifications were studied, which involved using different inlet angles. The fluid motion and the thermal conditions in the electric water heater have been simulated for two different mass flows during the operation m^{o}=0.06 and 0.10 kg/s. The validity of CFD model is assessed by comparison to the results from the experimental work: The results indicate that:

- Using inlet cold water configuration with angles (0°, 30°) and (0°, 45°) provide better thermal performance comparing to the (0°, 0°) inlet port; uniform temperature on the surface of electric heater coils and better thermal stratification are obtained for these angle; In addition, these configuration help to minimize the area of stagnant flow and promote uniform heating of fluid inside the heating tank to avoid such as hot spots being formed on the heating elements.
- The other entrance angles have little effect on improving the thermal performance in the tank.
- Temperature distributions indicate that the new shape of heating tank with the specific inlet angles of (0°, 30°) and (0°, 45°) are likely to improve the heating efficiency and reduce the occurrences of heater failure.
- For straight inlet angle of (0^{o}, 0^{o}), the water flows horizontally hitting another side of the water tank inducing the water flows directly to the top and less swirl flows.
- For cold water ports with inlet angles oriented in the vertical direction, some of the water flows upwards along the water tank after hitting the tank walls and some flows downwards along the water tank towards the bottom.

8.1.2 Effect of heating element and tank geometrical structures

The 3D model for an instantaneous electric water heaters were applied to predict flow mixing in the heating can, various modifications were studied, which involved using different can shape and heater coil structure, these can be constructed easily, economically and without disruption of the operation, the performance of water heater was studied by computational fluid dynamics simulation (CFD). The heater performances is characterized by decreasing the maximum temperature of the heating elements coils to avoid the heater failures.

From the comparison of the results the following conclusions were drawn:

- The shape of the heating tank has significant influence on the water mixing and circulation inside the heating tank heating tank.
- The structures of the heating elements coils have a strong effect on abstracting the inlet flow and maximum temperature of the heating elements coils.
- The use of guiding pipe such as two cans with joint helps to re-circulate the flow around the heating elements coils. Therefore, the use of guiding entrance improves the circulation efficiency and that model has been proposed for construction.
- Modification of the heating elements coils structure and geometry of the heating tank could be significant benefit to assist in smoothing the flow of fluid from inlet to outlet through the heating tank so that the heating elements do not interfere with the flow of fluid through the heating tank.
- The configuration of the heating tank with internal legs heating elements ensure that the space between the periphery of the heating elements and the interior surface of the side wall is relatively free of obstructions so that the heating elements do not detrimentally interfere with the flow of the water through the heating tank and that reduces loading of the heating elements coils which has a much lower maximum temperature and this more like to improve the durability.

8.1.3 Thermal management of residual heat in stored water tank

The use of phase change materials (PCMs) is an effective way of storing thermal energy with the advantages of high-energy storage density and the isothermal nature of the storage process. PCMs have been widely used in latent heat thermal storage systems for thermal control applications. In the present study an experimental unit was built and instrumented to investigate the thermal transfers in this LHTES (Latent Heat Thermal Energy Storages) device in laboratory conditions. The experimental findings indicated that, the use of PCM RT42 helps to stabilize the system temperature to an allowable working temperature of 40 ^{o}C and extends the usage time. The findings indicate that the melting time of the solid PCM is still a problem that needs to be resolved. The time for the PCM to completely melting is still long due to the poor thermal conductivity of PCM.

8.1.4 Ohmic heating for water heating

Ohmic heating is an advanced thermal heating technique, based on the passage of alternating electrical current (AC) through heating sample which serves as an electrical resistance and then heat is generated. The rate of heating is directly proportional to the electrical conductivity. In the current study, Ohmic heating experimental apparatus were conducted in a laboratory scale to evaluate the thermal performance of Ohmic heating based on different parameters such as, voltage gradient, electrical conductivity, heating rate and electrode materials.

The following are the main findings:

- The electric conductivity values have an increasing trend with increasing temperature.
- Ohmic heating is dependent on the voltage gradient used. As the voltage gradient is increased the heating time is decreased.
- The system performance coefficients (SPC) for water is in the range of 77.25 to 86.4%.
- The results show that the linear model is the most suitable model to describe the electrical conductivity curve of the Ohmic heating process of water.
- The results show that as the voltage gradient increased, the energy losses increased, in other words SPC values decreased.
- The effect of graphite electrodes resistivity is not significant on Ohmic heating performance.

- The heating rate for mesh electrodes is higher than graphite electrodes for any voltage gradient.
- A graphite electrode is the best choice based on the economical aspect.
- The graphite electrodes have effect on changing water color.
- The maximum heating rate for the mesh electrodes is 1.7 $^{o}C/min.cm^2.kg$ at the voltage gradient of 71.43 V/cm.
- The maximum heating rate for solid electrodes is 1.37 $^{o}C/min.cm^2.kg$ for the voltage gradient of 87 V/cm.

8.2. Recommendations for Further Work

Although substantial work has been carried out during this research, there are still quite research questions needing to be solved, and the performance of the water heating system can still be improved to some degree. These potential chances to improve the performance are in the following

- Future experimental work on various heating tank shapes
- During this research, static Ohmic heater was studied, continuous flow Ohmic heating should be investigated. Continuous flow Ohmic heating use a simple open geometry which prevents damage to products, reduces the effects of fouling and makes cleaning easier.
- The arrangement of the Ohmic heater electrodes and it configurations need to be studied.
- There are limited commercial ohmic heating applications due to the lack of knowledge on the economic cost of Ohmic heating.
- Commercialization of Ohmic heating technology depends, in part, on the development of adequate safety and quality-assurance protocols in order to obtain an approved filing of the process.
- Effectiveness of Ohmic heating against using traditional boiler in terms of cost analysis is not attempted to be investigated in this study, however the data provided

here will be essential for modeling methods to make fair and comprehensive comparison.

- One major drawback of thermal management of residual heat is the low thermal conductivity of most PCMs. Thus, thermal conductivity enhancement techniques are required in practical thermal management application with PCM.
- Using waste water heat recovery units absorb heat from the discharged waste shower water to heat the incoming supply of cold mains water to the shower inlet. This reduces the amount of energy for heating water required for each shower.

References

ASTM Manual Series MNL (1981) 'Special Technical Publication 470 B. Manual of the use of Thermocouples in Temperature Measurement, p' 14

Abrahams, E. and Ramakrishnan, T. V. (1980) 'Scaling Theory of Localization and Non-Ohmic Effects in Two Dimensions'. Journal of Non-Crystalline Solids 35-36 (PART 1), 15-20

Akhavan-Behabadi, M. A., Kumar, R., Salimpour, M. R., and Azimi, R. (2010) 'Pressure Drop and Heat Transfer Augmentation due to Coiled Wire Inserts during Laminar Flow of Oil Inside a Horizontal Tube'. International Journal of Thermal Sciences 49 (2), 373-379

Alamgholilou, A. and Esmaeilzadeh, E. (2012) 'Experimental Investigation on Hydrodynamics and Heat Transfer of Fluid Flow into Channel for Cooling of Rectangular Ribs by Passive and EHD Active Enhancement Methods'. Experimental Thermal and Fluid Science 38 (0), 61-73

Altuntop, N., Arslan, M., Ozceyhan, V., and Kanoglu, M. (2005) 'Effect of Obstacles on Thermal Stratification in Hot Water Storage Tanks'. Applied Thermal Engineering 25 (14–15), 2285-2298

Amatore, C., Berthou, M., and Hébert, S. (1998) 'Fundamental Principles of Electrochemical Ohmic Heating of Solutions'. Journal of Electroanalytical Chemistry 457 (1-2), 191-203

Anvari, A. R., Lotfi, R., Rashidi, A. M., and Sattari, S. (2011) 'Experimental Research on Heat Transfer of Water in Tubes with Conical Ring Inserts in Transient Regime'. International Communications in Heat and Mass Transfer 38 (5), 668-671

Assiry, A., Sastry, S. K., and Samaranayake, C. (2003) 'Degradation Kinetics of Ascorbic

Acid during Ohmic Heating with Stainless Steel Electrodes'. Journal of Applied Electrochemistry 33 (2), 187-196

Assiry, A. M. (2011) 'Application of Ohmic Heating Technique to Approach Near-ZLD during the Evaporation Process of Seawater'. Desalination 280 (1-3), 217-223

Assiry, A. M., Sastry, S. K., and Samaranayake, C. P. (2006) 'Influence of Temperature, Electrical Conductivity, Power and pH on Ascorbic Acid Degradation Kinetics during Ohmic Heating using Stainless Steel Electrodes'. Bioelectrochemistry 68 (1), 7-13

Assiry, A. M., Gaily, M. H., Alsamee, M., and Sarifudin, A. (2010) 'Electrical Conductivity of Seawater during Ohmic Heating'. Desalination 260 (1-3), 9-17

Ayadi, M. A., Leuliet, J. C., Chopard, F., Berthou, M., and Lebouché, M. (2004) 'Continuous Ohmic Heating Unit Under Whey Protein Fouling'. Innovative Food Science and Emerging Technologies 5 (4), 465-473

Baby, R. and Balaji, C. (2014) 'Thermal Performance of a PCM Heat Sink under Different Heat Loads: An Experimental Study'. International Journal of Thermal Sciences 79 (0), 240-249

Bansal, B. and Chen, X. D. (2006) 'Effect of Temperature and Power Frequency on Milk Fouling in an Ohmic Heater'. Food and Bioproducts Processing 84 (4 C), 286-291

Bourke, G., Bansal, P., and Raine, R. (2014) 'Performance of Gas Tankless (Instantaneous) Water Heaters Under various International Standards'. Applied Energy 131 (0), 468-478

Castro, I., Teixeira, J. A., Salengke, S., Sastry, S. K., and Vicente, A. A. (2004) 'Ohmic Heating of Strawberry Products: Electrical Conductivity Measurements and Ascorbic Acid Degradation Kinetics'. Innovative Food Science and Emerging Technologies 5 (1), 27-36

Chen, C., Abdelrahim, K., and Beckerich, I. (2010) 'Sensitivity Analysis of Continuous

Ohmic Heating Process for Multiphase Foods'. Journal of Food Engineering 98 (2), 257-265

Chen, H. C. and Patel, V. C. (1988) 'Near-Wall Turbulence Models for Complex Flows Including Separation.'. AIAA Journal 26 (6), 641-648

Chiu, Y. and Jang, J. (2009) '3D Numerical and Experimental Analysis for Thermal-Hydraulic Characteristics of Air Flow inside a Circular Tube with Different Tube Inserts'. Applied Thermal Engineering 29 (2-3), 250-258

Chompookham, T., Thianpong, C., Kwankaomeng, S., and Promvonge, P. (2010) 'Heat Transfer Augmentation in a Wedge-Ribbed Channel using Winglet Vortex Generators'. International Communications in Heat and Mass Transfer 37 (2), 163-169

Darvishi, H., Khostaghaza, M. H., and Najafi, G. (2013) 'Ohmic Heating of Pomegranate Juice: Electrical Conductivity and pH Change'. Journal of the Saudi Society of Agricultural Sciences 12 (2), 101-108

De Alwis, A. A. P. and Fryer, P. J. (1992) 'Operability of the Ohmic Heating Process: Electrical Conductivity Effects'. Journal of Food Engineering 15 (1), 21-48

De Alwis, A. A. P. and Fryer, P. J. (1990) 'The use of Direct Resistance Heating in the Food Industry'. Journal of Food Engineering 11 (1), 3-27

De Gracia, A., Oró, E., Farid, M. M., and Cabeza, L. F. (2011) 'Thermal Analysis of Including Phase Change Material in a Domestic Hot Water Cylinder'. Applied Thermal Engineering 31 (17–18), 3938-3945

Depaiwa, N., Chompookham, T., and Promvonge, P. (2010) 'Thermal Enhancement in a Solar Air Heater Channel using Rectangular Winglet Vortex Generators'. PEA-AIT Int.Conf.Energy and Sustainable Development: Issues and Strategies (ESD 2010), 1-7

Dewan, A., Mahanta, P., Raju, K. S., and Suresh Kumar, P. (2004) 'Review of Passive Heat

Transfer Augmentation Techniques'. Proceedings of the Institution of Mechanical Engineers, Part A: Journal of Power and Energy 218 (7), 509-527

Dong-won Yoo and Joshi, Y. K. (2004) 'Energy Efficient Thermal Management of Electronic Components using Solid-Liquid Phase Change Materials'. Device and Materials Reliability, IEEE Transactions on 4 (4), 641-649

Eiamsa-ard, S. (2010) 'Study on Thermal and Fluid Flow Characteristics in Turbulent Channel Flows with Multiple Twisted Tape Vortex Generators'. International Communications in Heat and Mass Transfer 37 (6), 644-651

Eiamsa-Ard, S. and Promvonge, P. (2010a) 'Thermal Characteristics in Round Tube Fitted with Serrated Twisted Tape'. Applied Thermal Engineering 30 (13), 1673-1682

Eiamsa-ard, S. and Promvonge, P. (2010b) 'Thermal Characterization of Turbulent Tube Flows Over Diamond-Shaped Elements in Tandem'. International Journal of Thermal Sciences 49 (6), 1051-1062

Eiamsa-ard, S. and Promvonge, P. (2006) 'Experimental Investigation of Heat Transfer and Friction Characteristics in a Circular Tube Fitted with V-Nozzle Turbulators'. International Communications in Heat and Mass Transfer 33 (5), 591-600

Eiamsa-ard, S., Seemawute, P., and Wongcharee, K. (2010) 'Influences of Peripherally-Cut Twisted Tape Insert on Heat Transfer and Thermal Performance Characteristics in Laminar and Turbulent Tube Flows'. Experimental Thermal and Fluid Science 34 (6), 711-719

Eiamsa-ard, S., Wongcharee, K., and Sripattanapipat, S. (2009) '3-D Numerical Simulation of Swirling Flow and Convective Heat Transfer in a Circular Tube Induced by Means of Loose-Fit Twisted Tapes'. International Communications in Heat and Mass Transfer 36 (9), 947-955

Eiamsa-ard, S., Rattanawong, S., and Promvonge, P. (2009) 'Turbulent Convection in

Round Tube Equipped with Propeller Type Swirl Generators'. International Communications in Heat and Mass Transfer 36 (4), 357-364

Eiamsa-ard, S., Wongcharee, K., Eiamsa-ard, P., and Thianpong, C. (2010) 'Thermohydraulic Investigation of Turbulent Flow through a Round Tube Equipped with Twisted Tapes Consisting of Centre Wings and Alternate-Axes'. Experimental Thermal and Fluid Science 34 (8), 1151-1161

Eiamsa-ard, S., Thianpong, C., Eiamsa-ard, P., and Promvonge, P. (2010) 'Thermal Characteristics in a Heat Exchanger Tube Fitted with Dual Twisted Tape Elements in Tandem'. International Communications in Heat and Mass Transfer 37 (1), 39-46

Eiamsa-ard, S., Wongcharee, K., Eiamsa-ard, P., and Thianpong, C. (2010a) 'Heat Transfer Enhancement in a Tube using Delta-Winglet Twisted Tape Inserts'. Applied Thermal Engineering 30 (4), 310-318

Eiamsa-ard, S., Nivesrangsan, P., Chokphoemphun, S., and Promvonge, P. (2010b) 'Influence of Combined Non-Uniform Wire Coil and Twisted Tape Inserts on Thermal Performance Characteristics'. International Communications in Heat and Mass Transfer 37 (7), 850-856

Eiamsa-ard, S., Thianpong, C., Eiamsa-ard, P., and Promvonge, P. (2009) 'Convective Heat Transfer in a Circular Tube with Short-Length Twisted Tape Insert'. International Communications in Heat and Mass Transfer 36 (4), 365-371

Eiamsa-ard, S., Pethkool, S., Thianpong, C., and Promvonge, P. (2008) 'Turbulent Flow Heat Transfer and Pressure Loss in a Double Pipe Heat Exchanger with Louvered Strip Inserts'. International Communications in Heat and Mass Transfer 35 (2), 120-129

Elshafei, E. A. M., Safwat Mohamed, M., Mansour, H., and Sakr, M. (2008) 'Experimental Study of Heat Transfer in Pulsating Turbulent Flow in a Pipe'. International Journal of Heat and Fluid Flow 29 (4), 1029-1038

Fan, L., Xiao, Y., Zeng, Y., Fang, X., Wang, X., Xu, X., Yu, Z., Hong, R., Hu, Y., and Cen, K. (2013) 'Effects of Melting Temperature and the Presence of Internal Fins on the Performance of a Phase Change Material (PCM)-Based Heat Sink'. International Journal of Thermal Sciences 70 (0), 114-126

Farid, M. M., Khudhair, A. M., Razack, S. A. K., and Al-Hallaj, S. (2004) 'A Review on Phase Change Energy Storage: Materials and Applications'. Energy Conversion and Management 45 (9–10), 1597-1615

Fernández-Seara, J., Uhı´a, F. J., and Sieres, J. (2007) 'Experimental Analysis of a Domestic Electric Hot Water Storage Tank. Part II: Dynamic Mode of Operation'. Applied Thermal Engineering 27 (1), 137-144

Fluent (2011). ANSYS FLUENT Release 13.0 User Manual

Fryer, P. J., de Alwis, A. A. P., Koury, E., Stapley, A. G. F., and Zhang, L. (1993) 'Ohmic Processing of Solid-Liquid Mixtures: Heat Generation and Convection Effects'. Journal of Food Engineering 18 (2), 101-125

Gang, L. (2013). Review of Thermal Energy Storage Technologies and Experimental Investigation of Adsorption Thermal Energy Storage for Residential Application

Gao, W., Liu, T., Lin, W., and Luo, C. (eds.) (2011) Procedia Environmental Sciences. 'Numerical Study on Mixing Characteristics of Hot Water Inside the Storage Tank of a Solar System with Different Inlet Velocities of the Supply Cold Water'

García, A., Vicente, P. G., and Viedma, A. (2005) 'Experimental Study of Heat Transfer Enhancement with Wire Coil Inserts in Laminar-Transition-Turbulent Regimes at Different Prandtl Numbers'. International Journal of Heat and Mass Transfer 48 (21-22), 4640-4651

García-Marí, E., Gasque, M., Gutiérrez-Colomer, R. P., Ibáñez, F., and González-Altozano, P. (2013) 'A New Inlet Device that Enhances Thermal Stratification during Charging in a Hot Water Storage Tank'. Applied Thermal Engineering 61 (2), 663-669

Ghnimi, S., Flach-Malaspina, N., Dresch, M., Delaplace, G., and Maingonnat, J. F. (2008) 'Design and Performance Evaluation of an Ohmic Heating Unit for Thermal Processing of Highly Viscous Liquids'. Chemical Engineering Research and Design 86 (6), 626-632

Goullieux, A. and Pain, J. (2005) '18 - Ohmic Heating'. in Emerging Technologies for Food Processing. ed. by Sun, D. London: Academic Press, 469-505

Green Energy Efficient Homes (2014) Electric Tankless Water Heater [online] available from <http://www.green-energy-efficient-homes.com/electric-tankless-water-heater.html> [07/27 2014]

Greening, B. and Azapagic, A. (2014) 'Domestic Solar Thermal Water Heating: A Sustainable Option for the UK?'. Renewable Energy 63 (0), 23-36

Gunes, S., Ozceyhan, V., and Buyukalaca, O. (2010) 'Heat Transfer Enhancement in a Tube with Equilateral Triangle Cross Sectioned Coiled Wire Inserts'. Experimental Thermal and Fluid Science 34 (6), 684-691

Guo, J., Fan, A., Zhang, X., and Liu, W. (2011) 'A Numerical Study on Heat Transfer and Friction Factor Characteristics of Laminar Flow in a Circular Tube Fitted with Center-Cleared Twisted Tape'. International Journal of Thermal Sciences 50 (7), 1263-1270

Habchi, C. and Harion, J.(2014) 'Residence Time Distribution and Heat Transfer in Circular Pipe Fitted with Longitudinal Rectangular Wings'. International Journal of Heat and Mass Transfer 74, 13-24

Halden, K., De Alwis, A. A. P., and Fryer, P. J. (1990) 'Changes in the Electrical Conductivity of Foods during Ohmic Heating'. International Journal of Food Science and Technology 25 (1), 9-25

Hasnain, S. M. (1998) 'Review on Sustainable Thermal Energy Storage Technologies, Part

I: Heat Storage Materials and Techniques'. Energy Conversion and Management 39 (11), 1127-1138

Hegazy, A. A. (2007) 'Effect of Inlet Design on the Performance of Storage-Type Domestic Electrical Water Heaters'. Applied Energy 84 (12), 1338-1355

Hegazy, A. A. and Diab, M. R. (2002) 'Performance of an Improved Design for Storage-Type Domestic Electrical Water-Heaters'. Applied Energy 71 (4), 287-306

Henze, G. P., Yuill, D. P., and Coward, A. H. (2009) 'Development of a Model Predictive Controller for Tankless Water Heaters'. HVAC&R Research 15 (1), 3-23

Hepbasli, A. and Kalinci, Y. (2009) 'A Review of Heat Pump Water Heating Systems'. Renewable and Sustainable Energy Reviews 13 (6-7), 1211-1229

Herrmann, C., Candas, V., Hoeft, A., and Garreaud, I. (1994) 'Humans under Showers: Thermal Sensitivity, Thermoneutral Sensations, and Comfort Estimates'. Physiology & Behavior 56 (5), 1003-1008

Ho, T. X., Kosinski, P., Hoffmann, A. C., and Vik, A. (2010) 'Effects of Heat Sources on the Performance of a Planar Solid Oxide Fuel Cell'. International Journal of Hydrogen Energy 35 (9), 4276-4284

Holman, J. P. (2001) 'Analysis of Experimental Data'. Experimental Methods for Engineers, 48-143

Huang, L., Chen, Y., and Morrissey, M. T. (1997) 'Coagulation of Fish Proteins from Frozen Fish Mince Wash Water by Ohmic Heating'. Journal of Food Process Engineering 20 (4), 285-300

Ibrahim, E. Z. (2011) 'Augmentation of Laminar Flow and Heat Transfer in Flat Tubes by Means of Helical Screw-Tape Inserts'. Energy Conversion and Management 52 (1), 250-257

Ibrahim, O., Fardoun, F., Younes, R., and Louahlia-Gualous, H. (2014) 'Review of Water-Heating Systems: General Selection Approach Based on Energy and Environmental Aspects'. Building and Environment 72 (0), 259-286

Icier, F. (2012) 'Novel Thermal and Non-Thermal Technologies for Fluid Foods'. Ohmic Heating of Fluid Foods, 305-367

Icier, F. and Ilicali, C. (2005) 'Temperature Dependent Electrical Conductivities of Fruit Purees during Ohmic Heating'. Food Research International 38 (10), 1135-1142

Ievers, S. and Lin, W. (2009) 'Numerical Simulation of Three-Dimensional Flow Dynamics in a Hot Water Storage Tank'. Applied Energy 86 (12), 2604-2614

Jaisankar, S., Radhakrishnan, T. K., and Sheeba, K. N. (2011) 'Experimental Studies on Heat Transfer and Thermal Performance Characteristics of Thermosyphon Solar Water Heating System with Helical and Left-Right Twisted Tapes'. Energy Conversion and Management 52 (5), 2048-2055

Jaisankar, S., Radhakrishnan, T. K., and Sheeba, K. N. (2009a) 'Experimental Studies on Heat Transfer and Friction Factor Characteristics of Thermosyphon Solar Water Heater System Fitted with Spacer at the Trailing Edge of Twisted Tapes'. Applied Thermal Engineering 29 (5-6), 1224-1231

Jaisankar, S., Radhakrishnan, T. K., and Sheeba, K. N. (2009b) 'Studies on Heat Transfer and Friction Factor Characteristics of Thermosyphon Solar Water Heating System with Helical Twisted Tapes'. Energy 34 (9), 1054-1064

Jaisankar, S., Radhakrishnan, T. K., and Sheeba, K. N. (2008) 'Experimental Studies on Heat Transfer and Friction Factor Characteristics of Forced Circulation Solar Water Heater System Fitted with Left-Right Twisted Tapes'. International Energy Journal 9 (3), 199-206

Jaisankar, S., Radhakrishnan, T. K., Sheeba, K. N., and Suresh, S. (2009c) 'Experimental

Investigation of Heat Transfer and Friction Factor Characteristics of Thermosyphon Solar Water Heater System Fitted with Spacer at the Trailing Edge of Left-Right Twisted Tapes'. Energy Conversion and Management 50 (10), 2638-2649

Jakób, A., Bryjak, J., Wójtowicz, H., Illeová, V., Annus, J., and Polakovic, M. (2010) 'Inactivation Kinetics of Food Enzymes during Ohmic Heating'. Food Chemistry 123 (2), 369-376

Jones, D. A., Lelyveld, T. P., Mavrofidis, S. D., Kingman, S. W., and Miles, N. J. (2002) 'Microwave Heating Applications in Environmental Engineering - A Review'. Resources, Conservation and Recycling 34 (2), 75-90

Kandasamy, R., Wang, X., and Mujumdar, A. S. (2008) 'Transient Cooling of Electronics using Phase Change Material (PCM)-Based Heat Sinks'. Applied Thermal Engineering 28 (8–9), 1047-1057

Kandasamy, R., Wang, X., and Mujumdar, A. S. (2007) 'Application of Phase Change Materials in Thermal Management of Electronics'. Applied Thermal Engineering 27 (17–18), 2822-2832

Kanjanapongkul, K., Wongsasulak, S., and Yoovidhya, T. (2010) 'Prediction of Clogging Time during Electrospinning of Zein Solution: Scaling Analysis and Experimental Verification'. Chemical Engineering Science 65 (18), 5217-5225

Kanjanapongkul, K., Tia, S., Wongsa-Ngasri, P., and Yoovidhya, T. (2009) 'Coagulation of Protein in Surimi Wastewater using a Continuous Ohmic Heater'. Journal of Food Engineering 91 (2), 341-346

Karagoz, I. and Kaya, F. (2007) 'CFD Investigation of the Flow and Heat Transfer Characteristics in a Tangential Inlet Cyclone'. International Communications in Heat and Mass Transfer 34 (9–10), 1119-1126

Knirsch, M. C., Alves dos Santos, C., Martins de Oliveira Soares Vicente,A.A., and

Vessoni Penna, T. C. (2010) 'Ohmic Heating a Review'. Trends in Food Science and Technology 21 (9), 436-441

Kongkaitpaiboon, V., Nanan, K., and Eiamsa-ard, S. (2010) 'Experimental Investigation of Heat Transfer and Turbulent Flow Friction in a Tube Fitted with Perforated Conical-Rings'. International Communications in Heat and Mass Transfer 37 (5), 560-567

Krishna, S. R., Pathipaka, G., and Sivashanmugam, P. (2009) 'Heat Transfer and Pressure Drop Studies in a Circular Tube Fitted with Straight Full Twist'. Experimental Thermal and Fluid Science 33 (3), 431-438

Krishna, S. R., Pathipaka, G., and Sivashanmugam, P. (2008) 'Studies on Heat Transfer Augmentation in a Circular Tube Fitted with Straight Half Twist Left-Right Inserts in Laminar Flow'. Journal of Environmental Research and Development 3, 437-441

Krishna, S. R., Pathipaka, G., and Sivashanmugam, P. (2009) 'Heat Transfer and Pressure Drop Studies in a Circular Tube Fitted with Straight Full Twist'. Experimental Thermal and Fluid Science 33 (3), 431-438

Kulshrestha, S. A. and Sastry, S. K. (2006) 'Low-Frequency Dielectric Changes in Cellular Food Material from Ohmic Heating: Effect of End Point Temperature'. Innovative Food Science and Emerging Technologies 7 (4), 257-262

Kumar, A. and Prasad, B. N. (2000) 'Investigation of Twisted Tape Inserted Solar Water heaters—heat Transfer, Friction Factor and Thermal Performance Results'. Renewable Energy 19 (3), 379-398

Kurtbas, I., Gülçimen, F., Akbulut, A., and Buran, D. (2009) 'Heat Transfer Augmentation by Swirl Generators Inserted into a Tube with Constant Heat Flux'. International Communications in Heat and Mass Transfer 36 (8), 865-871

Kusnadi, C. and Sastry, S. K. (2012) 'Effect of Moderate Electric Fields on Salt Diffusion into Vegetable Tissue'. Journal of Food Engineering 110 (3), 329-336

Lakkakula, N. R., Lima, M., and Walker, T. (2004) 'Rice Bran Stabilization and Rice Bran Oil Extraction using Ohmic Heating'. Bioresource Technology 92 (2), 157-161

Launder, B. E. and Spalding, D. B. (1974) 'The Numerical Computation of Turbulent Flows'. Computer Methods in Applied Mechanics and Engineering 3 (2), 269-289

Li, X., Meng, J., and Guo, Z. (2009) 'Turbulent Flow and Heat Transfer in Discrete Double Inclined Ribs Tube'. International Journal of Heat and Mass Transfer 52 (3-4), 962-970

Liebenberg, L. and Meyer, J. P. (2007) 'In-Tube Passive Heat Transfer Enhancement in the Process Industry'. Applied Thermal Engineering 27 (16), 2713-2726

Lima, M. and Sastry, S. K. (1999) 'Effects of Ohmic Heating Frequency on Hot-Air Drying Rate and Juice Yield'. Journal of Food Engineering 41 (2), 115-119

Lin, B. and Ouyang, X. (2014) 'Electricity Demand and Conservation Potential in the Chinese Nonmetallic Mineral Products Industry'. Energy Policy 68, 243-253

Liu, M., Saman, W., and Bruno, F. (2012) 'Review on Storage Materials and Thermal Performance Enhancement Techniques for High Temperature Phase Change Thermal Storage Systems'. Renewable and Sustainable Energy Reviews 16 (4), 2118-2132

Longeon, M., Soupart, A., Fourmigué, J., Bruch, A., and Marty, P. (2013) 'Experimental and Numerical Study of Annular PCM Storage in the Presence of Natural Convection'. Applied Energy 112 (0), 175-184

Lynette, J. (2014) Thermal Touch [online] available from <http://www.scholarpedia.org/article/Thermal_touch> [08/17 2014]

Mahmoud, S., Tang, A., Toh, C., AL-Dadah, R., and Soo, S. L. (2013) 'Experimental Investigation of Inserts Configurations and PCM Type on the Thermal Performance of PCM Based Heat Sinks'. Applied Energy 112 (0), 1349-1356

Malik, A. U., Al-Ghamdi, M. A., and Hodhan, A. H. (2001) 'Investigation on the Boiler

Tubes of Boiler #4, Jeddah-Testing for Microstructure and Life Prediction'. Ninth Middle East Corrosion Conference & Exhibition in Bahrain

Marra, F., Zell, M., Lyng, J. G., Morgan, D. J., and Cronin, D. A. (2009) 'Analysis of Heat Transfer during Ohmic Processing of a Solid Food'. Journal of Food Engineering 91 (1), 56-63

Martemianov, S. and Okulov, V. L. (2004) 'On Heat Transfer Enhancement in Swirl Pipe Flows'. International Journal of Heat and Mass Transfer 47 (10-11), 2379-2393

Marvin, M. (0000). Smith.Electrical Thermal Storage Heat Sink for Space Heater

McConnel, S. V. and Olsson, R. P. (1938) . Wiener Vending Machine

McKenna, B. M., Lyng, J., Brunton, N., and Shirsat, N. (2006) 'Advances in Radio Frequency and Ohmic Heating of Meats'. Journal of Food Engineering 77 (2), 215-229

McNabola, A. and Shields, K. (2013) 'Efficient Drain Water Heat Recovery in Horizontal Domestic Shower Drains'. Energy and Buildings 59 (0), 44-49

Mehling, H., Cabeza, L. F., Hippeli, S., and Hiebler, S. (2003) 'PCM-Module to Improve Hot Water Heat Stores with Stratification'. Renewable Energy 28 (5), 699-711

Meng, J., Liang, X., and Li, Z. (2005) 'Field Synergy Optimization and Enhanced Heat Transfer by Multi-Longitudinal Vortexes Flow in Tube'. International Journal of Heat and Mass Transfer 48 (16), 3331-3337

Milward (2005) Electric Tankless Water Heating: Competitive Assessment: Global Energy Partners, LLC

Milward, R. and Prijyanonda, J. (2005). Electric Tankless Water Heating: Competitive Assessment

Moawed, M. (2011) 'Heat Transfer and Friction Factor Inside Elliptic Tubes Fitted with

Helical Screw-Tape Inserts'. Journal of Renewable and Sustainable Energy 3 (2)

Moeini Sedeh, M. and Khodadadi, J. M. (2013) 'Energy Efficiency Improvement and Fuel Savings in Water Heaters using Baffles'. Applied Energy 102 (0), 520-533

Muñoz-Esparza, D. and Sanmiguel-Rojas, E. (2011) 'Numerical Simulations of the Laminar Flow in Pipes with Wire Coil Inserts'. Computers and Fluids 44 (1), 169-177

Murphy, A. B., Powell, K. J., and Morrow, R. (1991) 'Thermal Treatment of Sewage Sludge by Ohmic Heating'. IEE Proceedings A: Physical Science.Measurement and Instrumentation.Management and Education.Reviews 138 (4), 242-248

Murugesan, P., Mayilsamy, K., and Suresh, S. (2010) 'Heat Transfer and Friction Factor Studies in a Circular Tube Fitted with Twisted Tape Consisting of Wire-Nails'. Chinese Journal of Chemical Engineering 18 (6), 1038-1042

Murugesan, P., Mayilsamy, K., Suresh, S., and Srinivasan, P. S. S. (2011) 'Heat Transfer and Pressure Drop Characteristics in a Circular Tube Fitted with and without V-Cut Twisted Tape Insert'. International Communications in Heat and Mass Transfer 38 (3), 329-334

Murugesan, P., Mayilsamy, K., Suresh, S., and Srinivasan, P. S. S. (2009) 'Heat Transfer and Pressure Drop Characteristics of Turbulent Flow in a Tube Fitted with Trapezoidal-Cut Twisted Tape Insert'. International Journal of Academic Research 1 (1), 123-128

Nabavitabatabayi, M., Haghighat, F., Moreau, A., and Sra, P. (2014) 'Numerical Analysis of a Thermally Enhanced Domestic Hot Water Tank'. Applied Energy 129 (0), 253-260

Naga Sarada, S., Sita Rama Raju, A. V., Kalyani Radha, K., and Shyam Sunder, L. (2010) 'Enhancement of Heat Transfer using Varying Width Twisted Tape Inserts'. Int J Eng, Sci Technol 2 (6), 107-118

Naga, S., Sita, R., Raju, Kalyani, R., and Shyam, S. (2010) 'Enhancement of Heat Transfer using Varying Width Twisted Tape Inserts'. International Journal of Engineering, Science and Technology 2 (6), 107-118

Naphon, P., Nuchjapo, M., and Kurujareon, J. (2006) 'Tube Side Heat Transfer Coefficient and Friction Factor Characteristics of Horizontal Tubes with Helical Rib'. Energy Conversion and Management 47 (18-19), 3031-3044

Napp, T. A., Gambhir, A., Hills, T. P., Florin, N., and Fennell, P. S. (2014) 'A Review of the Technologies, Economics and Policy Instruments for Decarbonising Energy-Intensive Manufacturing Industries'. Renewable and Sustainable Energy Reviews 30, 616-640

Nayak, K. C., Saha, S. K., Srinivasan, K., and Dutta, P. (2006) 'A Numerical Model for Heat Sinks with Phase Change Materials and Thermal Conductivity Enhancers'. International Journal of Heat and Mass Transfer 49 (11–12), 1833-1844

Nguyen, L. T., Choi, W., Lee, S. H., and Jun, S. (2013) 'Exploring the Heating Patterns of Multiphase Foods in a Continuous Flow, Simultaneous Microwave and Ohmic Combination Heater'. Journal of Food Engineering 116 (1), 65-71

Nkwetta, D. N., Vouillamoz, P., Haghighat, F., El Mankibi, M., Moreau, A., and Desai, K. (2014) 'Phase Change Materials in Hot Water Tank for Shifting Peak Power Demand'. Solar Energy 107 (0), 628-635

Noothong, W., Eiamsa-Ard, S., and Promvonge, P. (2006) 'Effect of Twisted-Tape Inserts on Heat Transfer in a Tube'. The 2nd Joint International Conference on Sustainable Energy and Environment (SEE 2006), 1-5

Palaniappan, S. and Sastry, S. K. (1991) 'Electrical Conductivities of Selected Solid Foods during Ohmic Heating'. Journal of Food Process Engineering 14 (3), 221-236

Park, H., Kim, D. H., and Kim, M. S. (2013) 'Performance Investigation of a Cascade Heat Pump Water Heating System with a Quasi-Steady State Analysis'. Energy 63, 283-294

Patankar, S. V. (1980) 'Numerical Heat Transfer and Fluid Flow.'

Pielichowska, K. and Pielichowski, K. (2014) 'Phase Change Materials for Thermal Energy Storage'. Progress in Materials Science 65 (0), 67-123

Pineau, D., Rivière, P., Stabat, P., Hoang, P., and Archambault, V. (2013) 'Performance Analysis of Heating Systems for Low Energy Houses'. Energy and Buildings 65 (0), 45-54

Promvonge, P. (2008) 'Thermal Performance in Circular Tube Fitted with Coiled Square Wires'. Energy Conversion and Management 49 (5), 980-987

Promvonge, P. (2008) 'Thermal Enhancement in a Round Tube with Snail Entry and Coiled-Wire Inserts'. International Communications in Heat and Mass Transfer 35 (5), 623-629

Promvonge, P. (2008) 'Thermal Augmentation in Circular Tube with Twisted Tape and Wire Coil Turbulators'. Energy Conversion and Management 49 (11), 2949-2955

Promvonge, P. (2008) 'Heat Transfer Behaviors in Round Tube with Conical Ring Inserts'. Energy Conversion and Management 49 (1), 8-15

Promvonge, P. and Eiamsa-ard, S. (2007a) 'Heat Transfer Behaviors in a Tube with Combined Conical-Ring and Twisted-Tape Insert'. International Communications in Heat and Mass Transfer 34 (7), 849-859

Promvonge, P. and Eiamsa-ard, S. (2007b) 'Heat Transfer in a Circular Tube Fitted with Free-Spacing Snail Entry and Conical-Nozzle Turbulators'. International Communications in Heat and Mass Transfer 34 (7), 838-848

Promvonge, P. and Eiamsa-ard, S. (2007c) 'Heat Transfer and Turbulent Flow Friction in a Circular Tube Fitted with Conical-Nozzle Turbulators'. International Communications in Heat and Mass Transfer 34 (1), 72-82

Promvonge, P. and Eiamsa-ard, S. (2007d) 'Heat Transfer Augmentation in a Circular Tube using V-Nozzle Turbulator Inserts and Snail Entry'. Experimental Thermal and Fluid Science 32 (1), 332-340

Promvonge, P. and Eiamsa-ard, S. (2006) 'Heat Transfer Enhancement in a Tube with Combined Conical-Nozzle Inserts and Swirl Generator'. Energy Conversion and Management 47 (18-19), 2867-2882

Promvonge, P., Khanoknaiyakarn, C., Kwankaomeng, S., and Thianpong, C. (2011) 'Thermal Behavior in Solar Air Heater Channel Fitted with Combined Rib and Delta-Winglet'. International Communications in Heat and Mass Transfer 38 (6), 749-756

Promvonge, P., Chompookham, T., Kwankaomeng, S., and Thianpong, C. (2010) 'Enhanced Heat Transfer in a Triangular Ribbed Channel with Longitudinal Vortex Generators'. Energy Conversion and Management 51 (6), 1242-1249

Raluy, R. G., Serra, L. M., Guadalfajara, M., and Lozano, M. A. (eds.) (2014) Energy Procedia. 'Life Cycle Assessment of Central Solar Heating Plants with Seasonal Storage'

Regin, A. F., Solanki, S. C., and Saini, J. S. (2008) 'Heat Transfer Characteristics of Thermal Energy Storage System using PCM Capsules: A Review'. Renewable and Sustainable Energy Reviews 12 (9), 2438-2458

Ruan, R., Ye, X., Chen, P., Doona, C. J., and Taub, I. (2001) '13 Ohmic Heating'. in Thermal Technologies in Food Processing. by Richardson, P. : Woodhead Publishing, 241-265

RUBITHERM® R (2014) Rt42 [online] available from <www.rubitherm.de> [08/2014 2014]

Russell, K., and Craig, A. (2006) 'Field Evaluation of Two Demand Electric Water Heaters'. ASHRAE Transactions CH-06(4), 426-435

Saha, S. K. (2010) 'Thermohydraulics of Turbulent Flow through Rectangular and Square Ducts with Axial Corrugation Roughness and Twisted-Tapes with and without Oblique Teeth'. Experimental Thermal and Fluid Science 34 (6), 744-752

Sakr, M. and Liu, S. (2014) 'A Comprehensive Review on Applications of Ohmic Heating (OH)'. Renewable and Sustainable Energy Reviews 39 (0), 262-269

Salengke, S. and Sastry, S. K. (2007) 'Experimental Investigation of Ohmic Heating of Solid-Liquid Mixtures Under Worst-Case Heating Scenarios'. Journal of Food Engineering 83 (3), 324-336

Samaranayake, C. P. and Sastry, S. K. (2005) 'Electrode and pH Effects on Electrochemical Reactions during Ohmic Heating'. Journal of Electroanalytical Chemistry 577 (1), 125-135

Samprovalaki, K., Robbins, P. T., and Fryer, P. J. (2012) 'A Study of Diffusion of Dyes in Model Foods using a Visual Method'. Journal of Food Engineering 110 (3), 441-447

Saraç, B. A. and Bali, T. (2007) 'An Experimental Study on Heat Transfer and Pressure Drop Characteristics of Decaying Swirl Flow through a Circular Pipe with a Vortex Generator'. Experimental Thermal and Fluid Science 32 (1), 158-165

Sarkis, J. R., Jaeschke, D. P., Tessaro, I. C., and Marczak, L. D. F. (2013) 'Effects of Ohmic and Conventional Heating on Anthocyanin Degradation during the Processing of Blueberry Pulp'. LWT - Food Science and Technology 51 (1), 79-85

Sarkis, J. R., Mercali, G. D., Tessaro, I. C., and Marczak, L. D. F. (2013) 'Evaluation of Key Parameters during Construction and Operation of an Ohmic Heating Apparatus'. Innovative Food Science and Emerging Technologies 18, 145-154

Sastry, S. (2008) 'Ohmic Heating and Moderate Electric Field Processing'. Food Science and Technology International 14 (5), 419-422

Sastry, S. K. and Palaniappan, S. (1992) 'Ohmic Heating of Liquid-Particle Mixtures'. Food Technology 46 (12), 64-67

Schade, A. (1951) . Prevention of Enzymatic Discoloration of Potatoes

Seemawute, P. and Eiamsa-ard, S. (2010) 'Thermohydraulics of Turbulent Flow through a Round Tube by a Peripherally-Cut Twisted Tape with an Alternate Axis'. International Communications in Heat and Mass Transfer 37 (6), 652-659

Sezai, I., Aldabbagh, L. B. Y., Atikol, U., and Hacisevki, H. (2005) 'Performance Improvement by using Dual Heaters in a Storage-Type Domestic Electric Water-Heater'. Applied Energy 81 (3), 291-305

Shabanian, S. R., Rahimi, M., Shahhosseini, M., and Alsairafi, A. A. (2011) 'CFD and Experimental Studies on Heat Transfer Enhancement in an Air Cooler Equipped with Different Tube Inserts'. International Communications in Heat and Mass Transfer 38 (3), 383-390

Shah, L. J. and Furbo, S. (2003) 'Entrance Effects in Solar Storage Tanks'. Solar Energy 75 (4), 337-348

Sharma, A., Tyagi, V. V., Chen, C. R., and Buddhi, D. (2009) 'Review on Thermal Energy Storage with Phase Change Materials and Applications'. Renewable and Sustainable Energy Reviews 13 (2), 318-345

Simpson, D. P. (1994). Internal Resistance Ohmic Heating Apparatus for Fluids

Singdeo, D., Dey, T., and Ghosh, P. C. (2011) 'Modelling of Start-Up Time for High Temperature Polymer Electrolyte Fuel Cells'. Energy 36 (10), 6081-6089

Singh, R. P. and Heldman, D. R. (1993). Introduction to Food Engineering

Sivasakthivel, T., Murugesan, K., and Thomas, H. R. (2014) 'Optimization of Operating Parameters of Ground Source Heat Pump System for Space Heating and Cooling by

Taguchi Method and Utility Concept'. Applied Energy 116, 76-85

Sivashanmugam, P. and Nagarajan, P. K. (2007) 'Studies on Heat Transfer and Friction Factor Characteristics of Laminar Flow through a Circular Tube Fitted with Right and Left Helical Screw-Tape Inserts'. Experimental Thermal and Fluid Science 32 (1), 192-197

Sivashanmugam, P. and Suresh, S. (2006) 'Experimental Studies on Heat Transfer and Friction Factor Characteristics of Laminar Flow through a Circular Tube Fitted with Helical Screw-Tape Inserts'. Applied Thermal Engineering 26 (16), 1990-1997

Skudder, P. J. (1988) 'Ohmic Heating: New Alternative for Aseptic Processing of Viscous Foods'. Food Engineering 60 (1), 99-101

Solano, J. P., Herrero, R., Espín, S., Phan, A. N., and Harvey, A. P. (2012) 'Numerical Study of the Flow Pattern and Heat Transfer Enhancement in Oscillatory Baffled Reactors with Helical Coil Inserts'. Chemical Engineering Research and Design 90 (6), 732-742

Somavat, R., Mohamed, H. M. H., and Sastry, S. K. (2013) 'Inactivation Kinetics of Bacillus Coagulans Spores under Ohmic and Conventional Heating'. LWT - Food Science and Technology 54 (1), 194-198

Somavat, R., Mohamed, H. M. H., Chung, Y., Yousef, A. E., and Sastry, S. K. (2012) 'Accelerated Inactivation of Geobacillus Stearothermophilus Spores by Ohmic Heating'. Journal of Food Engineering 108 (1), 69-76

Stancl, J. and Zitny, R. (2010) 'Milk Fouling at Direct Ohmic Heating'. Journal of Food Engineering 99 (4), 437-444

Suresh, K., Raju, K. S., Mahanta, P., and Dewan, A. (2005) 'Review of Passive Heat Transfer Augmentation Techniques'. Proceedings of the Institution of Mechanical Engineers (I-Mech-E) Part A, Journal of Power and Energy 218 (7), 509-527

Thianpong, C., Eiamsa-ard, P., Wongcharee, K., and Eiamsa-ard, S. (2009) 'Compound Heat Transfer Enhancement of a Dimpled Tube with a Twisted Tape Swirl Generator'. International Communications in Heat and Mass Transfer 36 (7), 698-704

Thostenson, E. T. and Chou, T. (1999) 'Microwave Processing: Fundamentals and Applications'. Composites Part A: Applied Science and Manufacturing 30 (9), 1055-1071

Toyoshima, M. and Okawa, S. (2013) 'An Effect of a Horizontal Buoyant Jet on the Temperature Distribution Inside a Hot Water Storage Tank'. International Journal of Heat and Fluid Flow 44 (0), 403-413

Tu, J., Yeoh, G., and Liu, C. (2013) 'Chapter 1 - Introduction'. in Computational Fluid Dynamics (Second Edition). ed. by Tu, J., Yeoh, G., and Liu, C. : Butterworth-Heinemann, 1-29

Tu, J., Yeoh, G. H., and Liu, C. (2008) 'Chapter 2 - CFD Solution Procedure—A Beginning'. in Computational Fluid Dynamics. by Tu, J., Yeoh, G. H., and Liu, C. Burlington: Butterworth-Heinemann, 29-64

Tulsiyan, P., Sarang, S., and Sastry, S. K. (2009) 'Measurement of Residence Time Distribution of a Multicomponent System inside an Ohmic Heater using Radio Frequency Identification'. Journal of Food Engineering 93 (3), 313-317

Tumpanuvatr, T. and Jittanit, W. (2012) 'The Temperature Prediction of some Botanical Beverages, Concentrated Juices and Purees of Orange and Pineapple during Ohmic Heating'. Journal of Food Engineering 113 (2), 226-233

U.S. Department of Energy (DOE) (2014) Improving Process Heating System Performance: [online] available from <https://www1.eere.energy.gov/manufacturing/tech_assistance/pdfs/proc_heat_sourcebook.pdf> [07/29 2014]

Versteeg, H. K. and Malalasekera, W. (1995). An Introduction to Computational Fluid Dynamics

Wang, W., and Sastry, S. K. (1993) 'Salt Diffusion into Vegetable Tissue as a Pretreatment for Ohmic Heating: Electrical Conductivity Profiles and Vacuum Infusion Studies'. Journal of Food Engineering 20 (4), 299-309

Wang, W., and Sastry, S. K. (1993) 'Salt Diffusion into Vegetable Tissue as a Pretreatment for Ohmic Heating: Determination of Parameters and Mathematical Model Verification'. Journal of Food Engineering 20 (4), 311-323

Wang, X., Yap, C., and Mujumdar, A. S. (2008) 'A Parametric Study of Phase Change Material (PCM)-Based Heat Sinks'. International Journal of Thermal Sciences 47 (8), 1055-1068

Warming, R. F. and Beam, R. M. (1976) 'Upwind Second-Order Difference Schemes and Applications in Aerodynamic Flows.'. AIAA Journal 14 (9), 1241-1249

Wolfshtein, M. (1969) 'The Velocity and Temperature Distribution in One-Dimensional Flow with Turbulence Augmentation and Pressure Gradient'. International Journal of Heat and Mass Transfer 12 (3), 301-318

Wong, L. T., Mui, K. W., and Guan, Y. (2010) 'Shower Water Heat Recovery in High-Rise Residential Buildings of Hong Kong'. Applied Energy 87 (2), 703-709

Wongcharee, K. and Eiamsa-ard, S. (2011a) 'Friction and Heat Transfer Characteristics of Laminar Swirl Flow through the Round Tubes Inserted with Alternate Clockwise and Counter-Clockwise Twisted-Tapes'. International Communications in Heat and Mass Transfer 38 (3), 348-352

Wongcharee, K. and Eiamsa-ard, S. (2011b) 'Heat Transfer Enhancement by Twisted Tapes with Alternate-Axes and Triangular, Rectangular and Trapezoidal Wings'. Chemical Engineering and Processing: Process Intensification 50 (2), 211-219

Yakhot, V. and Orszag, S. A. (1986) 'Renormalization Group Analysis of Turbulence. I. Basic Theory'. Journal of Scientific Computing 1 (1), 3-51

Yakut, K. and Sahin, B. (2004) 'The Effects of Vortex Characteristics on Performance of Coiled Wire Turbulators used for Heat Transfer Augmentation'. Applied Thermal Engineering 24 (16), 2427-2438

Yang, C. S., Jeng, D. Z., Yang, Y., Chen, H., and Gau, C. (2011) 'Experimental Study of Pre-Swirl Flow Effect on the Heat Transfer Process in the Entry Region of a Convergent Pipe'. Experimental Thermal and Fluid Science 35 (1), 73-81

Ye, X., Ruan, R., Chen, P., and Doona, C. (2004) 'Simulation and Verification of Ohmic Heating in Static Heater using MRI Temperature Mapping'. LWT - Food Science and Technology 37 (1), 49-58

Ye, X., Ruan, R., Chen, P., Chang, K., Ning, K., Taub, I. A., and Doona, C. (2003) 'Accurate and Fast Temperature Mapping during Ohmic Heating using Proton Resonance Frequency Shift MRI Thermometry'. Journal of Food Engineering 59 (2-3), 143-150

Yilmaz, M., Comakli, O., Yapici, S., and Sara, O. N. (2003) 'Heat Transfer and Friction Characteristics in Decaying Swirl Flow Generated by Different Radial Guide Vane Swirl Generators'. Energy Conversion and Management 44 (2), 283-300

Zell, M., Lyng, J. G., Morgan, D. J., and Cronin, D. A. (2011) 'Minimising Heat Losses during Batch Ohmic Heating of Solid Food'. Food and Bioproducts Processing 89 (2), 128-134

Zell, M., Lyng, J. G., Morgan, D. J., and Cronin, D. A. (2009) 'Development of Rapid Response Thermocouple Probes for use in a Batch Ohmic Heating System'. Journal of Food Engineering 93 (3), 344-347

Zhu, S. M., Zareifard, M. R., Chen, C. R., Marcotte, M., and Grabowski, S. (2010)

'Electrical Conductivity of Particle-Fluid Mixtures in Ohmic Heating: Measurement and Simulation'. Food Research International 43 (6), 1666-1672

Websites:

Web 1: http://www.tritonshowers.co.uk/

Web 2: http://www.rubitherm.de/english/index.htm

Web 3: http://www.ansys.com/

Web 4: http://uk.rs-online.com/web/

Web 5: http://www.omega.co.uk/

Web 6: http://www.datataker.com/

Web 7:http://www.schloetter.co.uk/plating-equipment/platinised-titanium-anodes.htm

Web 8: Gems, Turbine Flow Rate Sensor FT-110 Series, 2008.

Appendix (A)

Flow Rate Measurements

The water flow is measured by a Gems water turbine operating inline as shown in Figure (A-1). The signal is an impulse for each round which is transformed into digital 0-20 mA signal. The accuracy of 3 % within the normal range plus the uncertainty of 0.5 % concerning the repeatability.

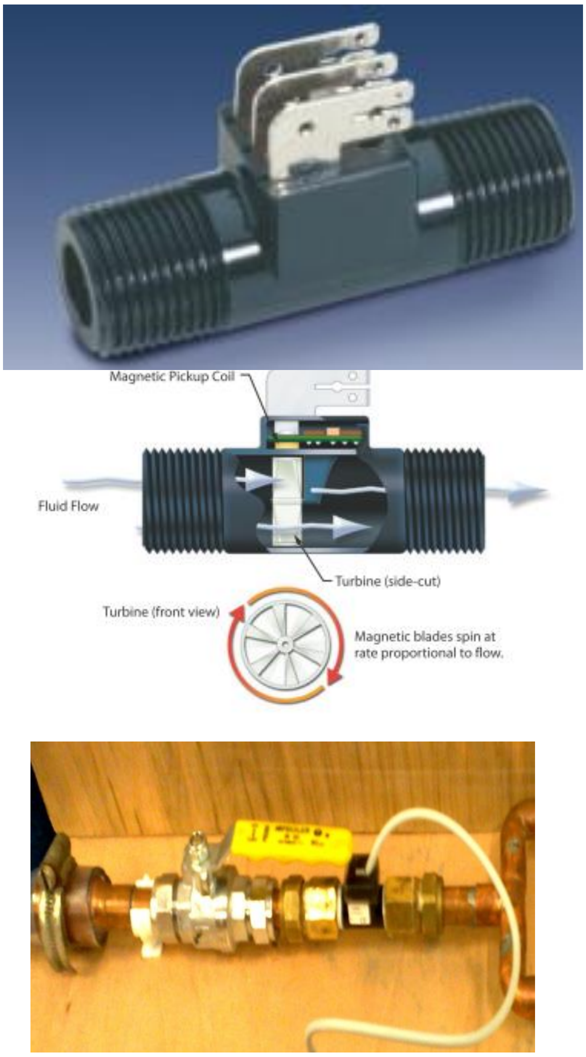

Figure A-1 Photos of flow meter turbine

Steps To Calibrate The Flow Meter Turbine Sensor.

1- Open the main vale to specific flow rate.

2- Record the water temperature to find calculates the water density.

3- Record the data taker reading of the flow rate.

4- at the same time collect specific quantity of water and record the time needed.

5- Measure the mass of the water.

6- Calculate the volume flow rate.

7- Calculate the percentage error= $\frac{Flow\ meter\ reading - Volume\ flow\ rate}{Flow\ meter\ reading}$ (A-1)

8- Repeating steps from (1-7) at different flow rate.

The results of the water flow turbine calibration are shown in Table (A-1).

Table A-1 Results of flow meter turbine calibration

Flow meter turbine(l/s)	**Mass of the water(g)**	**Time(s)**	**Water density(kg/m^3)**	**Volume flow rate(l/s)**	**Error%**
0.019	346	18.05	999.4	0.0192	0.95
0.0187	579	30.73	999.4	0.0189	0.82
0.0211	512	24.1	999.4	0.0213	0.75
0.0213	571	26.74	999.4	0.0214	0.31
0.0291	624	21.67	999.4	0.0288	0.99
0.0291	914.5	31.41	999.4	0.0291	0.11
0.0334	805	24.07	999.4	0.0335	0.19
0.0339	814.5	24.45	999.4	0.0333	1.67
0.0372	585.5	16.1	999.4	0.0364	2.18
0.0375	998	26.65	999.4	0.0375	0.08
0.0394	835.5	21.03	999.4	0.0398	0.90
0.0404	1037	26.27	999.4	0.0395	2.23
0.0419	1006	24.03	999.4	0.0419	0.03
0.0425	976	23.03	999.4	0.0424	0.22
0.0429	866.5	20.2	999.4	0.0429	0.05
0.048	976	20.2	999.4	0.0483	0.72
0.0504	800	16	999.4	0.0500	0.73

0.0503	756	15.14	999.4	0.0500	0.67
0.0542	709	13.1	999.4	0.0542	0.08
0.0516	845.5	16.25	999.4	0.0521	0.90
0.0545	956.5	17.66	999.4	0.0542	0.56
0.0549	1000	18.37	999.4	0.0545	0.78
0.0571	1000.5	17.53	999.4	0.0571	0.01
0.058	999	17.27	999.4	0.0579	0.21
0.0615	1015	16.64	999.4	0.0610	0.76
0.0655	917.5	13.95	999.4	0.0658	0.47
0.069	1010	14.7	999.4	0.0687	0.36
0.0678	784.5	11.59	999.4	0.0677	0.11
0.0729	968	13.27	999.4	0.0730	0.12
0.0724	884	12.19	999.4	0.0726	0.22
0.0772	879	11.37	999.4	0.0774	0.20
0.0804	985	12.24	999.4	0.0805	0.15
0.0881	977.5	10.94	999.4	0.0894	1.48
0.0872	878.5	9.85	999.4	0.0892	2.34
0.0974	1042.5	10.71	999.4	0.0974	0.00
0.0958	833.5	8.67	999.4	0.0962	0.41
0.111	973	8.62	999.4	0.1129	1.75

0.1126	956	8.49	999.4	0.1127	0.06
0.1206	989.5	8.24	999.4	0.1202	0.37
0.124	848	6.78	999.4	0.1251	0.93
0.129	824	6.37	999.4	0.1294	0.34
0.1287	778.5	6.01	999.4	0.1296	0.71
0.1359	872	6.47	999.4	0.1349	0.77
0.1484	1003.5	6.62	999.4	0.1517	2.21
0.1478	869.5	5.8	999.4	0.1500	1.49
0.156	716.5	4.5	999.4	0.1593	2.13
0.1559	744.5	4.81	999.4	0.1549	0.66
0.164	903	5.45	999.4	0.1658	1.09
0.182	682	3.77	999.4	0.1810	0.54
0.1817	840	4.63	999.4	0.1815	0.09
0.1946	834.5	4.24	999.4	0.1969	1.20

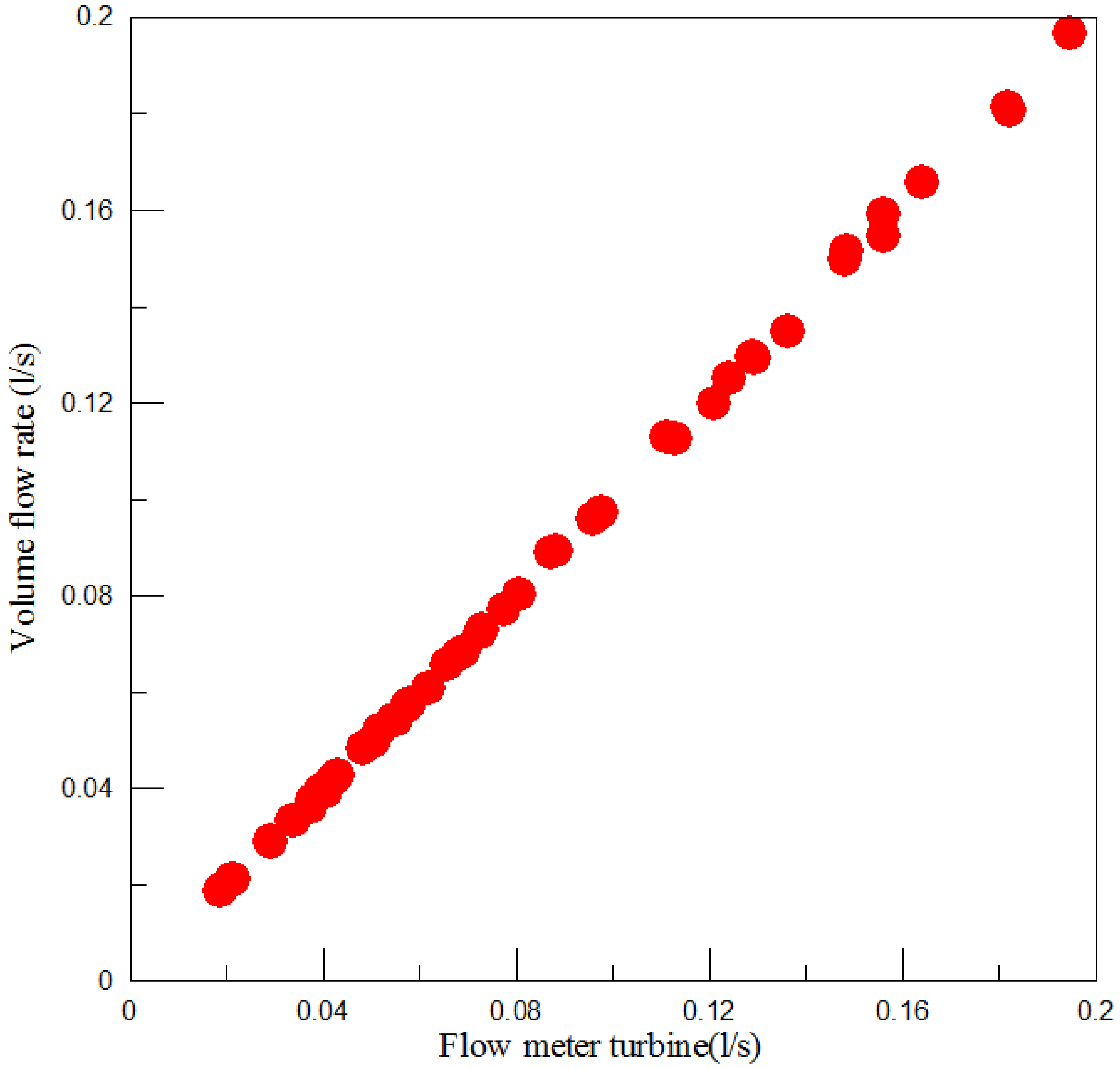

Figure A-2 The Validity of flow meter measurements

Appendix (B)

Calibration of Thermocouples

The thermocouples which are used in the present work are made of Nical-chromium - Alumel,((NiCr / NiAl)) (K type), of 0.2-mm wire diameter. Each wire is insulated. Thermocouples are used for measuring the water flow temperature inside the test section. The direct comparison calibration method is used to calibrate these thermocouples by using standard thermometer with scale from 0 ºC to 100 ºC. In this method, the hot junction of the thermocouple and mercury thermometer was submerged into water in a tank. The used water was heated very slowly with small increment of temperature. The water in the tank was stirred by a mechanical stirrer. The calibration circuit of thermocouples is shown in Figure B-1. The reading of thermocouples and the thermometer were recorded at different temperatures, while heating the oil very slowly up to 100 ºC. The reading of thermocouples is tabulated in Table B-1.

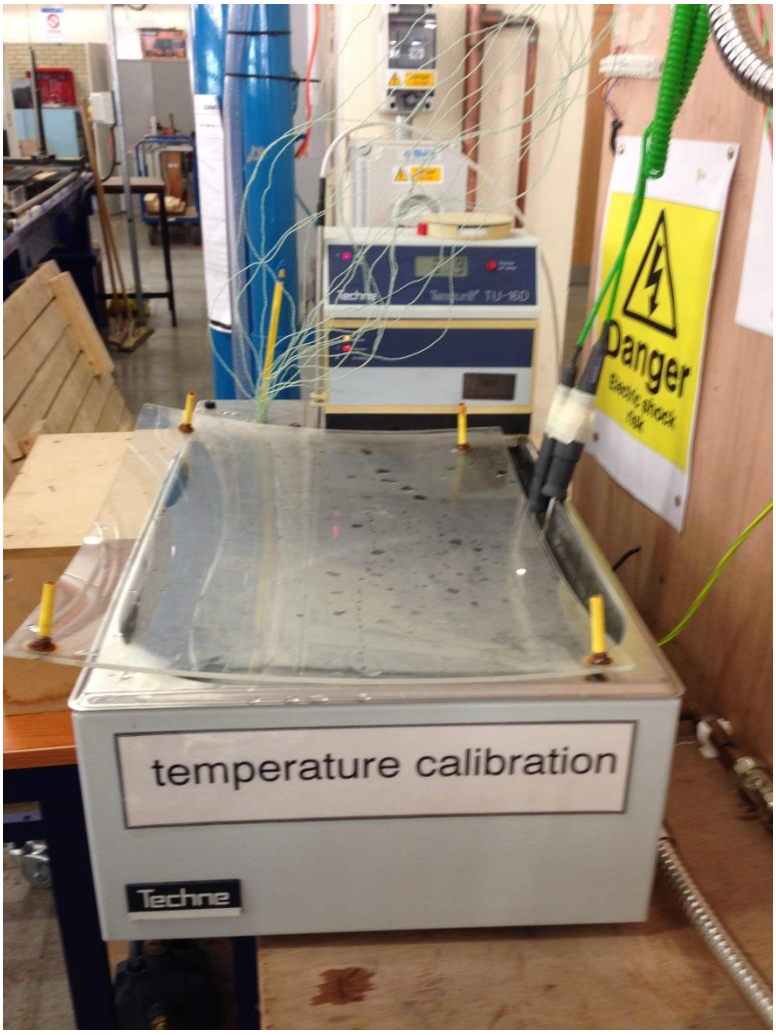

Figure B-1 Thermocouples calibration equipment

Table B-1 Calibration of the Thermocouples

Temperature calibrate	Thermometer	Thermocouple 1 (type K)	Thermocouple 2 (type k)	Thermocouple 3 (type K)	Thermocouple 4 (type K)
12.5	12.5	12.1	12.5	12.6	12.4
15	15	14.78	15.2	15.37	15.11
19.9	20	19.7	20.13	20.28	20.02
24.9	25	24.74	25.14	25.25	25
30	30	29.8	30.15	30.29	30
35	35	34.7	35.03	35.13	34.94
40	40	39.61	40	40.16	39.9
45	45	45.54	44.98	45.1	44.9
50.1	50	49.7	50.12	50.24	50.07
55.1	55	54.67	55	55.15	54.97
60.1	60	59.5	59.9	60	59.9
64.9	65	64.6	64.8	64.81	65.04
68.9	69	68.5	68.69	68.72	68.92

73.1	73	72.6	73.03	73.1	73.32
77.1	77	76.6	76.83	77.06	77.3
82.1	82	81.7	81.78	82	82.21
86.9	87	86.6	86.5	86.9	87.12
90.1	90	89.6	89.68	90	90.17

Appendix (C)

Data Sheet of PCM

EEC-Safety data sheet **page 1/2**

PHASE CHANGE MATERIAL

Appendix (D)

Sample of Measurements and Calculations for Ohmic heating Experiment

In this section, sample of measurements and calculations Ohmic heating experiment will be presented; the experiment is carried out for applied voltage 200 voltage and electrode gap, X=34 mm.

All the data shown in Table (D-1) are fed into data Excel program, through which the values of heated water average temperature, power and electrical conductivity are calculated.

Table D-1 Sample measurements and calculations for Ohmic heating, V= 200 Volt X=34 mm

Time	Time (S)	Voltage	Current	Top (ºC)	Bottom (ºC)	Side 1 (ºC)	Side 2 (ºC)	average (ºC)	Power (W)	Electric conductivity
16:06:04	1	199.7963	1.267757	20.80329	20.87699	20.97701	21.31985	20.99428	253.2932	0.06735
16:06:05	2	201.1415	1.285544	20.85757	20.92691	20.96612	21.31767	21.01707	258.5762	0.068295
16:06:06	3	201.3465	1.296584	21.0127	21.05173	20.98656	21.32977	21.09519	261.0627	0.068881
16:06:07	4	201.4121	1.301	21.23311	21.18538	20.98137	21.32875	21.18215	262.0371	0.069116
16:06:08	5	201.6084	1.314249	21.48044	21.34599	20.97701	21.35034	21.28845	264.9637	0.069819
16:06:09	6	201.4863	1.318664	21.76785	21.57265	20.98231	21.34711	21.41748	265.6928	0.070054
16:06:10	7	201.5429	1.331912	22.09195	21.77108	20.98989	21.31549	21.54211	268.4374	0.070758
16:06:11	8	201.7086	1.338536	22.4288	21.98668	21.00181	21.33612	21.68835	269.9942	0.07111
16:06:12	9	201.6868	1.338536	22.74279	22.13215	21.00835	21.32523	21.80213	269.9651	0.07111
16:06:13	10	201.6999	1.340806	23.08895	22.27504	21.0432	21.36008	21.94182	270.4404	0.07123
16:06:14	11	201.6781	1.343014	23.45319	22.37158	21.19191	21.40895	22.10641	270.8565	0.071348
16:06:15	12	200.7749	1.345222	23.78931	22.44838	21.36879	21.52066	22.28179	270.0869	0.071465
16:06:16	13	200.4037	1.349638	24.15857	22.51985	21.55734	21.62247	22.46456	270.4725	0.0717
16:06:17	14	200.2682	1.356262	24.53296	22.66164	21.74297	21.71703	22.66365	271.6162	0.072051
16:06:18	15	200.3644	1.362886	24.87684	22.82499	21.91968	21.80704	22.85714	273.0738	0.072403
16:06:19	16	200.3425	1.367302	25.21699	23.01758	22.08231	21.90021	23.05427	273.9287	0.072638
16:06:20	17	200.1153	1.376134	25.51425	23.21984	22.24137	21.99021	23.24142	275.3854	0.073107
16:06:21	18	200.2639	1.38055	25.82335	23.42965	22.35634	22.08759	23.42423	276.4744	0.073342
16:06:22	19	200.1852	1.387174	26.15175	23.61535	22.45156	22.14839	23.59176	277.6917	0.073694
16:06:23	20	200.1502	1.396006	26.49476	23.82918	22.56625	22.23282	23.78075	279.4109	0.074163
16:06:24	21	200.1765	1.404838	26.82045	23.97825	22.66382	22.3043	23.94171	281.2156	0.074632

16:06:25	22	200.1547	1.407046	27.11585	24.11424	22.76986	22.38445	24.0961	281.6269	0.074749
16:06:26	23	200.2027	1.41367	27.39486	24.22118	22.90718	22.4656	24.2472	283.0205	0.075101
16:06:27	24	200.2157	1.42471	27.65226	24.30632	23.04461	22.59892	24.40053	285.2493	0.075688
16:06:28	25	200.2244	1.427041	27.8911	24.37762	23.22416	22.6529	24.53645	285.7285	0.075812
16:06:29	26	200.2465	1.438081	28.13531	24.45416	23.40041	22.72538	24.67882	287.9707	0.076398
16:06:30	27	200.1635	1.444705	28.38474	24.53181	23.56453	22.83794	24.82976	289.1772	0.07675
16:06:31	28	200.0235	1.451329	28.65341	24.59424	23.77844	22.94832	24.9936	290.3	0.077102
16:06:32	29	200.2465	1.460161	28.90154	24.67956	23.99328	23.04244	25.1542	292.3921	0.077571
16:06:33	30	200.2901	1.466785	29.13021	24.76694	24.19296	23.13882	25.30723	293.7825	0.077923
16:06:34	31	200.124	1.47341	29.40377	24.89089	24.38612	23.26311	25.48597	294.8647	0.078275
16:06:35	32	200.0892	1.486718	29.66859	25.02764	24.55335	23.38302	25.65815	297.4762	0.078982
16:06:36	33	200.2944	1.497759	29.96568	25.1838	24.71844	23.50515	25.84327	299.9928	0.079568
16:06:37	34	200.2682	1.504383	30.2711	25.32515	24.86607	23.6272	26.02238	301.2801	0.07992
16:06:38	35	200.1722	1.511006	30.56101	25.46664	25.00723	23.74298	26.19446	302.4614	0.080272
16:06:39	36	200.111	1.517631	30.91746	25.58893	25.12899	23.83027	26.36641	303.6946	0.080624
16:06:40	37	200.0892	1.528671	31.2297	25.70124	25.26457	23.93839	26.53347	305.8706	0.081211
16:06:41	38	200.0717	1.539711	31.59096	25.80719	25.40945	24.02256	26.70754	308.0527	0.081797
16:06:42	39	200.0848	1.544127	31.92626	25.91735	25.55853	24.10678	26.87723	308.9563	0.082032
16:06:43	40	199.993	1.555167	32.29854	26.03398	25.74012	24.20165	27.06857	311.0226	0.082618
16:06:44	41	200.076	1.563999	32.67652	26.14737	25.91412	24.28913	27.25679	312.9187	0.083087
16:06:45	42	200.1897	1.572831	33.04546	26.26066	26.07932	24.39785	27.44582	314.8645	0.083557
16:06:46	43	200.124	1.579516	33.42715	26.38685	26.2963	24.48985	27.65004	316.0991	0.083912
16:06:47	44	200.1153	1.588349	33.81626	26.48609	26.52947	24.59319	27.85625	317.8529	0.084381
16:06:48	45	200.124	1.592765	34.17506	26.59832	26.77958	24.70106	28.06351	318.7505	0.084616
16:06:49	46	200.1414	1.610428	34.52706	26.72117	27.0446	24.8239	28.27918	322.3134	0.085554
16:06:50	47	200.1065	1.610428	34.86499	26.83882	27.30437	24.94152	28.48743	322.2572	0.085554

16:06:51	48	200.1197	1.614844	35.23266	26.95648	27.5726	25.05029	28.70301	323.1621	0.085789
16:06:52	49	200.0805	1.623676	35.57646	27.08038	27.7739	25.1655	28.89906	324.8659	0.086258
16:06:53	50	200.0148	1.634717	35.87868	27.2053	27.99335	25.24529	29.08066	326.9676	0.086844
16:06:54	51	199.971	1.639133	36.20308	27.33565	28.24814	25.36733	29.28855	327.7791	0.087079
16:06:55	52	200.0542	1.647965	36.53363	27.4551	28.50934	25.45713	29.4888	329.6823	0.087548
16:06:56	53	200.0323	1.656797	36.83724	27.5865	28.72219	25.5759	29.68046	331.4129	0.088017
16:06:57	54	200.0235	1.663421	37.17704	27.71561	28.94985	25.70558	29.88702	332.7234	0.088369
16:06:58	55	200.0585	1.672315	37.48556	27.86095	29.19351	25.8168	30.08921	334.5608	0.088842
16:06:59	56	200.0061	1.678938	37.81748	27.98245	29.40486	25.93452	30.28483	335.7978	0.089194
16:07:00	57	200.0935	1.689978	38.15969	28.11043	29.63131	26.06742	30.49221	338.1536	0.08978
16:07:01	58	199.945	1.68777	38.46027	28.244	29.84564	26.1797	30.6824	337.4611	0.089663
16:07:02	59	200.0148	1.698811	38.77566	28.37505	30.05348	26.2985	30.87568	339.7873	0.090249
16:07:03	60	200.0061	1.705434	39.08552	28.50077	30.27741	26.4463	31.0775	341.0972	0.090601
16:07:04	61	199.9798	1.70985	39.39428	28.65973	30.46587	26.59721	31.27927	341.9354	0.090836
16:07:05	62	200.0892	1.725306	39.6891	28.80806	30.66495	26.75049	31.47815	345.2151	0.091657
16:07:06	63	200.0979	1.736347	39.99648	28.98625	30.86827	26.90784	31.68971	347.4395	0.092243
16:07:07	64	199.722	1.738554	40.255	29.11069	31.09066	27.1147	31.89276	347.2276	0.092361
16:07:08	65	199.9493	1.745178	40.51329	29.26544	31.3087	27.29136	32.0947	348.947	0.092713
16:07:09	66	199.9318	1.756219	40.77263	29.42956	31.58775	27.39597	32.29648	351.124	0.093299
16:07:10	67	200.0717	1.762904	41.00744	29.57329	31.8248	27.53164	32.48429	352.7073	0.093654
16:07:11	68	199.8968	1.773944	41.26018	29.72649	32.07128	27.66397	32.68048	354.6057	0.094241
16:07:12	69	199.8837	1.780445	41.50625	29.88634	32.29095	27.82445	32.877	355.882	0.094586
16:07:13	70	199.9972	1.791486	41.73964	30.04603	32.49766	27.9761	33.06486	358.2922	0.095173
16:07:14	71	199.8925	1.795963	42.0015	30.24727	32.71166	28.14808	33.27713	358.9995	0.095411
16:07:15	72	199.9972	1.807003	42.25267	30.41649	32.93218	28.30948	33.47771	361.3955	0.095997
16:07:16	73	199.792	1.818043	42.50161	30.588	33.15047	28.4856	33.68142	363.2304	0.096584

16:07:17	74	199.8138	1.824667	42.77672	30.7602	33.38237	28.66297	33.89557	364.5936	0.096935
16:07:18	75	199.875	1.833499	43.02108	30.9014	33.58332	28.84357	34.08734	366.4706	0.097405
16:07:19	76	199.958	1.837915	43.27058	31.06077	33.81084	29.06344	34.30141	367.5058	0.097639
16:07:20	77	199.8268	1.848955	43.55821	31.20719	34.0554	29.27935	34.52504	369.4707	0.098226
16:07:21	78	199.888	1.857787	43.83664	31.39227	34.26989	29.50348	34.75057	371.3494	0.098695
16:07:22	79	199.9055	1.868827	44.11326	31.55772	34.51204	29.70831	34.97283	373.5888	0.099281
16:07:23	80	199.8531	1.879867	44.38654	31.74145	34.75945	29.93144	35.20472	375.6972	0.099868
16:07:24	81	199.8313	1.888761	44.65519	31.91658	34.96847	30.11998	35.41505	377.4336	0.10034
16:07:25	82	199.8444	1.895385	44.97039	32.10025	35.20286	30.34266	35.65404	378.782	0.100692
16:07:26	83	199.8706	1.908632	45.21359	32.30178	35.45842	30.56101	35.8837	381.4793	0.101396
16:07:27	84	199.8093	1.913049	45.50712	32.48149	35.70963	30.74529	36.11088	382.245	0.101631
16:07:28	85	199.7788	1.930652	45.8059	32.67105	35.95752	30.95164	36.34653	385.7034	0.102566
16:07:29	86	199.8531	1.935068	46.10956	32.83162	36.24032	31.20622	36.59693	386.7293	0.1028
16:07:30	87	199.8355	1.941691	46.40023	33.04349	36.49749	31.39655	36.83444	388.0188	0.103152
16:07:31	88	199.8006	1.952732	46.69423	33.2231	36.744	31.623	37.07108	390.157	0.103739
16:07:32	89	199.805	1.959355	46.99865	33.40897	37.01357	31.8215	37.31067	391.489	0.104091
16:07:33	90	199.8006	1.963772	47.28183	33.59951	37.29169	32.02448	37.54938	392.3628	0.104325
16:07:34	91	199.7614	1.981436	47.58398	33.77885	37.5545	32.27203	37.79734	395.8144	0.105264
16:07:35	92	199.7701	1.994684	47.89719	33.97844	37.80792	32.54151	38.05627	398.4783	0.105968
16:07:36	93	199.6958	2.001309	48.21448	34.14825	38.09072	32.82302	38.31912	399.6531	0.10632
16:07:37	94	199.8225	2.010202	48.52319	34.32651	38.36507	33.08743	38.57555	401.6836	0.106792
16:07:38	95	199.8618	2.023449	48.83596	34.53873	38.63923	33.33851	38.83811	404.4102	0.107496
16:07:39	96	199.7571	2.029951	49.16098	34.7467	38.90054	33.58964	39.09947	405.4971	0.107841
16:07:40	97	199.7308	2.038782	49.47651	34.91514	39.15213	33.84396	39.34694	407.2075	0.10831
16:07:41	98	199.7308	2.049884	49.78973	35.12404	39.4356	34.13442	39.62095	409.4249	0.1089
16:07:42	99	199.8225	2.060924	50.12046	35.33812	39.69976	34.36592	39.88107	411.819	0.109487

16:07:43	100	199.7658	2.069757	50.43626	35.5501	39.9659	34.59117	40.13586	413.4667	0.109956
16:07:44	101	199.7046	2.078588	50.7583	35.74688	40.25925	34.78398	40.3871	415.1035	0.110425
16:07:45	102	199.7701	2.091837	51.0727	35.92756	40.53241	35.05044	40.64578	417.8865	0.111129
16:07:46	103	199.6651	2.09846	51.4067	36.10734	40.81697	35.286	40.90426	418.9892	0.111481
16:07:47	104	199.6914	2.107292	51.74583	36.33489	41.11941	35.518	41.17953	420.8081	0.11195
16:07:48	105	199.6958	2.118271	52.05636	36.5208	41.42714	35.75965	41.44099	423.0099	0.112533
16:07:49	106	199.6127	2.127103	52.38156	36.74296	41.74074	36.00329	41.71714	424.5968	0.113002
16:07:50	107	199.6697	2.140351	52.719	36.93919	42.08811	36.24663	41.99823	427.3632	0.113706
16:07:51	108	199.5515	2.151392	53.03944	37.1484	42.38033	36.47298	42.26029	429.3134	0.114293
16:07:52	109	199.4685	2.158015	53.37769	37.36371	42.70821	36.70563	42.53881	430.456	0.114645
16:07:53	110	199.4989	2.166847	53.70018	37.55245	42.97998	36.95847	42.79777	432.2837	0.115114
16:07:54	111	199.5515	2.177949	54.02856	37.78556	43.28324	37.2046	43.07549	434.6129	0.115704
16:07:55	112	199.4028	2.188867	54.36211	37.97759	43.57497	37.46872	43.34585	436.4662	0.116284
16:07:56	113	199.4772	2.204384	54.67451	38.1819	43.83254	37.69032	43.59482	439.7243	0.117108
16:07:57	114	199.4464	2.213216	55.02829	38.39061	44.14492	37.9754	43.88481	441.4181	0.117577
16:07:58	115	199.4377	2.226463	55.34985	38.617	44.42015	38.2359	44.15573	444.0407	0.118281
16:07:59	116	199.4947	2.237504	55.66766	38.8189	44.70465	38.46776	44.41474	446.3701	0.118867
16:08:00	117	199.4072	2.246275	56.00106	39.04526	45.00062	38.71548	44.6906	447.9235	0.119333
16:08:01	118	199.3634	2.255107	56.33737	39.27049	45.29527	38.96188	44.96625	449.5859	0.119803
16:08:02	119	199.3985	2.266147	56.65178	39.46107	45.59721	39.21975	45.23245	451.8663	0.120389
16:08:03	120	199.4247	2.281603	57.0011	39.67962	45.90966	39.47178	45.51554	455.0079	0.12121
16:08:04	121	199.3677	2.294851	57.33552	39.89583	46.21102	39.722	45.7911	457.5193	0.121914
16:08:05	122	199.3416	2.30583	57.67513	40.10035	46.50517	39.97304	46.06342	459.6477	0.122497
16:08:06	123	199.3941	2.314662	58.03403	40.32919	46.8244	40.21478	46.3506	461.5299	0.122966
16:08:07	124	199.2803	2.325702	58.40691	40.55136	47.14123	40.4965	46.649	463.4666	0.123553
16:08:08	125	199.2191	2.341157	58.76525	40.77992	47.46438	40.74615	46.93892	466.4031	0.124374

16:08:09	126	199.2191	2.349929	59.12032	41.01794	47.78001	41.00954	47.23195	468.1507	0.12484
16:08:10	127	199.2673	2.365384	59.46464	41.25796	48.14341	41.27064	47.53416	471.3436	0.125661
16:08:11	128	199.2322	2.376424	59.82753	41.47883	48.48362	41.52955	47.82988	473.4602	0.126248
16:08:12	129	199.2278	2.387465	60.17038	41.67964	48.81626	41.80623	48.11813	475.6494	0.126834
16:08:13	130	199.346	2.398443	60.5266	41.8855	49.15794	42.01635	48.3966	478.12	0.127417
16:08:14	131	199.276	2.407275	60.86638	42.10289	49.49415	42.2885	48.68798	479.7122	0.127886
16:08:15	132	199.3503	2.422732	61.24088	42.35186	49.83652	42.52048	48.98744	482.9723	0.128708
16:08:16	133	199.3152	2.438249	61.60386	42.60185	50.21319	42.82111	49.31	485.9802	0.129532
16:08:17	134	199.3898	2.44475	61.96624	42.8515	50.56854	43.037	49.60582	487.4582	0.129877
16:08:18	135	199.3065	2.457998	62.33598	43.07068	50.92279	43.32336	49.9132	489.895	0.130581
16:08:19	136	199.2935	2.462415	62.70228	43.28235	51.27786	43.58545	50.21199	490.7433	0.130816
16:08:20	137	199.3416	2.484556	63.09479	43.51271	51.66363	43.84944	50.53014	495.2753	0.131992
16:08:21	138	199.2847	2.499889	63.4531	43.72535	52.03579	44.12902	50.83582	498.1897	0.132807
16:08:22	139	199.3898	2.510991	63.84522	43.95994	52.41693	44.38865	51.15269	500.6659	0.133396
16:08:23	140	199.3022	2.519823	64.22053	44.20674	52.81029	44.65229	51.47246	502.2063	0.133866
16:08:24	141	199.3241	2.532949	64.59342	44.43907	53.18866	44.91354	51.78367	504.8778	0.134563
16:08:25	142	199.2322	2.546258	64.97339	44.6952	53.57028	45.16959	52.10212	507.2966	0.13527
16:08:26	143	199.276	2.557297	65.34778	44.94186	53.9476	45.44533	52.42064	509.608	0.135856
16:08:27	144	199.1754	2.570423	65.71576	45.18224	54.34352	45.71479	52.73908	511.9651	0.136554
16:08:28	145	199.2016	2.583732	66.11614	45.42643	54.76383	45.9797	53.07153	514.6836	0.137261
16:08:29	146	199.1273	2.59698	66.48876	45.66348	55.18488	46.29168	53.4072	517.1297	0.137965
16:08:30	147	199.1886	2.607898	66.87935	45.87706	55.57444	46.58503	53.72897	519.4635	0.138545
16:08:31	148	199.1973	2.623415	67.26014	46.12742	55.96703	46.8696	54.05605	522.5772	0.139369
16:08:32	149	199.1711	2.638871	67.64993	46.38848	56.36648	47.1487	54.3884	525.5869	0.14019
16:08:33	150	198.9217	2.645435	68.0319	46.62292	56.76248	47.41621	54.70838	526.2345	0.140539
16:08:34	151	199.1186	2.658682	68.42686	46.88307	57.19218	47.71368	55.05395	529.3931	0.141242

16:08:35	152	199.1055	2.678554	68.83486	47.13187	57.57298	48.00406	55.38594	533.3147	0.142298
16:08:36	153	199.0748	2.685117	69.24152	47.37534	57.95245	48.25941	55.70718	534.5392	0.142647
16:08:37	154	199.0879	2.702781	69.63869	47.62165	58.33084	48.5432	56.03359	538.0909	0.143585
16:08:38	155	199.1404	2.715968	70.04565	47.87005	58.69429	48.82442	56.3586	540.8588	0.144286
16:08:39	156	199.1361	2.7248	70.45126	48.13384	59.05235	49.10877	56.68656	542.606	0.144755
16:08:40	157	199.1055	2.738048	70.8486	48.40288	59.40711	49.40243	57.01525	545.1603	0.145459
16:08:41	158	199.0836	2.757859	71.24695	48.67082	59.77709	49.72796	57.35571	549.0444	0.146511
16:08:42	159	199.0486	2.771107	71.66305	48.91976	60.15297	50.05577	57.69789	551.5851	0.147215
16:08:43	160	199.0222	2.782025	72.07743	49.14107	60.54735	50.3478	58.02841	553.6847	0.147795
16:08:44	161	199.0529	2.795334	72.50051	49.38053	60.94768	50.6572	58.37148	556.4195	0.148502
16:08:45	162	198.9392	2.810667	72.91129	49.64464	61.356	50.96231	58.71856	559.1518	0.149317
16:08:46	163	198.9655	2.821768	73.32324	49.91389	61.73632	51.25589	59.05734	561.4345	0.149906
16:08:47	164	199.0399	2.839432	73.71554	50.18404	62.12976	51.53352	59.39071	565.1603	0.150845
16:08:48	165	199.0442	2.854827	74.14563	50.46749	62.55243	51.88306	59.76216	568.2368	0.151663
16:08:49	166	198.9917	2.870283	74.56568	50.72696	62.98409	52.23321	60.12749	571.1625	0.152484
16:08:50	167	199.0486	2.8812	74.9951	50.99576	63.37945	52.55493	60.48131	573.4989	0.153064
16:08:51	168	199.0748	2.898926	75.43022	51.26223	63.76437	52.85784	60.82867	577.1032	0.154005
16:08:52	169	199.0442	2.918676	75.85402	51.50049	64.15828	53.21976	61.18314	580.9456	0.155055
16:08:53	170	199.0748	2.931862	76.26444	51.74583	64.53002	53.58482	61.53128	583.6599	0.155755
16:08:54	171	199.0092	2.942902	76.68829	52.05028	64.93164	53.89362	61.89096	585.6645	0.156342
16:08:55	172	198.9873	2.95615	77.10638	52.37002	65.30699	54.18446	62.24196	588.2362	0.157045
16:08:56	173	198.913	2.969337	77.54482	52.64414	65.68216	54.49602	62.59179	590.6397	0.157746
16:08:57	174	199.0004	2.982585	77.9781	52.87154	66.06424	54.78138	62.92381	593.5357	0.15845
16:08:58	175	198.9655	2.995772	78.39298	53.11721	66.47658	55.08958	63.26909	596.0553	0.15915
16:08:59	176	198.9435	3.011228	78.836	53.38724	66.91712	55.38907	63.63236	599.0642	0.159971
16:09:00	177	198.9873	3.028831	79.28103	53.70644	67.37147	55.72362	64.02064	602.6988	0.160907

16:09:01	178	198.9697	3.044226	79.72487	54.01615	67.82203	56.07374	64.4092	605.7087	0.161725
16:09:02	179	198.9917	3.059682	80.1625	54.29047	68.23366	56.41708	64.77593	608.8513	0.162546
16:09:03	180	198.9566	3.077284	80.61094	54.5303	68.64779	56.72632	65.12884	612.2461	0.163481
16:09:04	181	198.9173	3.088325	81.05642	54.79489	69.06569	57.09709	65.50352	614.3213	0.164067
16:09:05	182	198.8648	3.10372	81.5125	55.0947	69.49352	57.48638	65.89677	617.2207	0.164885
16:09:06	183	198.8561	3.121322	81.94508	55.38698	69.91783	57.81841	66.26708	620.6938	0.16582
16:09:07	184	198.7729	3.132362	82.40429	55.69369	70.36417	58.15672	66.65472	622.6288	0.166407
16:09:08	185	198.7291	3.145549	82.84867	55.97742	70.78655	58.51716	67.03245	625.1122	0.167107
16:09:09	186	198.7599	3.163091	83.30114	56.2402	71.21116	58.85277	67.40132	628.6957	0.168039
16:09:10	187	198.8253	3.176338	83.7524	56.5309	71.61844	59.16254	67.76607	631.5364	0.168743
16:09:11	188	198.7117	3.196149	84.20677	56.81204	72.00833	59.47084	68.12449	635.1121	0.169795
16:09:12	189	198.6941	3.20719	84.67102	57.1241	72.42851	59.87578	68.52485	637.2497	0.170382
16:09:13	190	198.7291	3.222584	85.13187	57.40795	72.84549	60.22696	68.90307	640.4213	0.1712
16:09:14	191	198.7553	3.237979	85.59772	57.71337	73.25936	60.53591	69.27659	643.5656	0.172018
16:09:15	192	198.7817	3.255642	86.02706	58.02276	73.68117	60.87362	69.65115	647.1619	0.172956
16:09:16	193	198.6897	3.273245	86.50776	58.31016	74.09389	61.23066	70.03562	650.3599	0.173891
16:09:17	194	198.7117	3.28864	86.97086	58.61291	74.51907	61.61509	70.42948	653.4912	0.174709
16:09:18	195	198.7553	3.304034	87.43596	58.88475	74.93397	61.96846	70.80579	656.6944	0.175527
16:09:19	196	198.7117	3.323784	87.91071	59.1933	75.34088	62.301	71.18647	660.4747	0.176576
16:09:20	197	198.6941	3.337093	88.36851	59.51711	75.77083	62.66122	71.57942	663.0607	0.177283
16:09:21	198	198.6371	3.359051	88.84942	59.83567	76.22007	63.08564	71.9977	667.2323	0.17845
16:09:22	199	198.7599	3.37003	89.33076	60.13447	76.65361	63.46154	72.39509	669.8268	0.179033
16:09:23	200	198.6941	3.38984	89.81552	60.43194	77.12262	63.77066	72.78518	673.5412	0.180085
16:09:24	201	198.6984	3.405296	90.27134	60.72223	77.58756	64.11621	73.17434	676.6269	0.180906
16:09:25	202	198.7248	3.420692	90.77356	61.04355	78.02573	64.47599	73.57971	679.7765	0.181724
16:09:26	203	198.7071	3.436087	91.26146	61.34986	78.49434	64.77212	73.96944	682.775	0.182542

16:09:27	204	198.6941	3.447127	91.7462	61.65725	78.98822	65.12642	74.37952	684.9238	0.183129
16:09:28	205	198.7117	3.464728	92.25014	61.97991	79.44821	65.46701	74.78632	688.4819	0.184064
16:09:29	206	198.633	3.477854	92.77374	62.29387	79.87181	65.86457	75.201	690.8165	0.184761
16:09:30	207	198.646	3.502081	93.25992	62.60271	80.26566	66.18349	75.57795	695.6745	0.186048
16:09:31	208	198.646	3.515268	93.73572	62.92159	80.6576	66.52849	75.96085	698.294	0.186749
16:09:32	209	198.5803	3.526308	94.19422	63.26802	81.09801	66.89674	76.36425	700.2554	0.187335
16:09:33	210	198.4883	3.54391	94.63437	63.55244	81.60384	67.2521	76.76069	703.4248	0.18827
16:09:34	211	198.4928	3.559305	95.07933	63.91584	82.10275	67.71211	77.20251	706.4963	0.189088
16:09:35	212	198.554	3.572492	95.50362	64.27467	82.56863	68.16329	77.62755	709.3326	0.189789
16:09:36	213	198.5453	3.590034	95.95338	64.59762	83.03544	68.54617	78.03315	712.7843	0.190721
16:09:37	214	198.554	3.601073	96.44839	64.91712	83.5761	68.91734	78.46474	715.0075	0.191307
16:09:38	215	198.576	3.618676	96.9252	65.24675	84.11043	69.30261	78.89625	718.5824	0.192242

Appendix (E)

Uncertainty Analysis Uncertainty for Ohmic Heating Experiment

Uncertainty analysis of various measured parameters was carried out in order to estimate the accuracy of the experimental results.

In the present study, temperatures, voltage gradients, current, water mass and times were measured with appropriate instruments clarified before and total uncertainties for all these parameters were calculated separately. The sensitivity of temperature sensors were ±0.1^{o}C, reading errors for temperature measurements were assumed as ±0.1 ^{o}C. The sensitivity of digital scale used in measuring mass of the water was ±1.0 g and reading errors were ±1.0 g. The uncertainty caused from vibration of timer was assumed as ±0.02 s errors came from the periodic measuring was assumed as ±0.1 s and error occurred while recording of temperature data were as ±0.1 s.

According to all these uncertainties and errors, an uncertainty analysis was performed using the method described by Holman (2001). The method is based on careful specifications of the uncertainties in the various primary experimental measurements. Suppose that the result; R is a given function of the independent variables $X_1,X_2,X_3,X_4,\ldots\ldots,X_n$. Thus:

$R = R(X_1, X_2, X_3, X_4 \ldots X_n)$

Let W_R be the uncertainty in the result and W_1, W_2, W_3………*and* W_n are the uncertainties in the independent variables. The uncertainty in the result is given as:

$$W_R = \left[\left(\frac{\partial R}{\partial x_1}W_1\right)^2 + \left(\frac{\partial R}{\partial x_2}W_2\right)^2 + \left(\frac{\partial R}{\partial x_3}W_3\right)^2 + \ldots\ldots\ldots\ldots + \left(\frac{\partial R}{\partial x_n}W_n\right)^2\right]^{1/2} \quad \text{(E-1)}$$

Uncertainty in Energy Input; E_{in}

The relative uncertainty in the measured voltages and currents each estimated to be about 1%. Hence the relative uncertainty in energy input becomes:

$$\frac{w_E}{E} = \left[(0.01)^2 + (0.01)^2 + (0.02)^2\right]^{\frac{1}{2}} = 2.45\%$$

Uncertainty in average temperature, $T_{average}$

The relative uncertainties of the mean temperature considering the minimum and maximum temperatures are:

For T_{min} = 15°C, the uncertainty becomes:

$$\frac{w_{Taverage}}{T_{average}} = 0.77\ \%$$

For T_{max} = 100°C, the uncertainty becomes:

$$\frac{w_{Taverage}}{T_{average}} = 0.10\ \%$$

Uncertainty in mass of the water: m

The relative uncertainty of the mass of the water is:

$$\frac{w_m}{m} = 0.27\ \%$$

Uncertainty in heat absorbed; $Q_{absorbed}$

The relative uncertainty of the heat taken up by water is:

$$\frac{w_Q}{Q} = \left[(0.0077)^2 + (0.0027)^2\right]^{\frac{1}{2}} = 0.815\%$$

Table E-1 summarizes the calculated values of the uncertainty of the measured quantities.

Table E-1 Uncertainties of measured quantities

Parameter	**Absolute Uncertainty**	**Relative Uncertainty**
Mass of the water	±1.0 g	±0.27 %
Energy input		± 2.45 %
Average temperature	±0.1 °C	
Heat absorbed		±0.815 %

Appendix (F)

Published Papers and Patents

Papers

1- Mohamed Sakr and Shuli Liu, "**A Comprehensive Review on Applications of Ohmic Heating (OH)**". Renewable and Sustainable Energy Reviews 39, (2014), 262-269.

2- Shuli Liu and Mohamed Sakr, "**A Comprehensive Review on Passive Heat transfer Enhancements in Pipe Exchangers**". Renewable and Sustainable Energy Reviews 19, (2013), 64-81.

Patents

1.**A device for the passage of a volume of fluid**. UK.

Application Number: GB1305613.0

Application Source: Form 1

Publication Number: GB2512353

Status: Application Published

Filing Date: 27 March 2013

Publication Date: 01 October 2014

2.**A device for the passage of a volume of fluid**. UK.

Application Number :GB1305617.1

Application Source :Form 1

Publication Number :GB2512354

Status :Application Published

Filing Date :27 March 2013

Publication Date :01 October 2014

3.**A device for the passage of water.** UK.

Application Number: GB1314203.9

Application Source: Form 1

Publication Number: GB2516953

Status: Application Published

Filing Date: 08 August 2013

Publication Date: 11 February 2015

Renewable and Sustainable Energy Reviews 39 (2014) 262–269

Renewable and Sustainable Energy Reviews 19 (2013) 64–81

4

At least one drawing originally filed was informal and the print reproduced here is taken from a later filed formal copy.

2

This item has been removed due to third party copyright. The unabridged version of the thesis can be viewed at the Lanchester library, Coventry University

6

This item has been removed due to third party copyright. The unabridged version of the thesis can be viewed at the Lanchester library, Coventry University

INTELLECTUAL
PROPERTY OFFICE

INTELLECTUAL
PROPERTY OFFICE

At least one drawing originally filed was informal and the print reproduced here is taken from a later filed formal copy.

1 / 3

3

5

8

9